NOSC TD 1209
Volume 2

(4)

AD-A192 311

NAVAL OCEAN SYSTEMS CENTER San Diego, California 92152-5000

NOSC

Technical Document 1209
Volume 2
January 1988

Antenna Heights for the Optimum Utilization of the Oceanic Evaporation Duct

Part III: Results from the Mediterranean Measurements

J. H. Richter
H. V. Hitney

Approved for public release, distribution is unlimited.

NAVAL OCEAN SYSTEMS CENTER
San Diego, California 92152-5000

E. G. SCHWEIZER, CAPT, USN
Commander

R. M. HILLYER
Technical Director

ADMINISTRATIVE INFORMATION

This reissue of Naval Electronics Laboratory Center (NELC) Technical Notes 2031, 2371, and 2569 was funded by the Office of Naval Technology, Arlington, VA 22217. The authors are currently members of the Marine Sciences and Technology Department, Naval Ocean Systems Center, San Diego, CA 92152-5000.

Released by
H.V. Hitney, Head
Tropospheric Branch

Under authority of
J.H. Richter, Head
Ocean and Atmospheric
Sciences Division

LH

UNCLASSIFIED
SECURITY CLASSIFICATION OF THIS PAGE

REPORT DOCUMENTATION PAGE

1a. REPORT SECURITY CLASSIFICATION: UNCLASSIFIED	1b. RESTRICTIVE MARKINGS
2a. SECURITY CLASSIFICATION AUTHORITY	3. DISTRIBUTION/AVAILABILITY OF REPORT: Approved for public release; distribution is unlimited.
2b. DECLASSIFICATION/DOWNGRADING SCHEDULE	
4. PERFORMING ORGANIZATION REPORT NUMBER(S): NOSC TD 1209, Vol. 2	5. MONITORING ORGANIZATION REPORT NUMBER(S)
6a. NAME OF PERFORMING ORGANIZATION: Naval Ocean Systems Center; 6b. OFFICE SYMBOL (if applicable): Code 54	7a. NAME OF MONITORING ORGANIZATION
6c. ADDRESS (City, State and ZIP Code): San Diego, CA 92152-5000	7b. ADDRESS (City, State and ZIP Code)
8a. NAME OF FUNDING/SPONSORING ORGANIZATION: Office of Naval Technology, Office of Chief of Naval Research; 8b. OFFICE SYMBOL (if applicable)	9. PROCUREMENT INSTRUMENT IDENTIFICATION NUMBER
8c. ADDRESS (City, State and ZIP Code): Arlington, VA 22217	10. SOURCE OF FUNDING NUMBERS

PROGRAM ELEMENT NO	PROJECT NO	TASK NO	AGENCY ACCESSION NO
62435N	N01A	RA35G80/ RU35G80	DN888 715

11. TITLE (include Security Classification)

ANTENNA HEIGHTS FOR THE OPTIMUM UTILIZATION OF THE OCEANIC EVAPORATION DUCT
Part III: Results from the Mediterranean Measurements

12. PERSONAL AUTHOR(S)

J.H. Richter and H.V. Hitney

13a. TYPE OF REPORT	13b. TIME COVERED	14. DATE OF REPORT (Year, Month, Day)	15. PAGE COUNT
	FROM ______ TO ______	January 1988	291

16. SUPPLEMENTARY NOTATION

Volume 2 of 2; first published as an informal working document with limited distribution, NELC Technical Note 2569 has been reissued as a formal NOSC Technical Document approved for unlimited distribution.

17. COSATI CODES			18. SUBJECT TERMS (Continue on reverse if necessary and identify by block number)
FIELD	GROUP	SUB-GROUP	Evaporation ducting
			Propagation

19. ABSTRACT (Continue on reverse if necessary and identify by block number)

Extensive evaporation ducting measurements were conducted in the Eastern Mediterranean. The purpose of the measurements was to provide data for model validations and to determine if existing climatologies could be used for estimating the probability of occurrence for evaporation ducting conditions. Keywords.

20. DISTRIBUTION/AVAILABILITY OF ABSTRACT: ☐ UNCLASSIFIED/UNLIMITED ☒ SAME AS RPT ☐ DTIC USERS	21. ABSTRACT SECURITY CLASSIFICATION: UNCLASSIFIED
22a. NAME OF RESPONSIBLE INDIVIDUAL: J.H. Richter	22b. TELEPHONE (include Area Code): (619) 553-3053; 22c. OFFICE SYMBOL: Code 54

DD FORM 1473, 84 JAN

83 APR EDITION MAY BE USED UNTIL EXHAUSTED
ALL OTHER EDITIONS ARE OBSOLETE

UNCLASSIFIED
SECURITY CLASSIFICATION OF THIS PAGE

FOREWORD

In the early 1970s, a series of extensive evaporation ducting measurements was conducted in different ocean areas. The purpose of the measurements was to provide data for model validations and to determine if existing climatologies could be used for estimating the probability of occurrence for evaporation ducting conditions. Both objectives were successfully met and documented in Naval Electronics Laboratory Center (NELC) Technical Notes 2031, 2371, and 2569. (NELC was a predecessor of the Naval Ocean Systems Center.)

Technical Notes carry a limited distribution statement and cannot be referenced in documents approved for unlimited distribution. Because the information in Technical Notes 2031, 2371, and 2569 is still extensively used, the Technical Notes have been reissued in this NOSC Technical Document approved for unlimited distribution. As a formal, Center-approved publication, this Technical Document can be referenced.

This reissue is presented in two volumes. Volume 1 presents Part I: Results from the Pacific Measurements (formerly NELC TN 2031) and Part II: Results from the Key West Measurements (formerly NELC TN 2371). Volume 2 presents Part III: Results from the Mediterranean Measurements (formerly NELC TN 2569).

Part III: Results from the Mediterranean Measurements

CONTENTS

SUMMARY

Radio propagation measurements in the 1-40 GHz frequency range were performed during 1972 in the Eastern Mediterranean. A propagation link between the islands of Mykonos and Naxos in the Aegean Sea was operated during four measurement periods, each lasting approximately two weeks. The receiver terminal was equipped with vertically spaced antennas in order to obtain information on optimum shipboard antenna heights. The measurements showed that evaporation ducting is an important phenomenon, in particular for frequencies above S-band. For example, signal enhancements from evaporation ducting were measured 99% of the time for X-band frequencies. It was determined that the evaporation duct strongly affects propagation for all shipboard antenna heights. Under conditions of strong ducting, low sited antennas (e.g. 15 feet above mean sea level) may receive higher signals than more conventional antenna heights (e.g. 60-70 feet above msl). For all measurements in the Mediterranean the low sited X-band antenna received equal or higher signals than the high antenna 47.4% of the time. During 20% of the time signals received at the low sited X-band antenna exceeded those received on the high sited antenna by 10 dB. From the measurements one may conclude that the optimum location for an antenna is high on the ship. When economics justify two antennas, an advantage can be obtained with both a high and low antenna.

The evaporation ducting effect appears to have a broad maximum in the X- to Ku-band frequency range. Atmospheric absorption and sea surface roughness apparently counteract the effectiveness of the duct expected at higher frequencies.

Simple meteorological measurements were found to be quite sufficient to describe ducting conditions. Horizontal homogeneity of the duct was found to be good for the propagation path used in this investigation. Ducting effects deduced from long term meteorological averages compared well with the actual measurements, permitting estimates of ducting conditions to be made for any oceanic area for which such statistical meteorological data are available.

I. BACKGROUND

Parts I and II of this series of reports (references 1 and 2) described microwave propagation measurements in the oceanic evaporation duct performed off the California and Florida coast. Ducting conditions were found to be significantly different in the two areas. At X-band antenna reversals (i.e. an antenna 64' above mean sea level received less signal strength than an antenna at 16' above mean sea level) occurred less than 10% of the time in California and 60% of the time in Florida. The apparent dependency of ducting conditions on geographic locations makes it important for Naval operations to be able to estimate occurrence and effects of ducting in various oceanic areas. As it is impractical to perform long term measurements in all oceanic areas of interest, one has to rely on available meteorological statistics. Available statistical meteorological data (from sources like the National Weather Records Center in Ashville, North Carolina) were not gathered with the accuracy one would like to describe evaporation duct parameters. However, one can hope that in the absence of any constant bias in the data the averages of long term statistical data are of sufficient quality to make reliable judgements of evaporation ducting conditions. In order to check this assumption, it was decided to perform extensive measurements during one year in a strategically important area which encounters a wide range of ducting conditions. The Mediterranean meets these conditions and two islands in the Aegean Sea were selected for the measurements. In order to encounter the full range of seasonal variations, measurements were performed in four different seasons during 1972.

II. OBJECTIVES

Perform extensive radio propagation measurements in the microwave range in the Mediterranean. Compare the measurements with calculations based on in situ meteorological measurements and long term meteorological statistics, and assess the influence of the evaporation duct on various shipboard antenna heights.

III. APPROACH

Following the approach described in reference 1, a propagation link was established between the islands of Mykonos and Naxos in the Aegean Sea. The transmitter was placed on the island of Naxos. The geographical location of the propagation path is shown in figure 1. The UTM coordinates (zone 35) for the transmitter and receiver sites were 4108.35; 355.70 and 4143.32; 351.65 respectively. The links were operated during four different periods each of which lasted for two weeks. Table 1 lists frequencies and duration of the various measurement periods. The block diagrams for transmitters and receivers are given in references 1-3. Table 2 compiles the propagation link characteristics for all five frequencies used during the Mediterranean measurements. Three vertically spaced antennas were used for L-, S-, X-, and Ku-band and two for Ka-band. Figure 2 shows the receiving terminal at Ornos Beach, Mykonos. The equipment was housed in the trailer to the left of the mast. Figure 3 shows some of the receiving equipment inside the trailer. The upper row of receivers and recorders was for L-, S-, X-, and Ku-band while the equipment of the lower shelf belonged to the Ka-band receiving system described in reference 3. Figure 4 shows the transmitting antennas at Naxos. The 3' antenna to the right radiated at L-, S-, and X-band frequencies, the 1.5' center antenna at Ku-band and the 3' antenna to the left at Ka-band frequencies. Commercial power was used during all measurement periods at Naxos and during the summer and fall periods at Mykonos. In the winter and spring periods, diesel generators were used at Mykonos.

IV. RESULTS

A. Propagation Measurements

Figures 5-134 and tables 3-62 show the results of the measurements in graphical and tabular form. The time indicated on the figures is eastern European standard time. Grouping was done by measurement period and frequency. Figures 5-11 summarize the L-band measurements for the winter period. The upper part of figure 5 gives the path loss as a function of time for the high L-band antenna. The upper parts of figures 6 and 7 show path loss for the middle and the low antennas. Two dashed reference lines in this presentation represent free space path loss and path loss due to diffraction assuming a standard atmosphere. The L-band path loss values for all three antenna heights stay close to the diffraction field value which means that the evaporation duct heights encountered have little influence on L-band frequencies. The lower part of figures 5-7 shows the path loss difference for different antenna configurations. Positive differences mean higher signals on the higher antennas and negative values higher signals on the lower antennas. In all three cases (high-low, mid-low, high mid) the higher antenna received higher signals than the lower antenna. This is what one would expect if evaporation ducting is not a significant factor influencing propagation conditions. Fading for the three antenna heights is plotted in figure 8. Fading is here defined as the maximum deviation from the mean signal during a five minute period. Rapid fluctuations were suppressed by a four second time constant in the receiver. In figure 8, fading increases with decreasing antenna height or, in other words, higher fluctuations were observed for the weaker signals. Except for path loss, the information graphically displayed in

figures 5-8 is presented in tabular form in table 3. The upper portion of this table gives the percentage of time the difference between an antenna pair exceeds a certain value in dB. As an example, signals received on the high antenna during the February measurement period exceeded those received on the low antenna by more than 15 dB during 54.5% of the time. The lower portion of table 3 lists for the three antennas the percentage of time certain fading values in dB were exceeded. As an example, the fading observed on the high antenna exceeded 3 dB during 0.6% of the time. Figures 9-11 present the statistical information in graphic form. Figure 9 shows the percentage of occurrence of path loss values in 5 dB intervals. The distribution shifts toward higher path loss values with decreasing antenna height. Fading distributions in 0.5 dB intervals are displayed in figure 10. The numerical values of figures 9 and 10 are listed in table 4. Figure 11 shows the frequency distribution of path loss difference between antennas plotted for 2 dB intervals. The path loss differences are always positive and are highest for maximum antenna separation. Table 5 contains the corresponding numerical values.

Figures 12-18 and tables 6-8 contain the S-band propagation measurements for the winter period. Path loss values as shown in the upper portions of the figures are consistently above diffraction field values which means that S-band frequencies were apparently influenced by ducting conditions. However, the path loss differences between antennas are almost always positive, i.e. received signal strength increased with antenna height. One may conclude that ducting conditions were not strong enough to cause trapping of 10 cm waves. Fading in figure 15 follows the

same trend observed at L-band frequencies, it increases with decreasing antenna height (or decreasing signals).

While L-band frequencies were apparently not affected by ducting conditions, and S-band frequencies only moderately so, there is a strong influence on propagation of X-band frequencies as evidenced in figures 19-28 and tables 9-12. The upper portions of figures 19-21 show that observed path loss values approach and even become less than the free space path loss value. Also, the differences between path loss values measured at the three different antenna heights frequently assume negative values, i.e. higher signals are observed on antennas closer to the surface. The statistical comparison of antenna performance in table 9 shows that during 49.3% of the time the high antenna observed higher signals than the low antenna. In other words, for the ducting conditions encountered during this measurement period, none of the three antenna heights showed a distince advantage over the other. Also, the fading (figure 22 and table 9) is quite similar for all antennas. Figures 23-25 show the frequency distributions of path loss, fading, and path loss differences. The spread of path loss difference values is largest for the maximum antenna separation (high-low) and smallest for the antennas which are closest to each other (mid-low). This spread is both an indication of stronger ducting effects on lower antennas and spatial decorrelation between antennas.

The format for presenting the data shown so far has been carefully chosen to provide a systems designer with the maximum information on systems performance under varying ducting conditions and the relative merits of antennas at different heights. Path loss was chosen as the primary

parameter in this format. While path loss represents an excellent quantity independent of specific systems parameters, it was realized that this very independence might limit its usefulness under specific operational circumstances. Therefore, it was attempted to translate propagation conditions into an operationally important parameter for judging radar performance. The parameter chosen was detection range. Surveillance radar performance is often described by the range a target with a specified radar cross section (e.g. one square meter) can be detected under free space propagation conditions. All of the calculations presented here assume a free space detection range of 200 nautical miles at 9.6 GHz and all detection range figures thus have units of nautical miles. The procedure for the detection range calculations is described in Appendix A. Figure 26 shows the frequency distribution of detection range calculated for the propagation conditions encountered during the winter measurement period. In the absence of any ducting the detection ranges would have been 16, 14, and 12 nautical miles for the high, middle, and low antenna respectively. Figure 26 illustrates the fact that detection ranges due to ducting are significantly extended a large percentage of the time. It also shows that extreme extensions of detection ranges are obtained for the lowest antenna under conditions of strong ducting. The mean detection ranges were 28 n miles for the high and the middle antenna and 31 n miles for the low antenna. These mean detection ranges represent range extensions compared to no ducting of 75%, 100%, and 158% for the high, middle, and low antenna respectively. Figure 27 shows the cumulative distribution of detection range. In analogy to the path loss difference presentations of figure 25, detection range differences are plotted in figure 28. The

abscissa in this presentation is in nautical miles and the graphs show the percentage of time for which one antenna exceeds the detection range of another antenna by a certain value. Positive values mean longer detection ranges for the higher antenna and negative values longer detection ranges for the lower antenna.

The spring measurements were conducted during 18 April to 1 May 1972. Power and equipment failures caused the loss of some data during the period. The path loss curves for the three L-band antennas in figures 29-31 show more variation compared to the winter period. In particular, during the second half of the spring period the signals vary between free space and diffraction values which is an indication of highly variable atmospheric refractive conditions. The higher variability is also reflected in the fading of figure 32. S-band frequencies are even more affected as seen from the path loss curves for the three antenna heights in figures 36-39. Free space values are exceeded for over 20% of the time for the high antenna, 14% for the middle antenna and 11% for the low antenna. Signal reversals between high and low antenna occurred during 4.4% of the time (table 16). Also for S-band frequencies the fading was somewhat higher than during the winter period. The path loss values measured during the spring period for X-band frequencies exceed free space values 70% of the time at the high antenna and 57% of the time at the middle and low antennas (figures 43-45). However these low path loss (or high signal) values are accompanied by strong fading (figure 46). The low antenna received higher signals than the high antenna 27.9% of the time. It is interesting to note that even though atmospheric refractive condition caused higher signals compared to the winter period,

antenna reversals occurred less frequently in the spring period than in winter. A qualitative explanation will be given later in discussion of meteorological measurements. Path loss in terms of detection range is shown in figures 50 and 51. The interval of 190-200 nautical miles in figure 50 includes all detection ranges exceeding 200 nautical miles. The mean detection ranges calculated from the presentation in figure 50 for the three antenna heights are 113 n mi. (high), 94 n mi (mid), 98 n mi (low).

The summer measurement period from 31 July - 14 August 1972 also encountered strong ducting conditions. L-band signals again varied between diffraction and free space values (figures 53-55) and exhibited deep fading during periods of high signal enhancement. During 1% of the time did the signal received on the low antenna equal or exceed that received on the high antenna (table 23). S-band signals (figures 60-62) during this period were consistently enhanced and exceeded the free space path loss value a significant portion of the time. The low antenna received equal or higher signals than the high antenna during 8.6% of the time (table 26). The most dramatic effect of the ducting conditions during the summer measurement period was experienced for X-band frequencies. Signals on the lower antenna fell below free space values only 7% of the time which is an indication of unusually persistent ducting conditions. Signals received on the lower antenna equaled or exceeded those received on the higher antenna 93% of the time. Figure 70 shows a decrease of fading with antenna height which may be interpreted as a result of more complete trapping of energy for the lower antenna. The higher signals on the low antenna are of course reflected in longer detection ranges of

figures 74 and 75. The median detection range for the high antenna is 40 n mi, for the middle antenna 70 n mi, and 148 n mi for the low antenna. (Median rather than mean detection range was used because of the large number of cases in the 200 n mi and above category). During the summer period an additional frequency (Ku-band) was added to the propagation link and the path loss values are shown in figures 77-79. Using free space path loss values as a reference, Ku-band is less enhanced than X-band which may be an indication that ducting is accompanied by losses from rough boundaries. Figure 80 also shows that deep fading was encountered for all antenna heights.

The last measurement period during fall (5-21 November 1972) gave for L-band frequencies quite similar results compared with the winter period. Path loss values (figures 84-86) are generally around diffraction field values and show little variation apart from a brief period around 16 November. Path loss values for S-band (figures 91-93) show a greater variation, occasionally even exceeding free space and diffraction values. Also X-band signals were quite variable (figures 98-100). Signals on the lower antenna equaled or exceeded those received on the high antenna during 14.2% of the time. The mean detection ranges were 47, 46 and 42 n mi for the high, middle, and low antenna respectively. The path loss values for Ku-band are shown in figures 108-110. The lower antenna received equal or higher signals compared to the high antenna during 56.5% of the time. An additional frequency in Ka-band (37.44 GHz) was added to the propagation link in the fall measurement period. This frequency extension into the mm-wave band provided some interesting insight into frequency dependency of

ducting. While ducting should increase with increasing frequency, absorption and roughness of the boundaries (noteably sea surface roughness) became more important for higher frequencies. Therefore, not all of the signal enhancements expected from ducting will be realized. Estimates of signal losses due to atmospheric absorption and sea surface roughness are given in reference 4. The path loss values for Ka-band shown in figures 115 and 116 (only two antenna heights at 8.6 and 3.6 m above msl were used) do not reach or exceed free space values as it was observed for X- and Ku-band frequencies. Nontheless, the received signal levels were consistently high and most of the time within 30-65 dB above the value one would expect without ducting. Figure 115 shows path loss as a function of time for the receiving antenna located at 8.6 m above msl. The received signal levels are consistently above the diffraction values, most of the time 30-45 dB, but not quite as high as the signals on the lower antenna. A comparison of the signal levels of the two vertically spaced receiving antennas shows that the lower antenna receives higher signals a larger percentage of the time. The difference in the path loss values is plotted in figure 115. The zero level on the ordinate represents equal power on both antennas. Positive values indicate higher signals on the higher antenna and negative values higher signals on the lower antenna. The information in figure 115 is also expressed in table 49 which gives the percentage of time the path loss difference received on the two antennas exceeds a certain value. For example, the higher antenna received signals at least 10 dB larger than the lower antenna 1.8% of the time; likewise, the lower antenna exceeded the signal levels received on the higher antenna 65.7% of the time. Figure 117 shows the fading observed on both receiving antennas. Fading is here defined as maximum peak

to peak deviation from the mean signal level during a 7.5 minute interval. Again a four second time constant at the recorder suppressed rapid fluctuations. Table 49 also lists the percentage of time fading exceeds certain dB values. The percentages for the lower antenna are slightly less than for the higher antenna. The lesser fading on the lower antenna may be explained by the more complete trapping of electromagnetic energy close to the water surface. The path loss information of figures 115 and 116 may be represented as a frequency distribution for path loss intervals. This is done in figure 118 for 5 dB intervals. The antenna labelled "mid" is the one at 8.6 m, the one labelled "low" at 3.6 m above mean sea level. The distribution curve for the lower antenna is shifted toward the left for lower path loss values (higher signals) compared to the higher antenna. Table 50 contains the numerical values plotted in figure 118. The frequency distributions of path loss difference between the two vertically spaced antennas and the fading for each antenna are shown in figure 119, the corresponding numerical values are listed in table 51.

The foregoing description of propagation conditions encountered during four observational periods distributed over one calendar year underlined the strong variability of ducting conditions. As mentioned earlier, one objective of this measurement program was to encounter a wide range of evaporation ducting conditions. Another objective was an attempt to gather enough information to permit a comparison of the data with long term meteorological statistics. To facilitate such a comparison, the data were averaged for all seasons. Figure 190 shows the frequency distributions of path loss for the three L-band antennas. Likewise, fading and path loss differences between

antennas are averaged in figures 121 and 122. The corresponding numerical values are listed in tables 52 and 53. The S-band data are averaged in figures 123-125 and tables 54 and 55. Table 56 shows the percentage of time path loss differences between high and low X-band antennas exceed certain dB values. For example, for all seasons combined, signals received on the high antenna exceeded those received on the low antenna during 52.6% of the time. During 20% of the time the signal received at the low X-band antenna exceeded that received at the high antenna by 10 dB. The frequency distributions of path loss for X-band in figure 126 show again the wider spread for the low antenna. The detection ranges for the hypothetical 200 n mi free space detection range radar are shown in figures 129 and 130. The mean detection ranges calculated from this presentation are 60, 61, and 79 n mi for the high, middle, and low antenna respectively. Figures 132-134 show the Ku-band data averaged for the summer and fall season.

B. Meteorological Comparisons

Three aspects were pursued in the meteorological phase of the program. First, the complex processes in the oceanic boundary layer demand sophisticated measurements for their detailed description; however, only simple meteorological measurements can be performed under operational conditions and only simple meteorological measurements are routinely performed by meteorological offices around the world. Therefore, the assessment of evaporation ducting effects on radio propagation becomes practical only if simple measurements can be used to estimate ducting phenomena. For this reason, it was decided to use routinely obtained data from a meteorological station of the Greek Weather Service on Naxos. The data consisted

of surface temperature and humidity measurements taken every three hours and water temperatures measured twice daily. Figures 135-146 show the air-sea temperature difference, air temperature, relative humidity, wind speed, and duct height calculated from these measurements for the four measurement periods. Duct height δ was calculated according to the following formulas (log-linear profile):

$$\delta = -\left[\frac{0.0013\left(\ln\frac{z_1}{z_o} + \frac{z_1}{L'}\right)}{\phi_A - \phi_S} + \frac{\alpha}{L'}\right]^{-1} \text{cm}$$

$$\phi_A = \frac{77.6}{T_A}\left[1000 + \frac{4810}{T_A}\, e\right]$$

$$\phi_S = \frac{77.6}{T_{SW}}\left[1000 + \frac{4810}{T_{SW}}\, e_{SW}\right]$$

$$L' = \frac{\dfrac{(u \cdot 51.4444)^2}{980(T_A - T_{SW})/T_{SW}} - \alpha z_1}{\ln(z_1/z_o)} \text{ cm}$$

z_1 = 500 cm

z_o = 0.0015 cm

α = 2.0

u = wind speed in knots

T_A = air temperature in Kelvin

T_{SW} = sea water surface temperature in Kelvin

e = partial vapor pressure in mb

e_{SW} = saturated vapor pressure at sea surface in mb

Conditions of thermal stability with bulk Richardson's numbers exceeding 0.1 were eliminated for duct height calculations. Bulk Richardson's number is given by

$$R_{ib} = 6.4 \frac{T_A - T_{SW}}{u^2}$$

T in Kelvin, u in knots

The meteorological measurements at Naxos have several limitations. They are measured over land and may not be representative of open sea conditions, being measurements taken at one point they do not permit any statement about the horizontal extent of ducting conditions, and they do not include elevated refractive layers which may affect propagation conditions. These potential error sources were addressed in the second aspect of the meteorological program. During the fall measurement period a meteorological ground station was established at the receiver site in Mykonos and measurements shown in figures 147 and 148 were taken similar to the ones at Naxos. Figure 149 shows duct heights calculated from the Naxos and the Mykonos measurements. Duct heights for both places agree remarkably well considering the serious short-comings pointed out earlier. Both the questions of horizontal homogeneity and duct heights over open water were investigated by performing measurements from a small fishing

boat traveling along the propagation path. Duct heights were calculated from sea water temperate, air temperature, relative humidity, and wind speed measurements using the above formulas. Figures 150-156 show duct heights versus range. The measurements at the end points of the propagation path (asterisks) are the previously described data from Naxos and Mykonos. Date and time interval during which the measurements were performed are marked on the figures (EEST = eastern European standard time). In general ducting conditions appeared horizontally homogeneous. Duct height changes which were observed may have been temporal rather than spatial changes as the measurements along the path extended for several hours. Figure 157 shows a comparison between duct heights measured at Mykonos, Naxos, and along the path. The dotted areas represent the range of duct heights measured along the path for the time during which the measurements were taken. The agreement between the various duct heights is, again, considered excellent. During the fall measurement period radiosondes were launched from the receiver station at Mykonos. This was done to check for the presence and influence of elevated layers. The radiosondes (403 MHz system) were tracked optically for wind information. No significant layers were observed that occurred low enough to influence propagation conditions along the Naxos - Mykonos path. The individual profiles are included in Appendix B.

Figures 158-161 are overlays of measured path loss values for the low X-band antenna in each of the four measurement periods and duct heights calculated from the Naxos meteorological data. In general, there is an excellent agreement in the trend between path loss and duct height. The

agreement is particularly good for the winter and fall periods. The agreement in the trend between duct heights and path loss might be improved by using different models to calculate duct height for thermally stable and unstable conditions. Those models are described in reference 5. Figure 162 shows the measured path loss for the low X-band antenna during the fall period and path loss values calculated from the Naxos duct height (indicated by circles). The relationship between duct height and path loss for the geometry under consideration shown in figure 163, has been calculated with NELC's full wave solution wave guide computer program which will be described in a report which is presently under preparation. The general agreement between calculated and measured path loss values in figure 162 is very good if one considers the shortcomings of the meteorological measurements. The correlation coefficient between calculated values and corresponding measured values was claculated to be 0.63. If one eliminates in this comparison duct heights associated with wind speeds of less than 5 knots, the correlation coefficient increases to 0.71. (The elimination of duct heights for wind speeds less than 5 knots may be justified on the basis that wind measurements in this range are quite unreliable but may have a strong influence on atmospheric stability and duct height). Both correlation coefficients 0.63 and 0.71 are significant at the 99% level. This means there is only a 1% probability that the data are actually uncorrelated. One may conclude that the comparison between the meteorological and radio data shows that simple in situ meteorological measurements are quite adequate to estimate propagation conditions.

The third aspect of the meteorological phase of this program was to check the usefulness of available long-term meteorological statistics to predict radio propagation conditions. Only if this can be done, can successfull predictions of ducting conditions be made without actually performing extensive measurements. Figure 164 is the frequency distribution of duct height based on five years of meteorological averages and the duct height distributions based on the Naxos meteorological measurements taken during the four measurement periods in 1972. The agreement between the two distributions is considered quite good. These duct height distributions may also be used to estimate antenna reversals, i.e., the percentage of time the low antenna receives equal or higher signals than the high antenna. From a family of height-gain functions generated with the previously mentioned waveguide program it was concluded that reversals would be expected for duct heights between 10 and 30 m. Table 62 shows that for individual seasons calculated and measured values may differ appreciably. One really would not expect a specific two week period to be identical with a five year seasonal average. However, all measured data averaged (thereby forming a larger sample size) compare quite favorably with the average for the entire five year period. Based on these and similar previous comparisons for the California off-shore area (reference 1), one may conclude that long term meteorological statistics are quite useful in estimating average ducting conditions for oceanic areas.

V. CONCLUSIONS

Extensive radio propagation measurements in the Mediterranean have shown that evaporation ducting is an important phenomenon in particular for frequencies above S-band. For example, signal enhancements from evaporation ducting have been measured 99% of the time for X-band frequencies. It was determined that the evaporation duct strongly affects all shipboard antenna heights. Under conditions of strong ducting, low sited antennas (e.g. 15 feet above mean sea level) may receive higher signals than more conventional antenna heights (e.g. 60-70 feet above msl). For all measurements in the Mediterranean the low sited X-band antenna received equal or higher signals than the high antenna 47.4% of the time. During 20% of the time signals received at the low sited X-band antenna exceeded those received on the high sited antenna by 10 dB. From the measurements one may conclude that the optimum location for an antenna is high on the ship. When economics justify two antennas, an advantage can be obtained with both a high and low antenna.

The evaporation ducting effect appears to have a broad maximum in the X- to Ku-band frequency range. Atmospheric absorption and sea surface roughness apparently counteract the effectiveness of the duct expected at higher frequencies.

Simple meteorological measurements were found to be quite sufficient to describe ducting conditions. Horizontal homogeneity of the duct was found to be good for the propagation path used in this investigation. Ducting effects deduced from long term meteorological averages compared well

with the average of all measurements for the year permitting estimates of average ducting conditions to be made for any oceanic area for which such statistical meteorological data are available.

VI. RECOMMENDATIONS

The path loss information obtained from the propagation measurements had been translated in this report into detection range information for X-band. Hypothetical radar parameters were assumed for this purpose. Target height versus detection range plots for various ground based duct heights can be generated for actual radars (reference 6). Those curves could be easily used under operational conditions in connection with simple meteorological measurements performed on board ship and in connection with duct height distributions calculated from long term meteorological averages. It is, therefore, recommended to apply this technique to a suitable surface surveillance radar (e.g. SPS - 55) and conduct an evaluation under operational conditions.

VII. REFERENCES

1. Richter, J. H. and H. V. Hitney, "Antenna heights for optimum utilization of the oceanic surface evaporation duct", Part I: Results from the Pacific measurements, NELC TN 2031, 4 May 1972.

2. Richter, J. H. and H. V. Hitney, "Antenna heights for optimum utilization of the oceanic surface evaporation duct", Part II: Results from the Key West measurements, NELC TN 2371, 10 May 1973.

3. Richter, J. H., H. V. Hitney, K. D. Anderson, and M. L. Phares, "Propagation measurements of 37 GHz in the oceanic surface evaporation duct", NELC TN 2422, 3 July 1973.

4. Hitney, H. V., "Propagation Calculations of 37 GHz in the oceanic evaporation duct", NELC TN 2421, 3 July 1973.

5. Jeske, H., "The state of radar-range prediction over sea", AGARD Conference Proceedings No. 70, Part II, p. 50.1 - 50.10, February 1971.

6. Hitney, H. V., "The influence of the oceanic surface evaporation duct on detection range for a 3.3 GHz radar", NELC TN 2322, 15 March 1973.

VIII. FIGURES

PAGE

PAGE

PAGE

ALL SEASONS COMBINED

PAGE

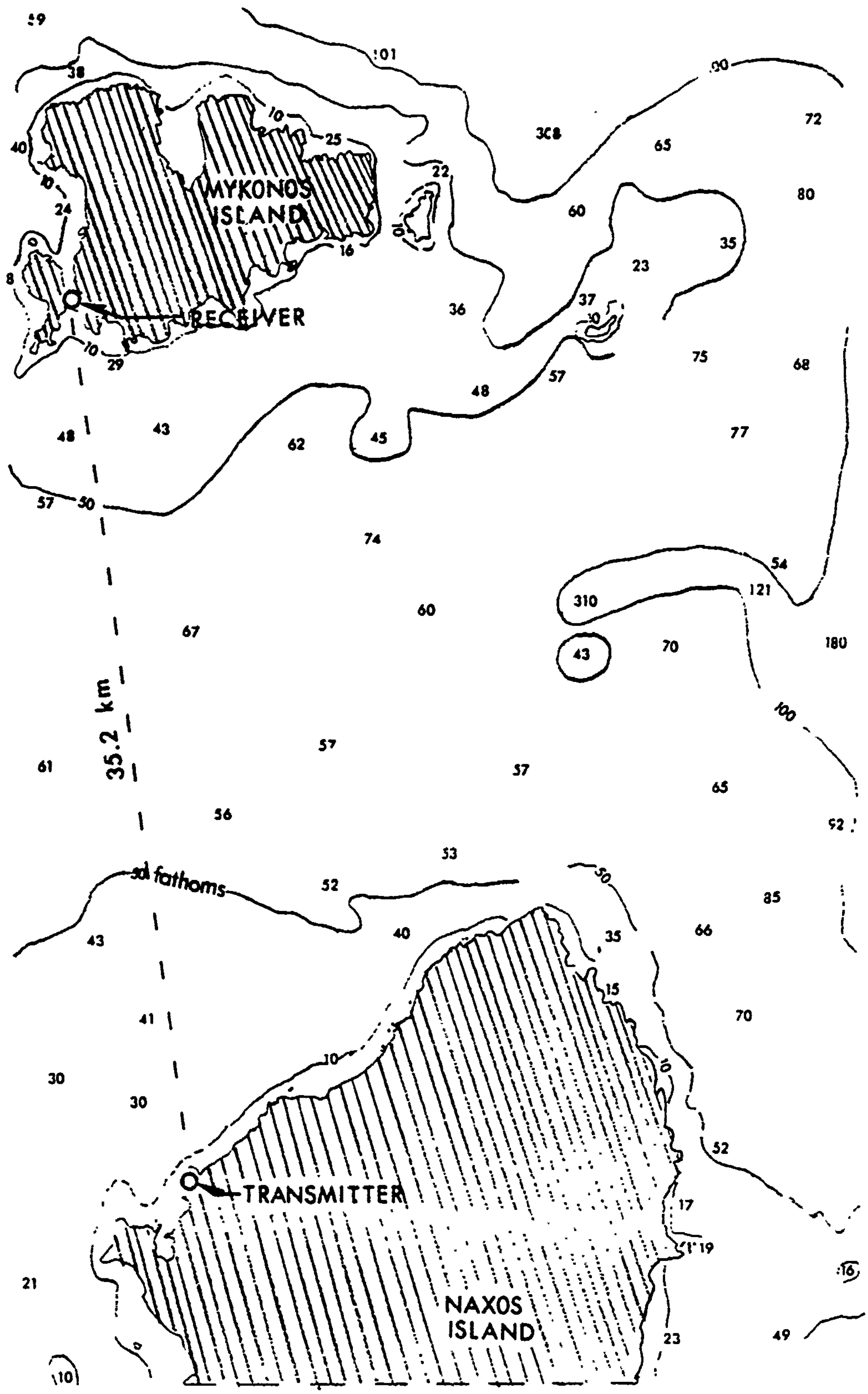

Figure 1. Geographic location of propagation path

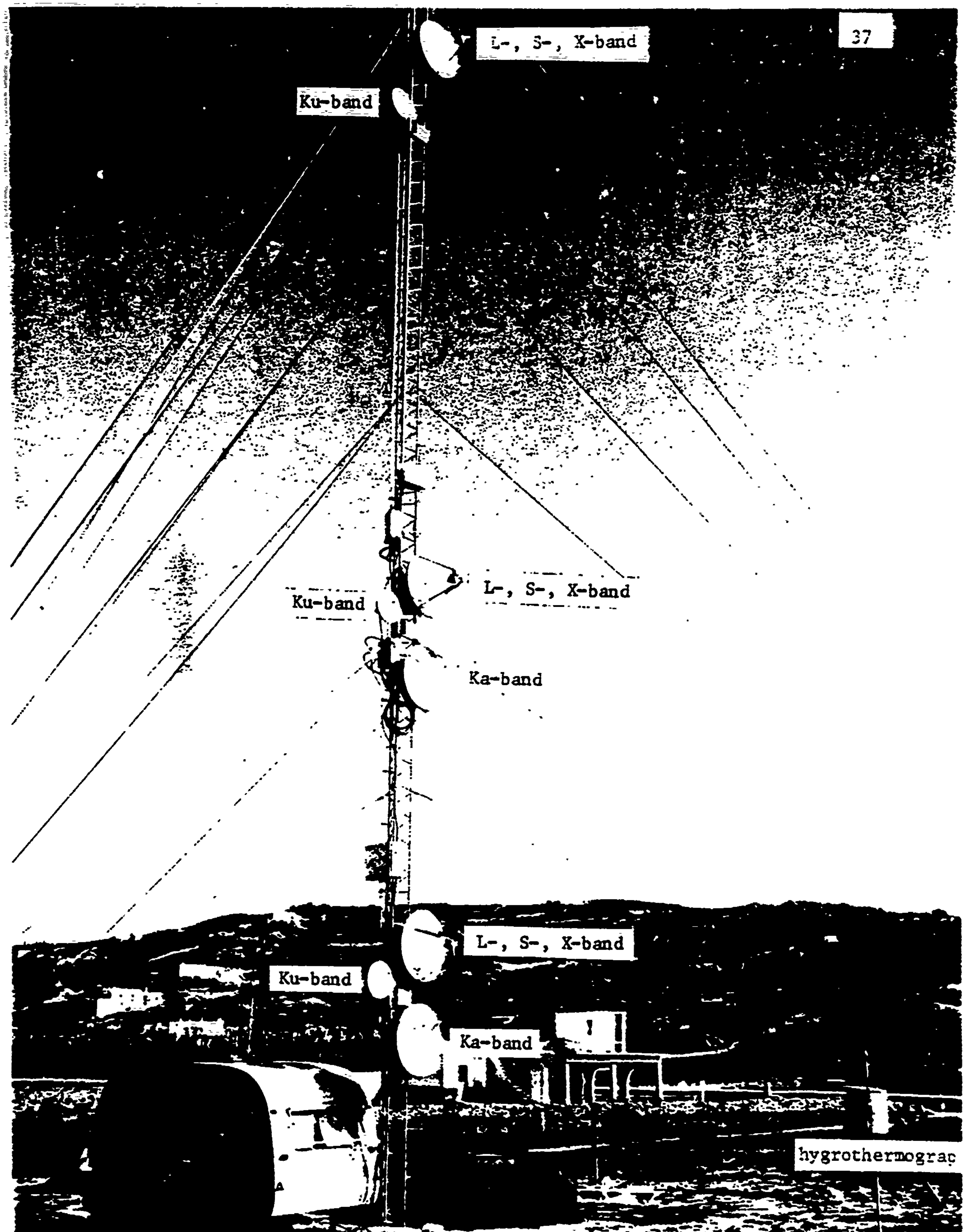

Figure 1. Receiving terminal at Ornos Beach, Mykonos

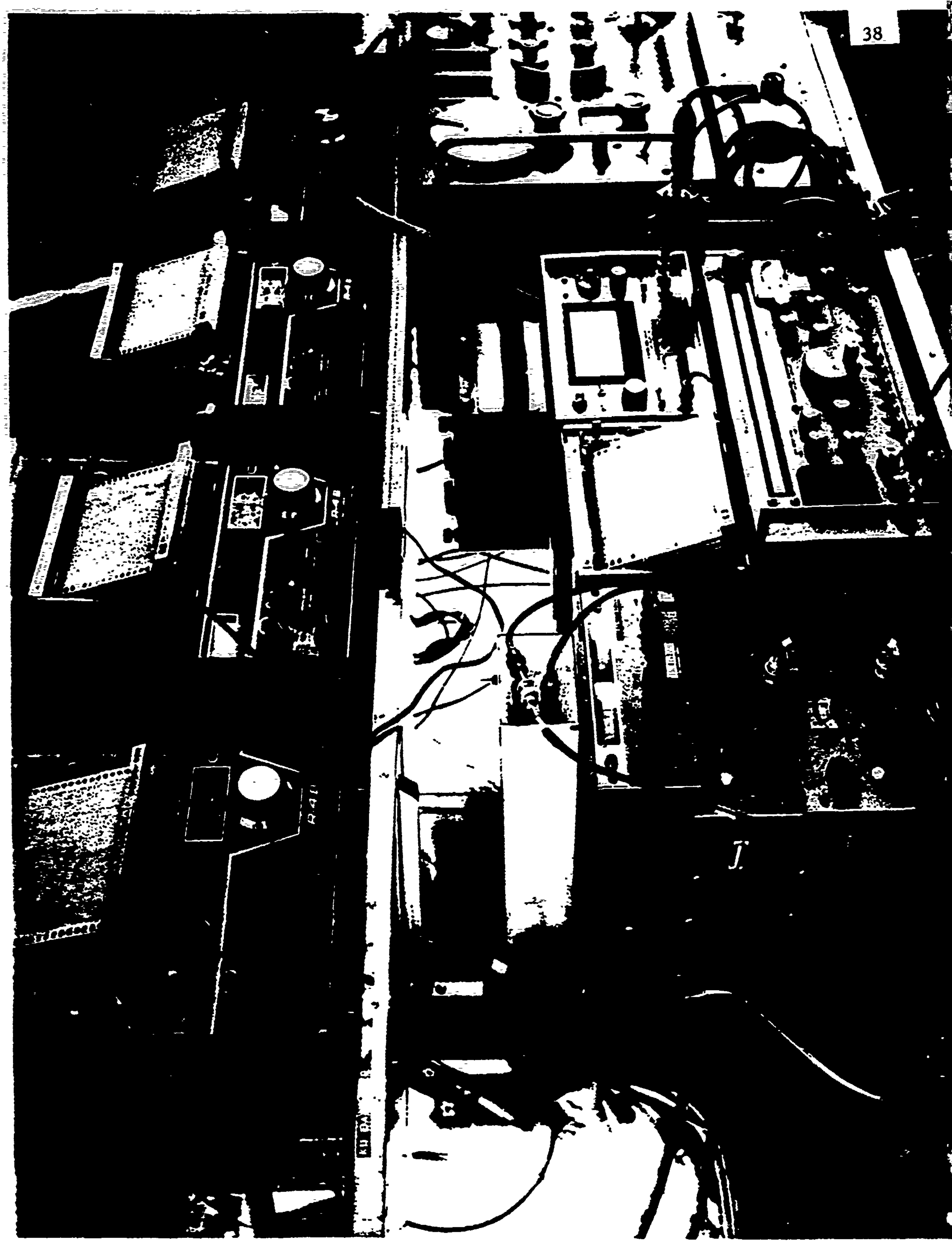
38

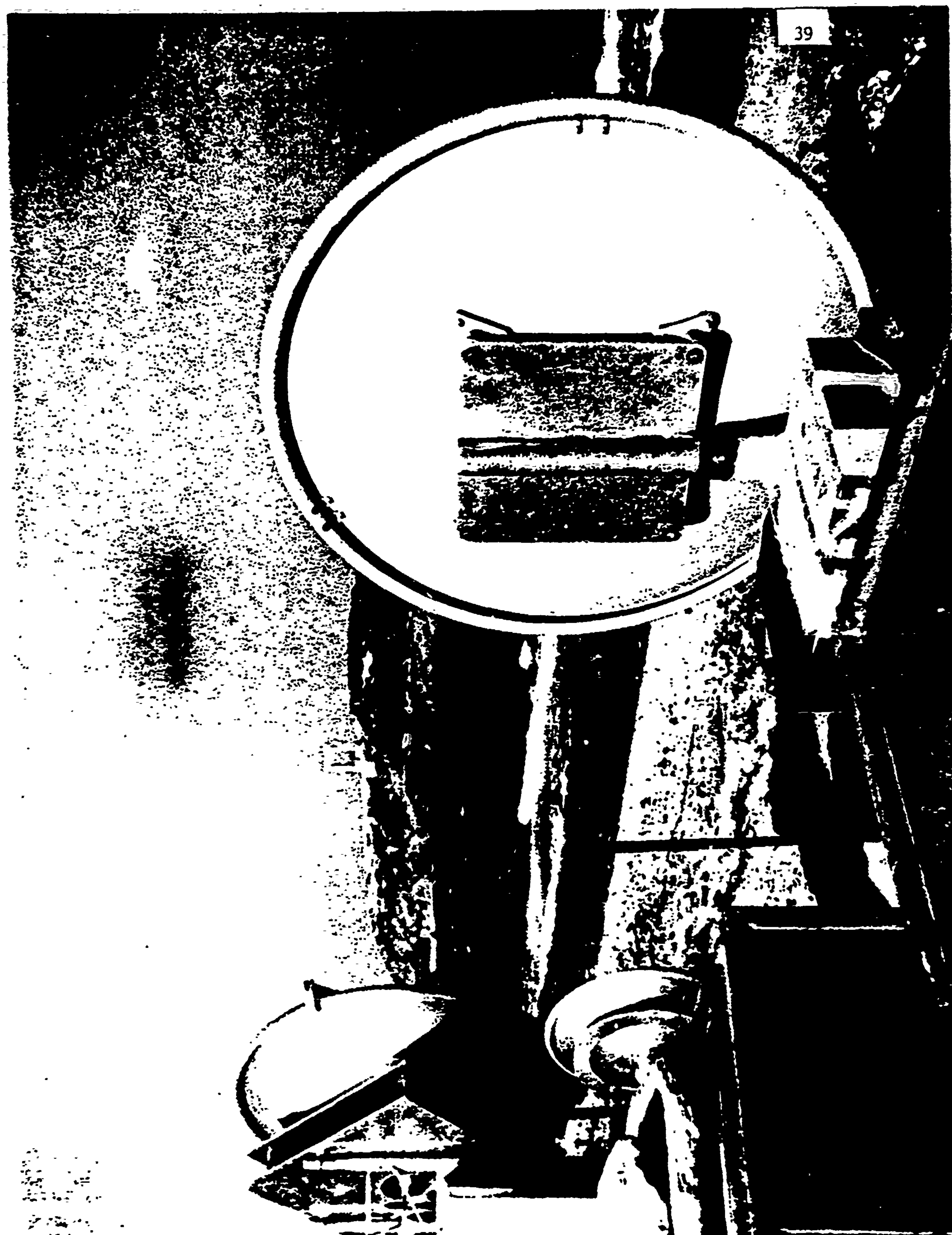
39

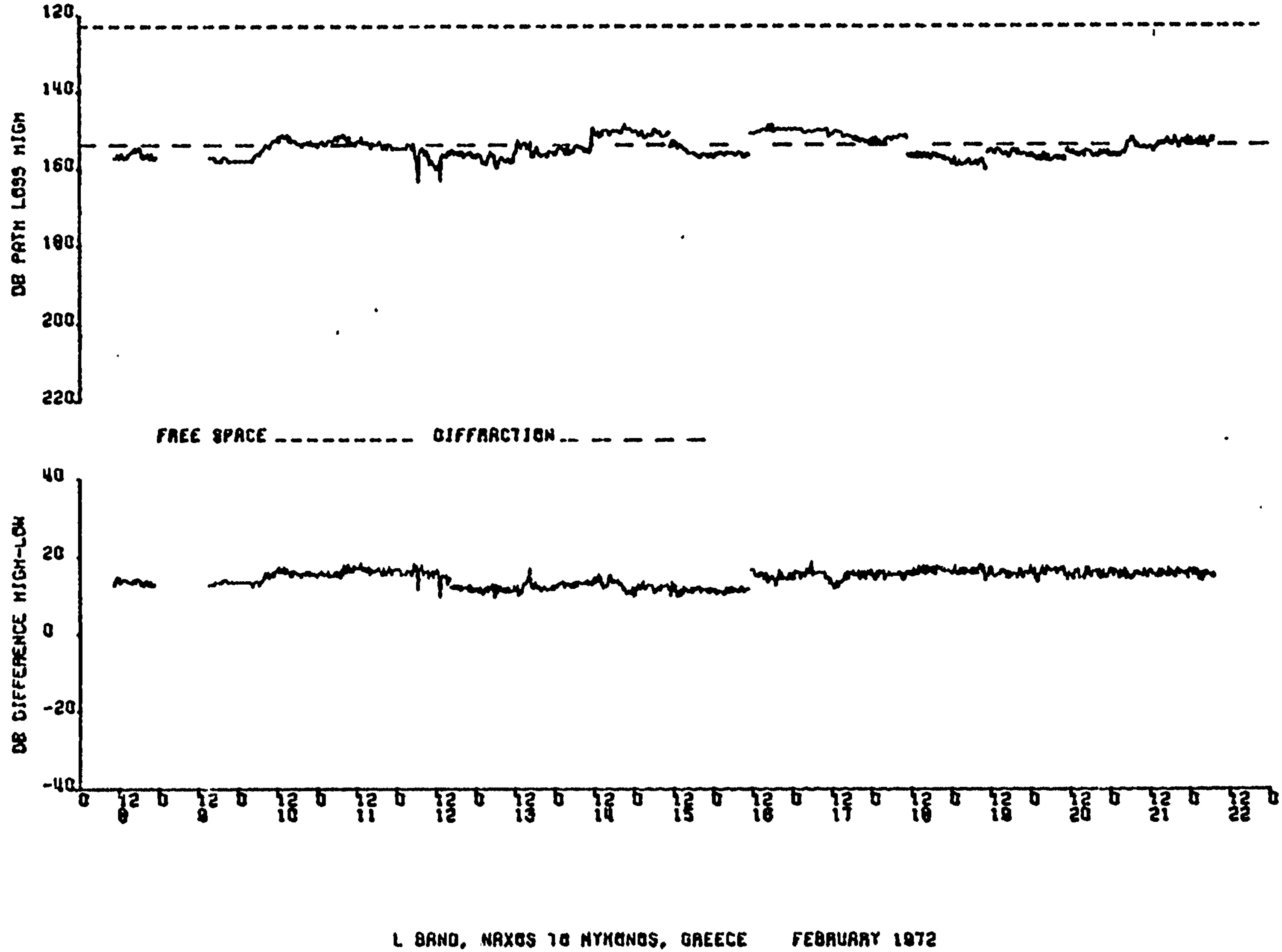

Figure 5. Path loss for high L-band antenna and path loss difference high-low antenna

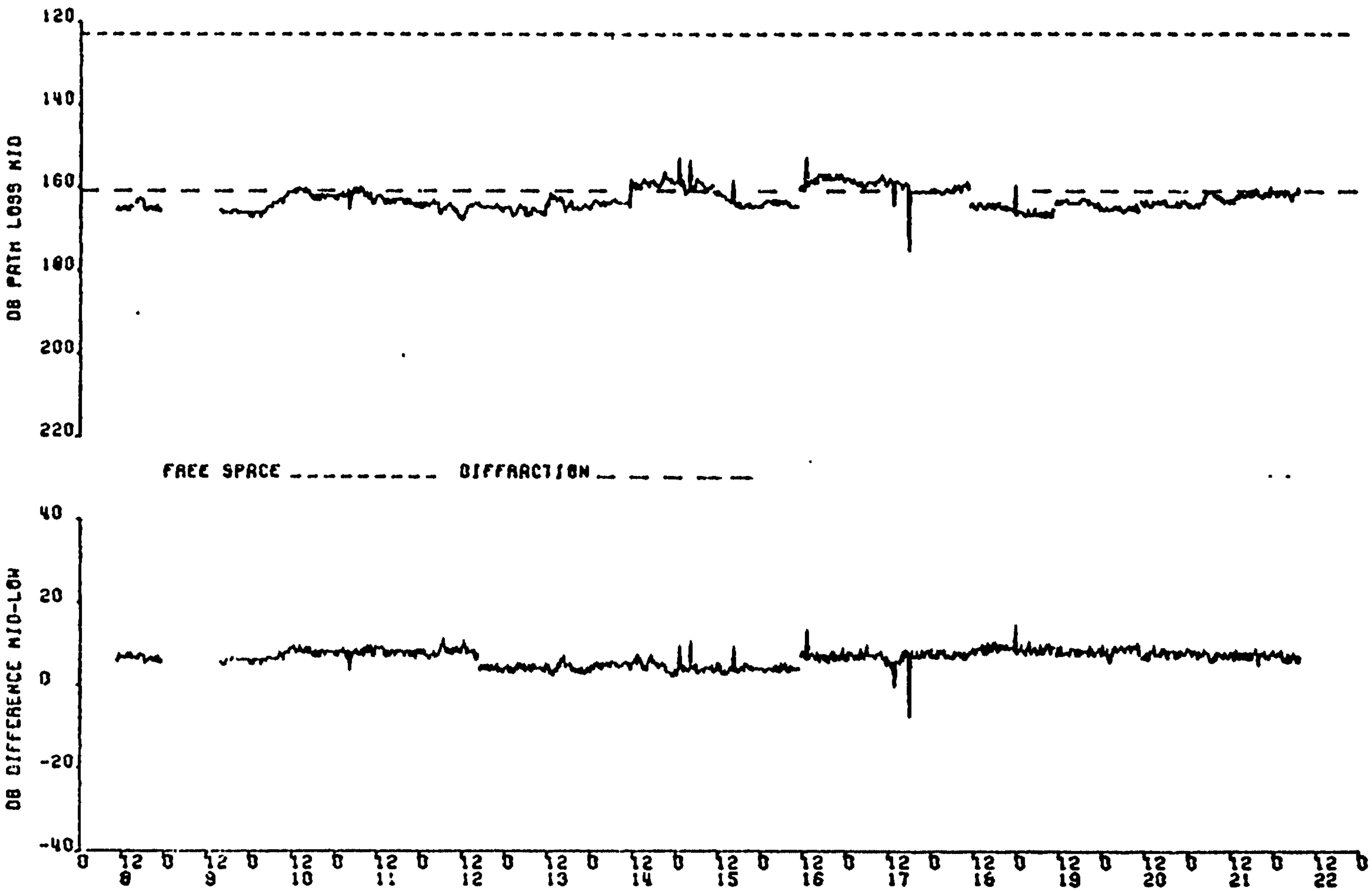

L BAND, NAXOS TO MYKONOS, GREECE FEBRUARY 1972

Figure 6. Path loss for middle L-band antenna and path loss difference mid-low antenna

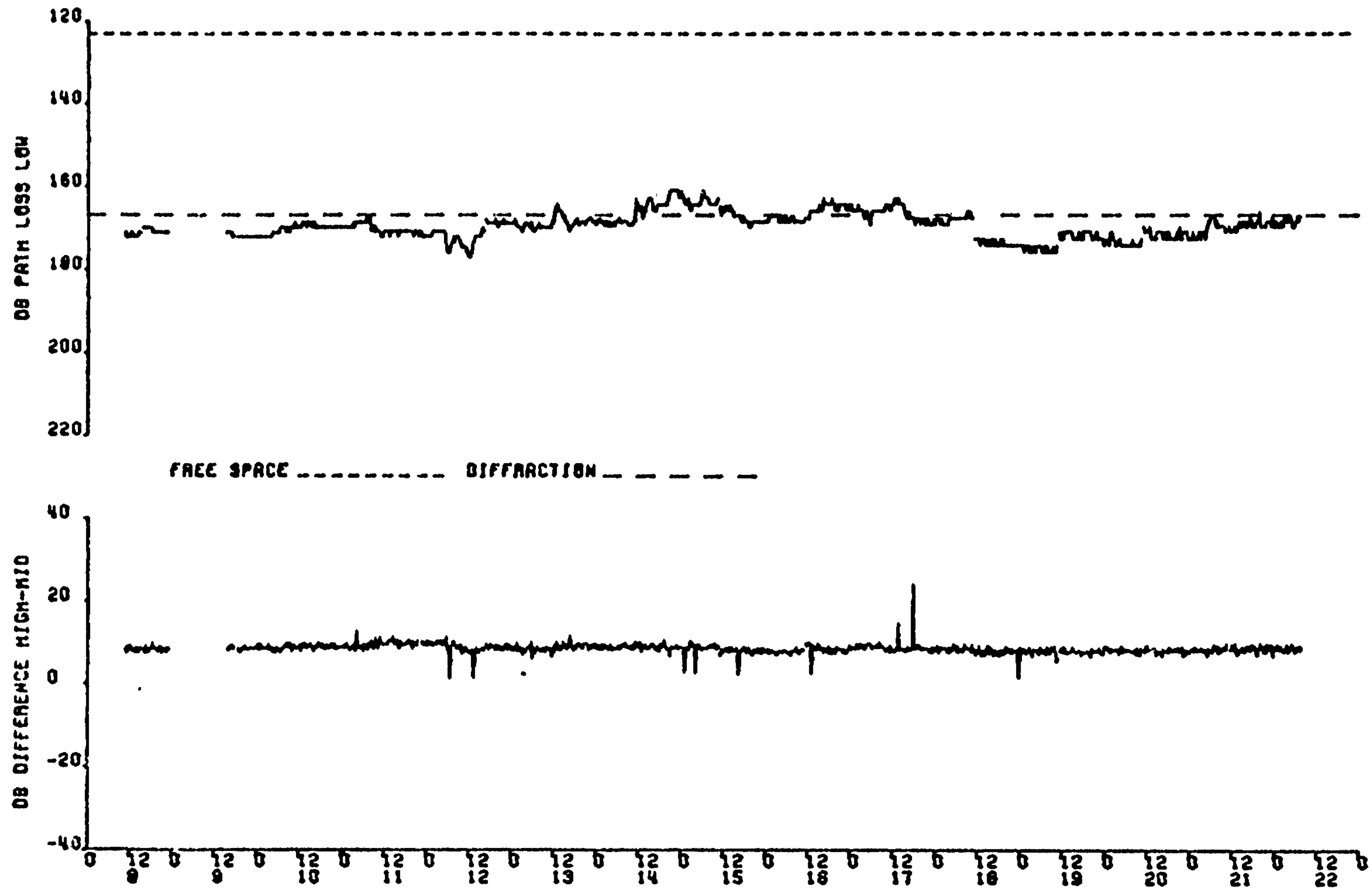

L BAND, NAXOS TO MYKONOS, GREECE FEBRUARY 1972

Figure 7. Path loss for low L-band antenna and path loss difference high-mid antenna

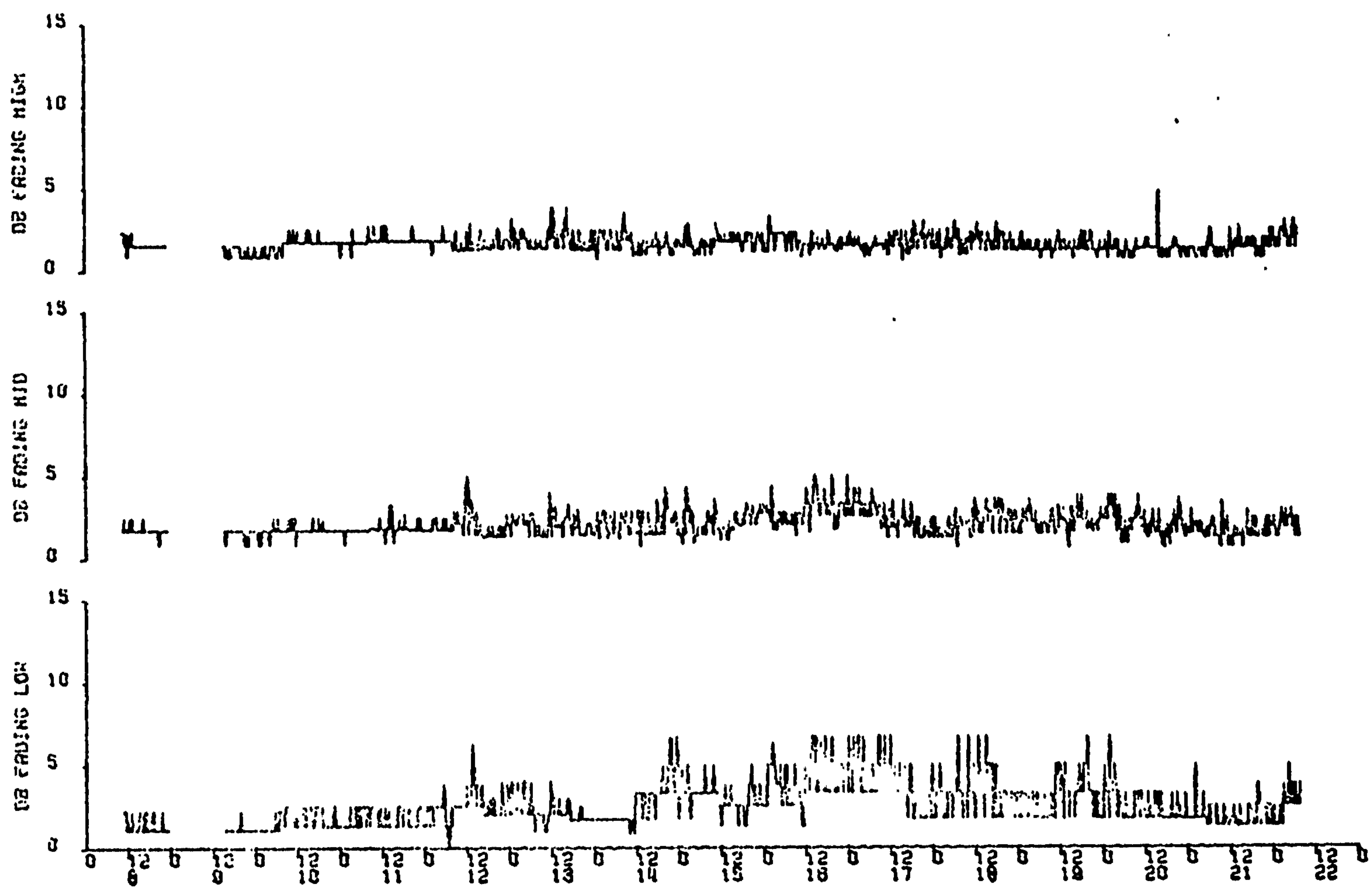

L BAND, NAXOS TO MYKONOS, GREECE FEBRUARY 1972

Figure 8. Fading L-band

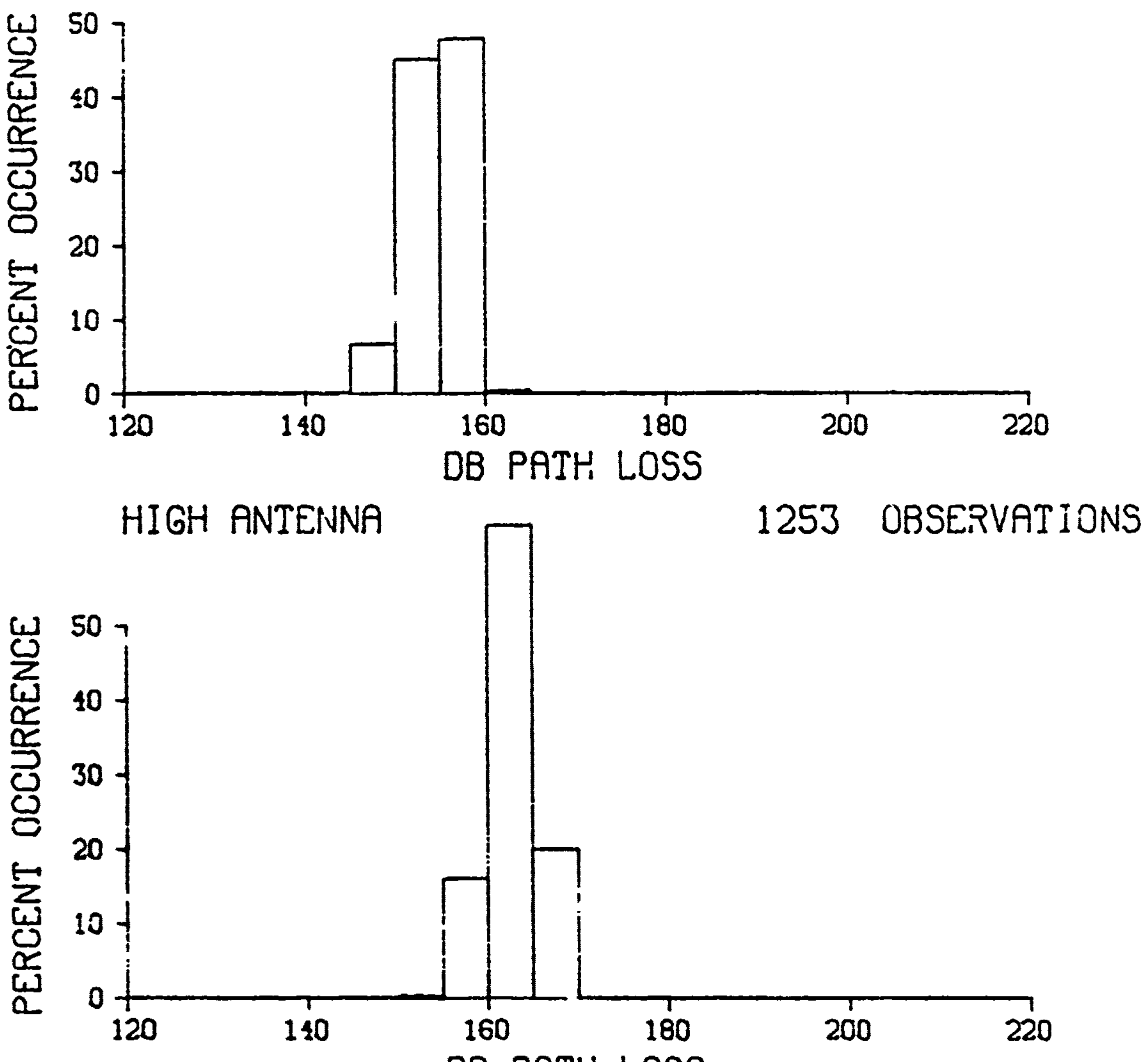

Figure 9. Frequency distributions of path loss for L-band

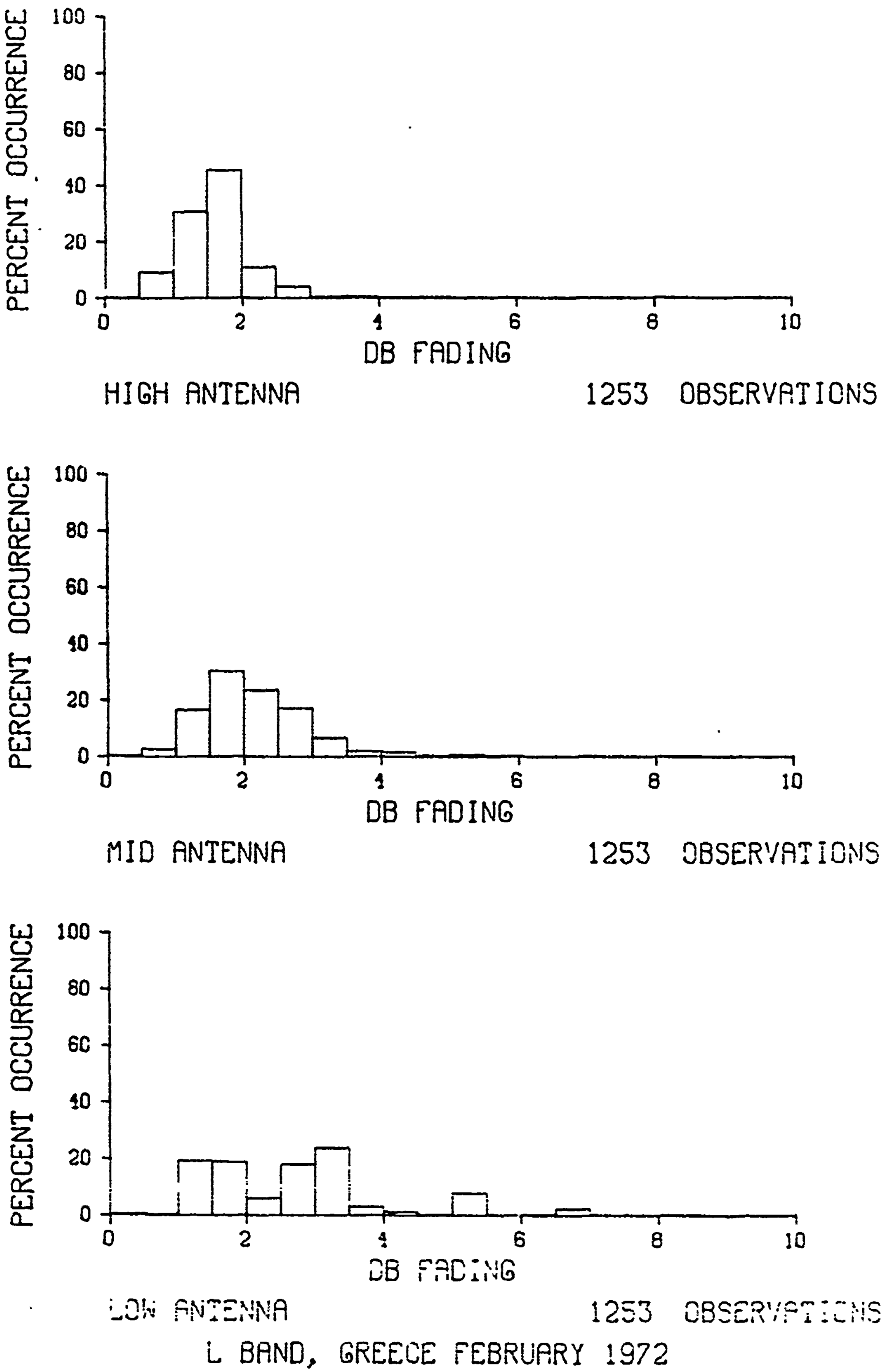

Figure 10. Frequency distributions of fading L-band

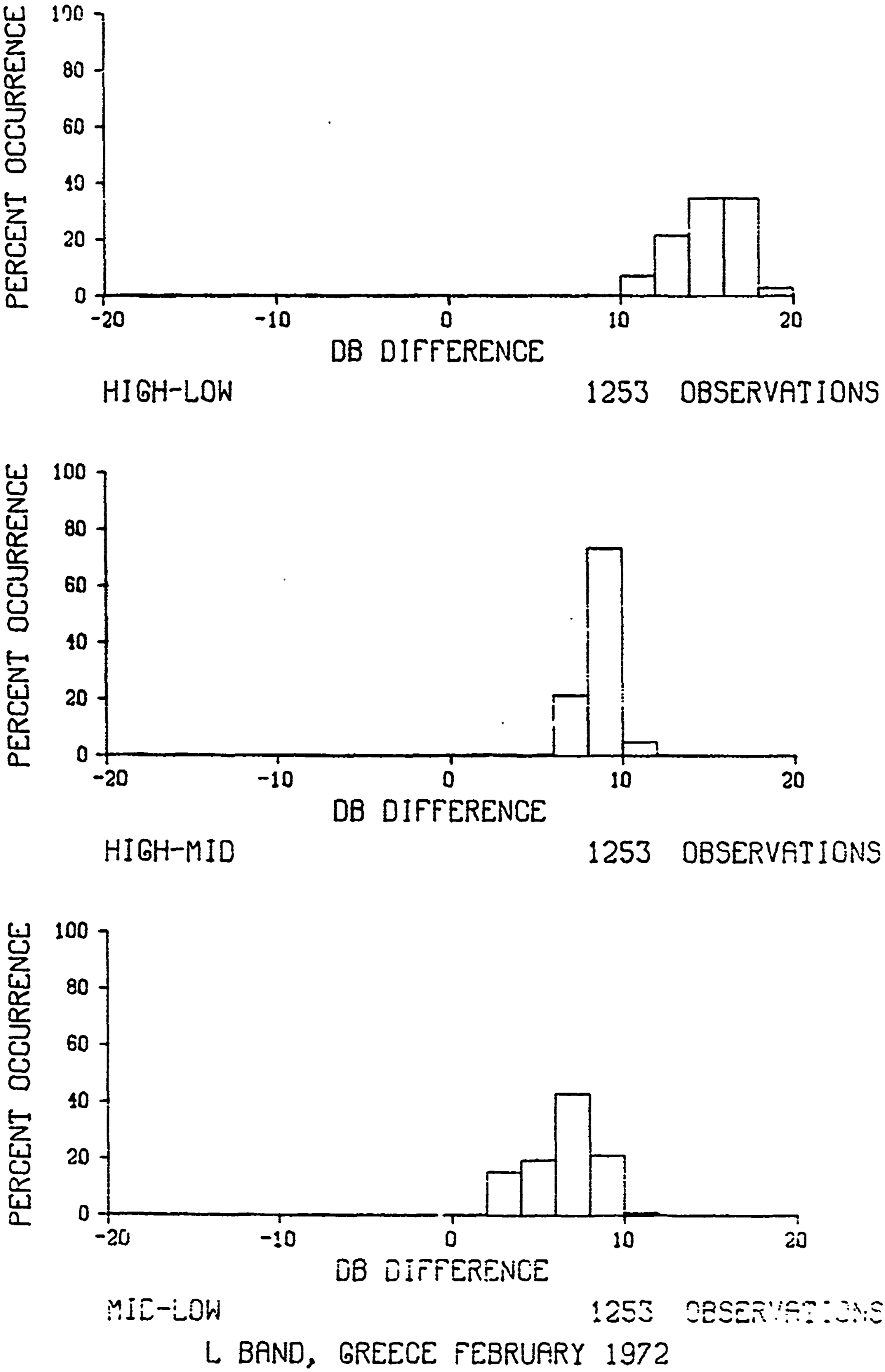

Figure 11. Frequency distributions of path loss differences between antennas for L-band

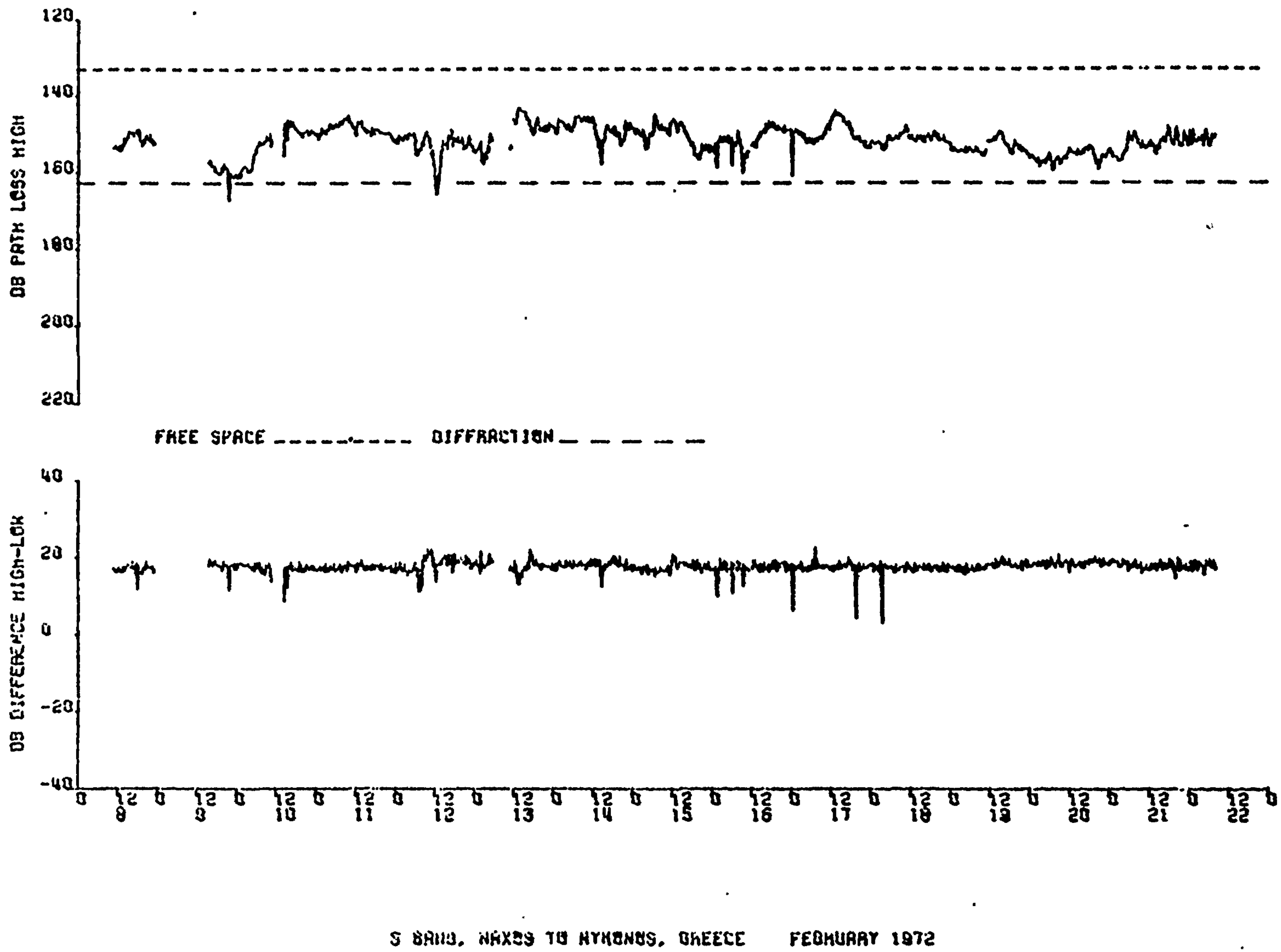

Figure 12. Path loss for high S-band antenna and path loss difference high-low antenna

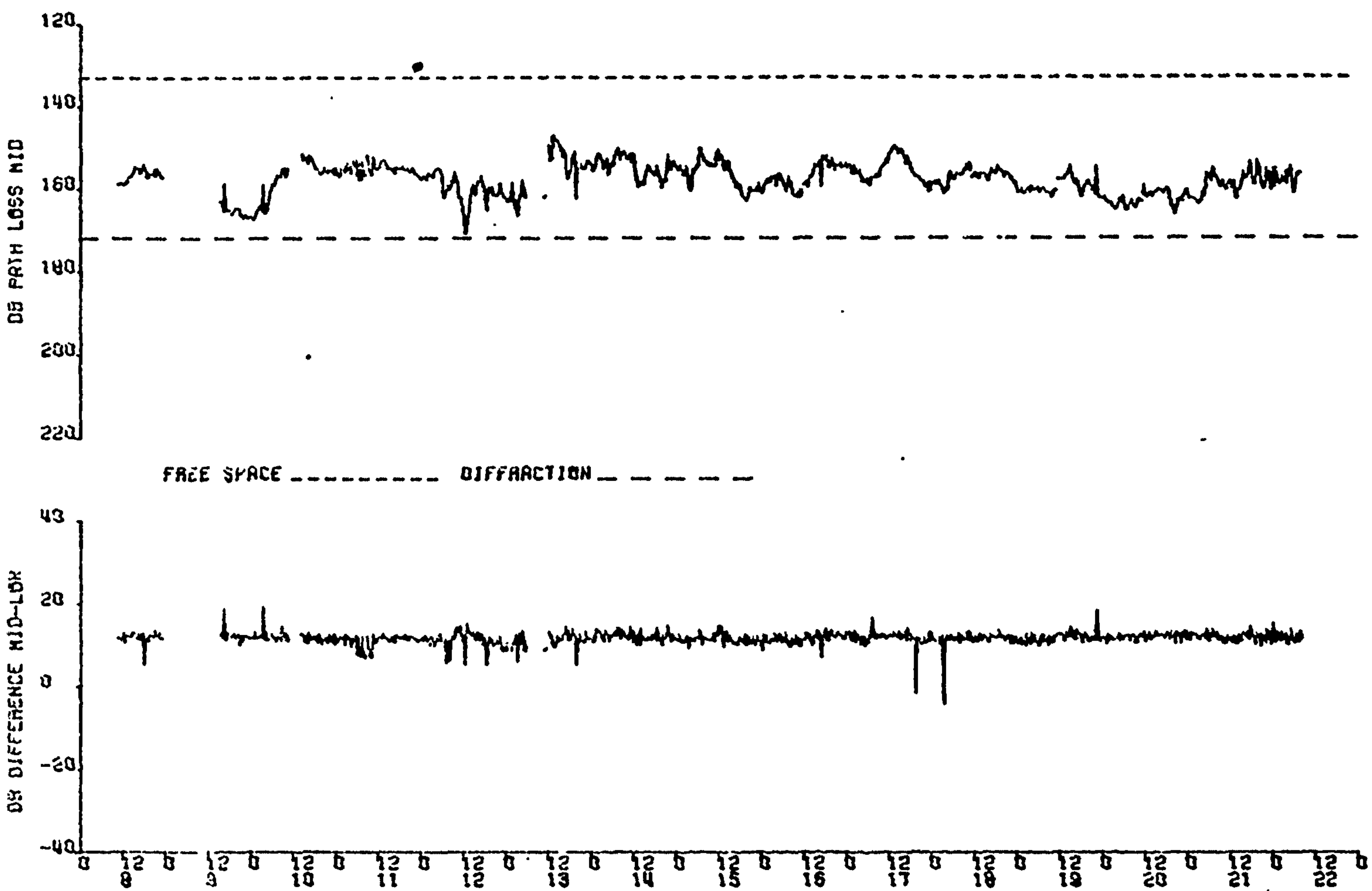

S BAND, NAXOS TO MYKONOS, GREECE   FEBRUARY 1972

Figure 13. Path loss for middle S-band antenna and path loss difference mid-low antenna

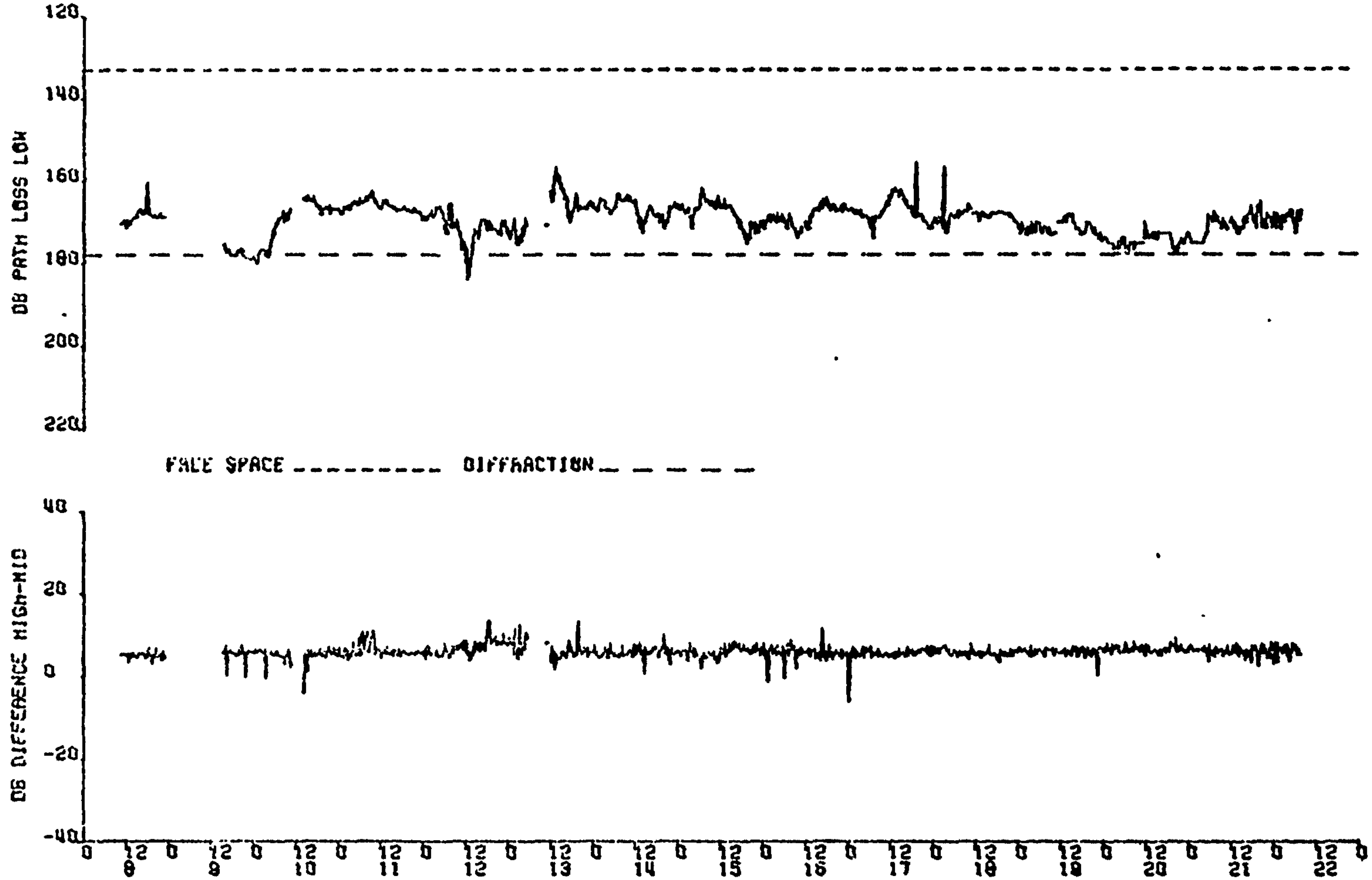

S BAND. NAXOS TO MYKONOS, GREECE FEBRUARY 1972

Figure 14. Path loss for low S-band antenna and path loss difference high-mid antenna

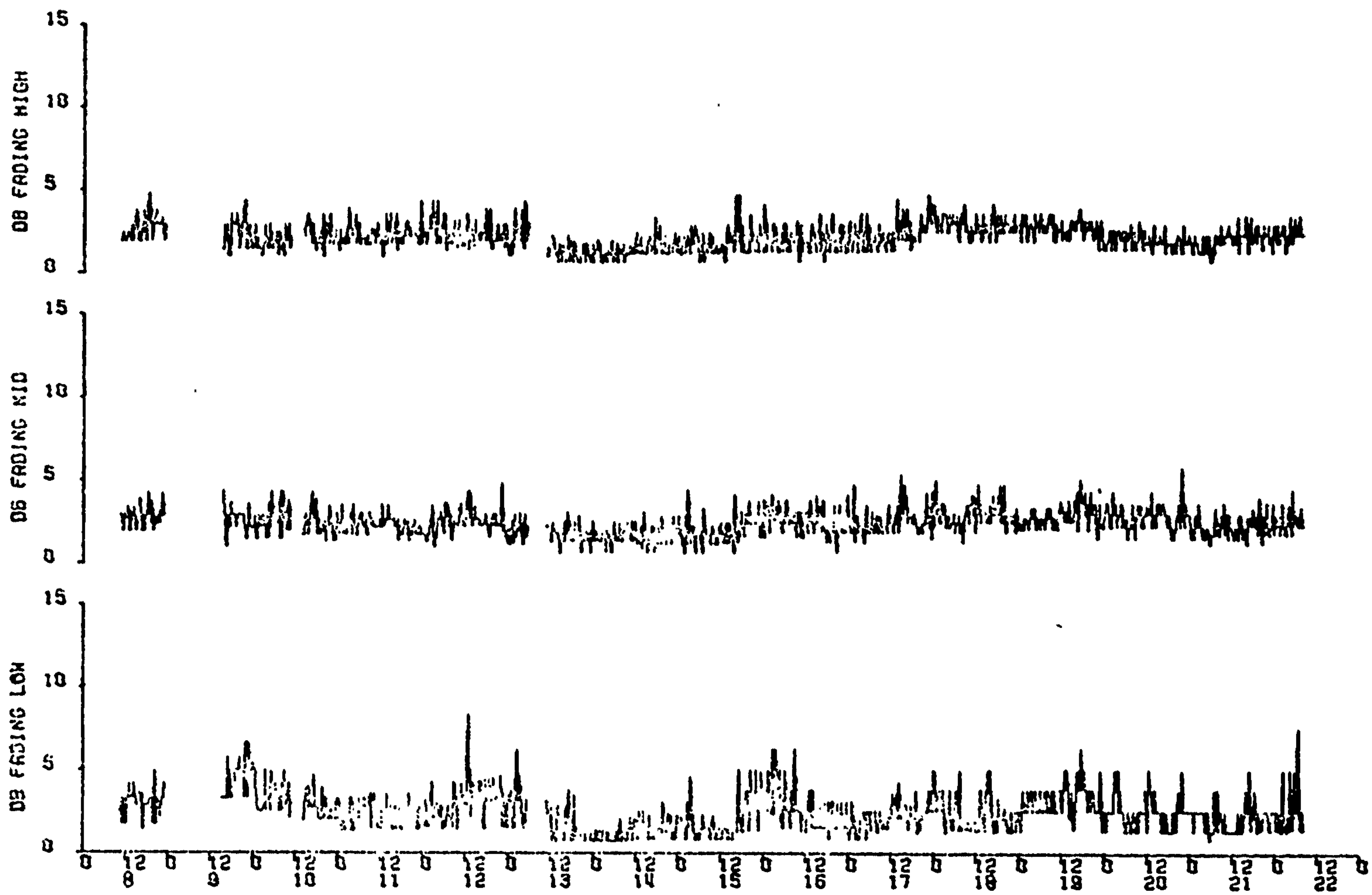

S BAND, NAXOS TO MYKONOS, GREECE FEBRUARY 1972

Figure 15. Fading S-band

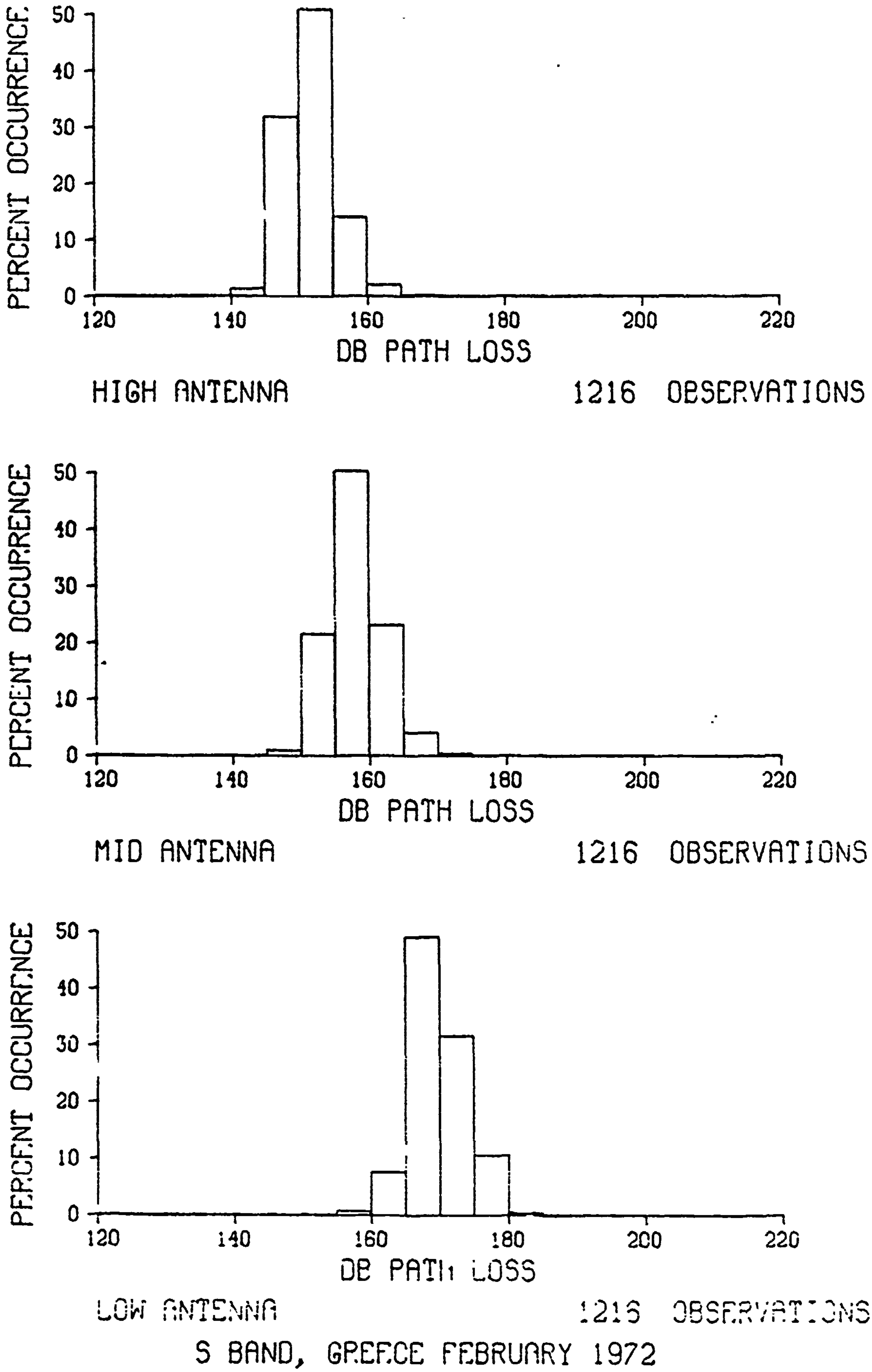

Figure 16. Frequency distributions of path loss for S-band

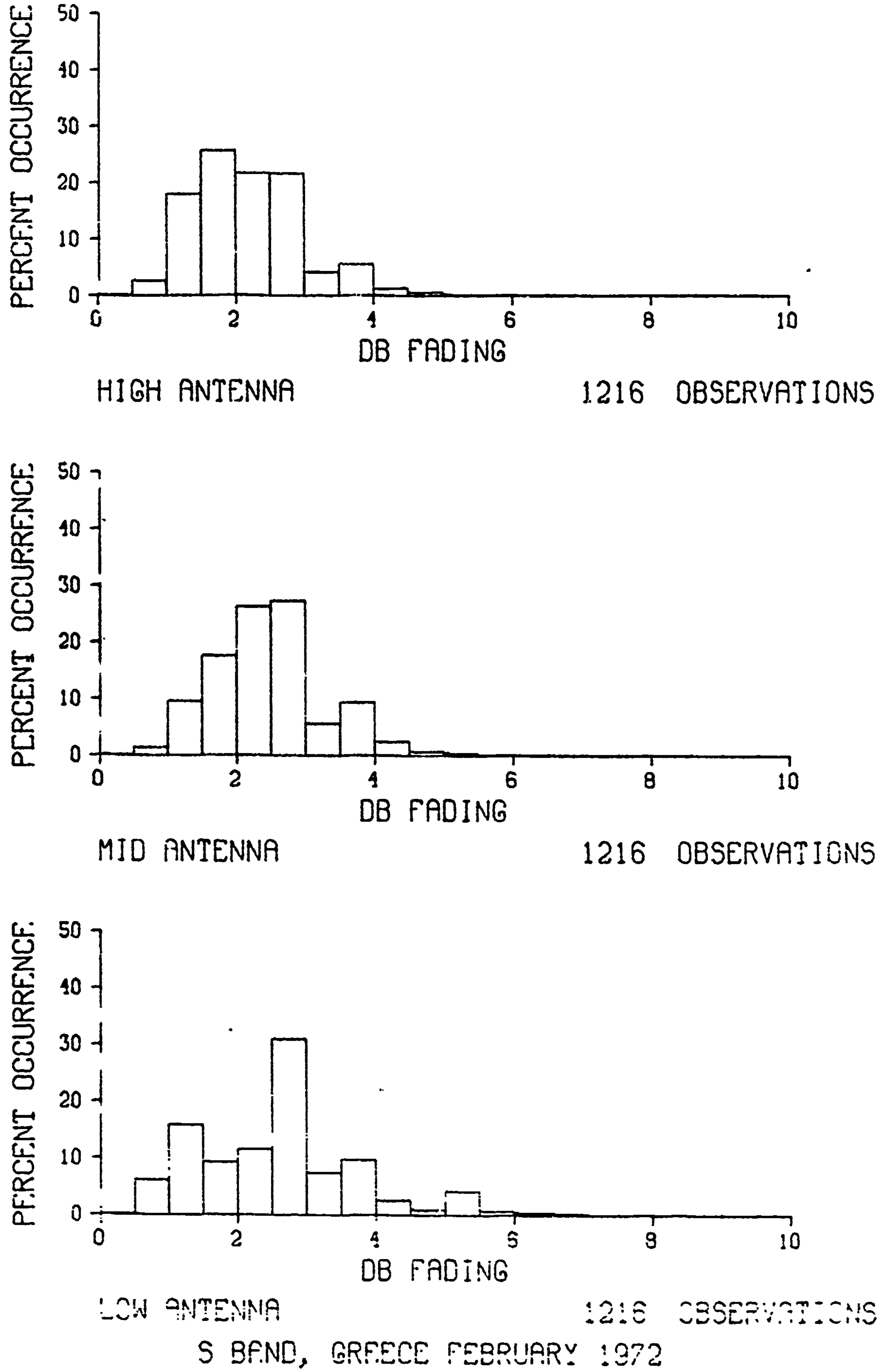

Figure 17. Frequency distributions of fading for S-band

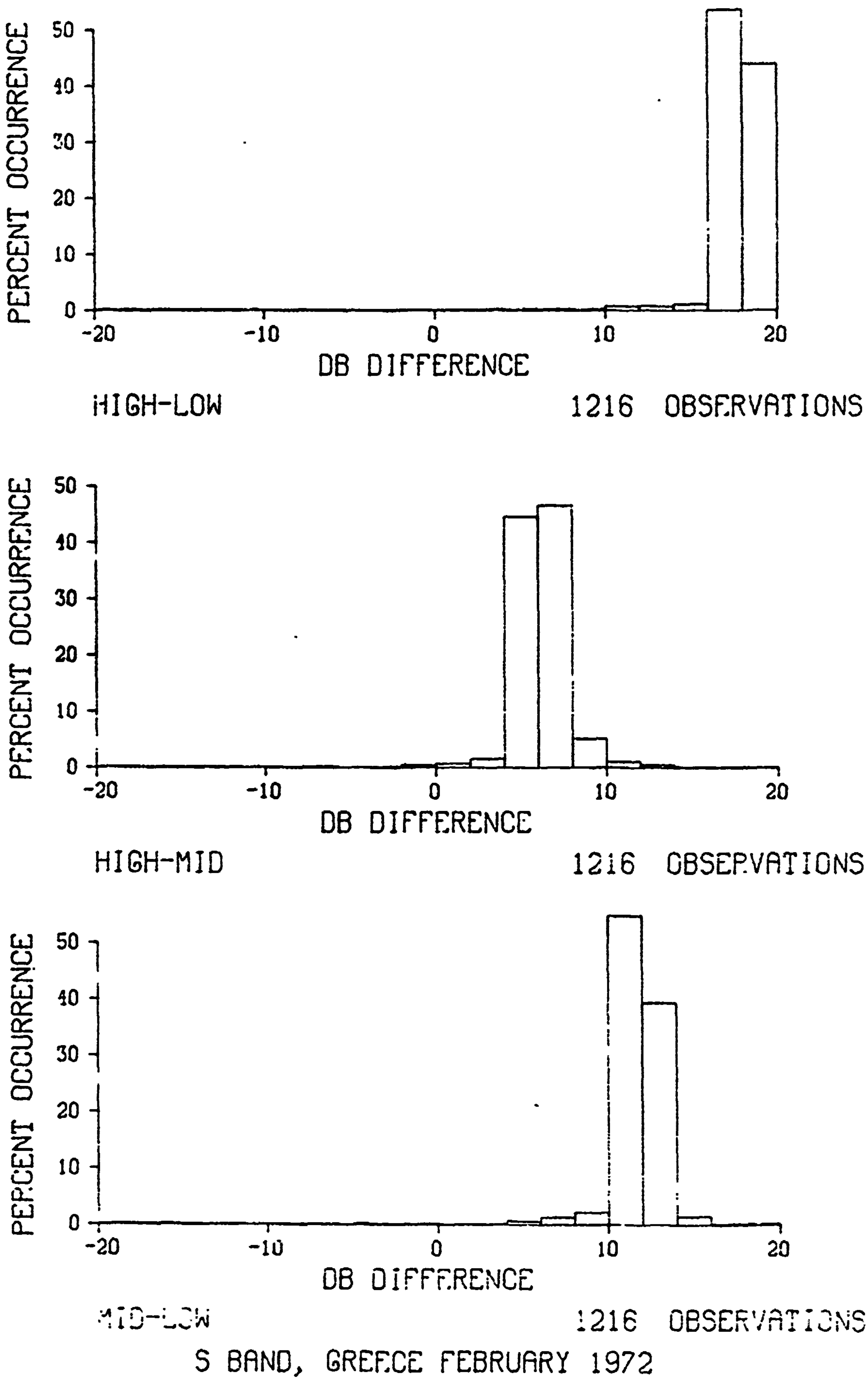

Figure 18. Frequency distributions of path loss differences between antennas for S-band

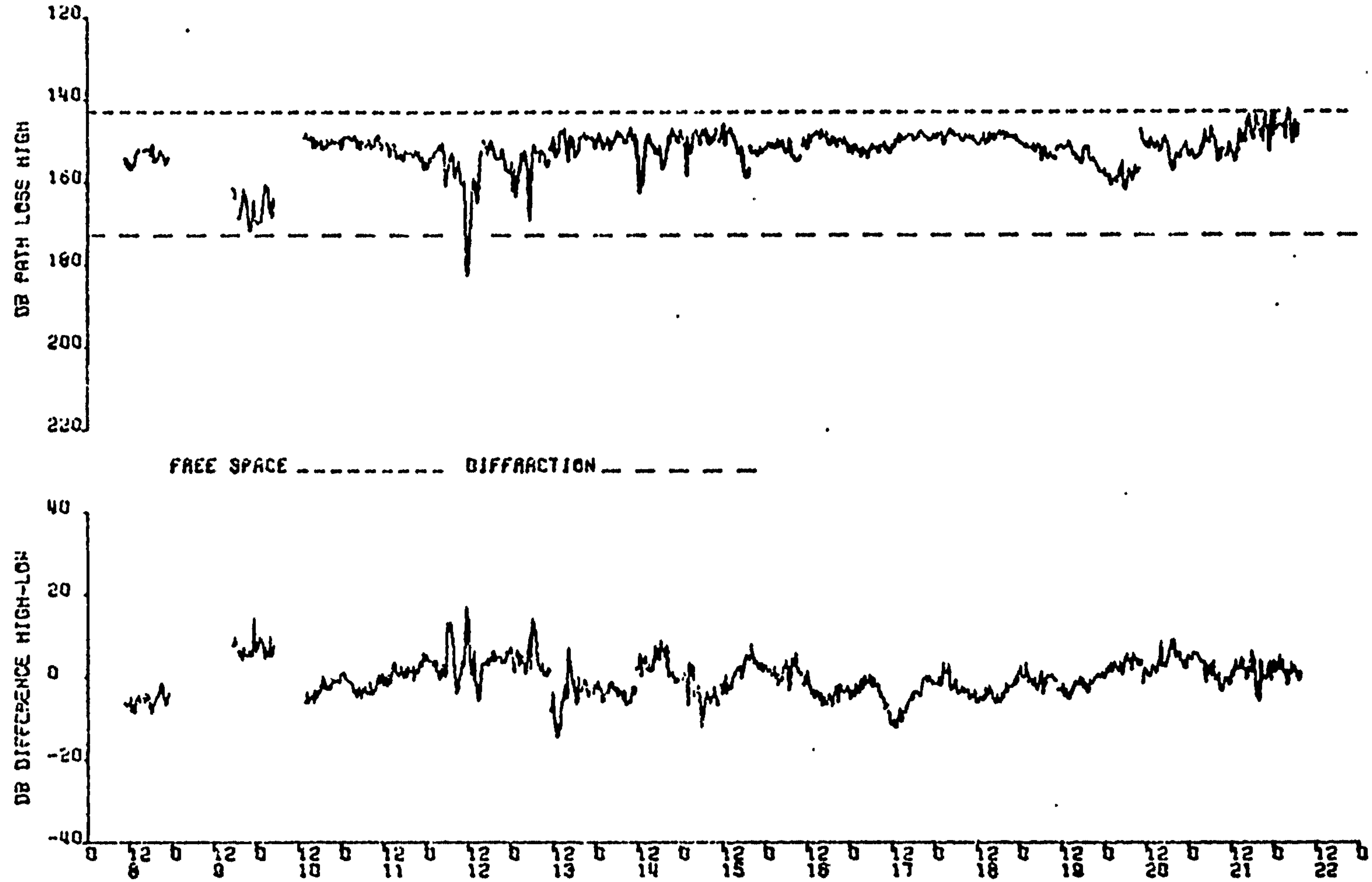

X BAND, NAXOS TO MYKONOS, GREECE   FEBRUARY 1972

Figure 19. Path loss for high X-band antenna and path loss difference high-low antenna

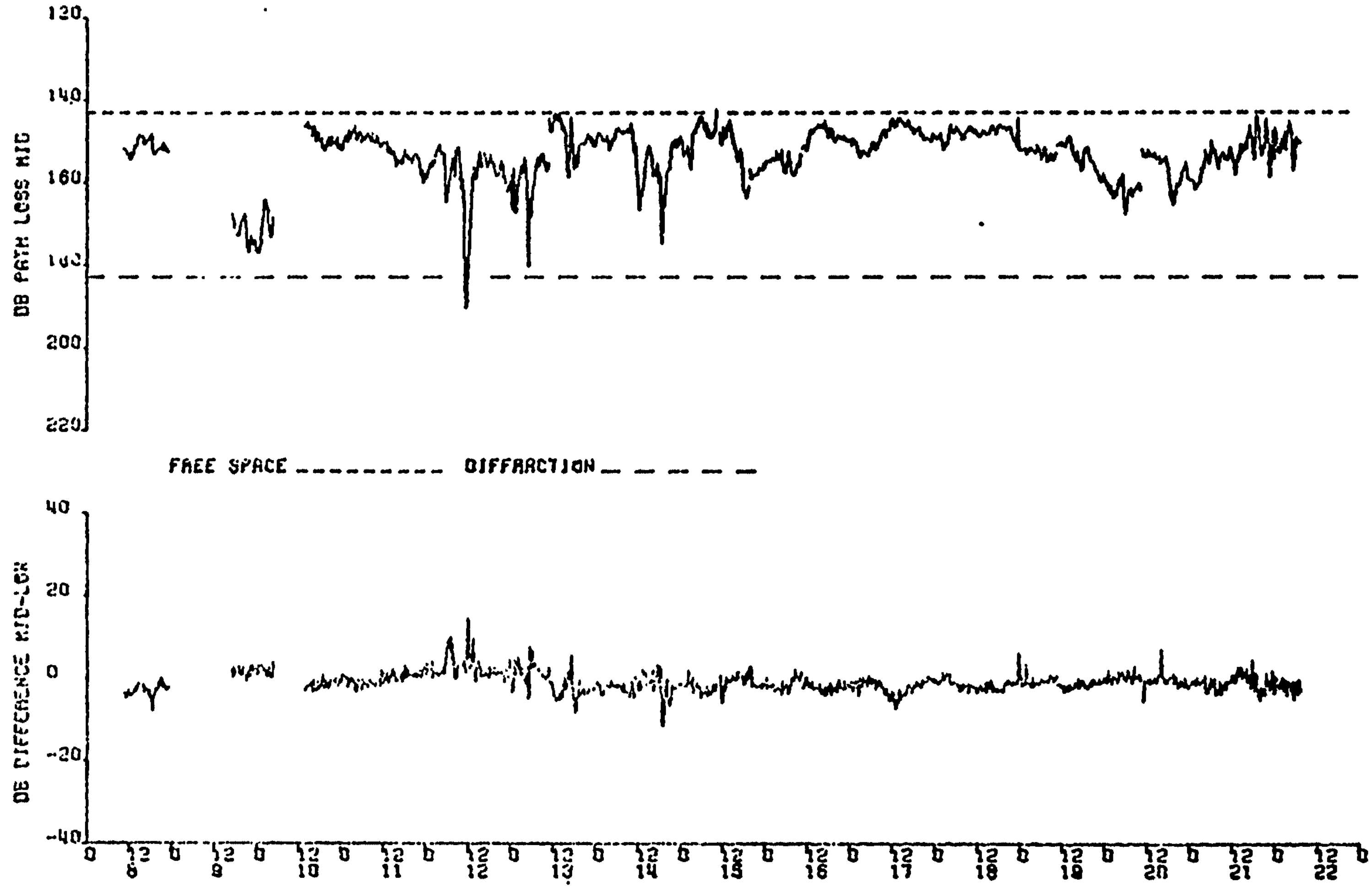

X BAND, NAXOS TO MYKONOS, GREECE FEBRUARY 1972

Figure 20. Path loss middle X-band antenna and path loss difference mid-low antenna

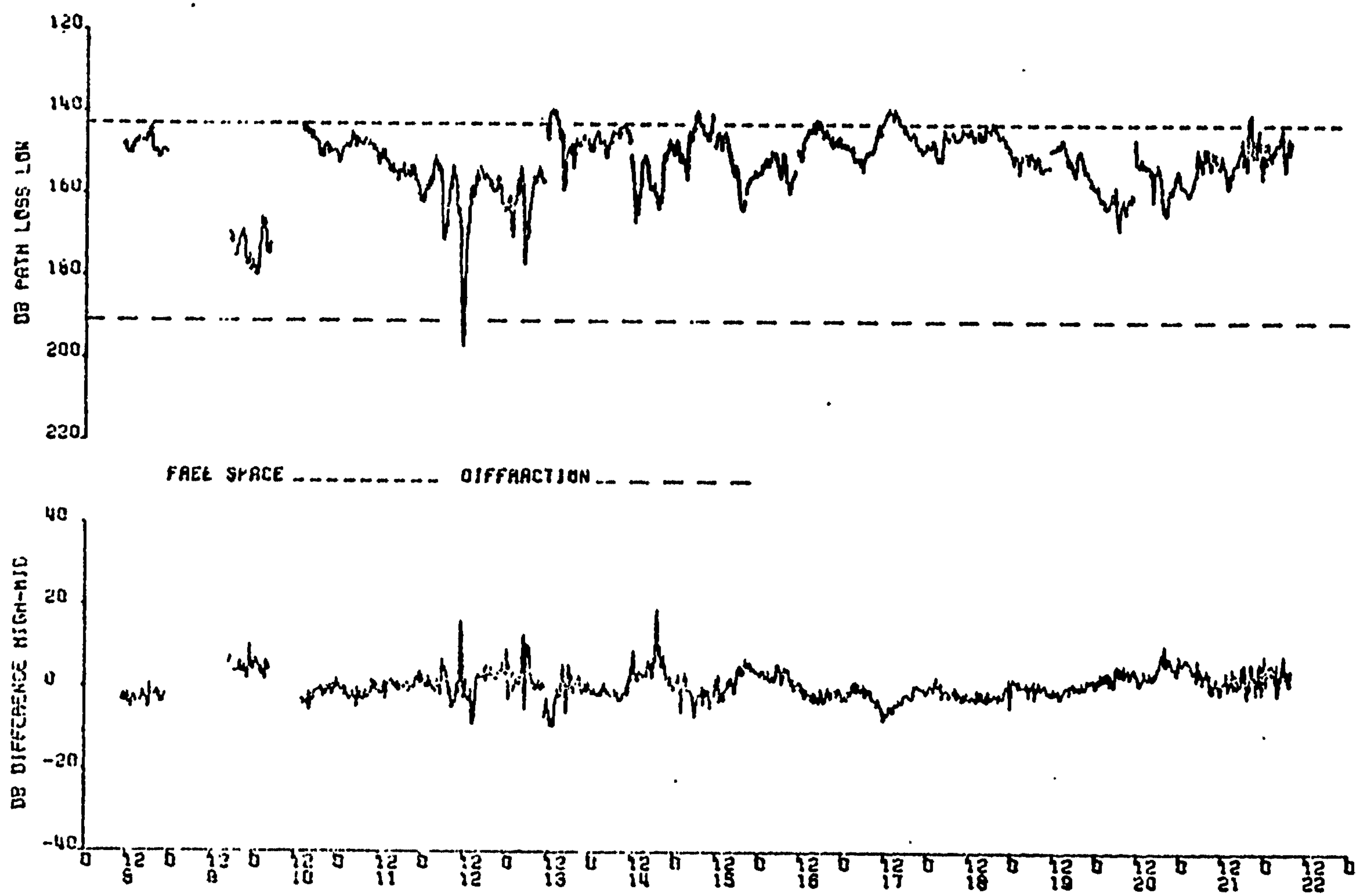

X BAND, NAXOS TO HYMETTUS, GREECE   FEBRUARY 1972

Figure 21. Path loss low X-band antenna and path loss difference high-mid antenna

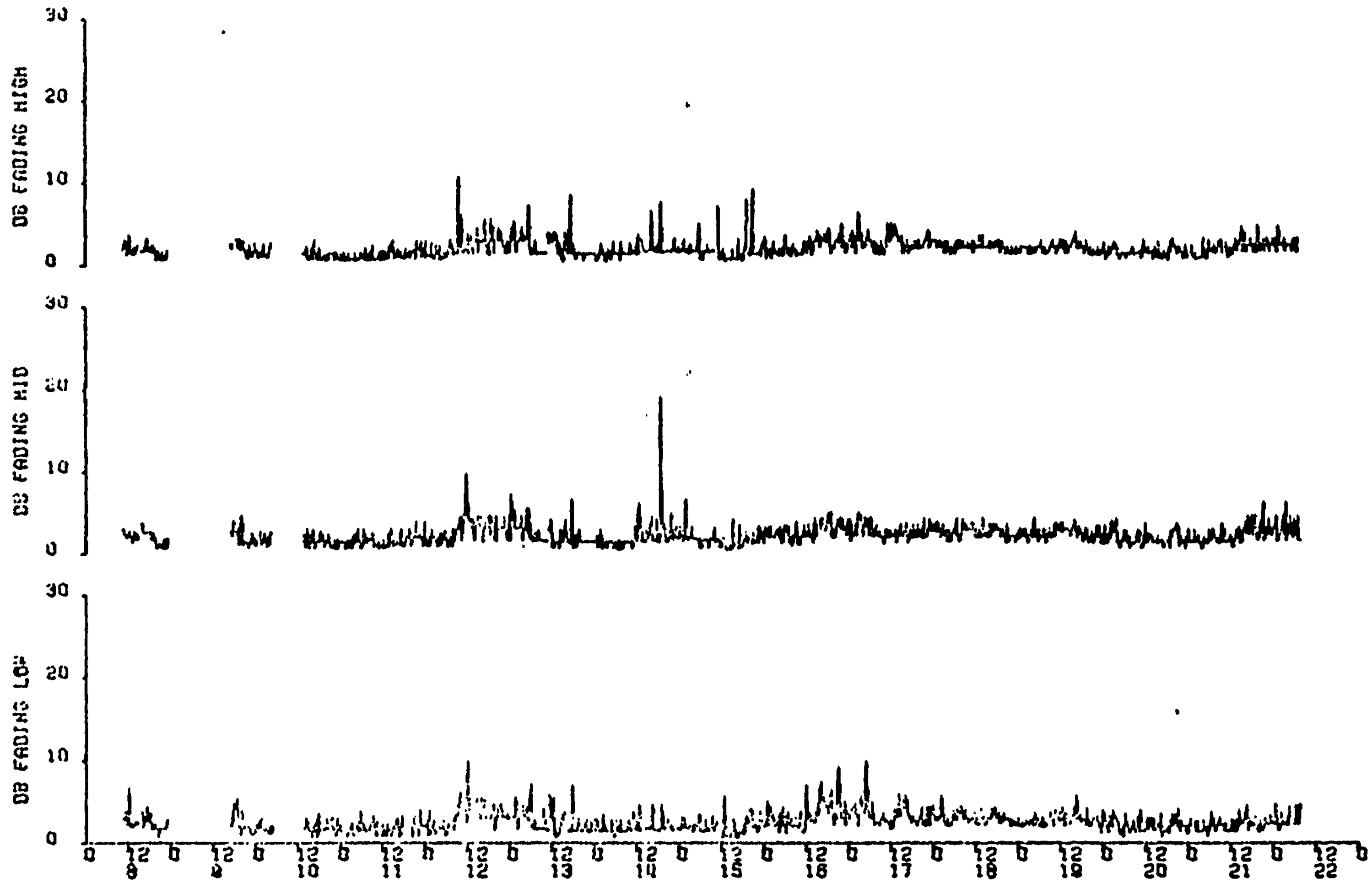

X BAND, NAXOS TO MYKONOS, GREECE   FEBAURAY 1972

Figure 22. Fading X-band

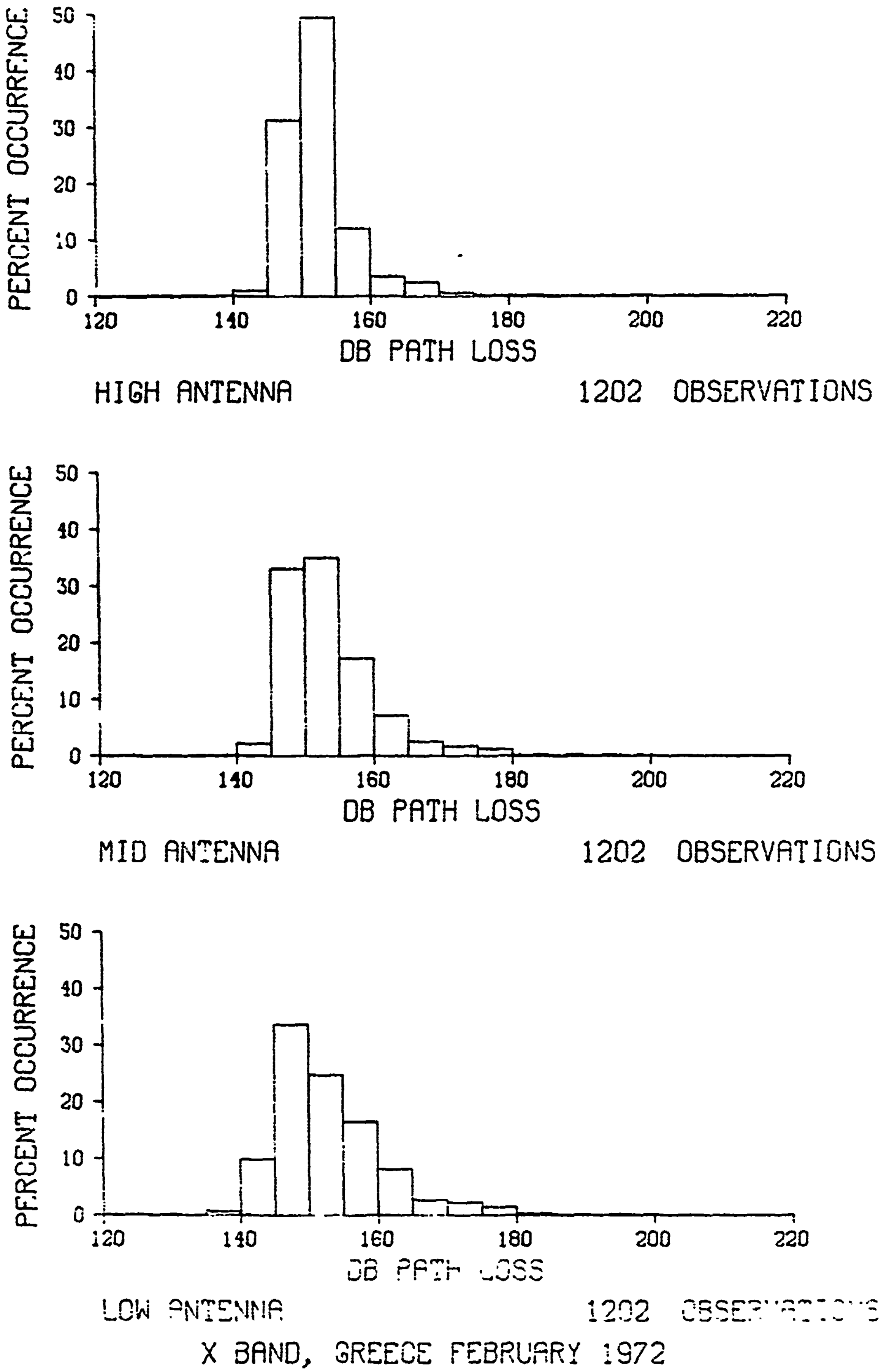

Figure 23. Frequency distribution of path loss for X-band

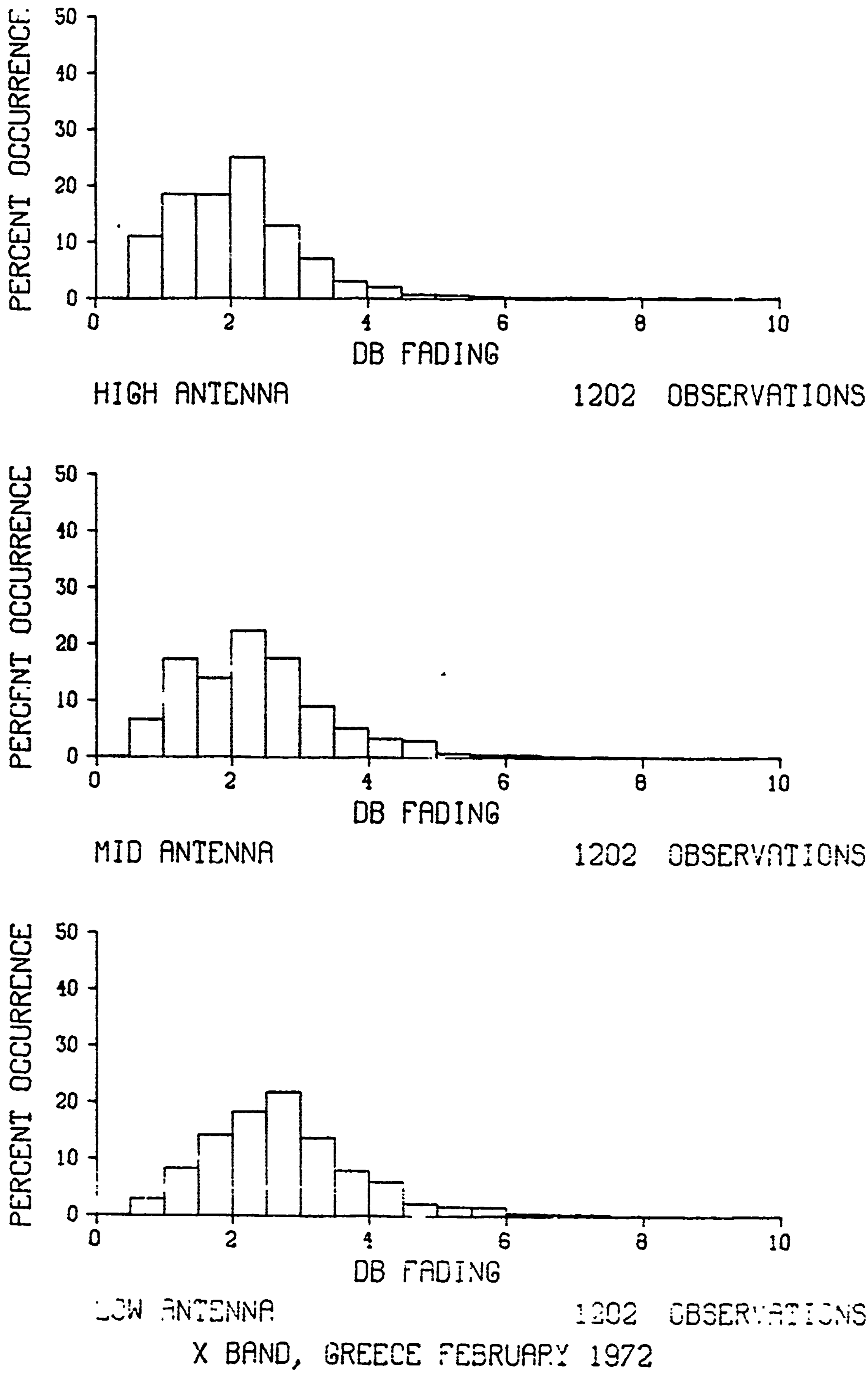

Figure 24. Frequency distribution of fading X-band

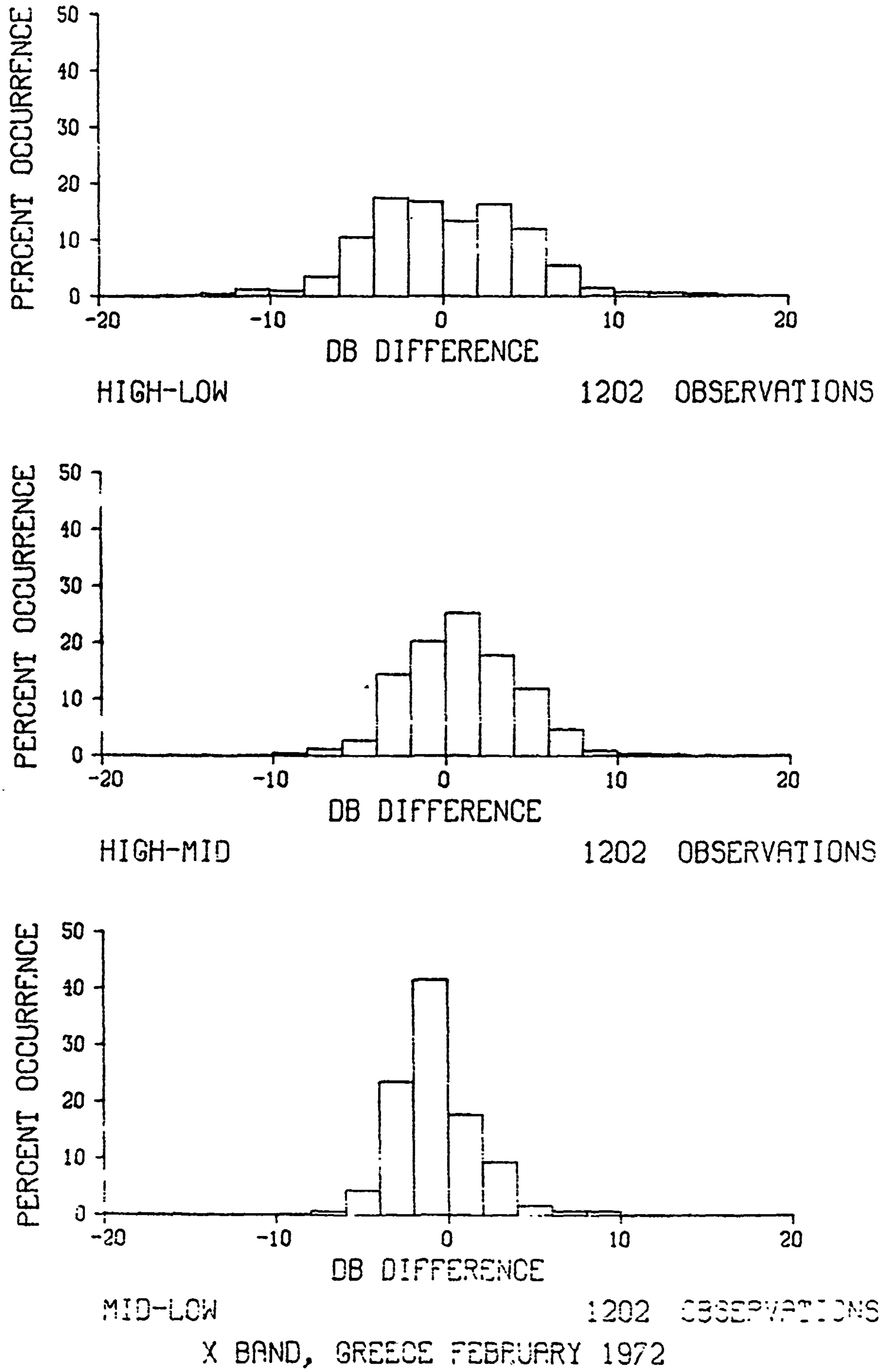

Figure 25. Frequency distribution of differences between antennas for X-band

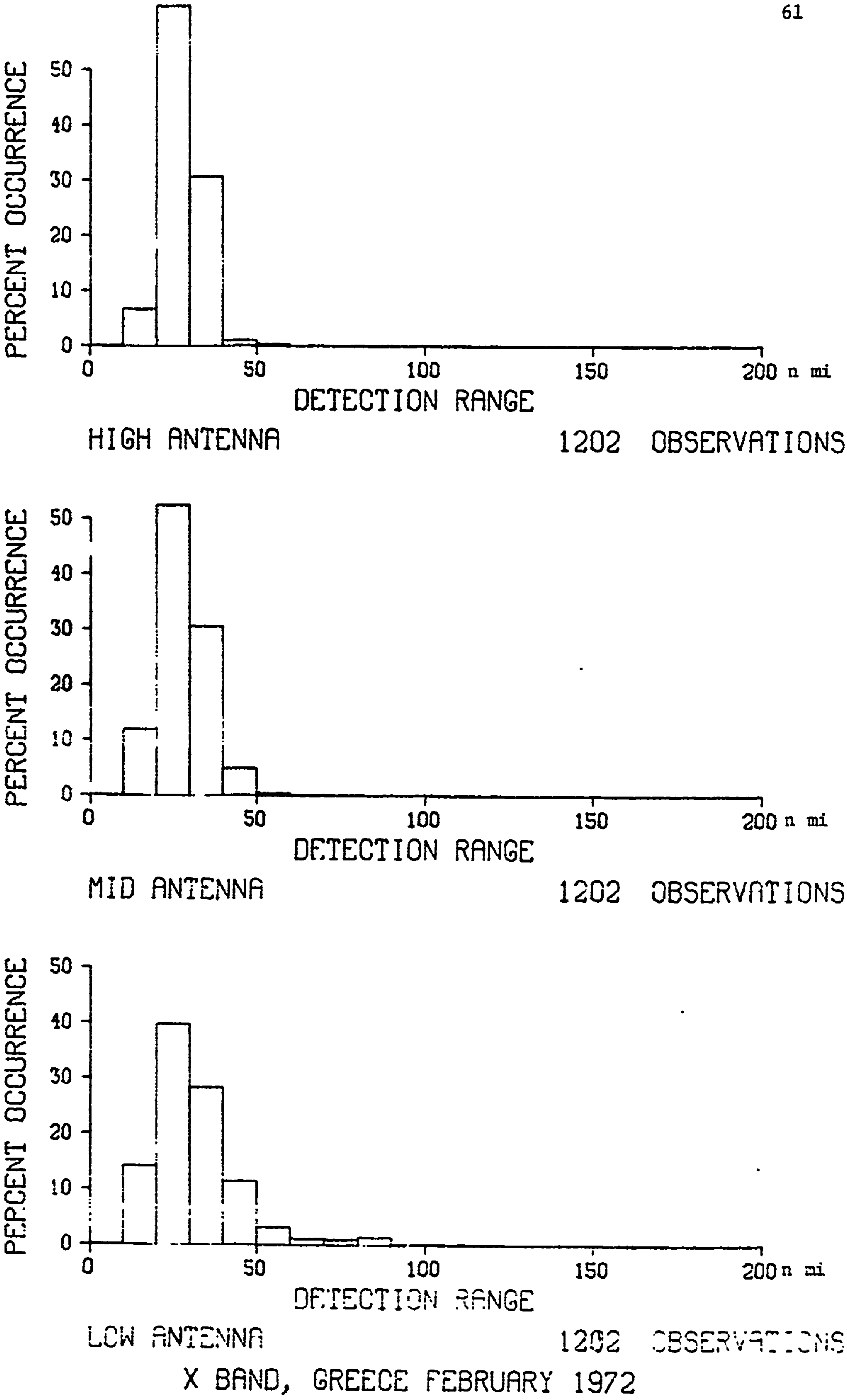

Figure 26. Frequency distribution of detection range for X-band

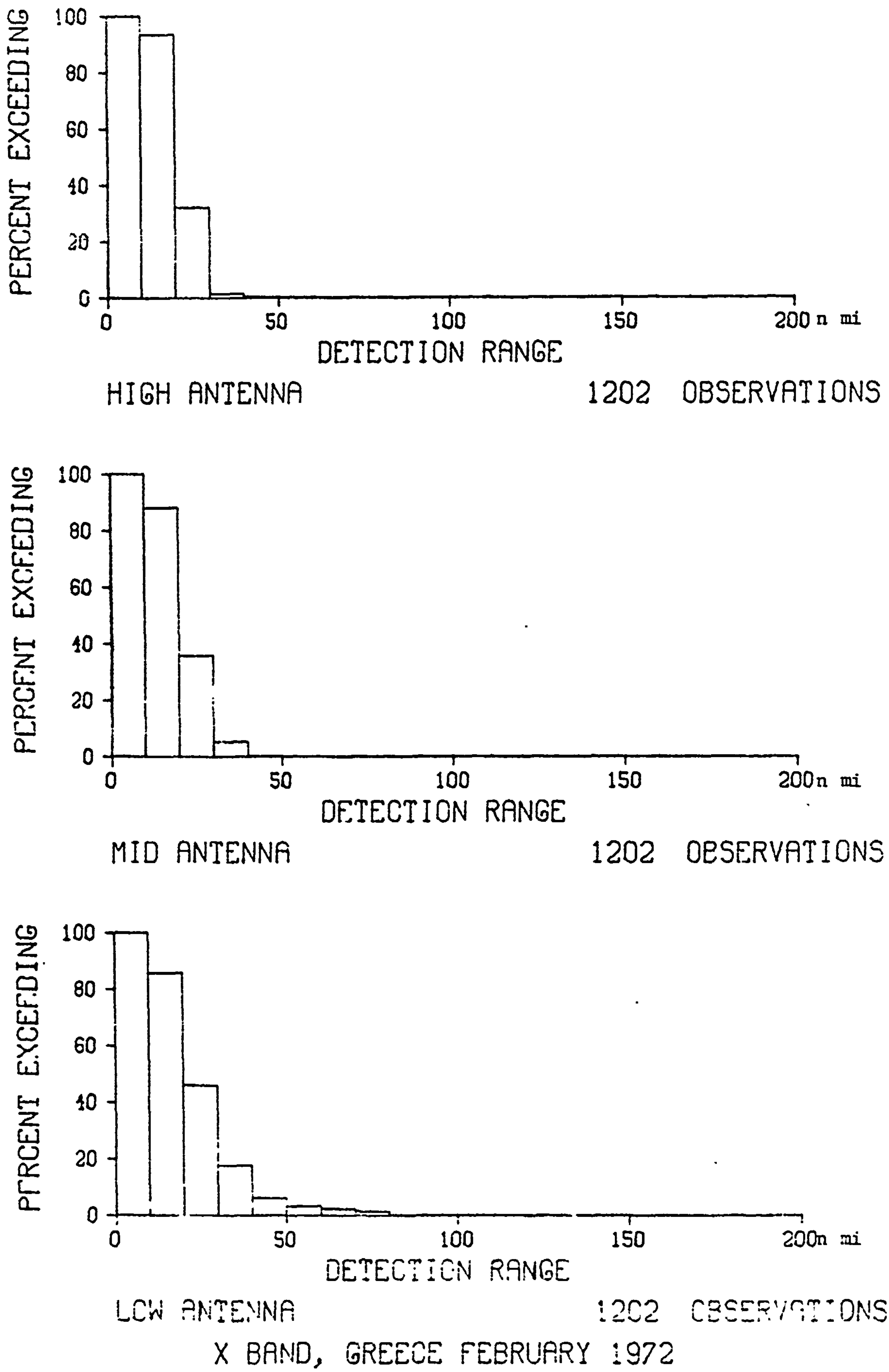

Figure 27. Cumulative distribution of detection range for X-band

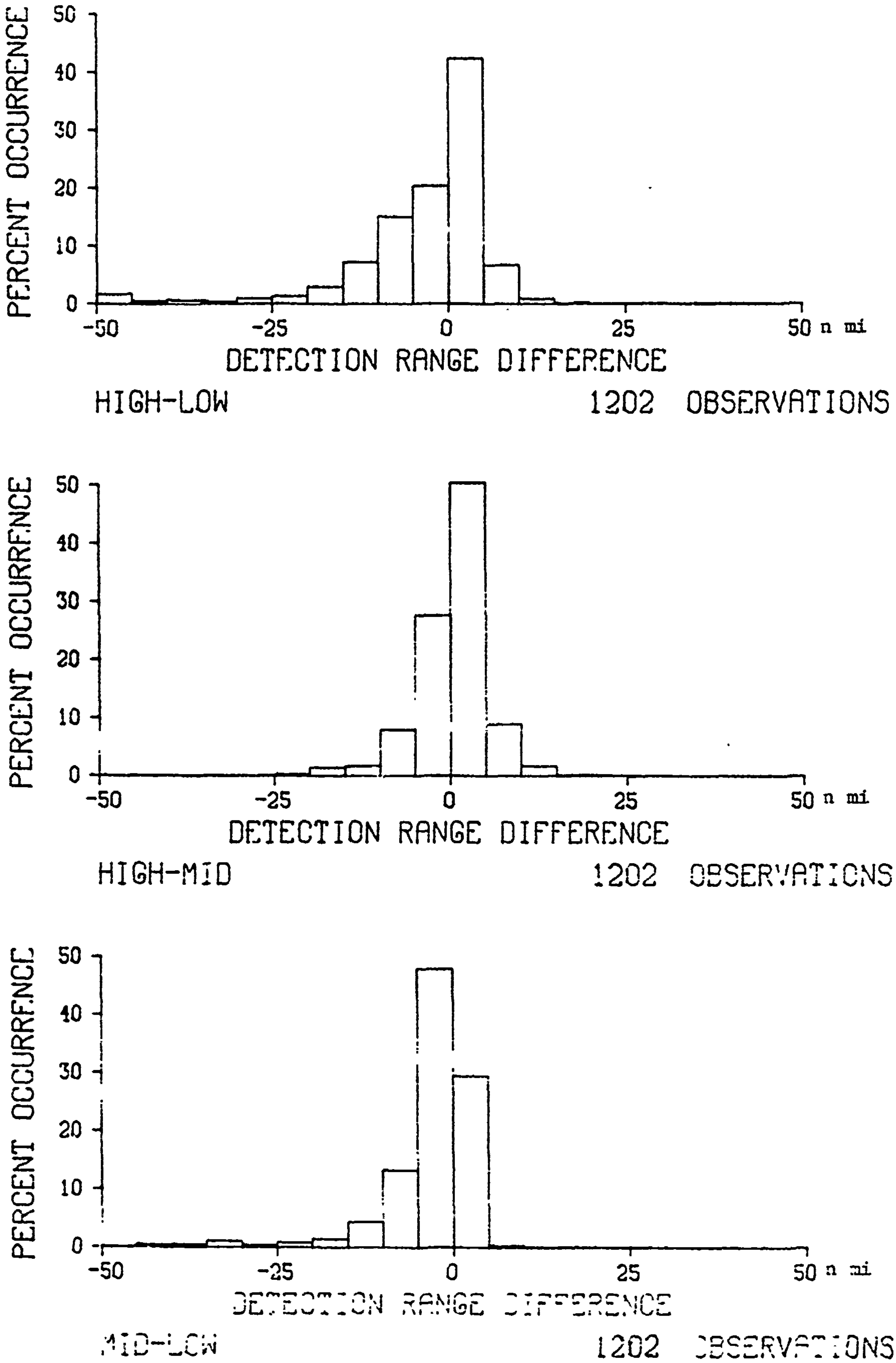

Figure 28. Frequency distribution of detection range differences between antennas for X-band

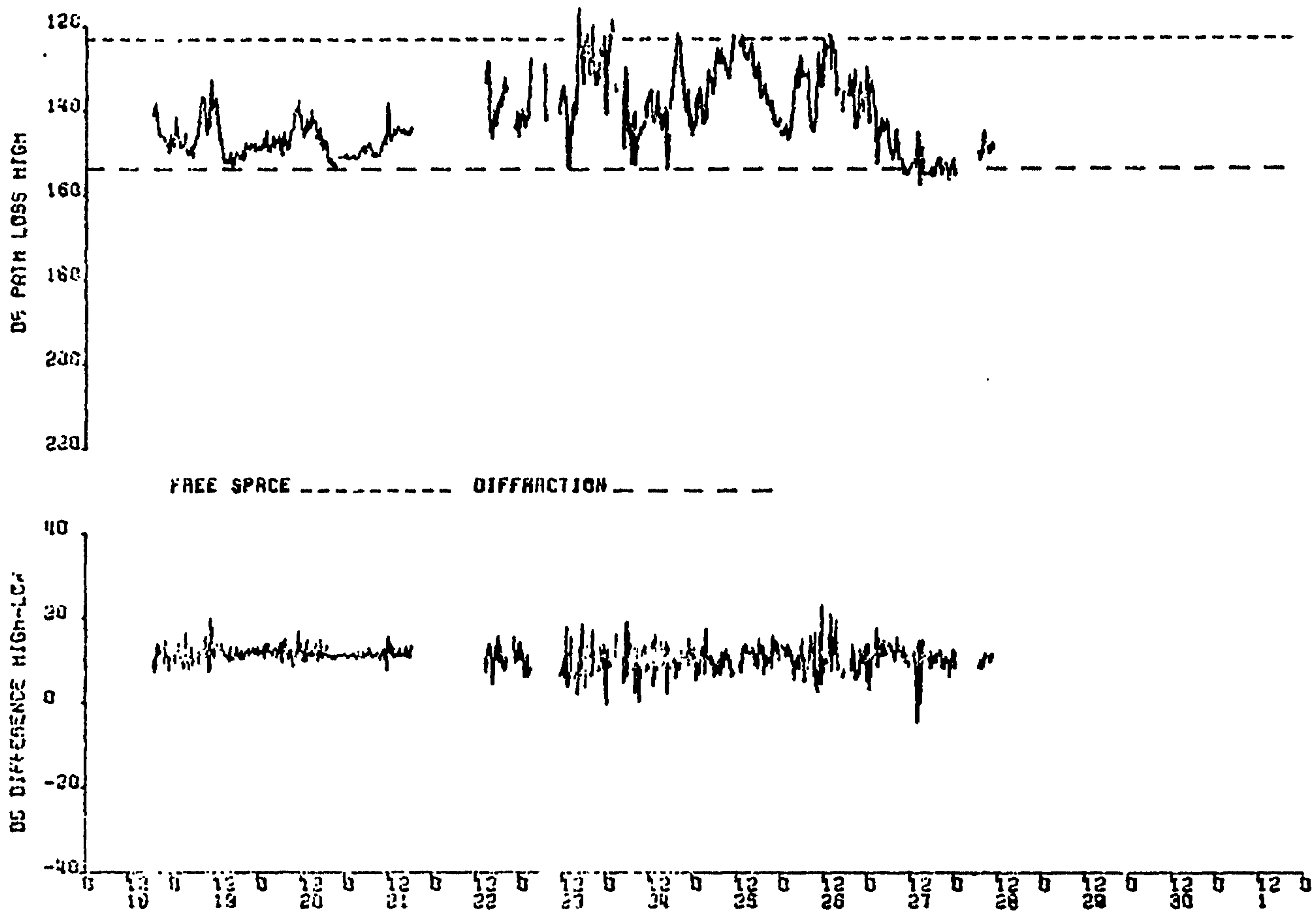

L BAND, NAXOS TO ATHENS, GREECE APRIL 1972

Figure 29. Path loss for high L-band antenna and path loss difference high-low antenna

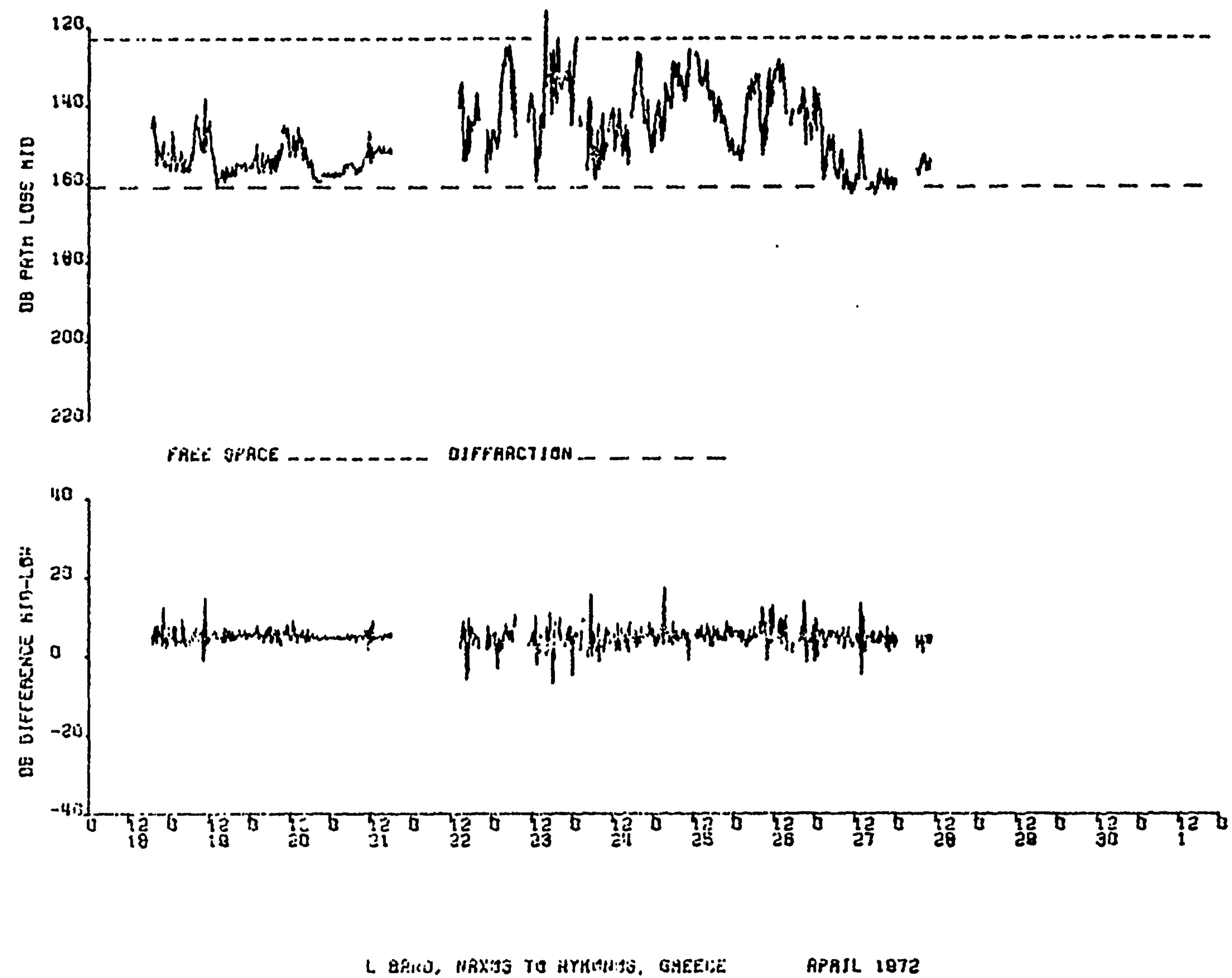

Figure 30. Path loss for middle L-band antenna and path loss difference mid-low antenna

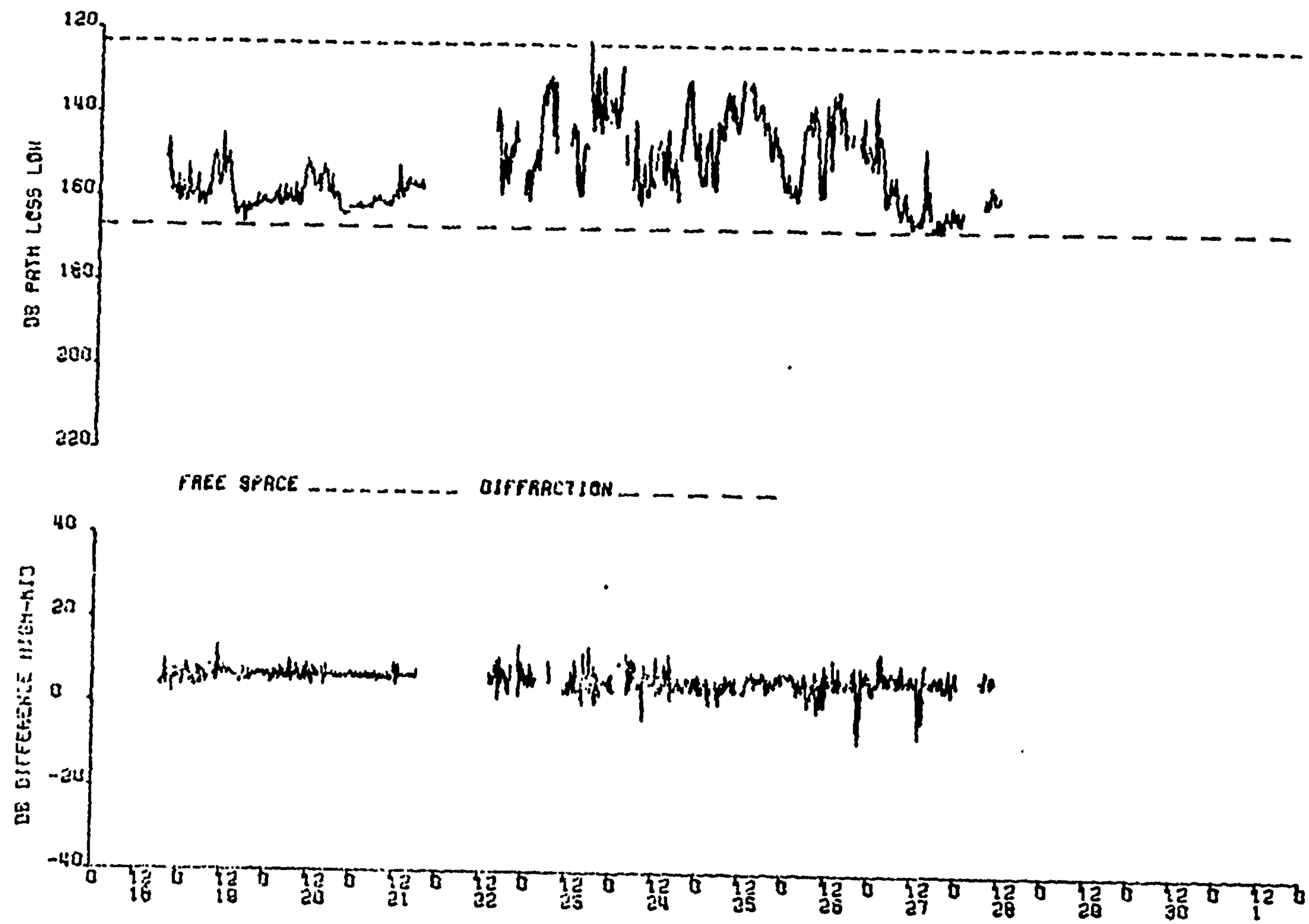

L BAND, NAXOS TO MYKONOS, GREECE APRIL 1972

Figure 31. Path loss for low L-band antenna and path loss difference high-mid antenna

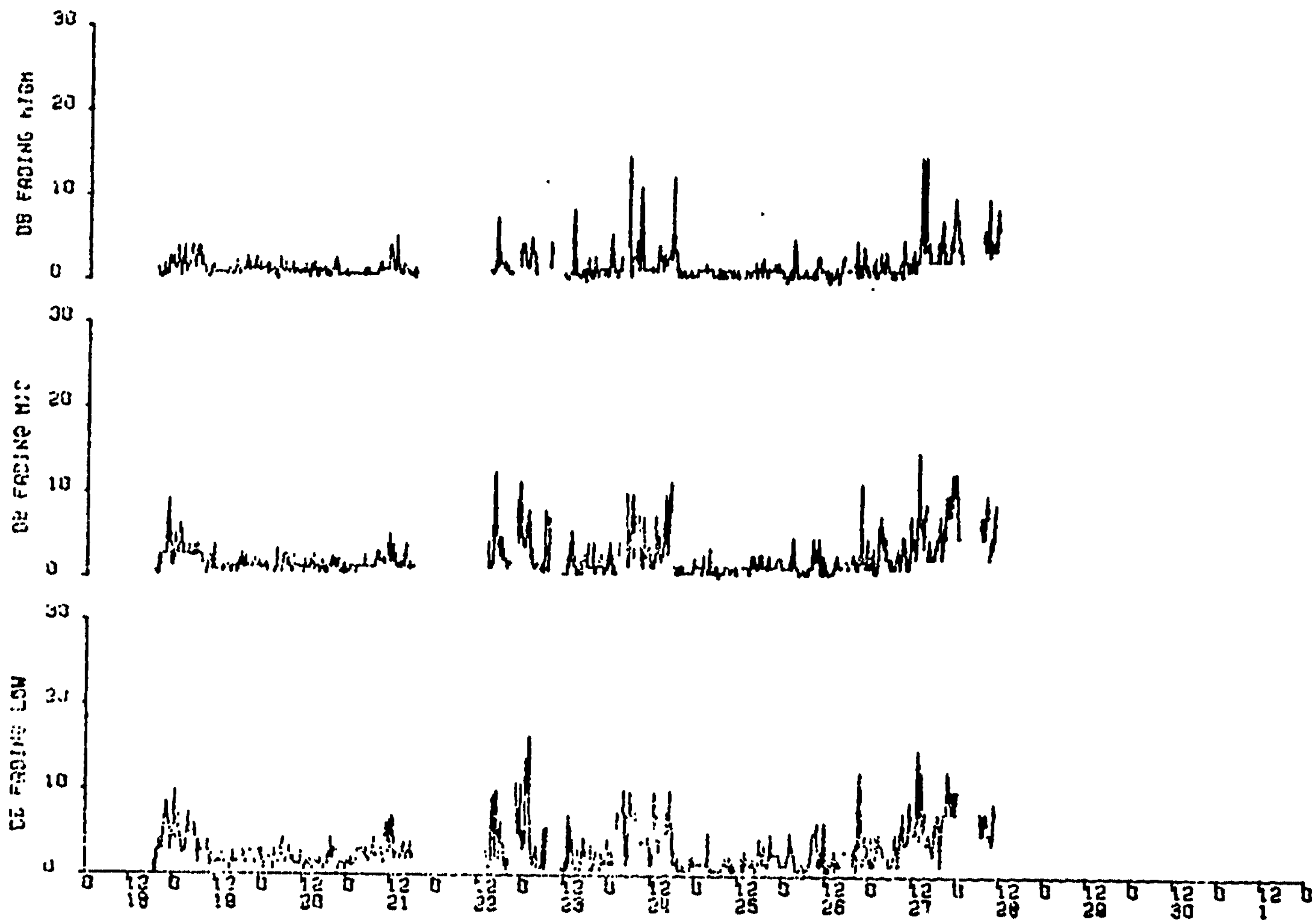

L BAND, NAXOS TO AYKONOS, GREECE APRIL 1972

Figure 32. Fading L-band

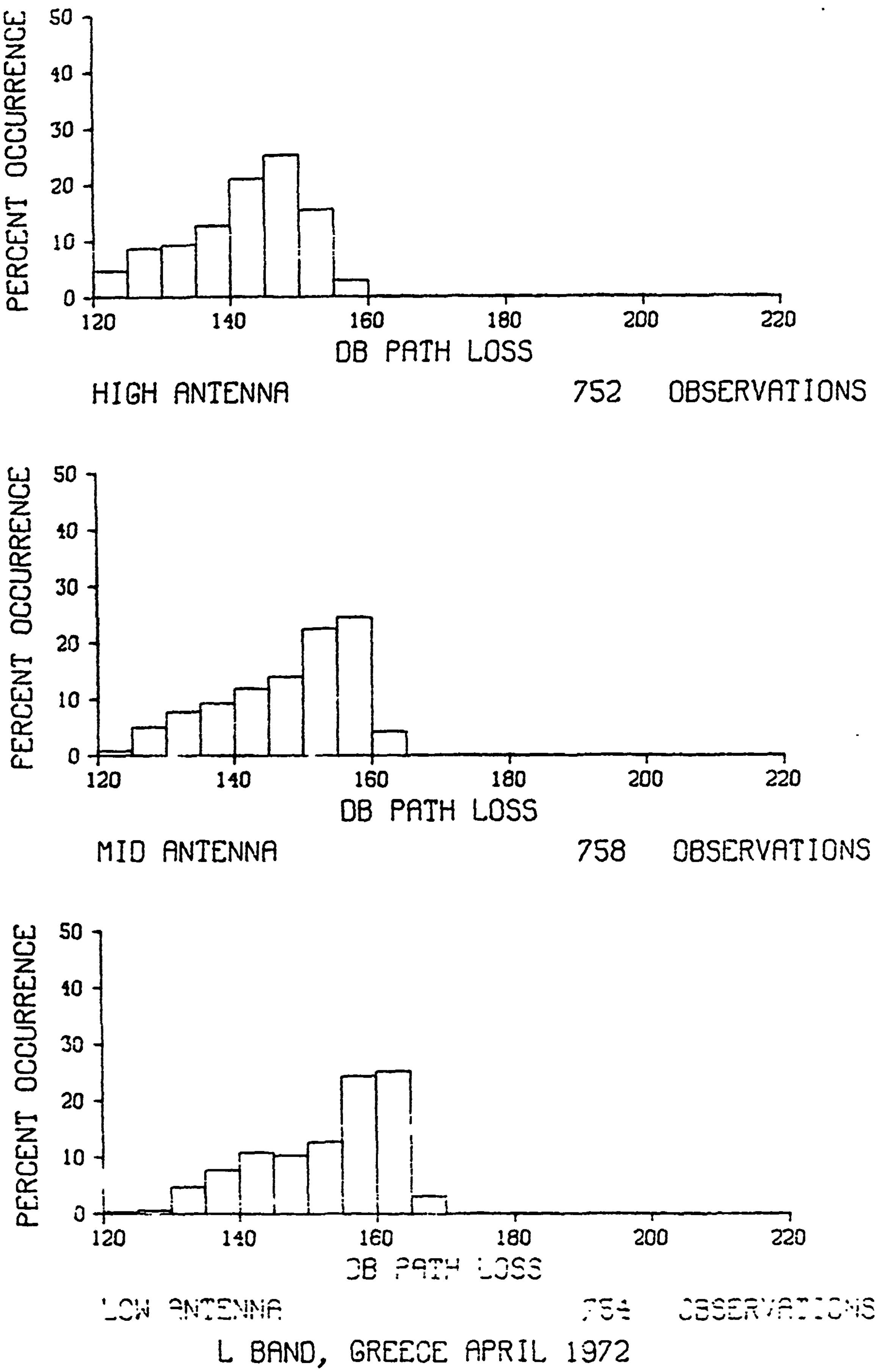

Figure 33. Frequency distributions of path loss for L-band

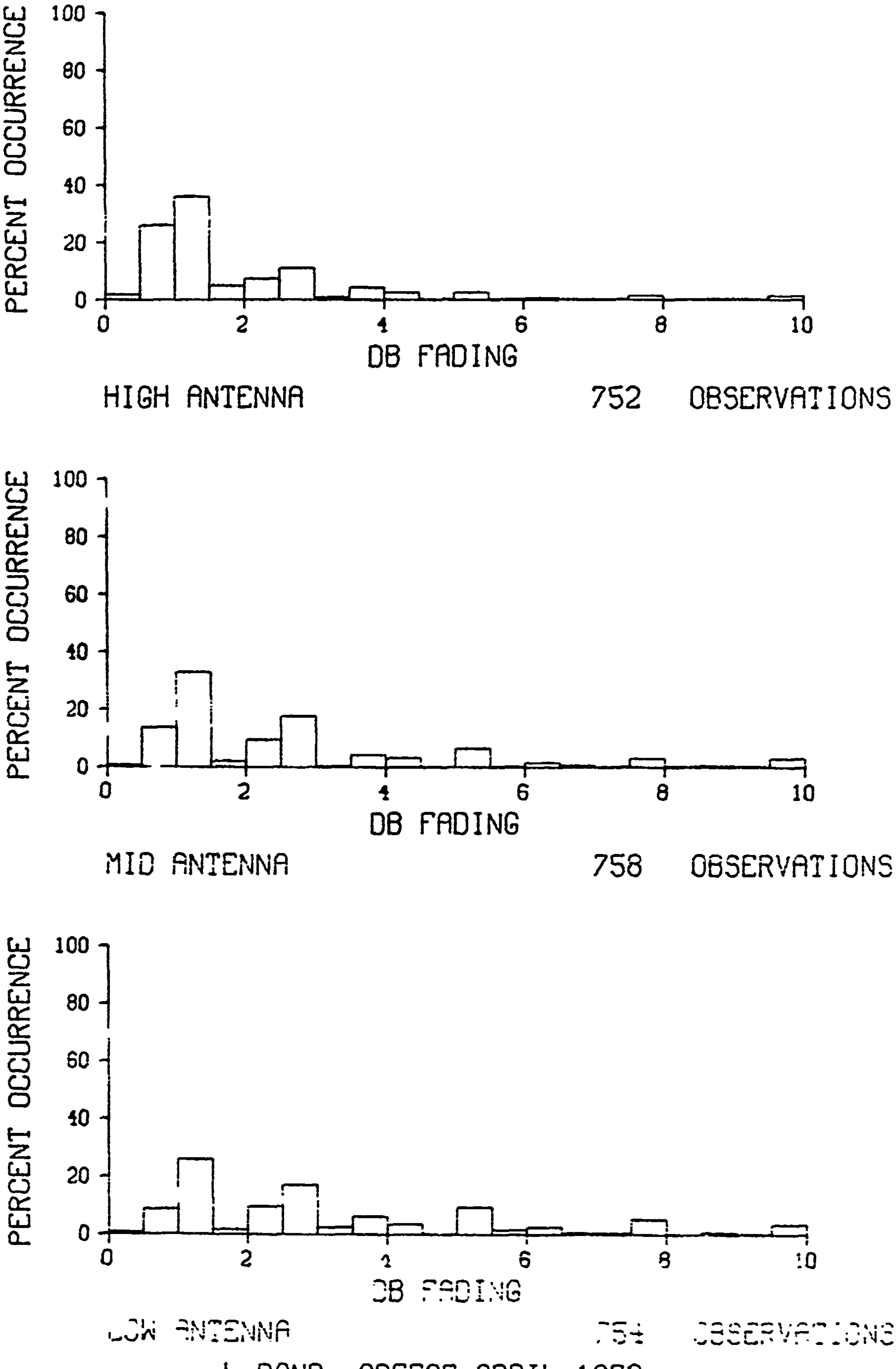

Figure 34. Frequency distributions of fading L-band

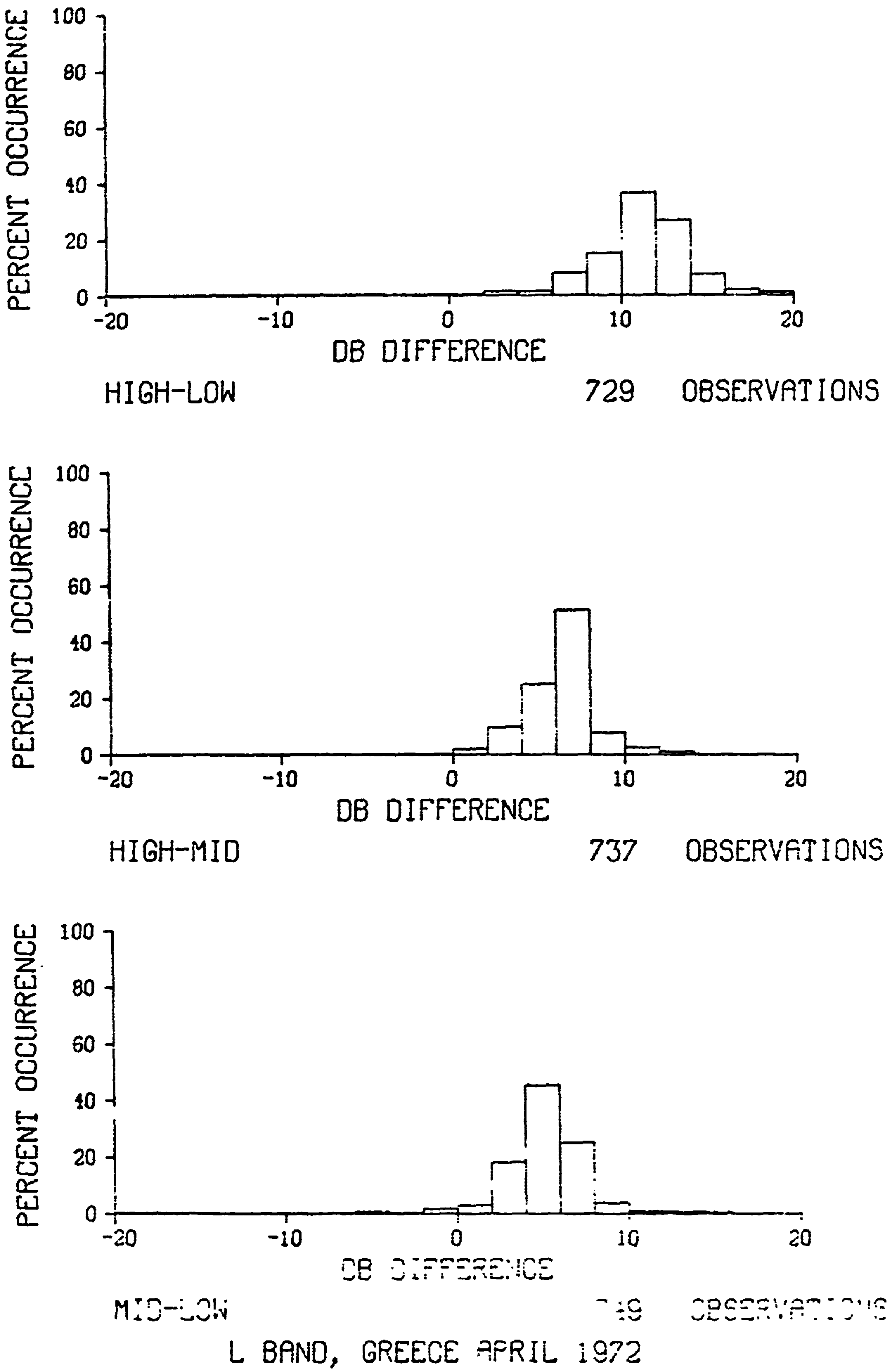

Figure 35. Frequency distributions of path loss differences between antennas for L-band

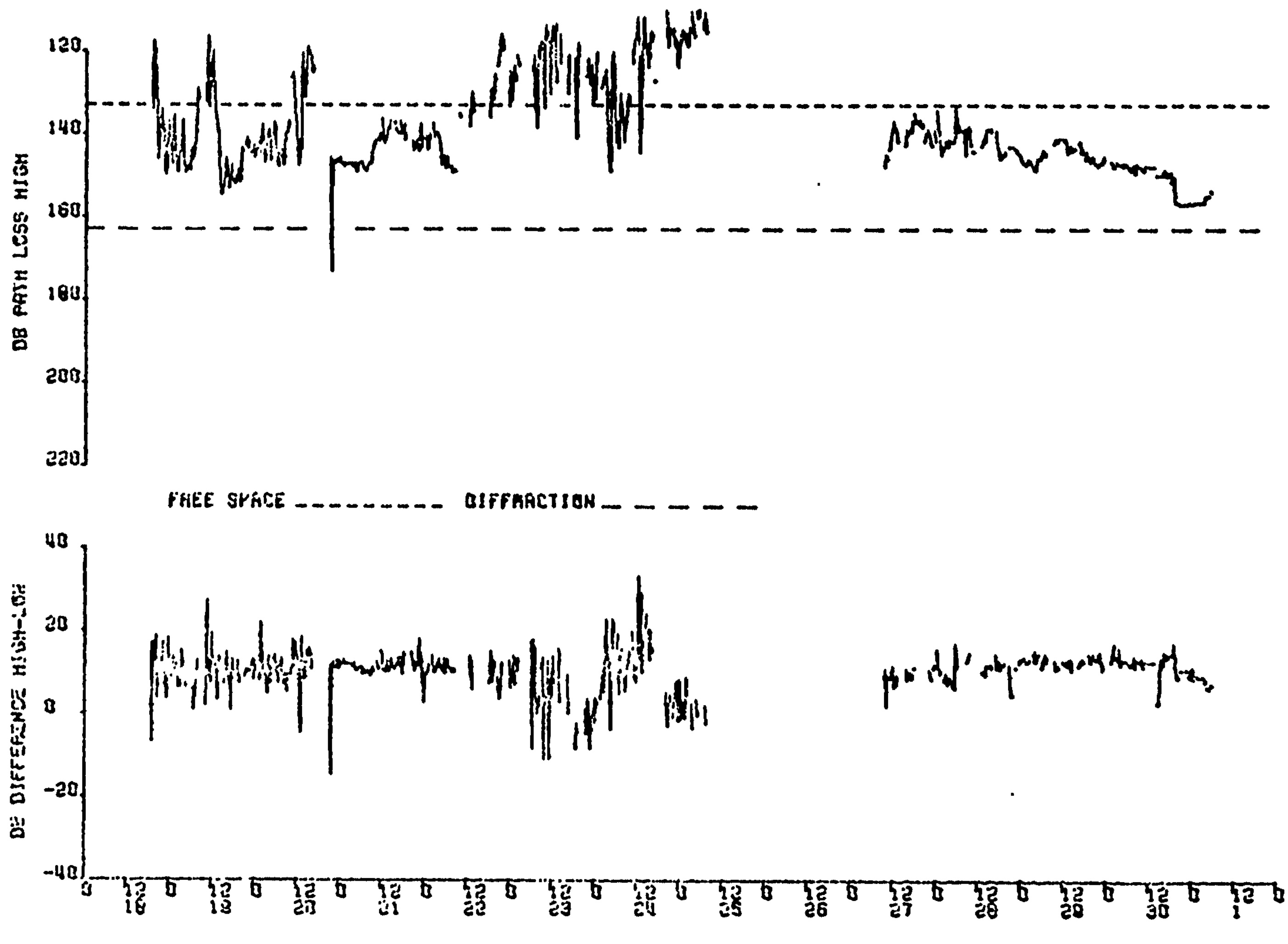

S BAND, NAXOS TO MYKONOS, GREECE   APRIL 1973

Figure 3b. Path loss for high S-band antenna and path loss difference high-low antenna

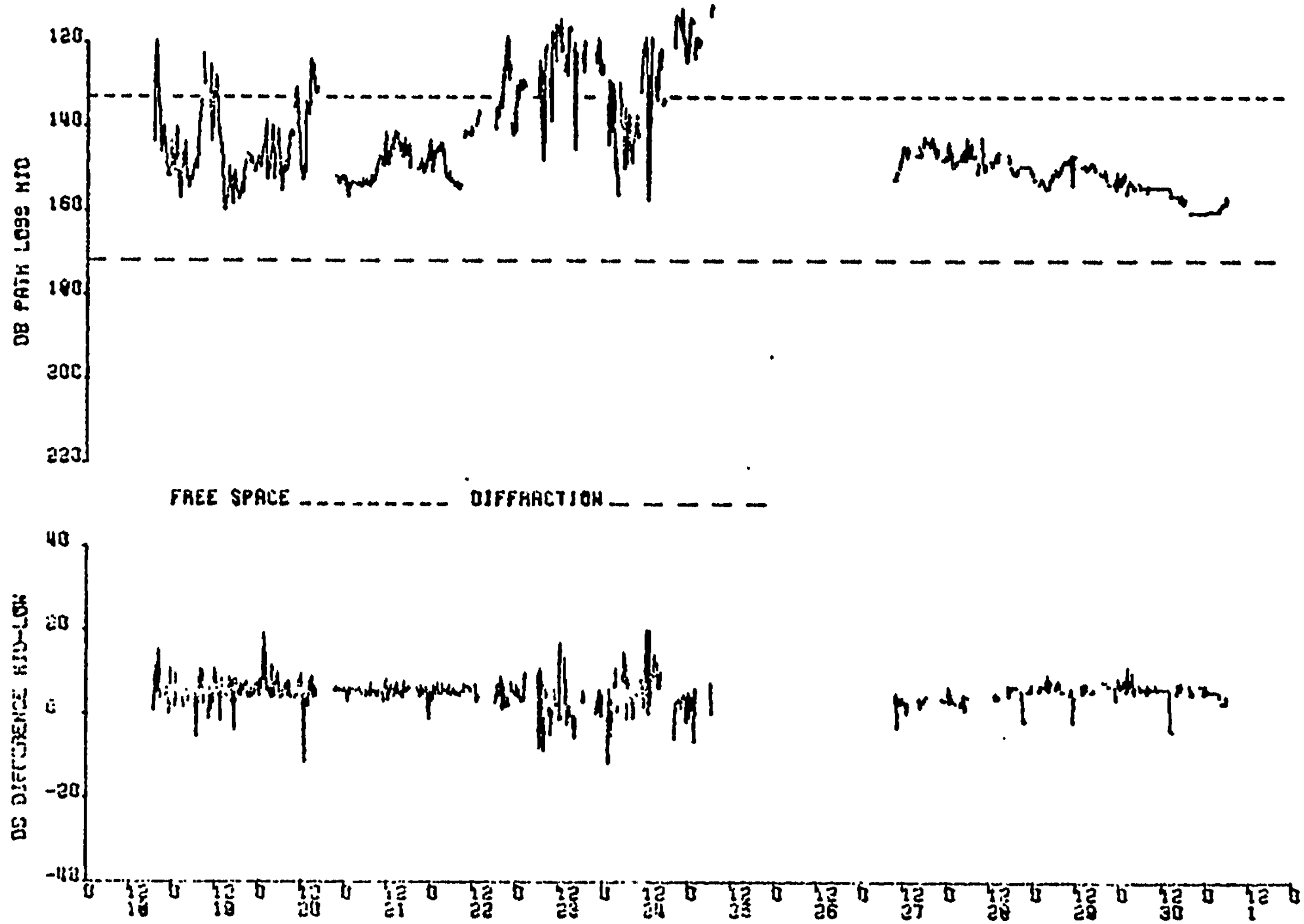

S BAND, NAXOS TO ATHENS, GREECE APRIL 1972

Figure 37. Path loss for middle S-band antenna and path loss difference mid-low antenna

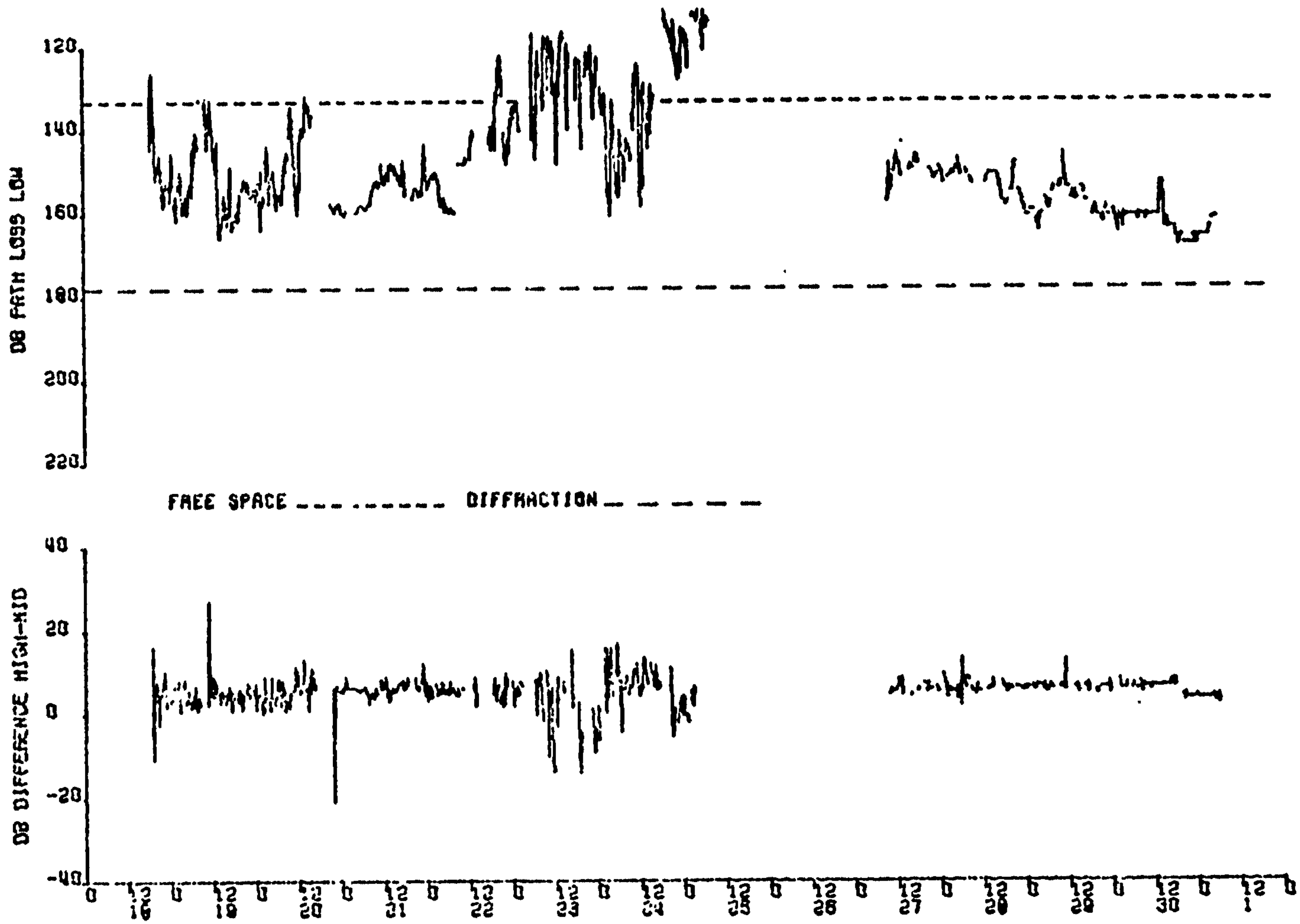

S BAND, NAXOS TO NYMENOS, GREECE APRIL 1972
Figure 38. Path loss for low S-band antenna and path loss difference high-mid antenna

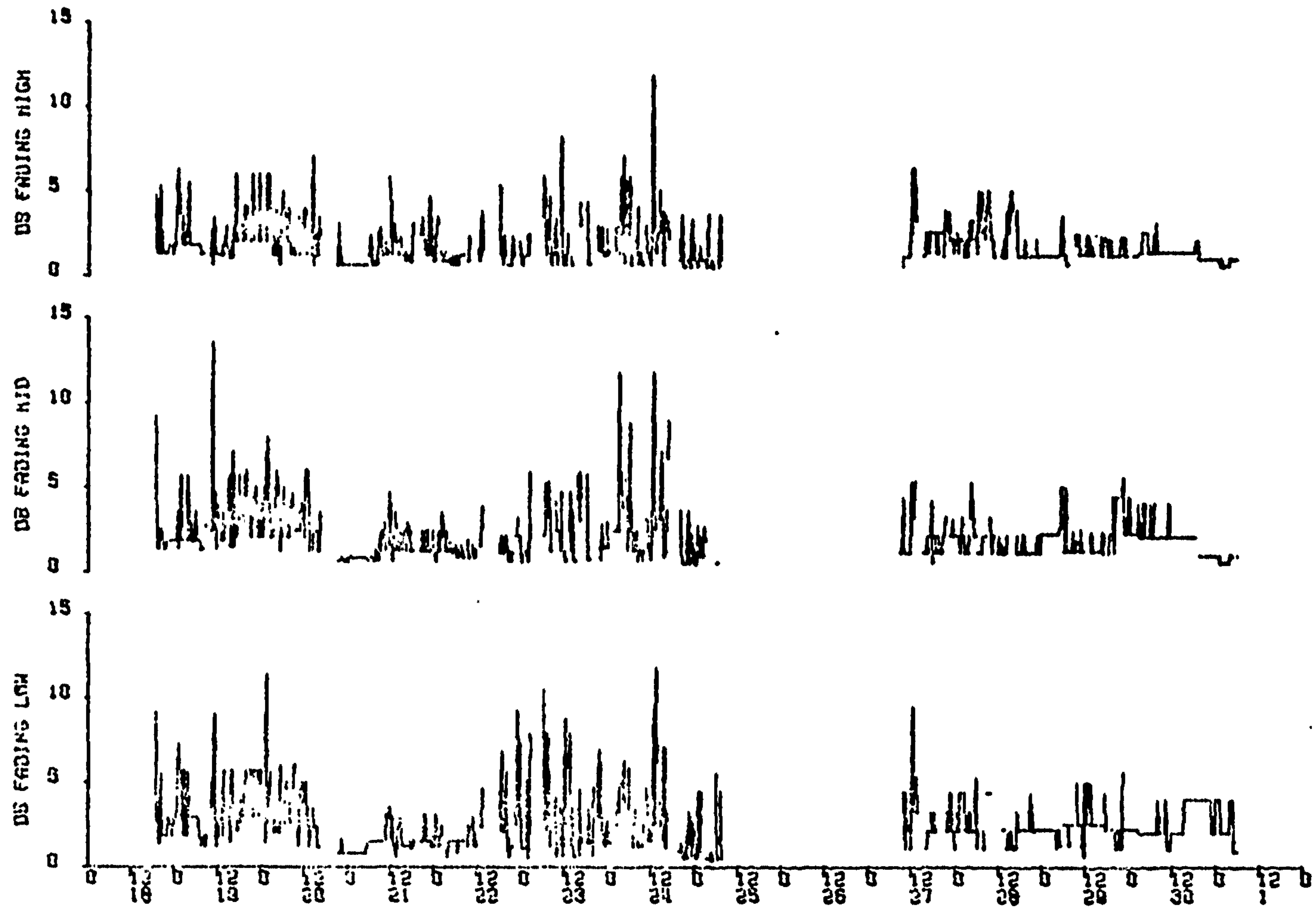

S BAND, NAXOS TO [illegible], GREECE APRIL 1972

Figure 39. Fading S-band

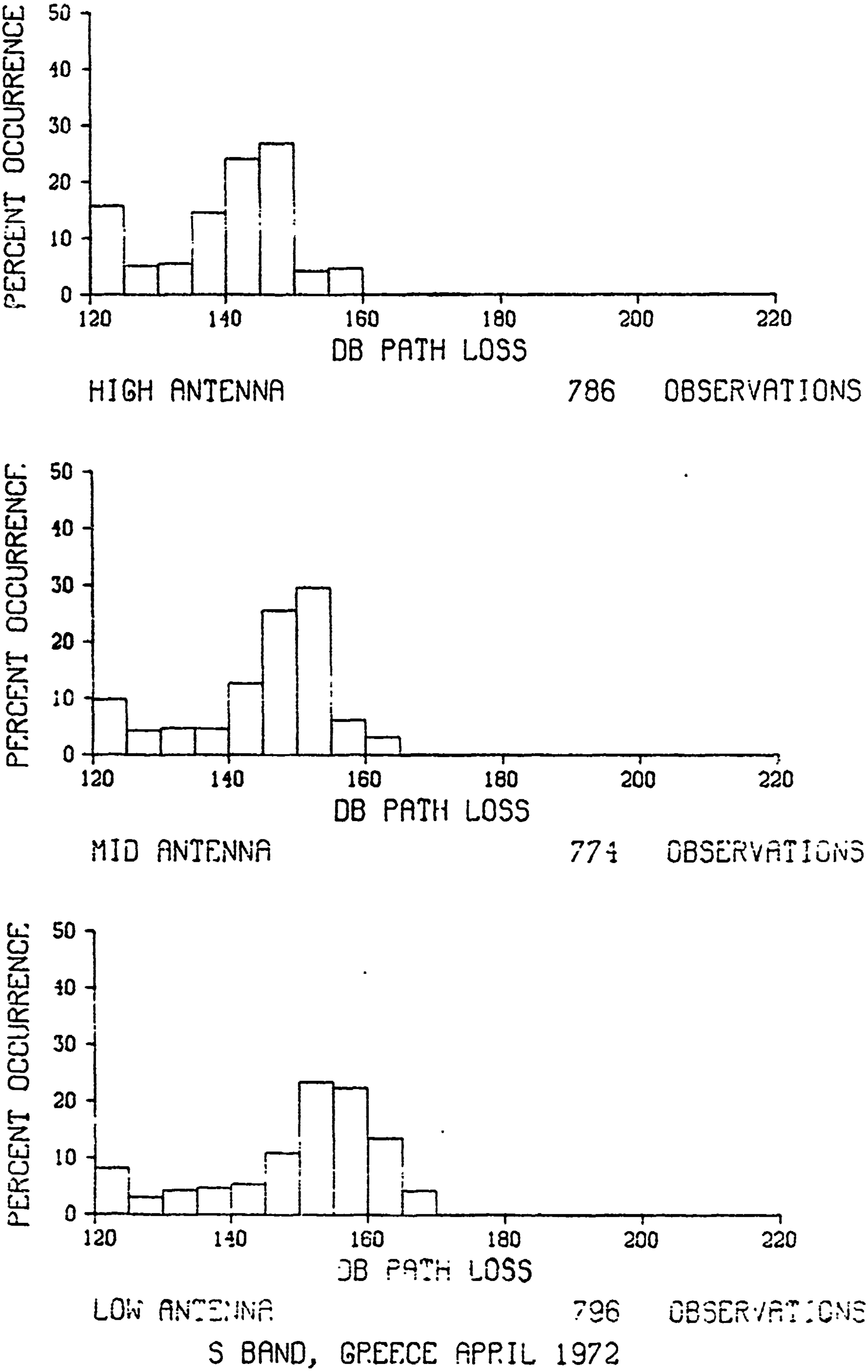

Figure 40. Frequency distributions of path loss for S-band

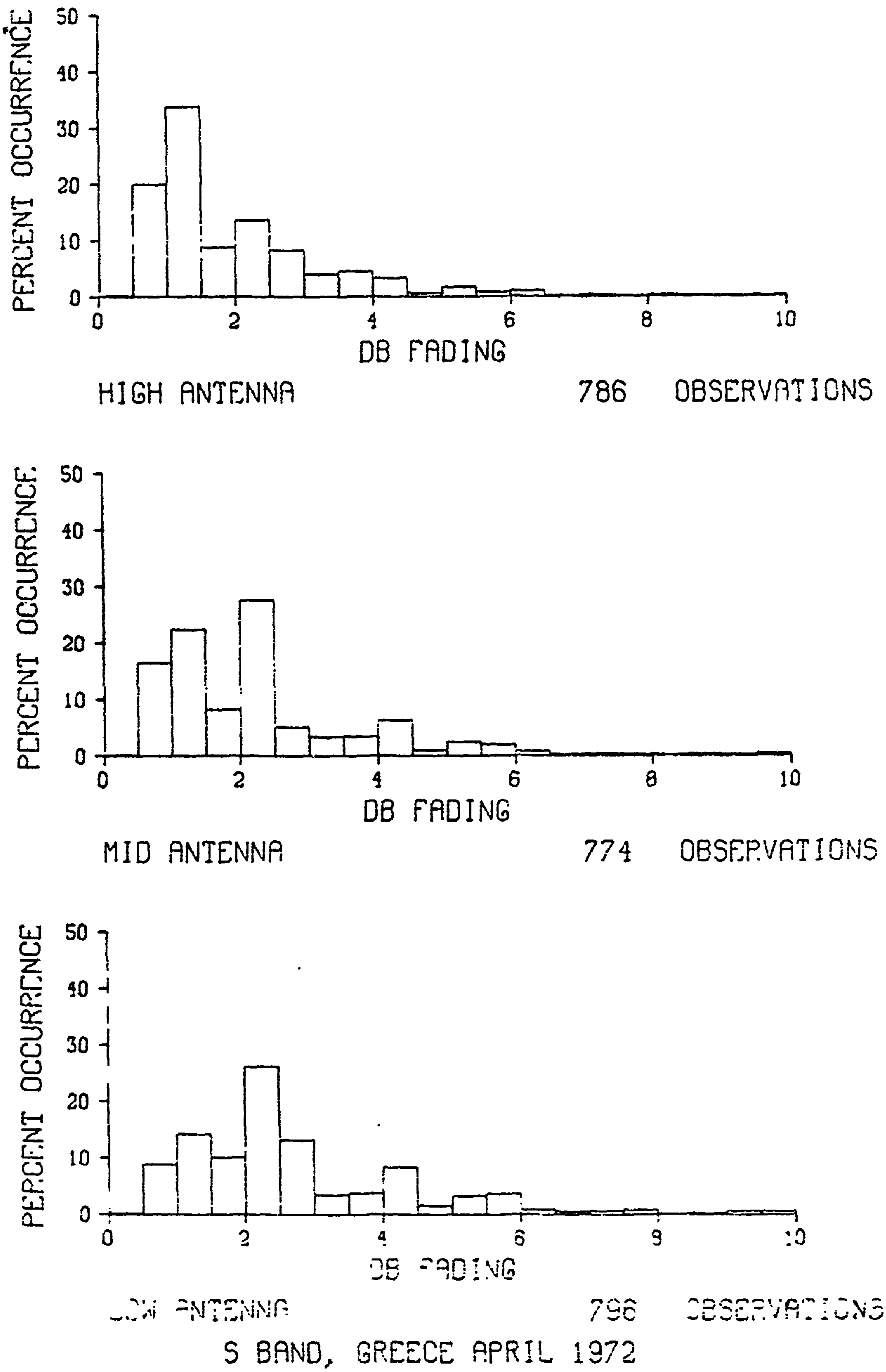

Figure 41. Frequency distributions of fading for S-band

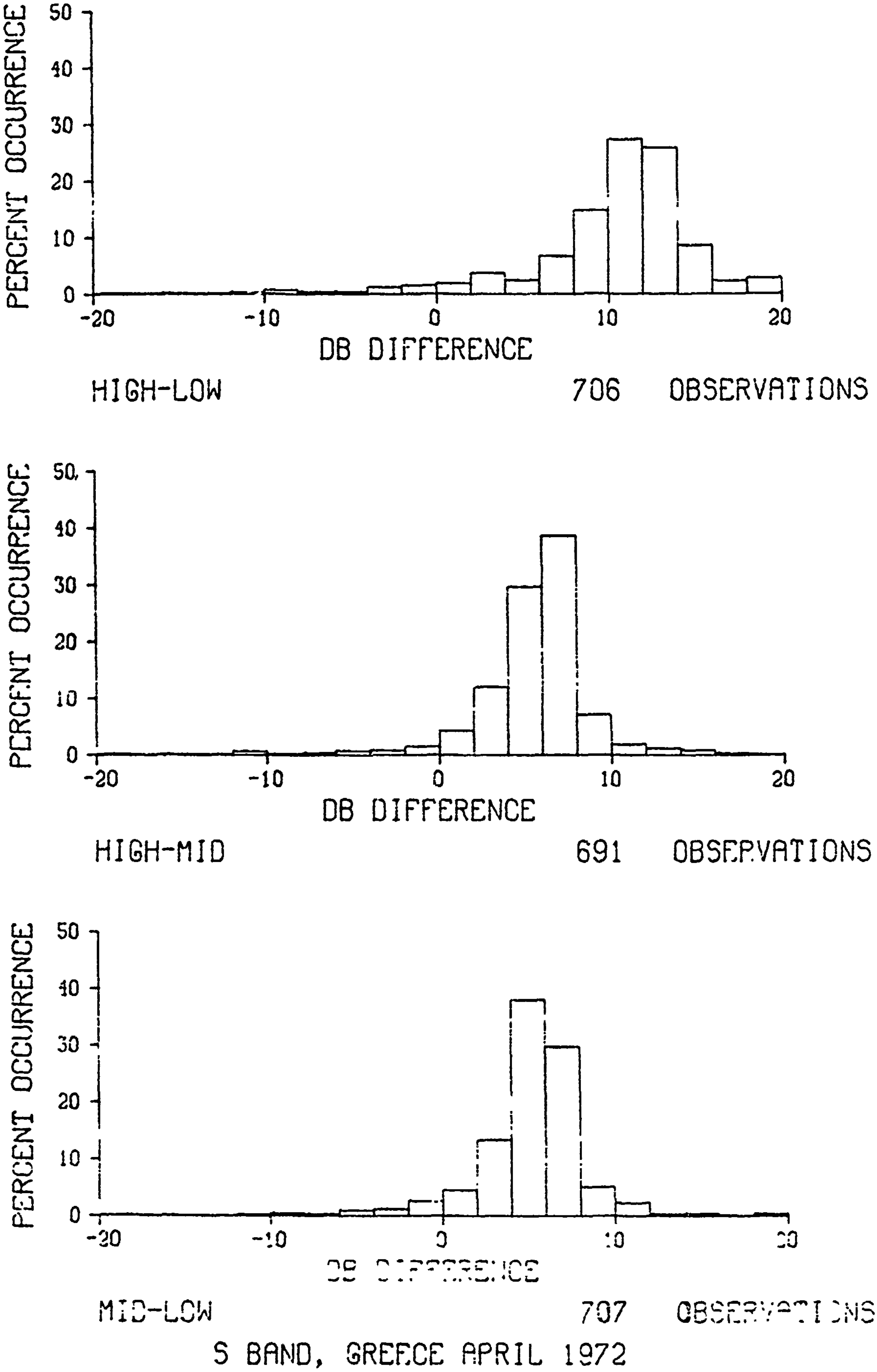

Figure 42. Frequency distributions of path loss differences between antennas for S-band

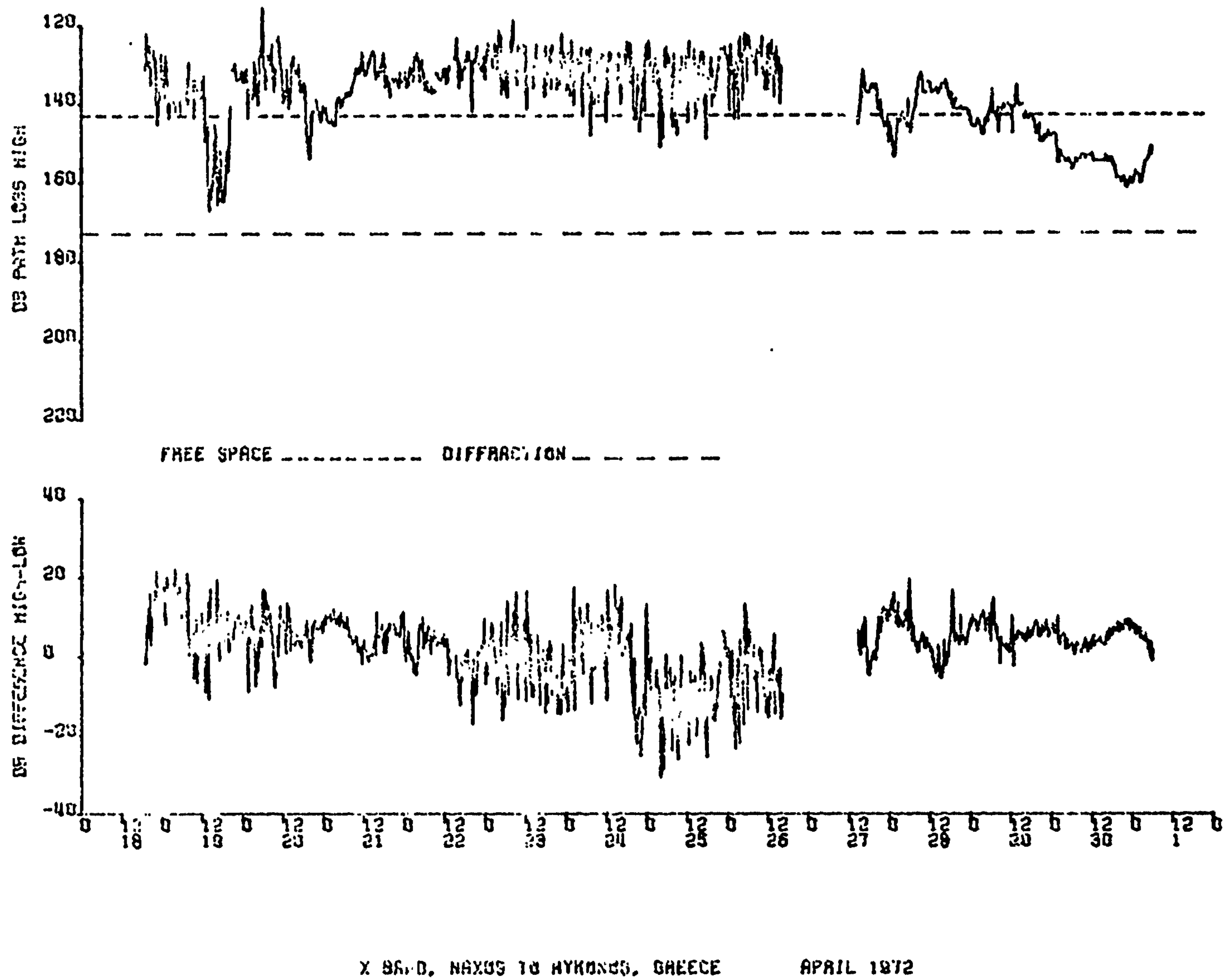

Figure 43. Path loss for high X-band antenna and path loss difference high-low antenna

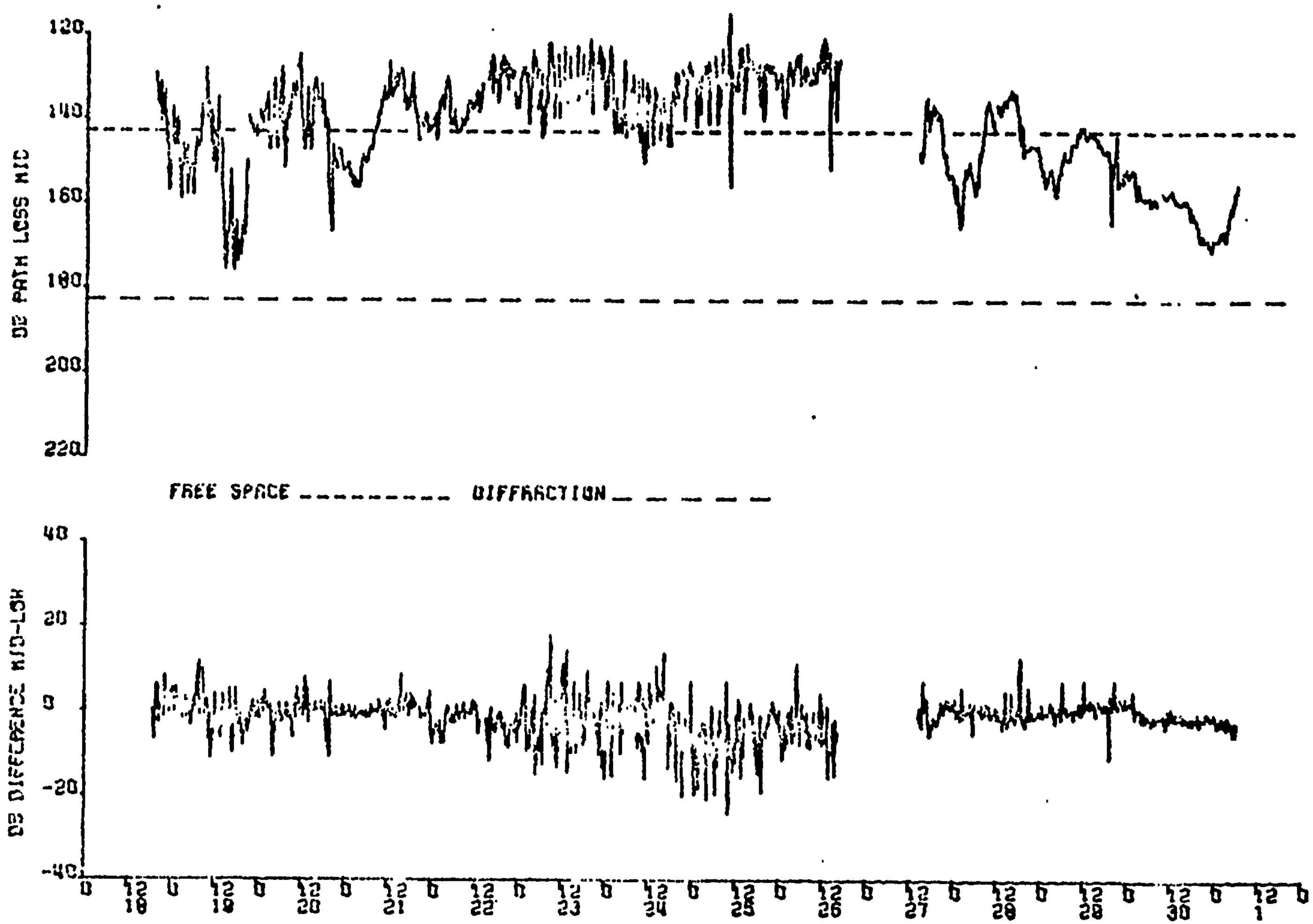

X BAND, NAXOS TO MYKONOS, GREECE APRIL 1972

Figure 44. Path loss middle X-band antenna and path loss difference mid-low antenna

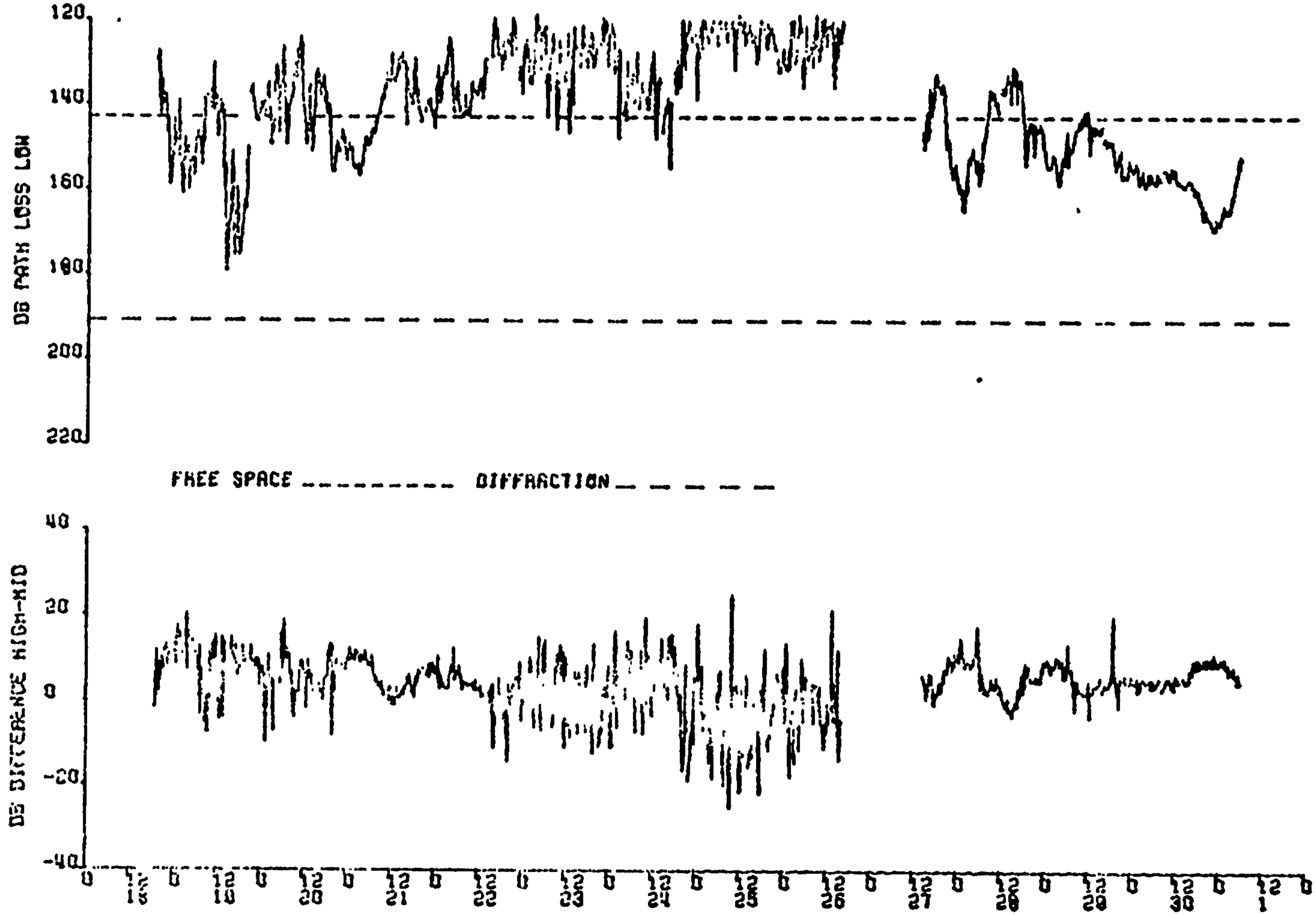

X BAND, NAXOS TO MYKONOS, GREECE APRIL 1972

Figure 45. Path loss low X-band antenna and path loss difference high-mid antenna

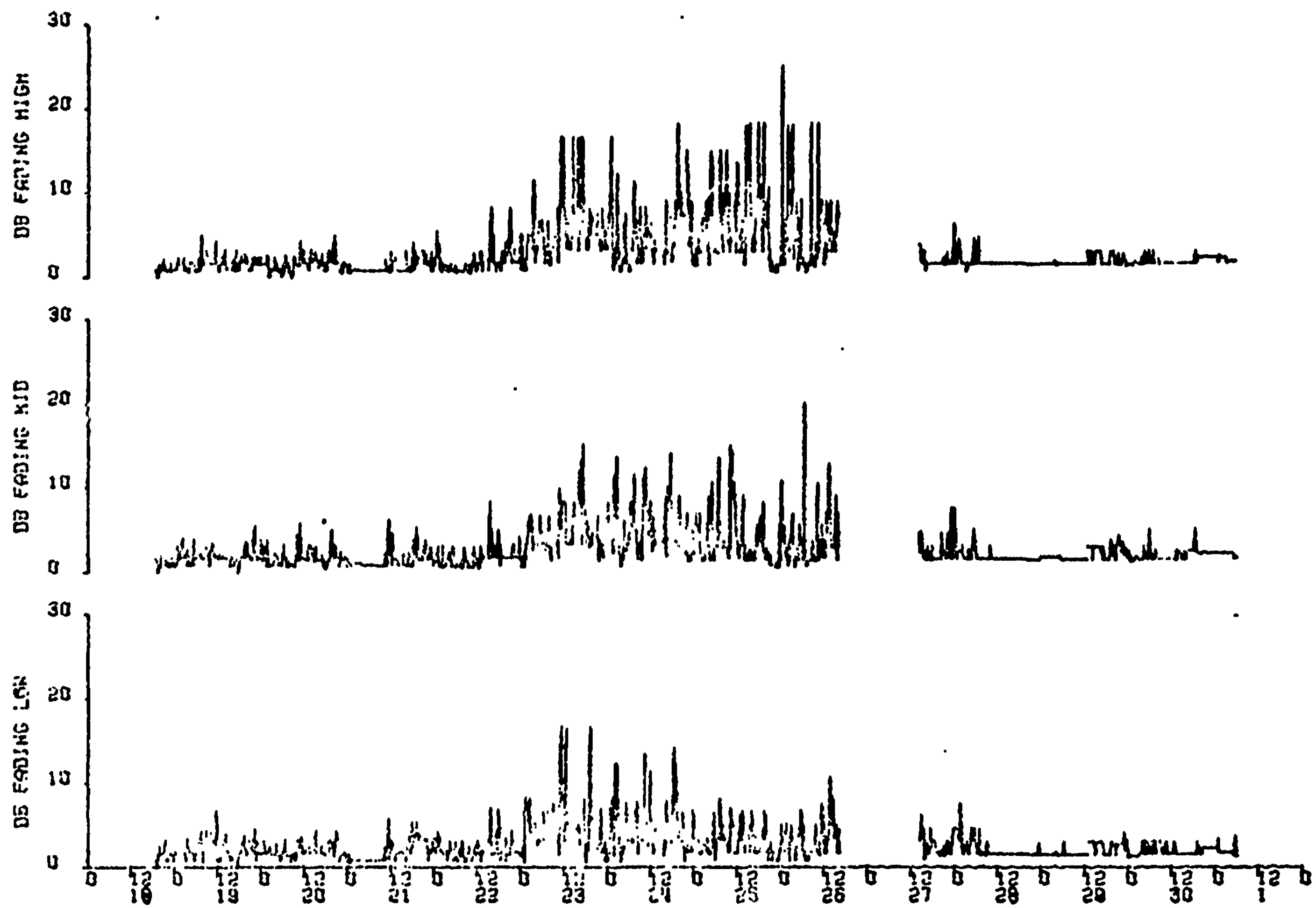

X BAND, NAXOS TO MYKONOS, GREECE APRIL 1972

Figure 46. Fading X-band

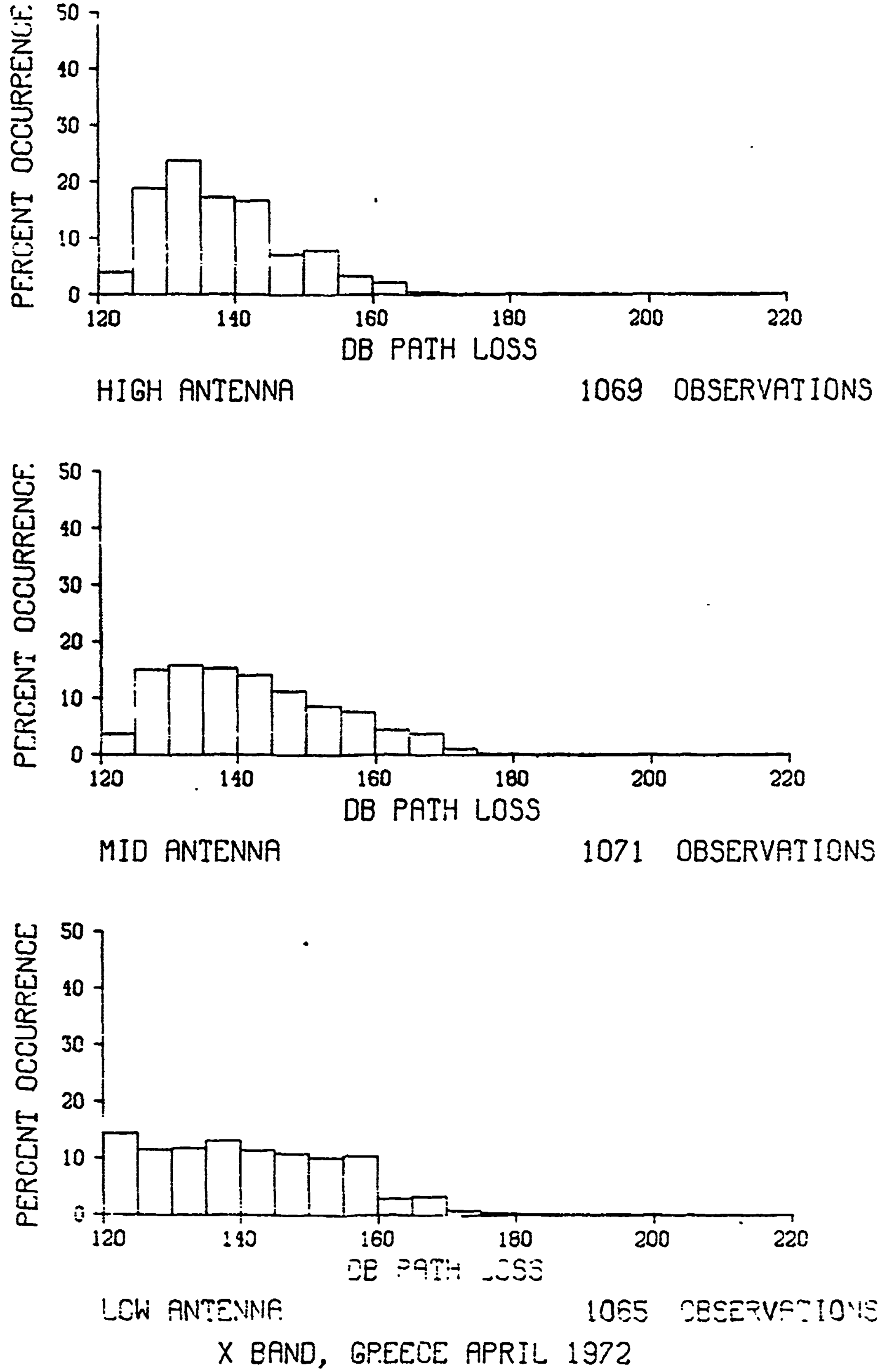

Figure 47. Frequency distribution of path loss for X-band

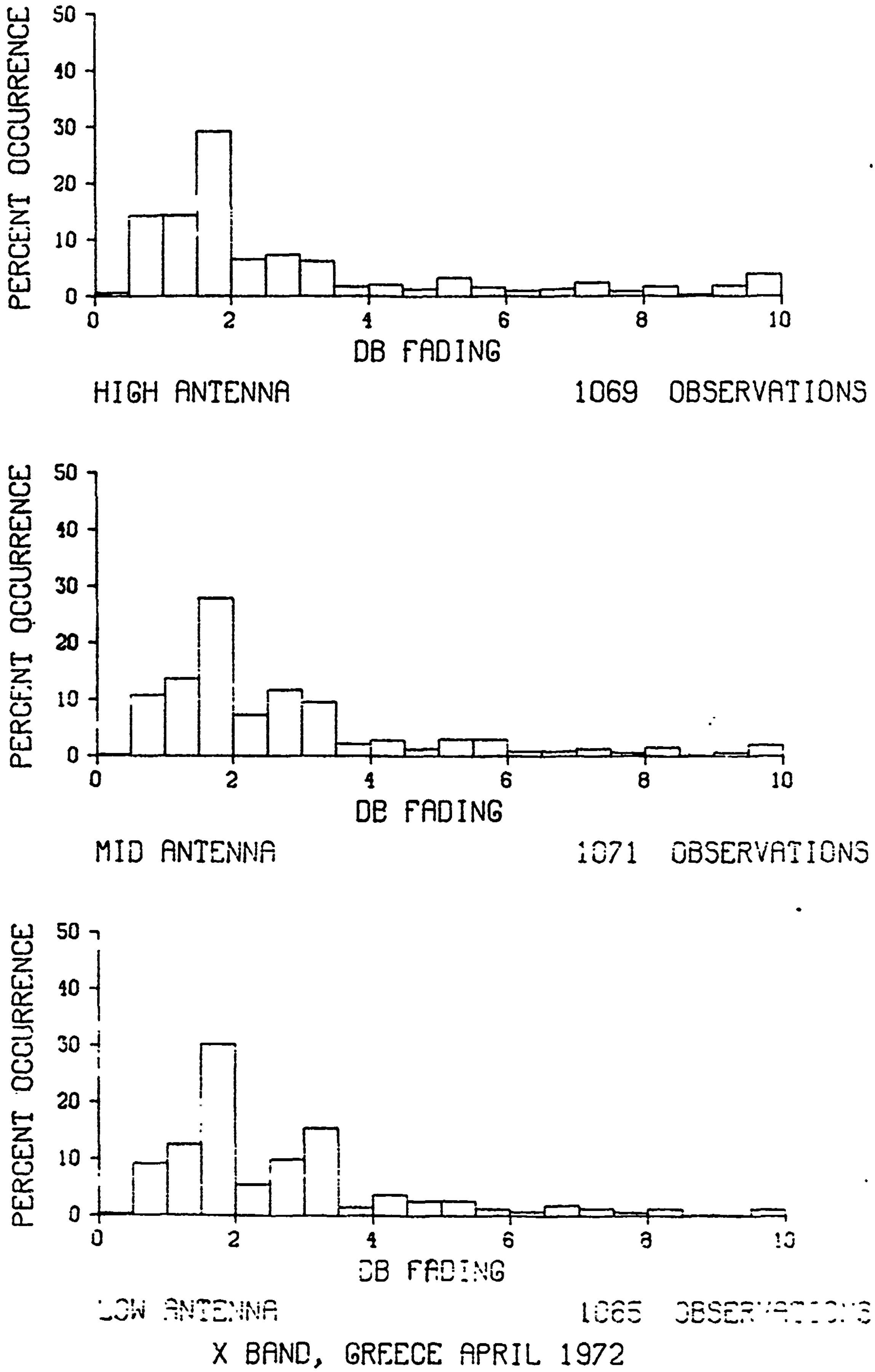

Figure 48. Frequency distribution of fading X-band

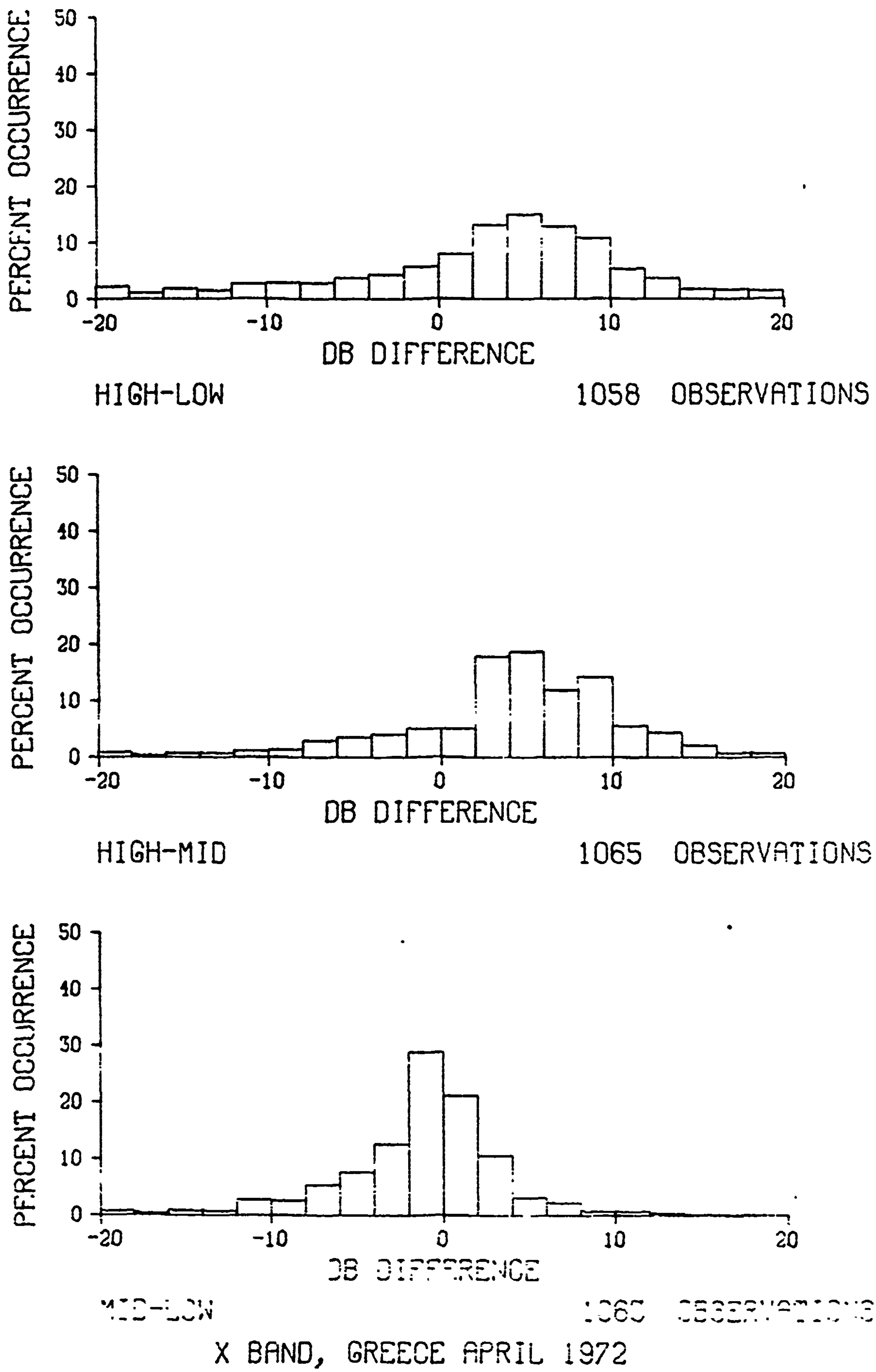

Figure 49. Frequency distribution of differences between antennas for X-band

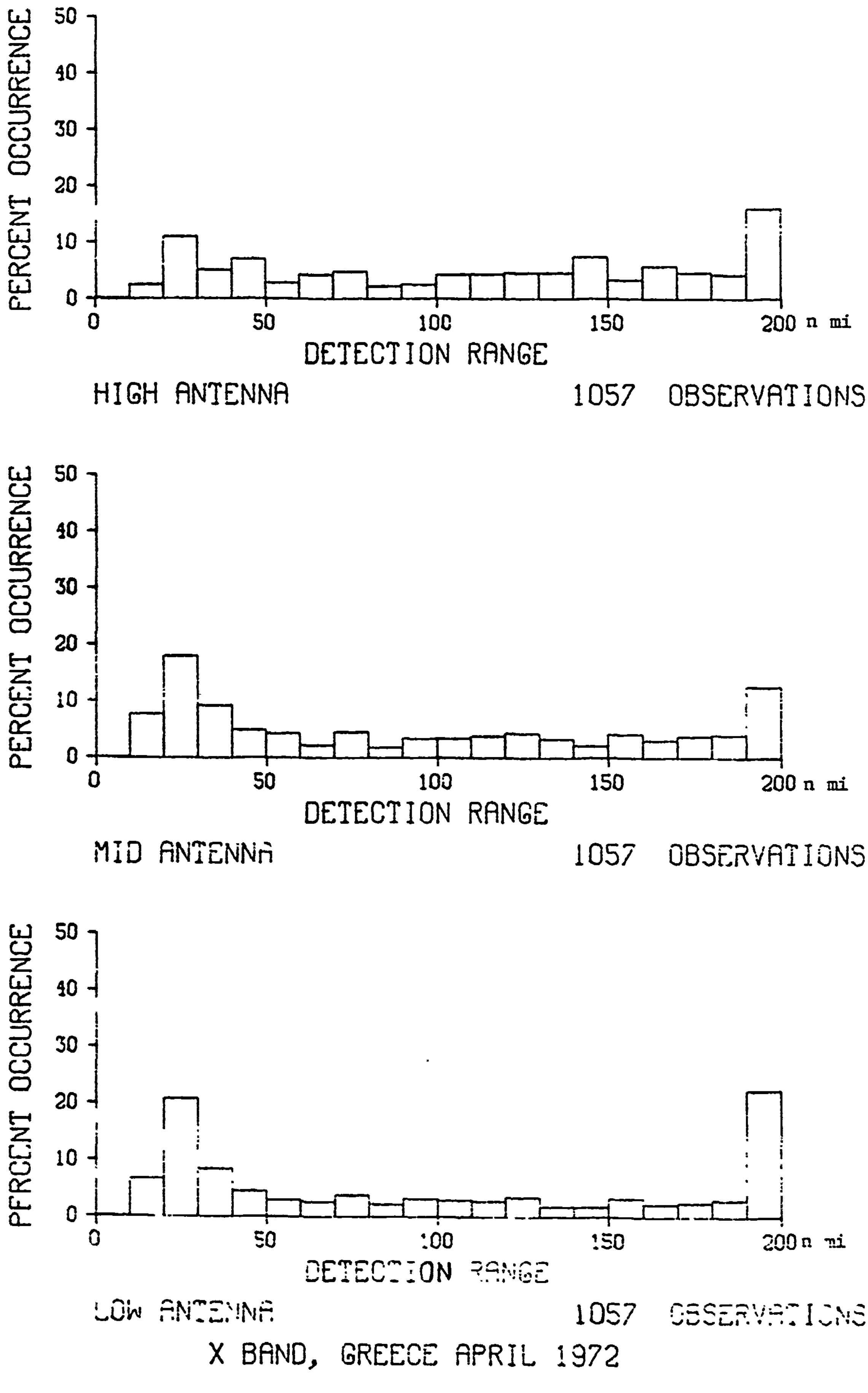

Figure 50. Frequency distribution of detection range for X-band

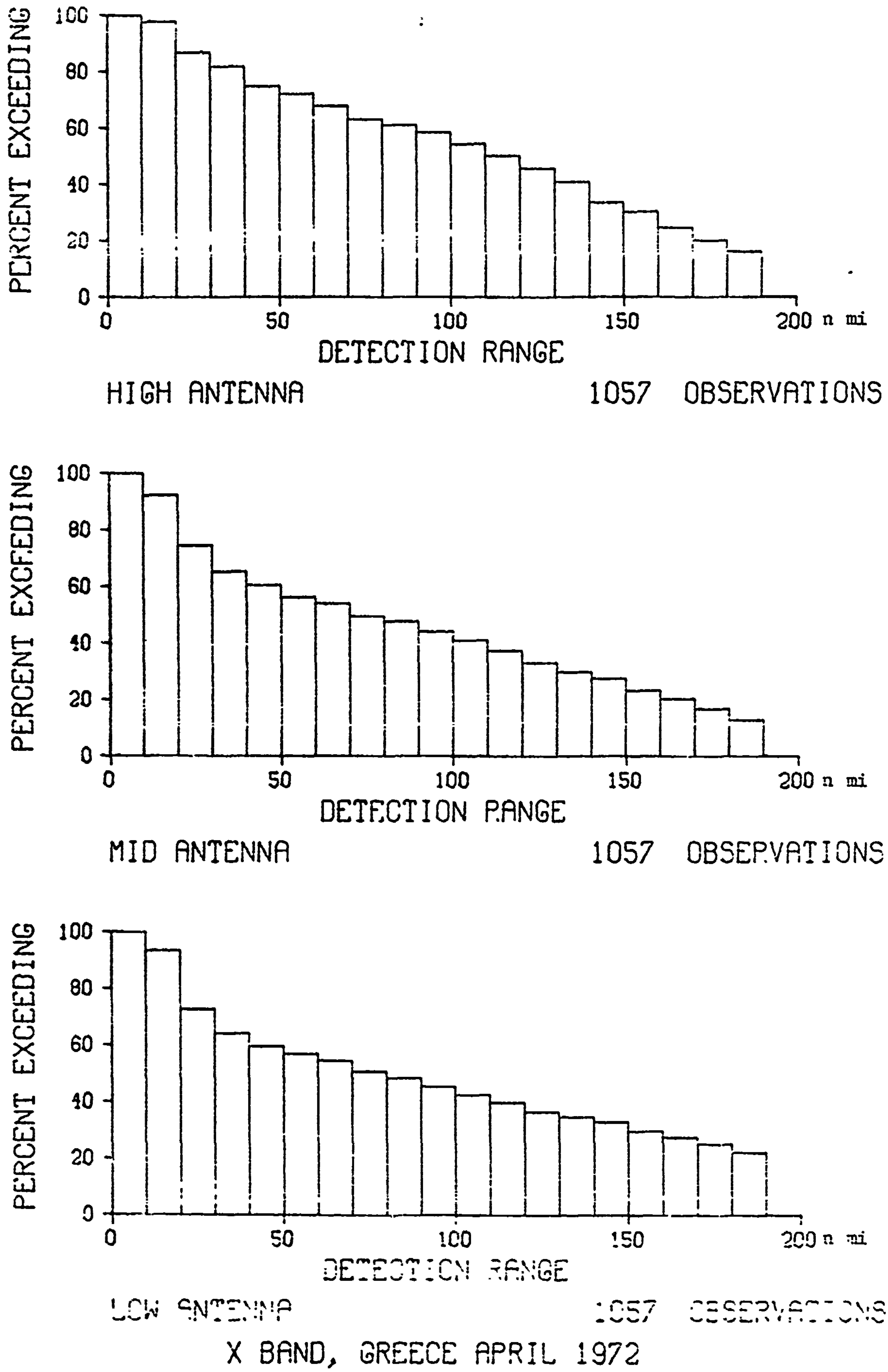

Figure 51. Cumulative distribution of detection range for X-band

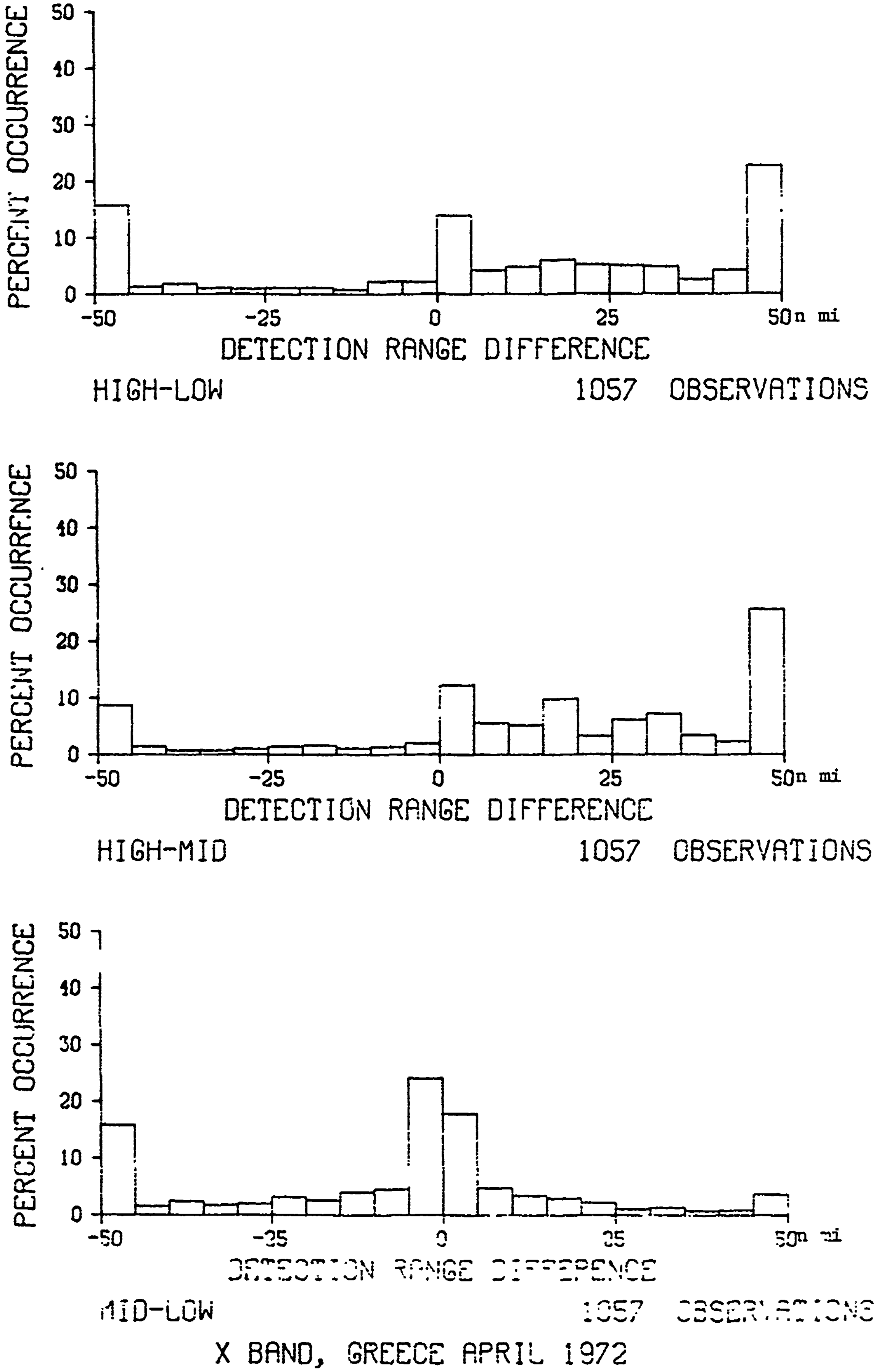

Figure 52. Frequency distribution of detection range differences between antennas for X-band

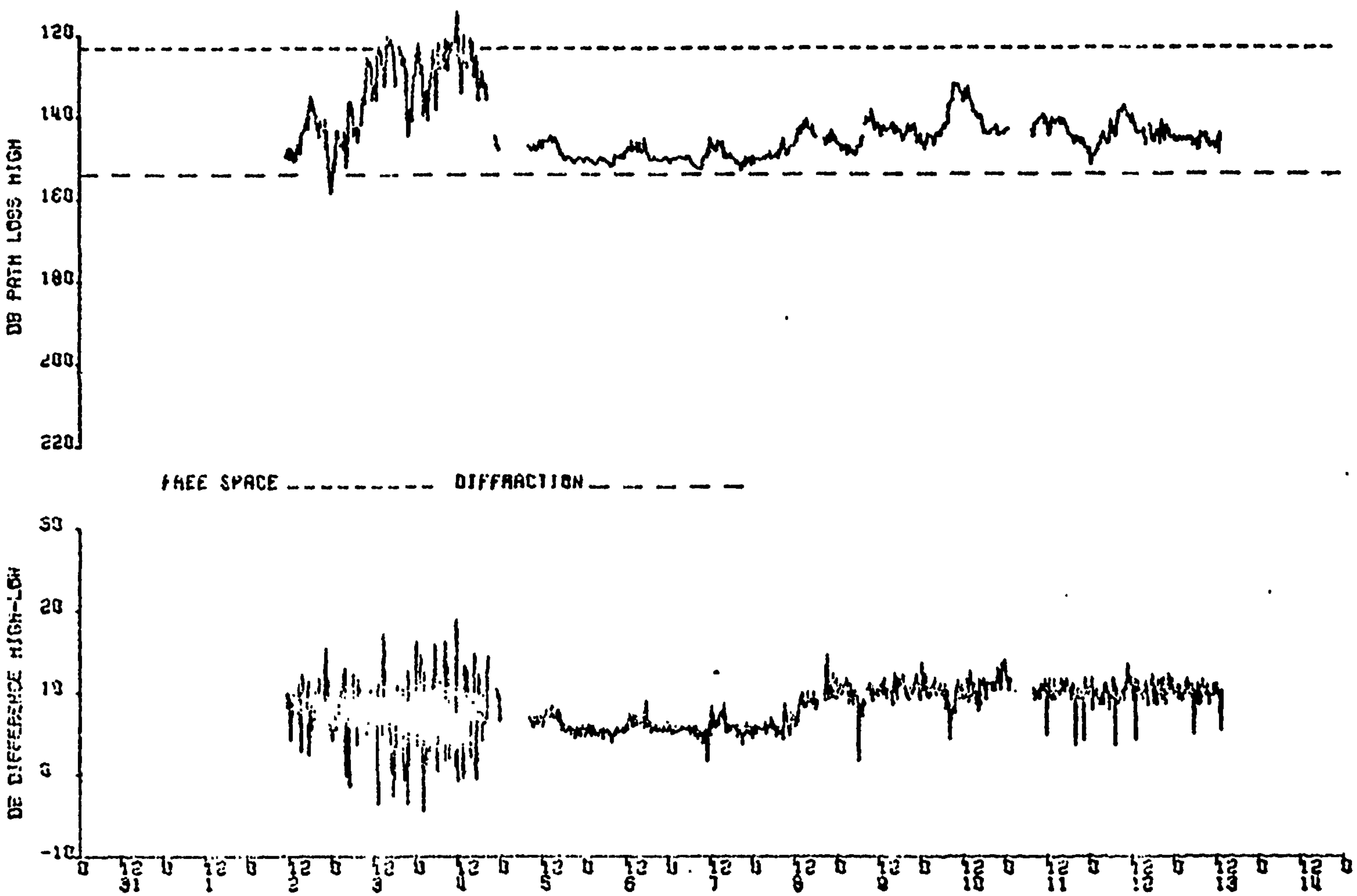

L BAND, NAXOS TO MYKONOS, GREECE AUGUST 1972

Figure 53. Path loss for high L-band antenna and path loss difference high-low antenna

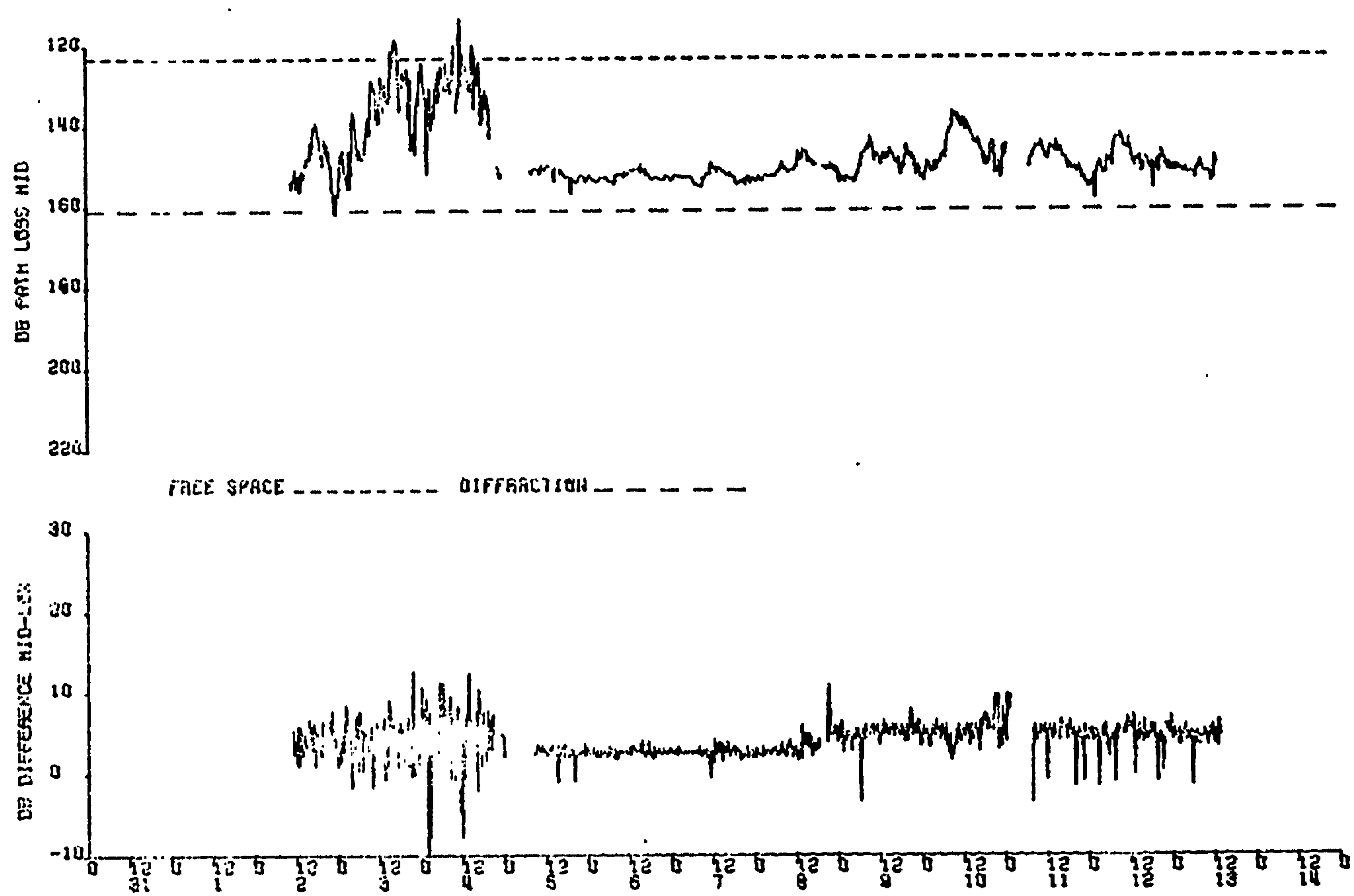

L BAND, NAXOS TO MYKONOS, GREECE AUGUST 1972

Figure 54. Path loss for middle L-band antenna and path loss difference mid-low antenna

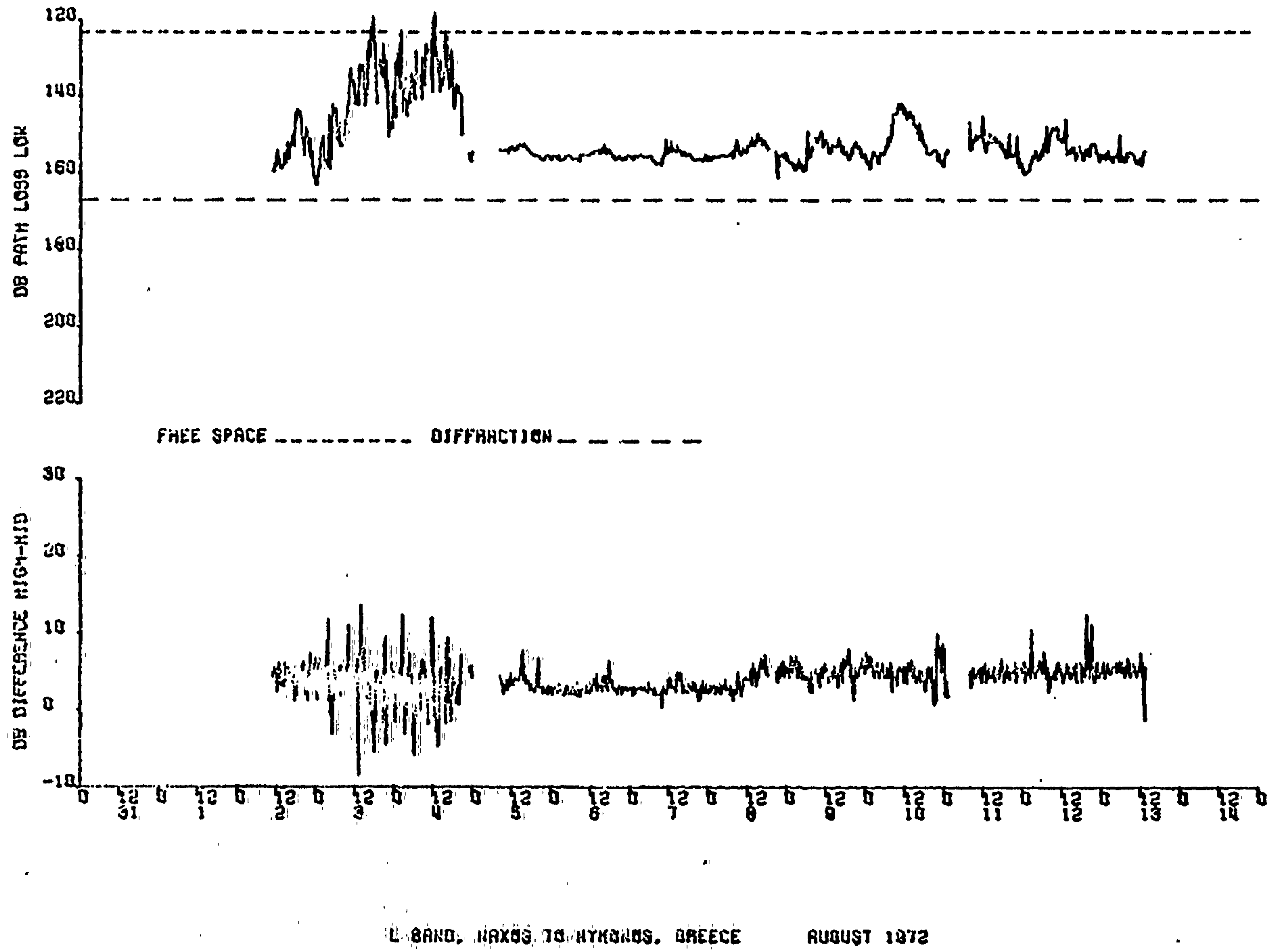

Figure 55. Path loss for low L-band antenna and path loss difference high-mid antenna

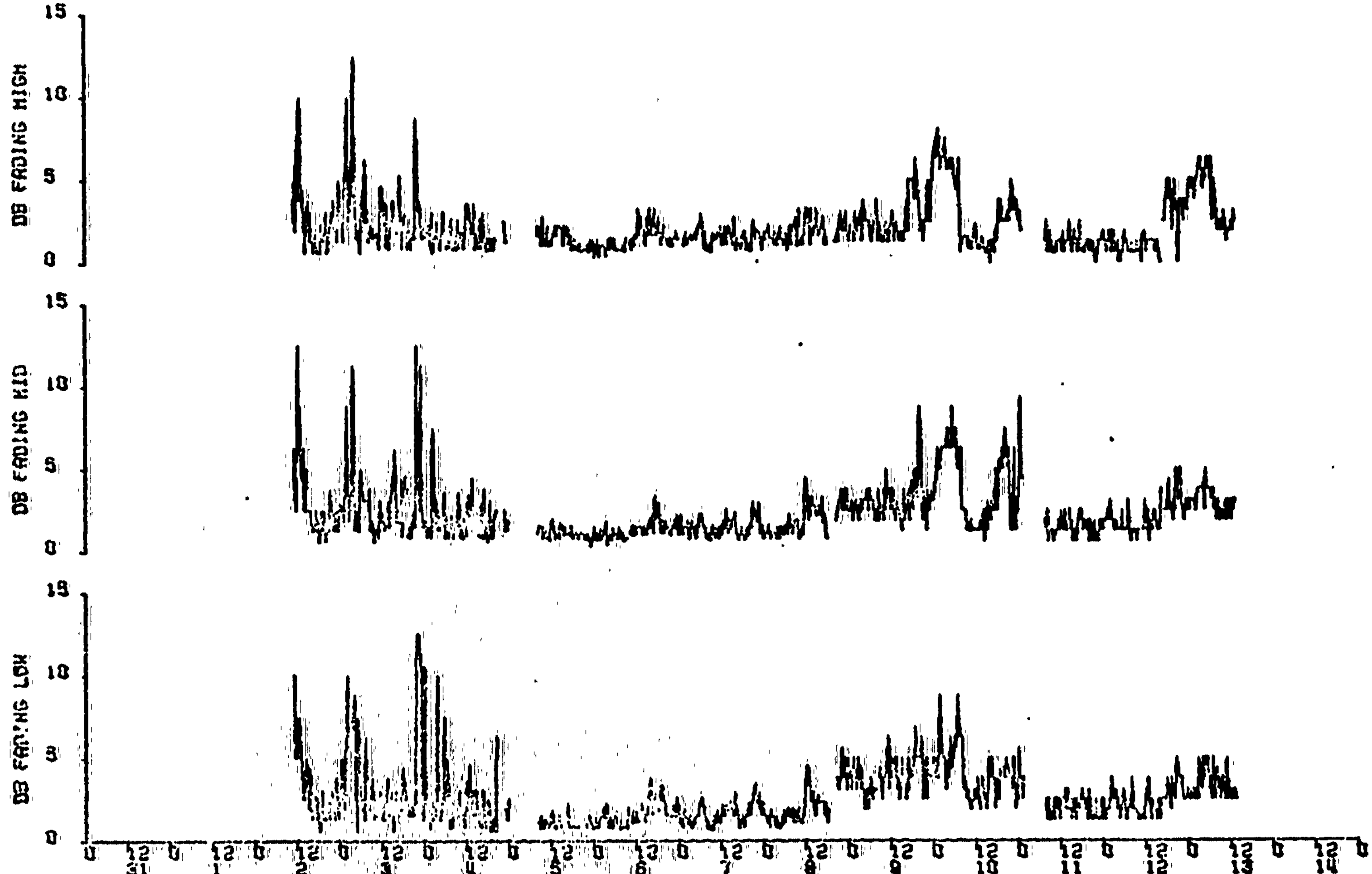

L BAND, NAXOS TO MYKONOS, GREECE AUGUST 1972

Figure 56. Fading L-band

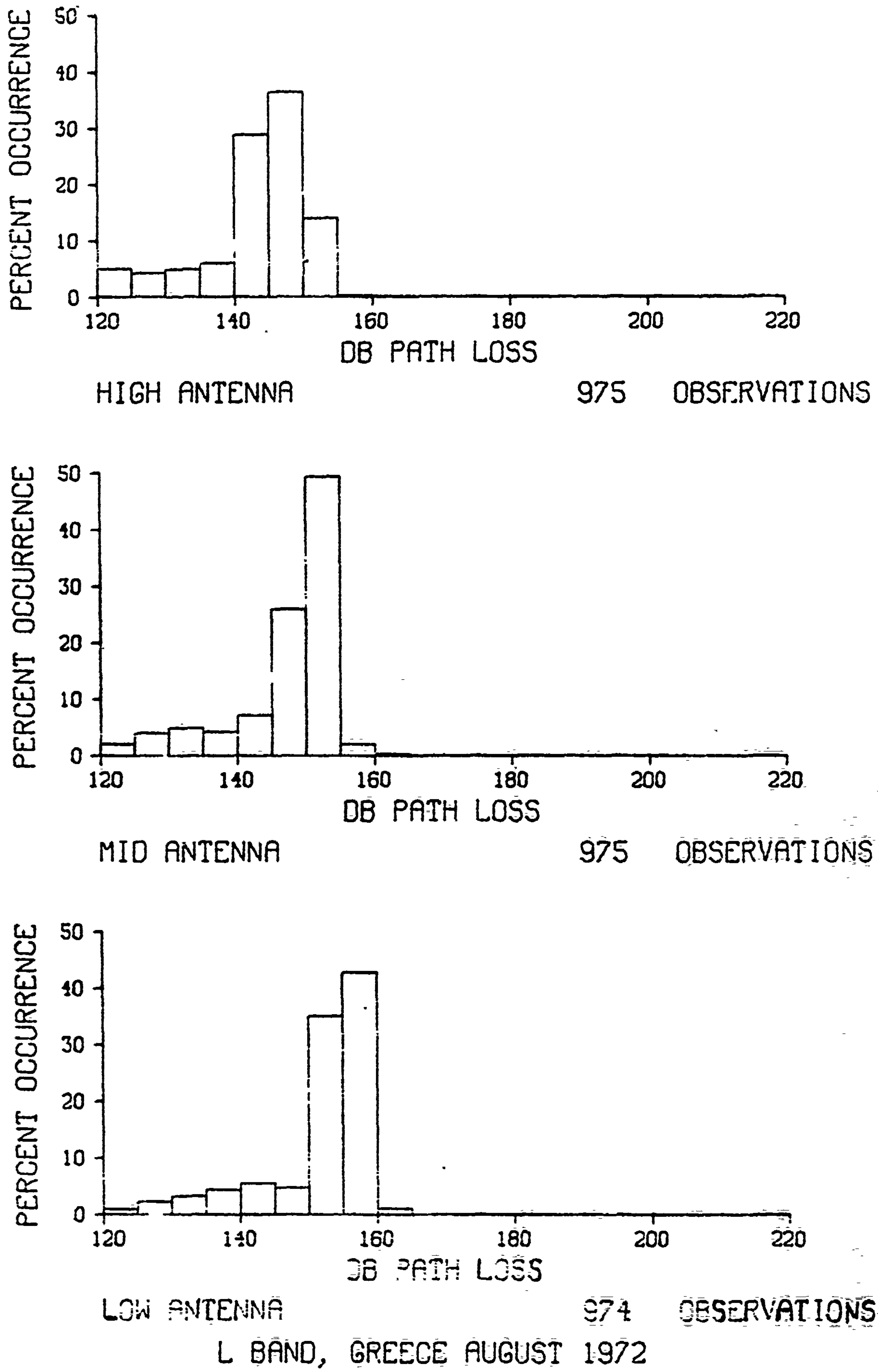

Figure 57. Frequency distributions of path loss for L-band

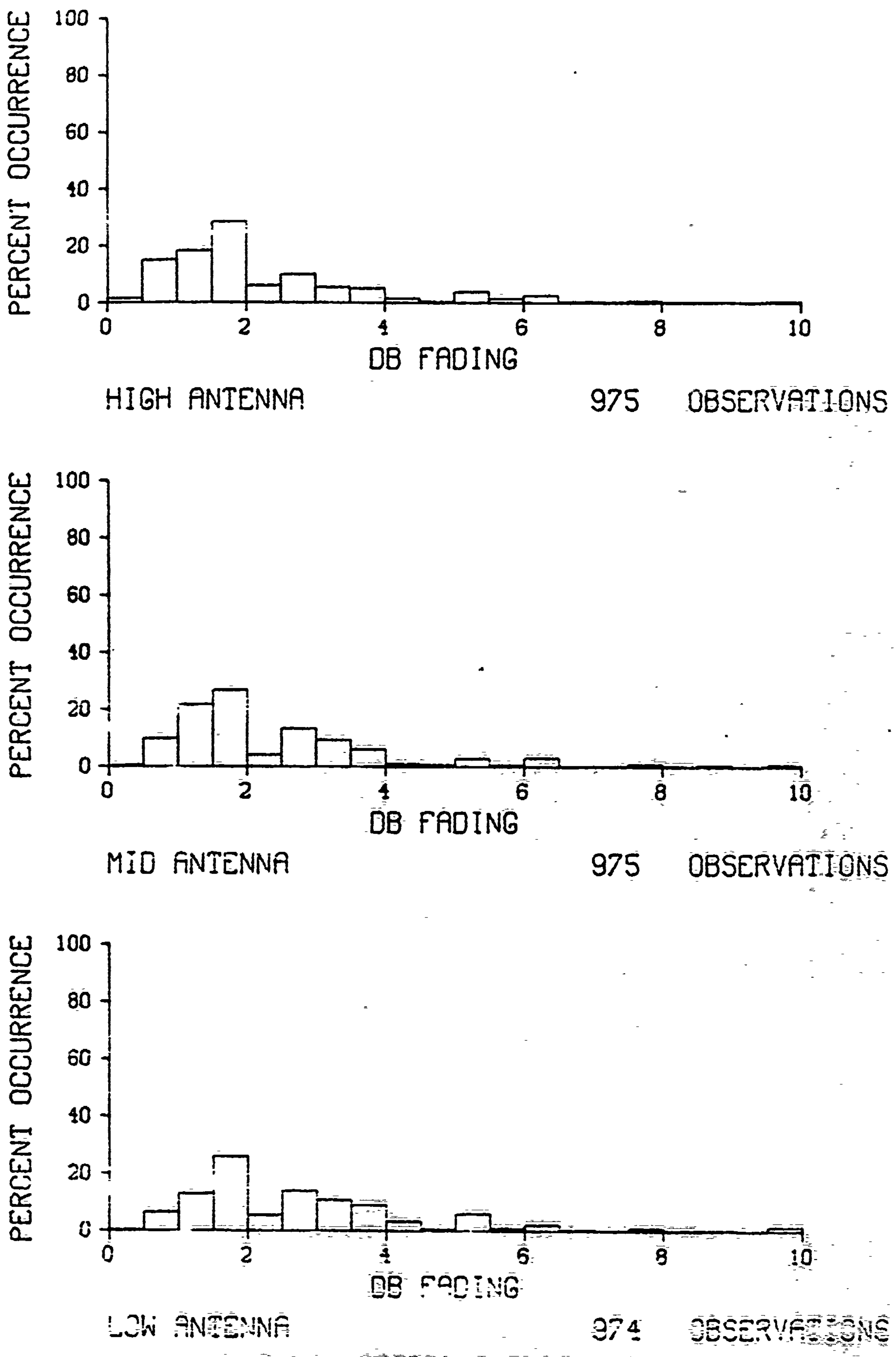

Figure 58. Frequency distributions of fading L-band

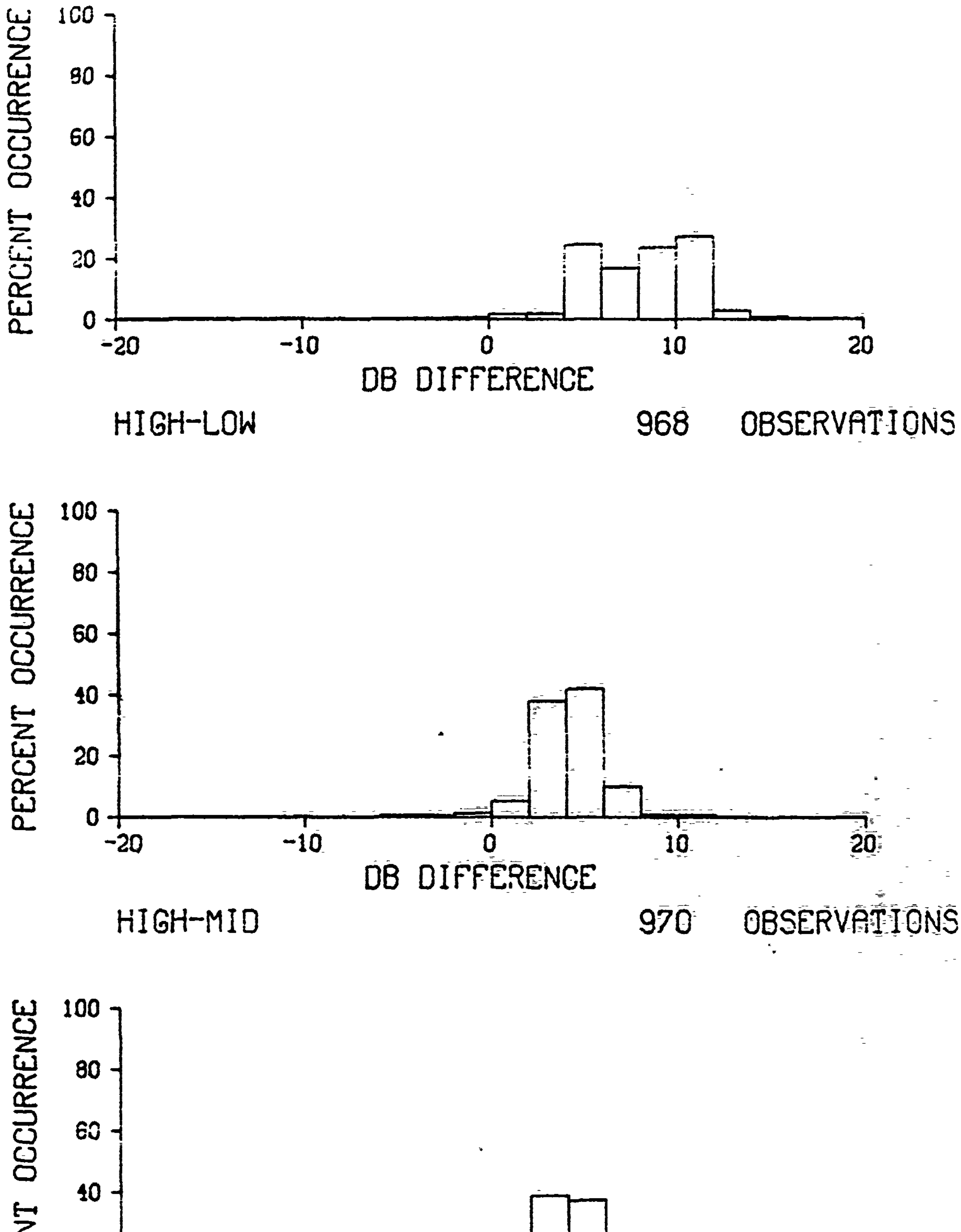

Figure 59. Frequency distributions of path loss differences between antennas for L-band

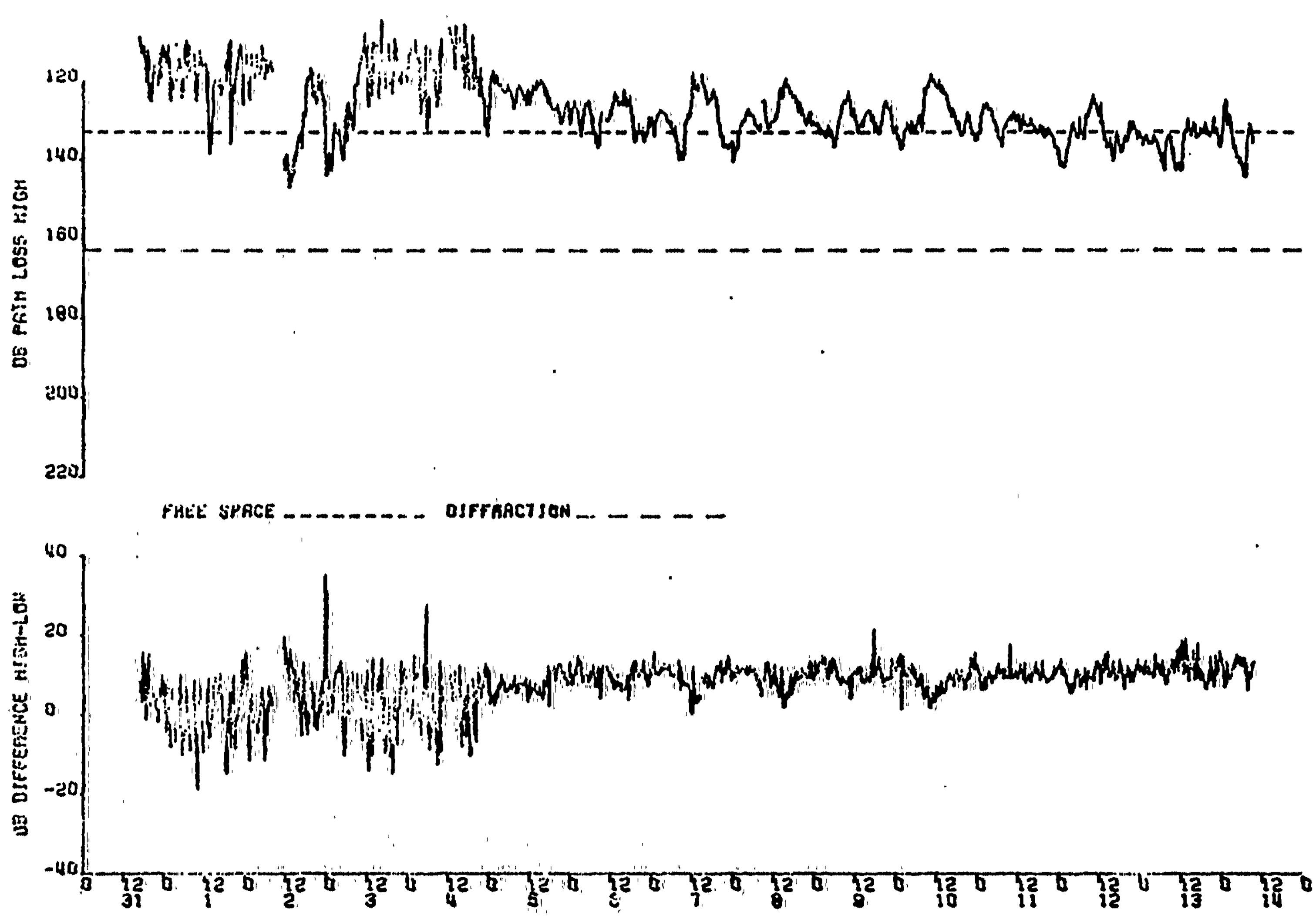

Figure 60. Path loss for high S-band antenna and path loss difference high-low antenna

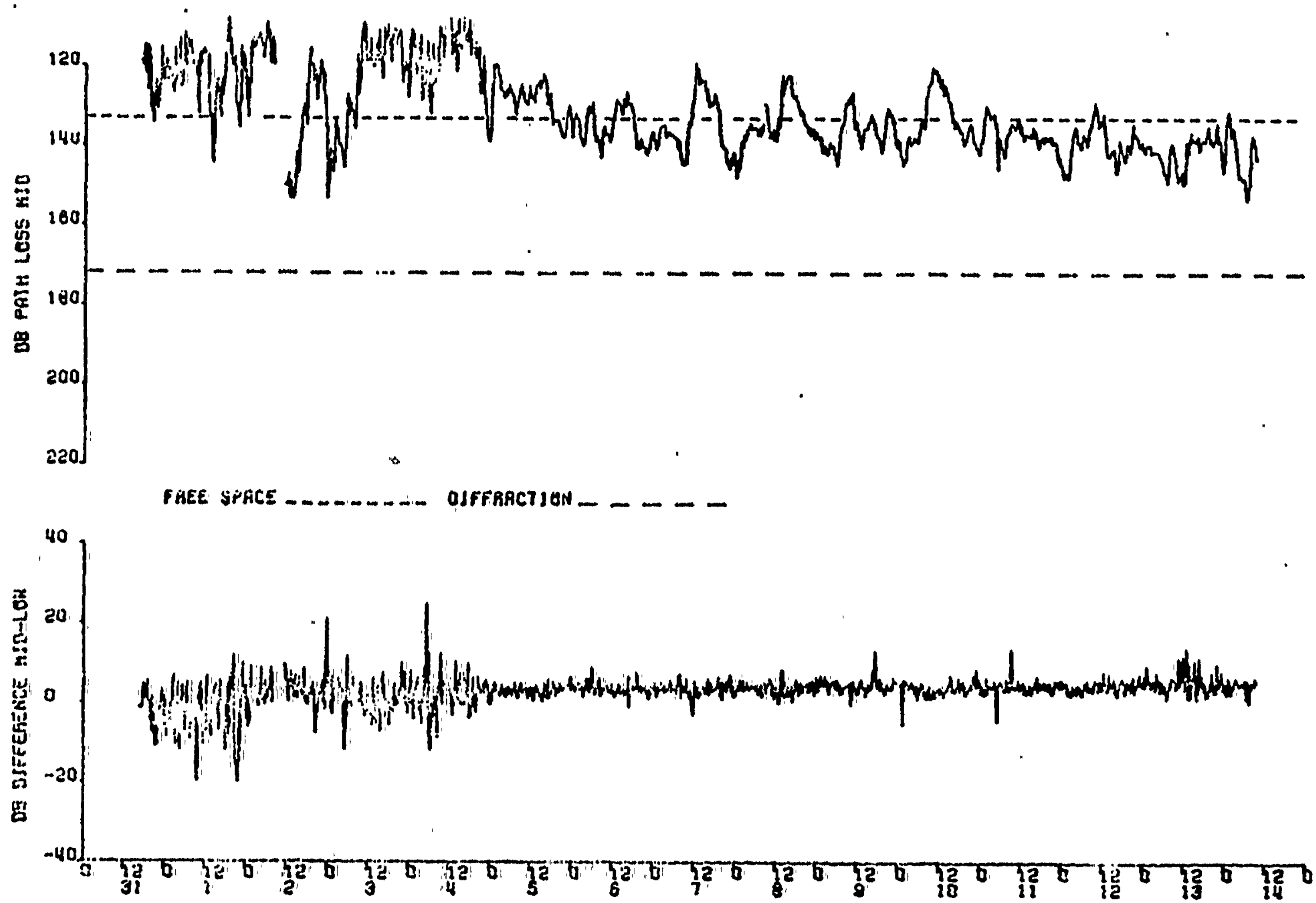

S BAND, NAXOS TO HYMETTUS, GREECE AUGUST 1972

Figure 61. Path loss for middle S-band antenna and path loss difference mid-low antenna

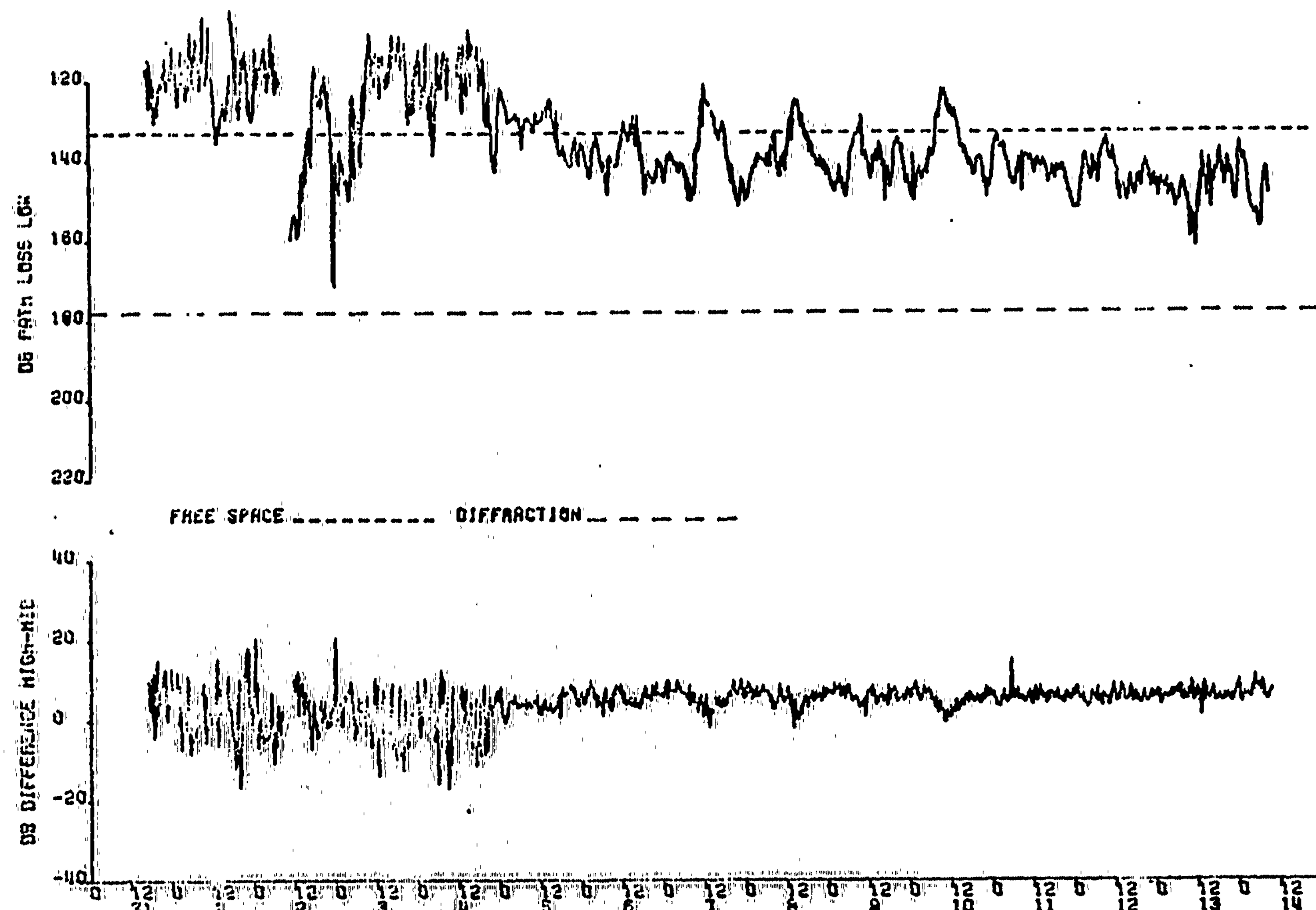

S BAND, NAXOS TO MYKONOS, GREECE   AUGUST 1972

Figure 62. Path loss for low S-band antenna and path loss difference high-mid antenna

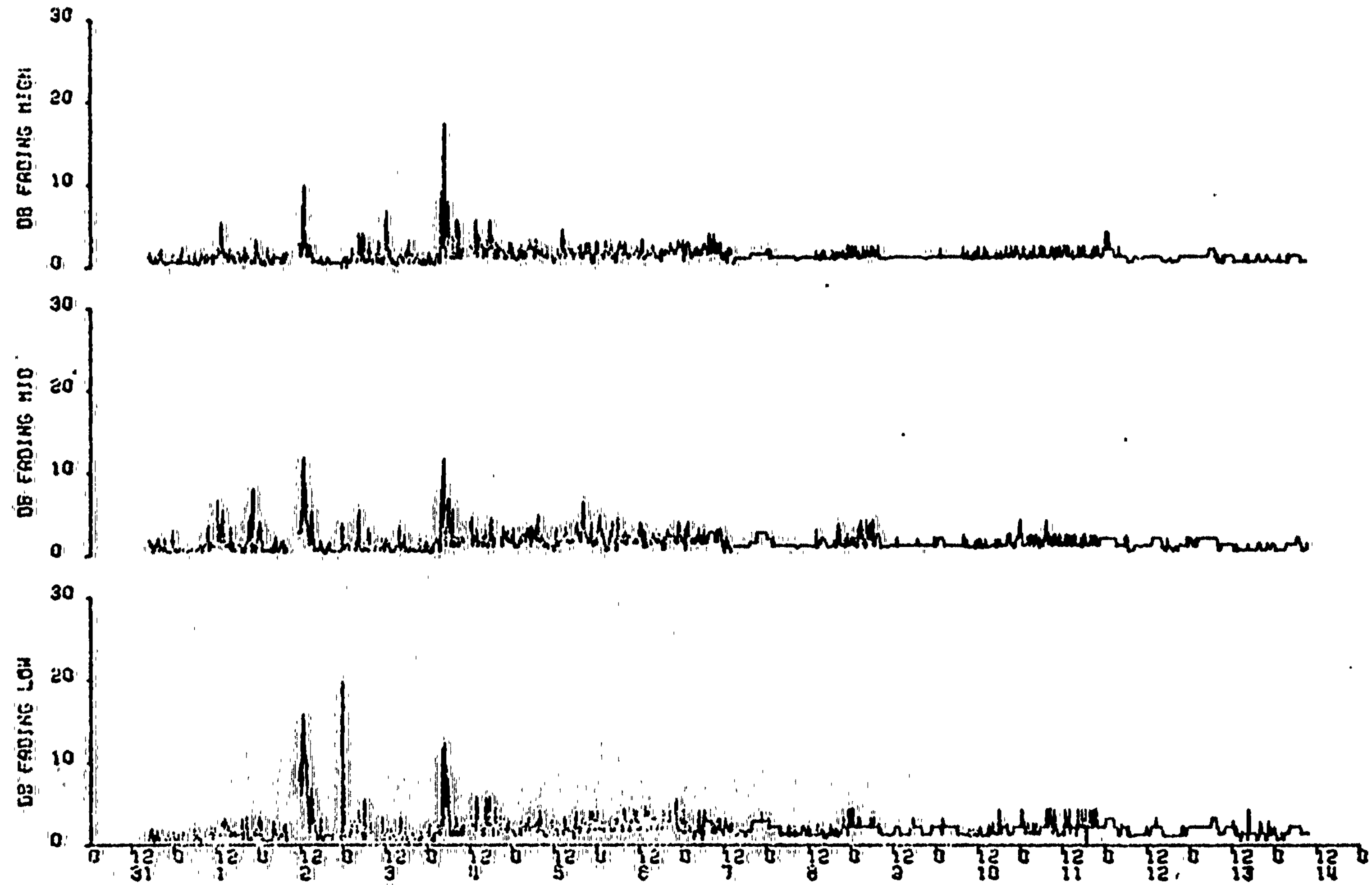

S BAND, NAXOS TO MYKONOS, GREECE AUGUST 1972

Figure 63. Fading S-band

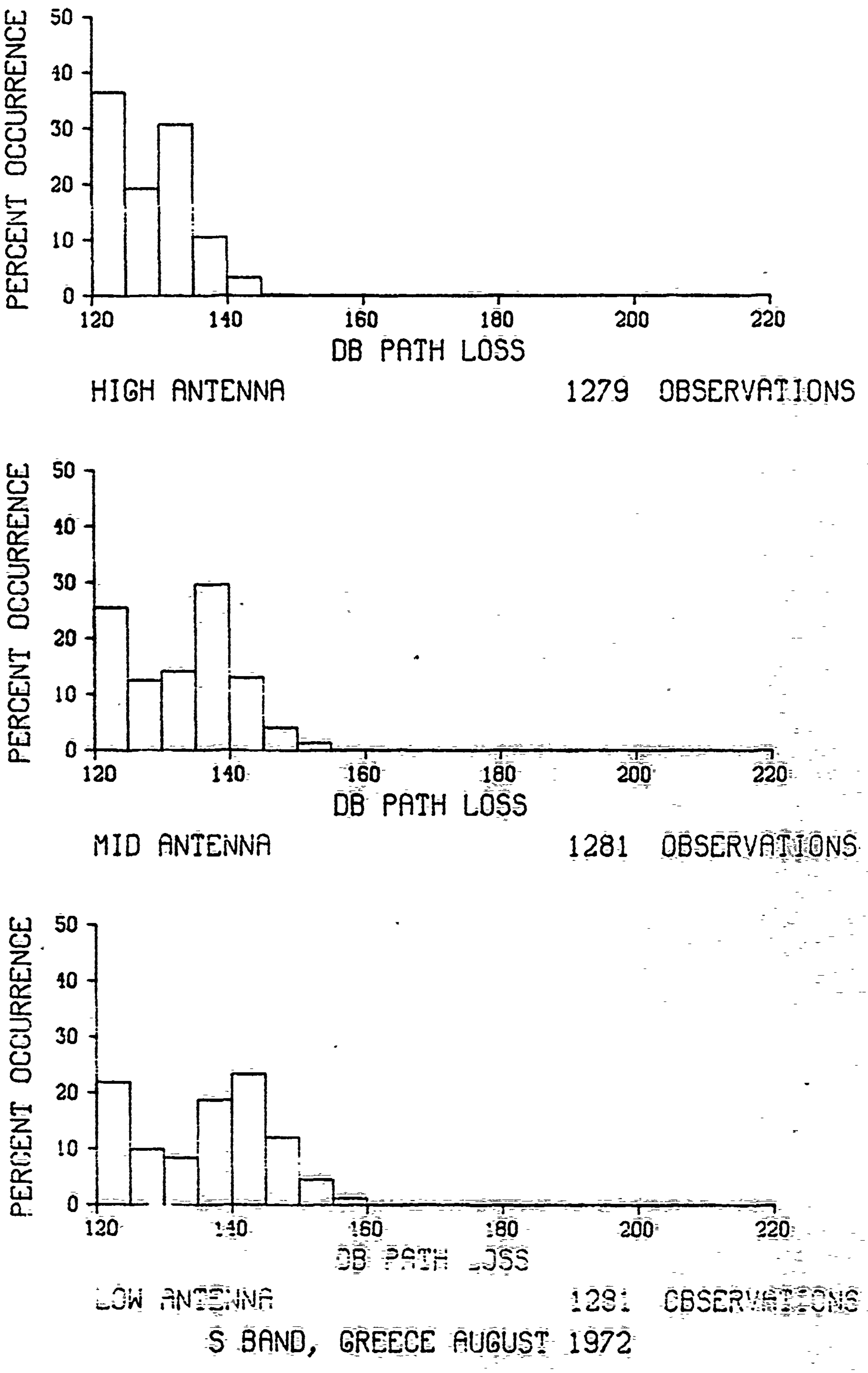

Figure 64. Frequency distributions of path loss for S-band

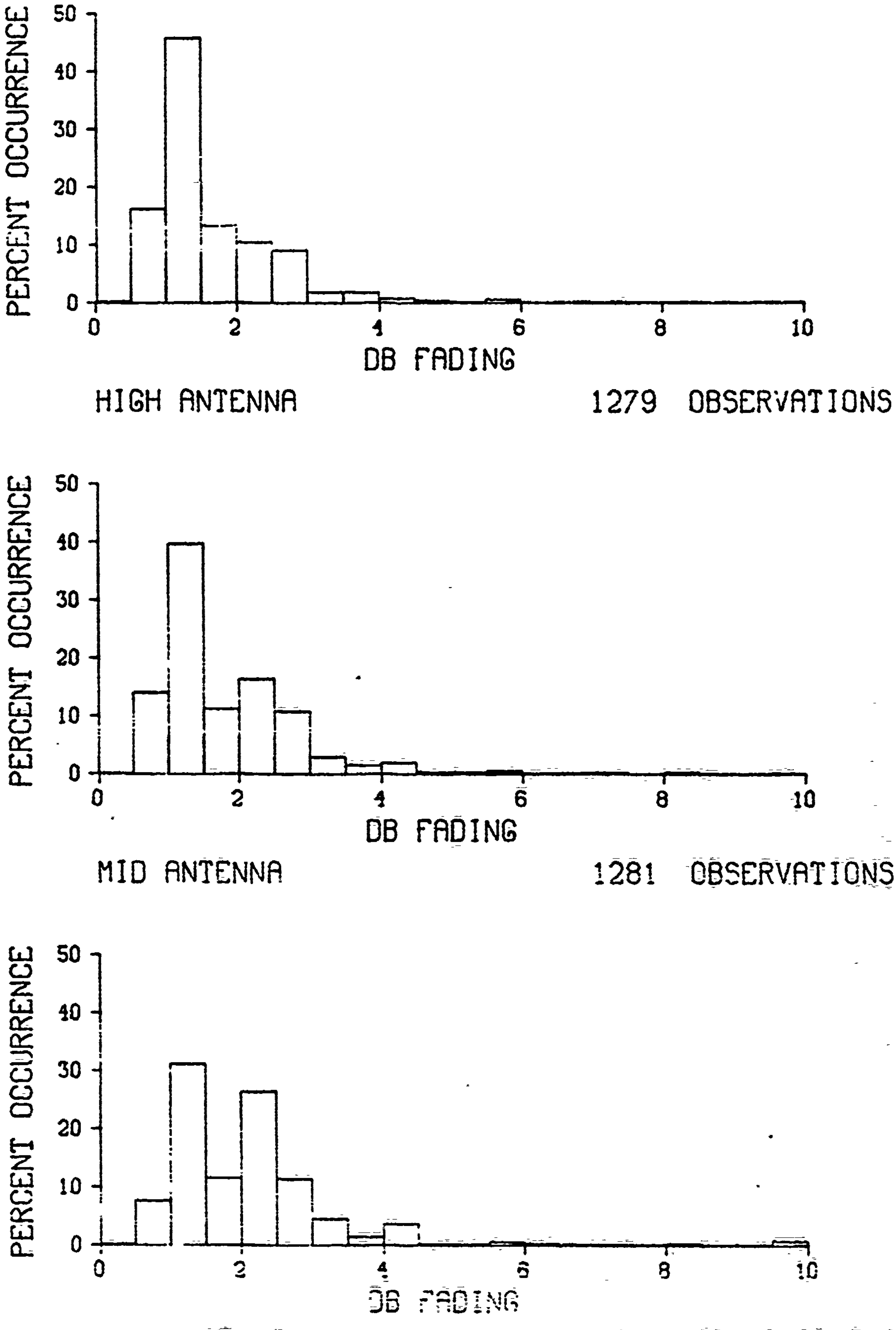

Figure 65. Frequency distributions of fading for S-band

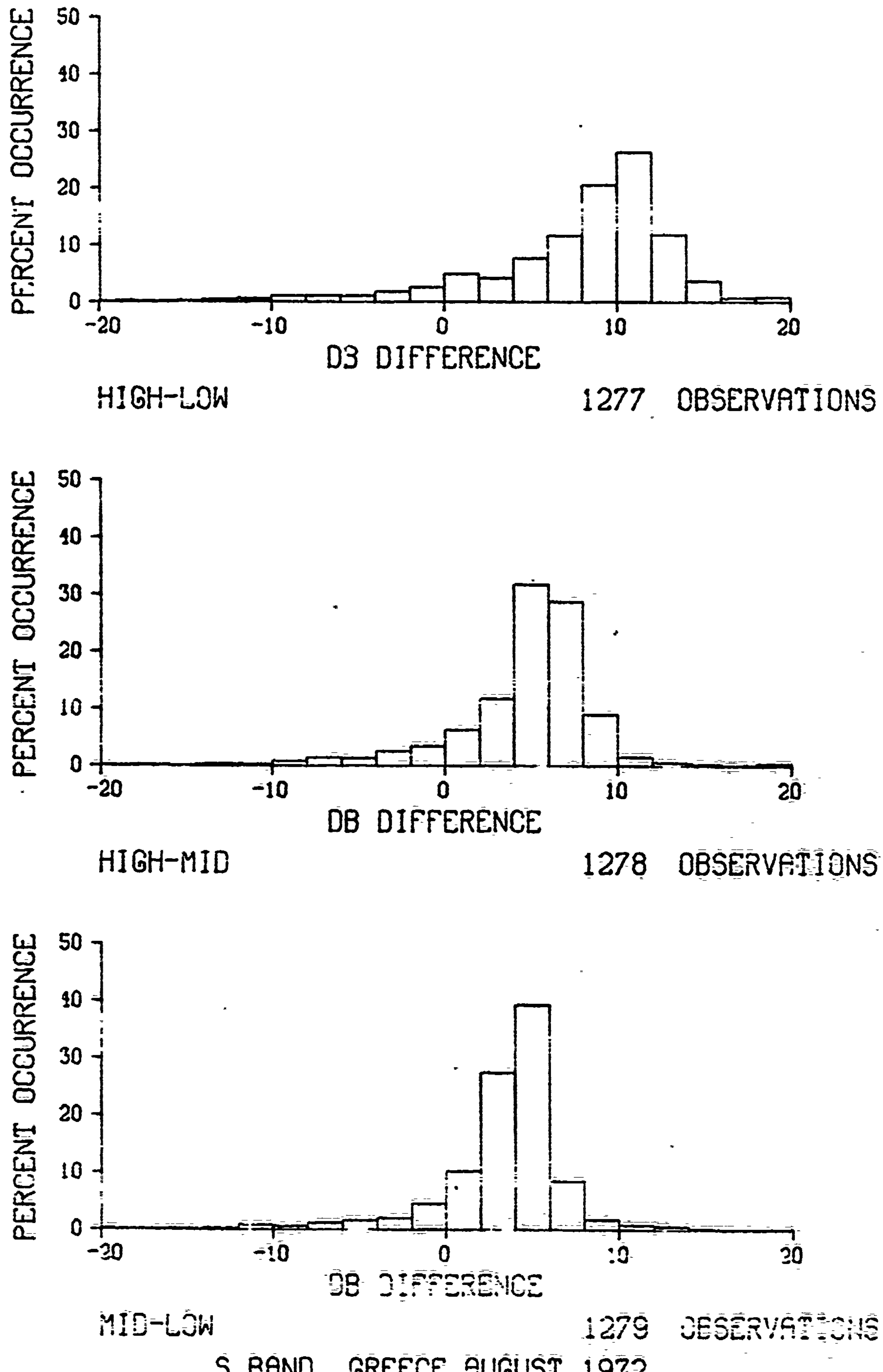

Figure 66. Frequency distributions of path loss differences between antennas for S-band

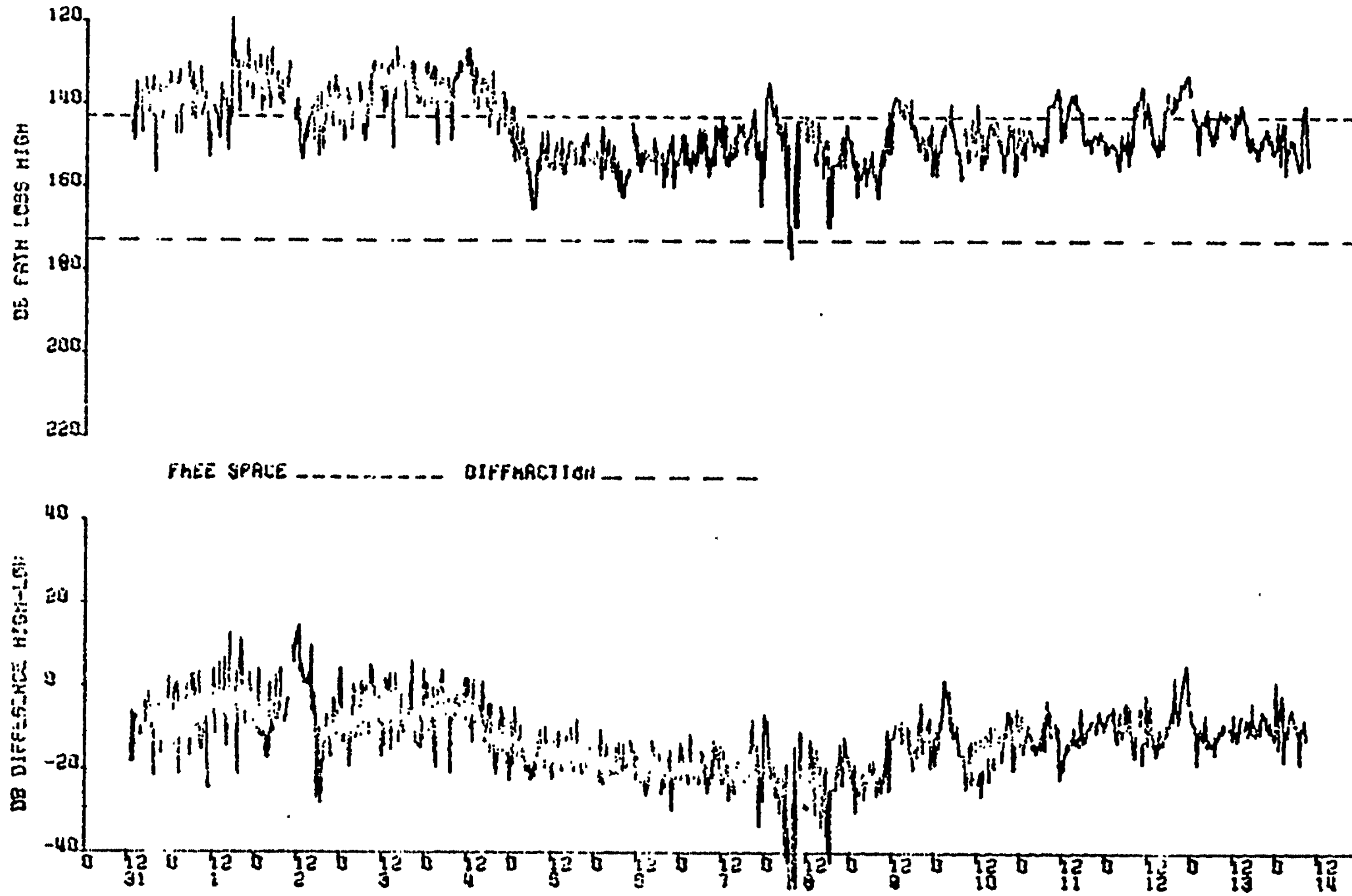

X BAND, NAXOS TO MYKONOS, GREECE AUGUST 1972

Figure 67. Path loss for high X-band antenna and path loss difference high-low antenna

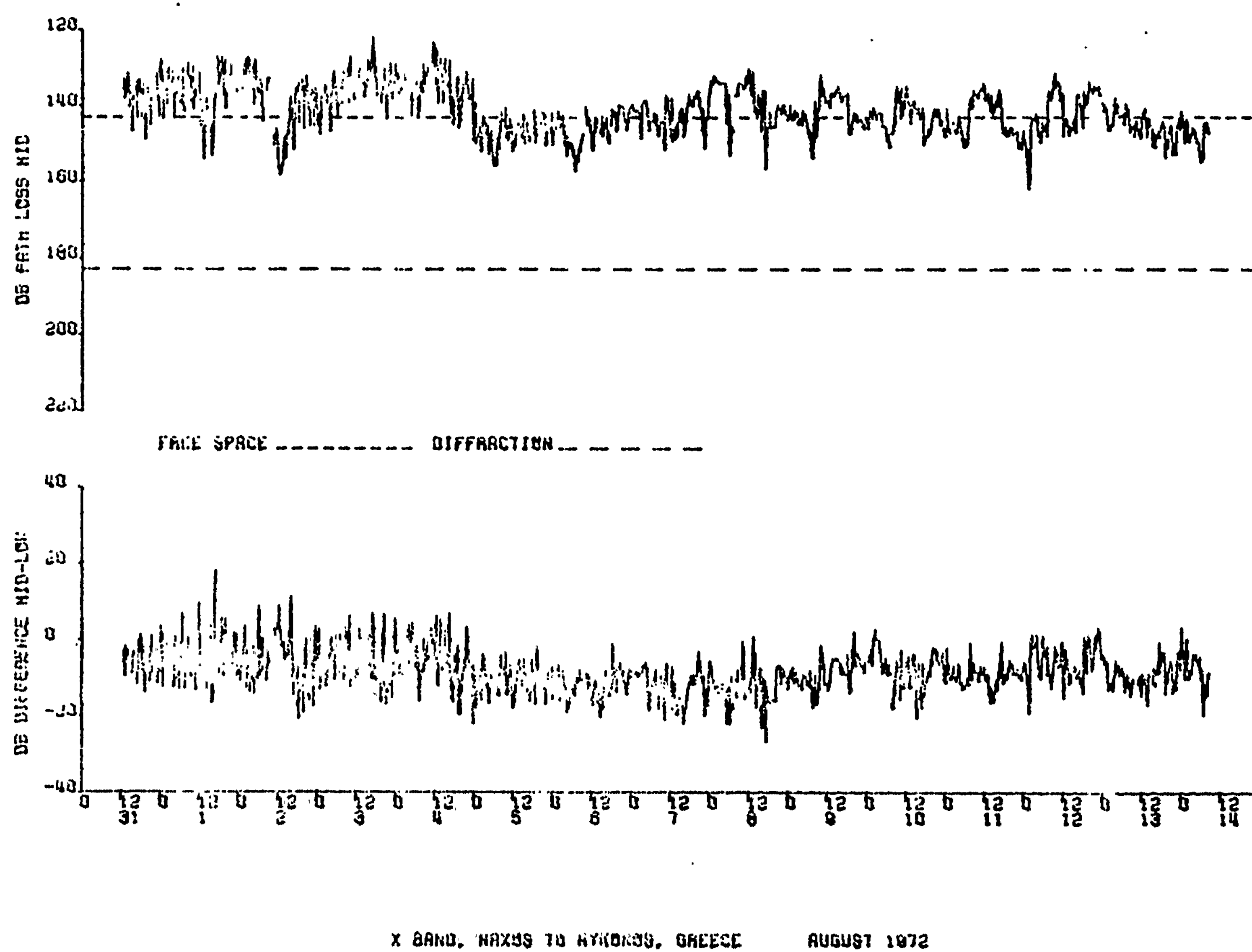

Figure 68. Path loss middle X-band antenna and path loss difference mid-low antenna

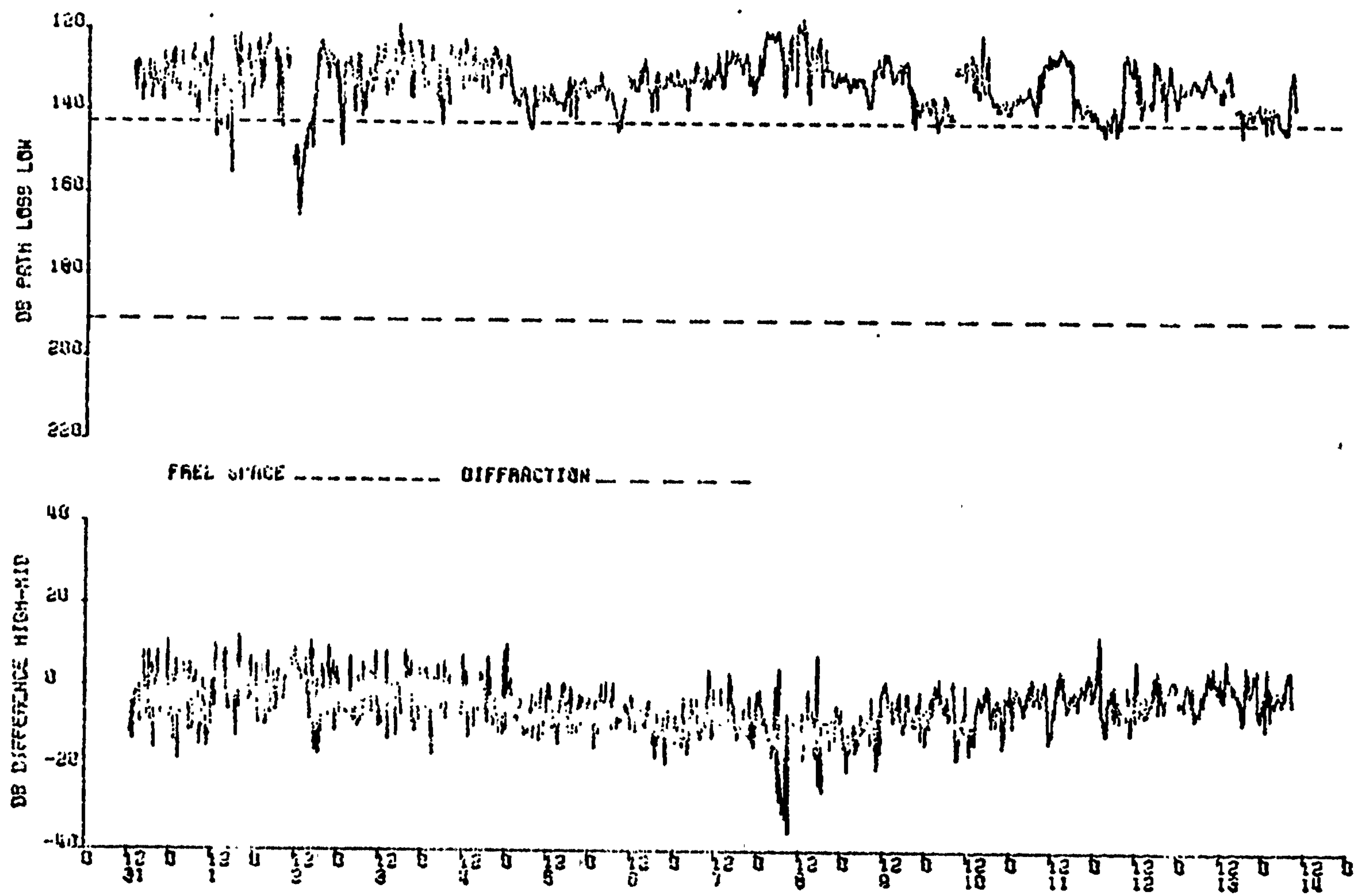

X BAND, NAXOS TO HYMETTOS, GREECE AUGUST 1972

Figure 69. Path loss low X-band antenna and path loss difference high-mid antenna

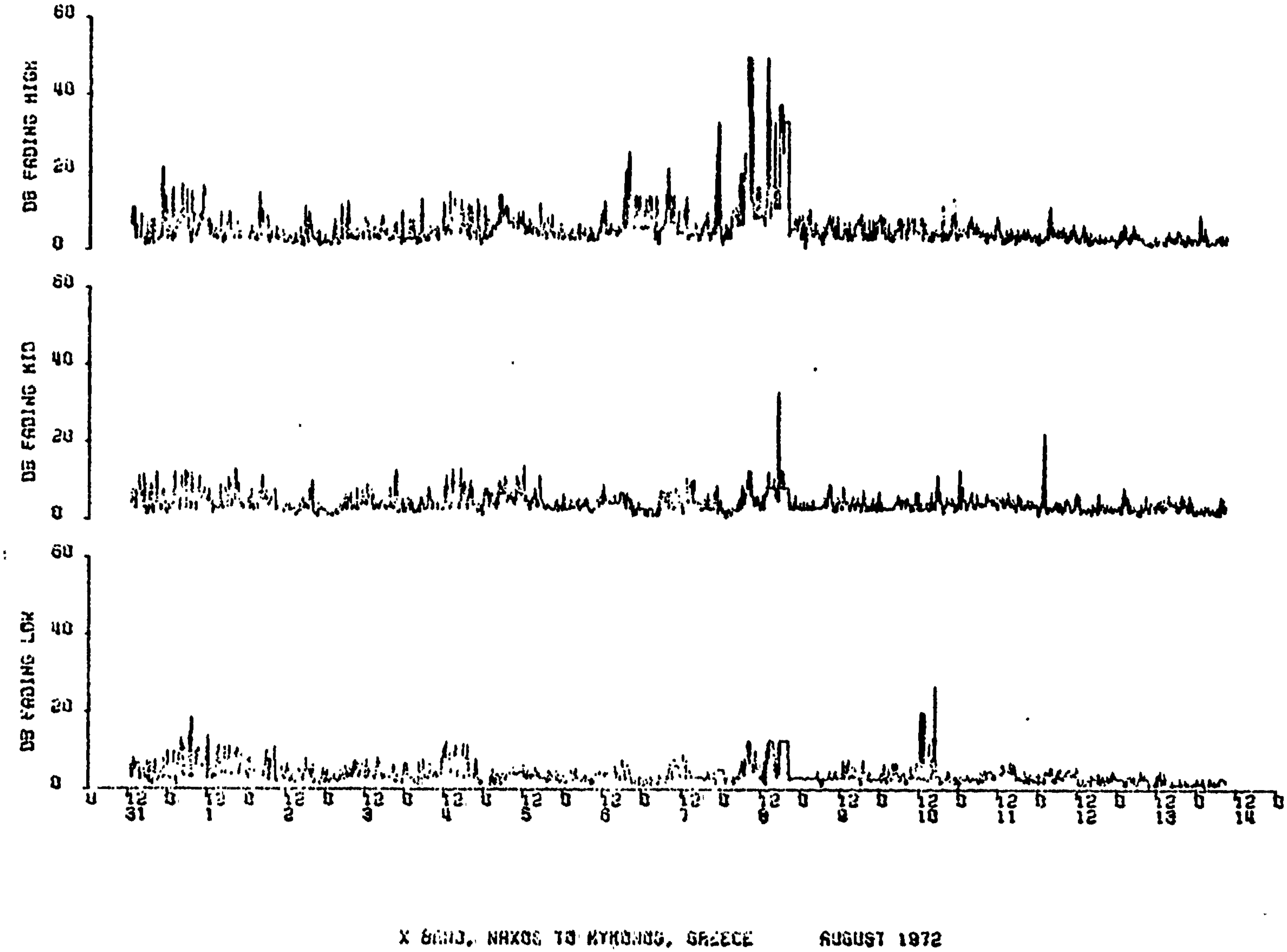

Figure 70. Fading X-band

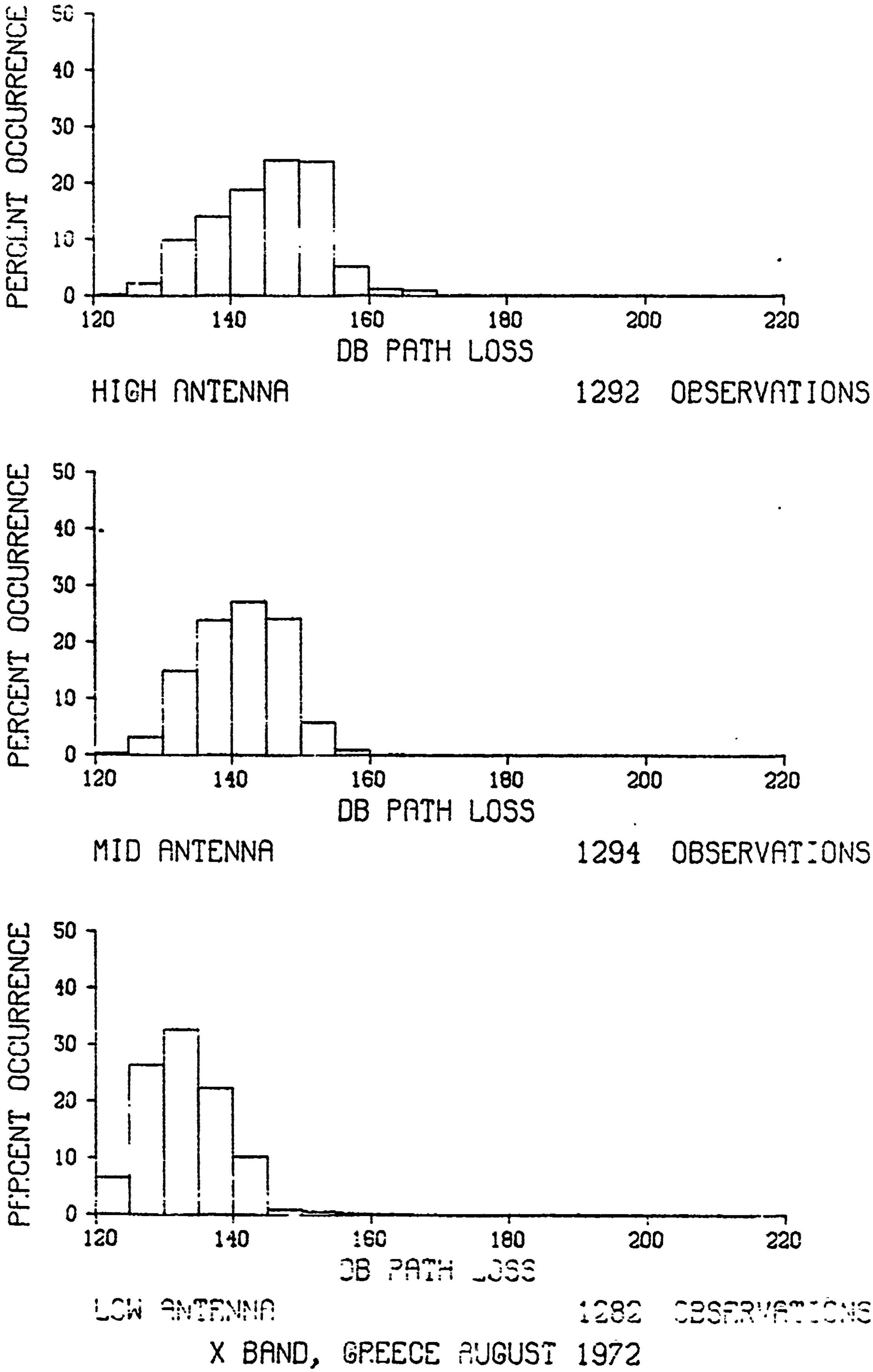

Figure 71. Frequency distribution of path loss for X-band

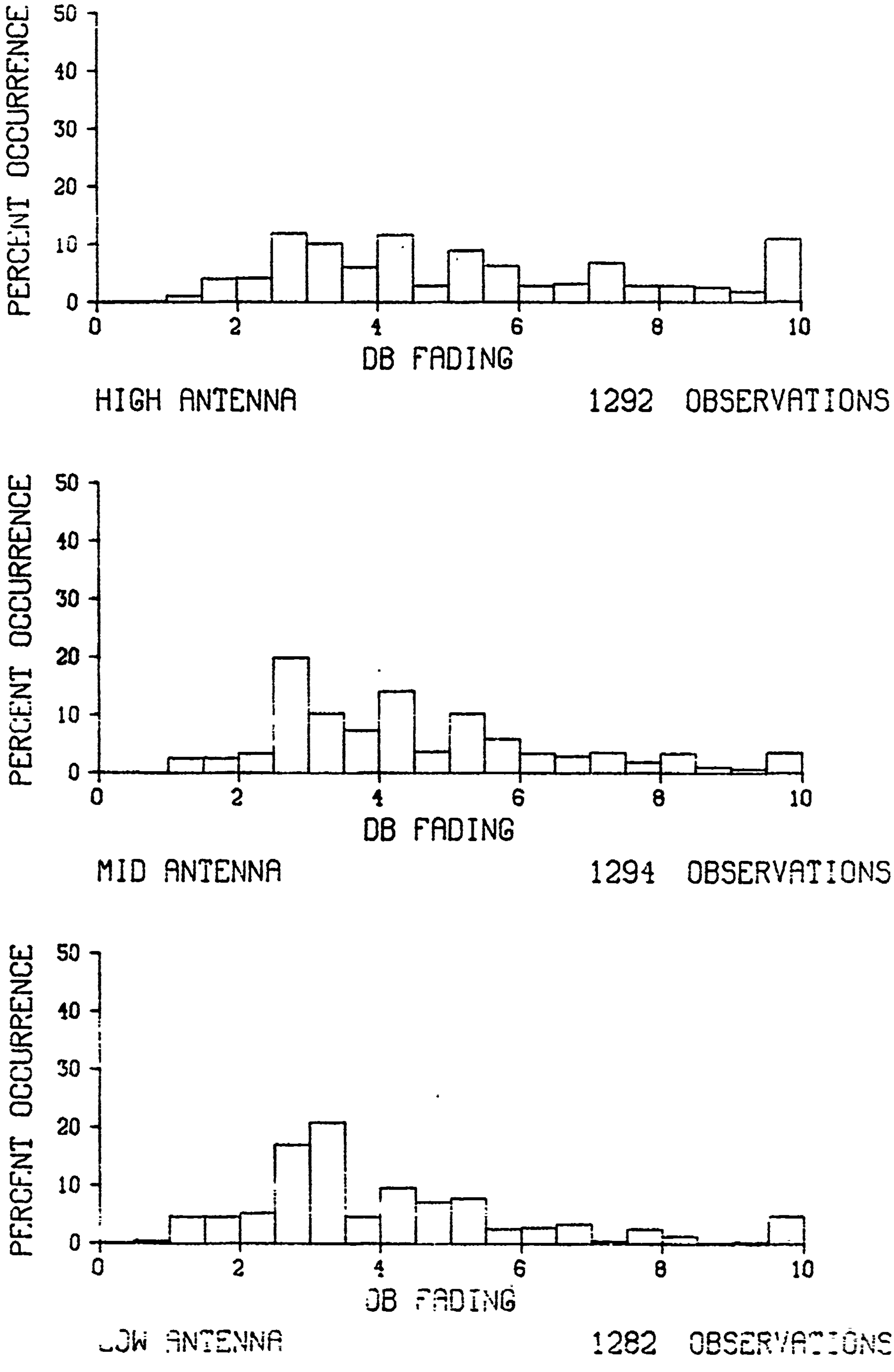

Figure 72. Frequency distribution of fading X-band

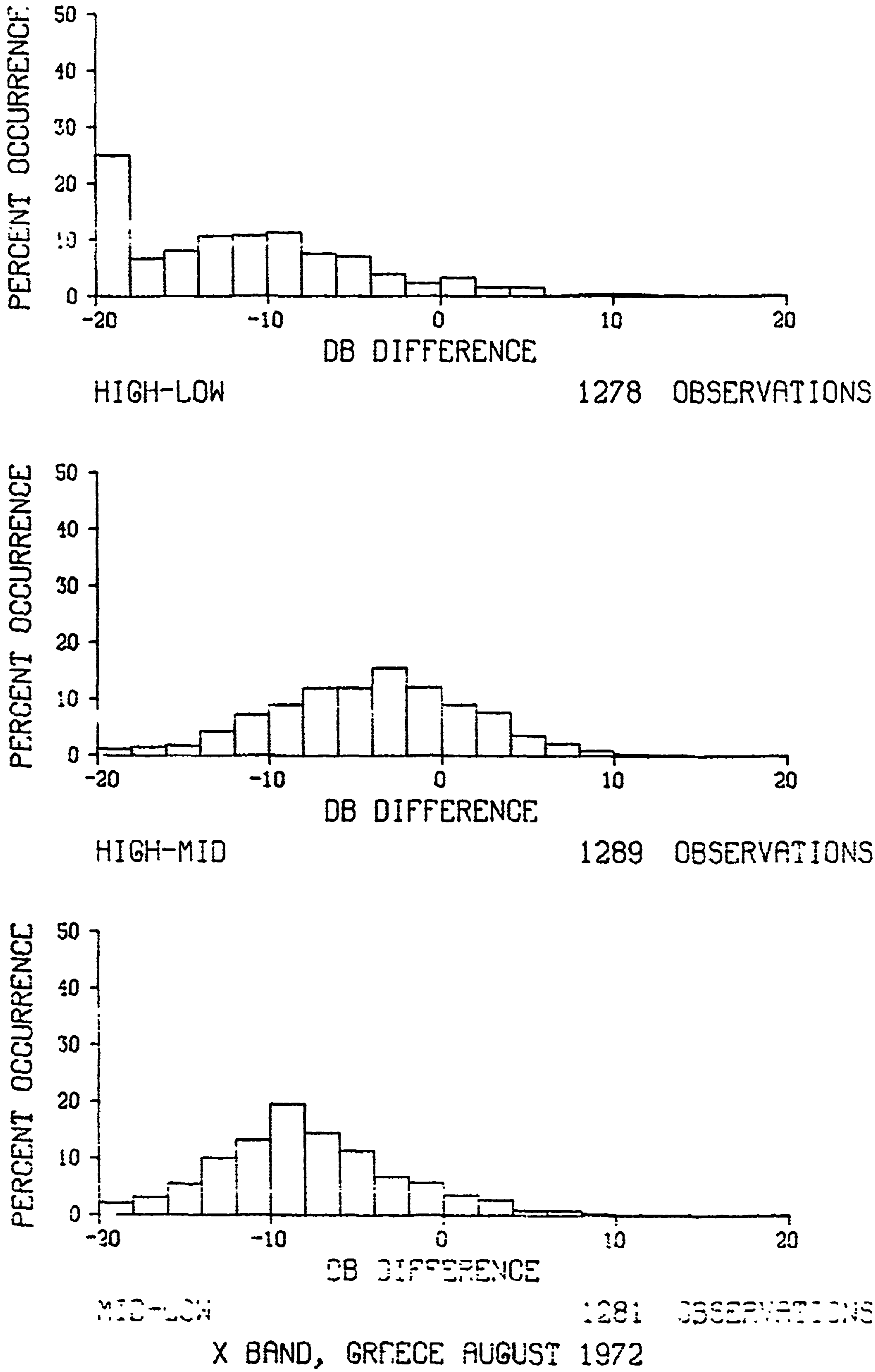

Figure 73. Frequency distribution of differences between antennas for X-band

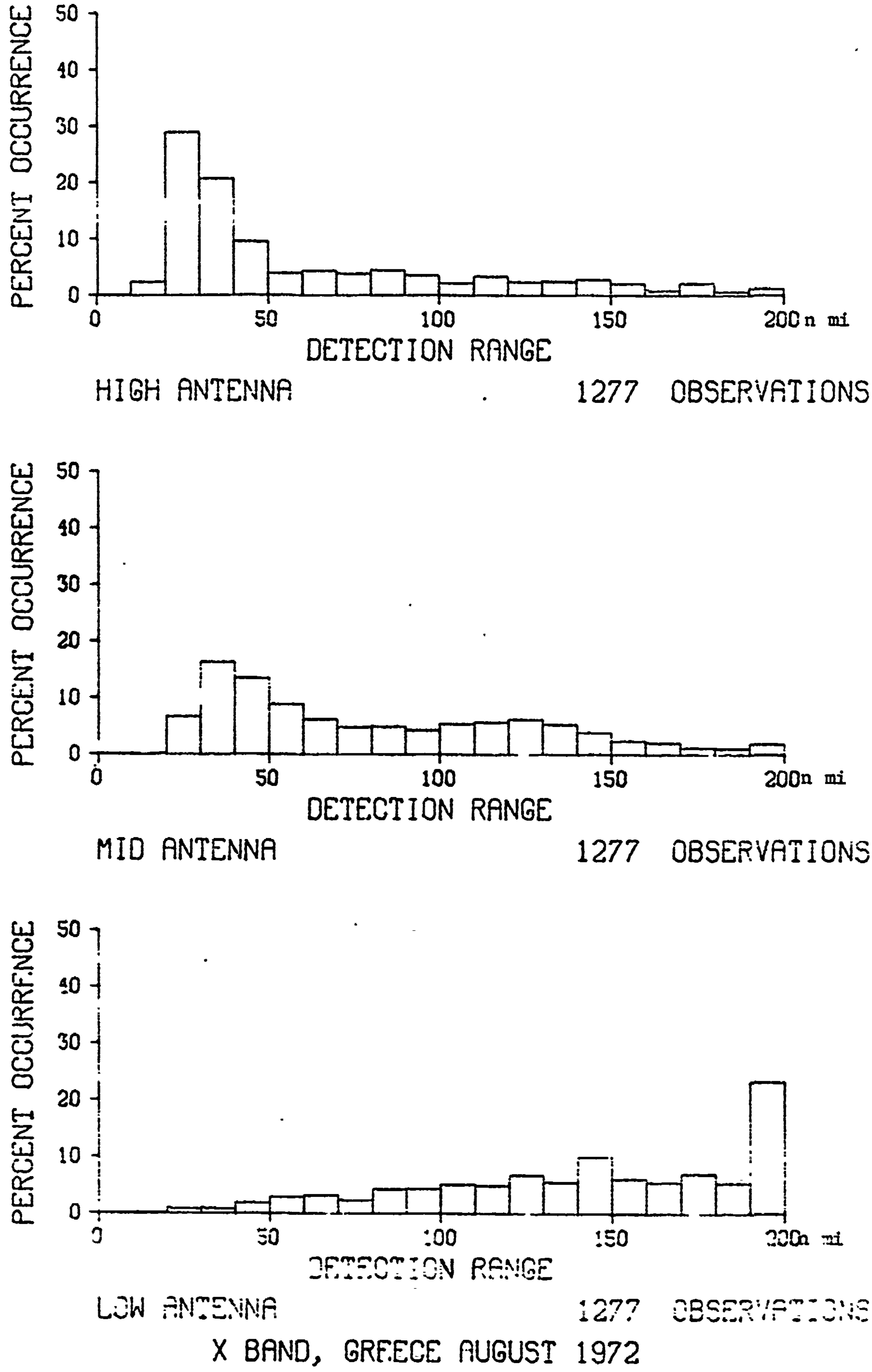

Figure 74. Frequency distribution of detection range for X-band

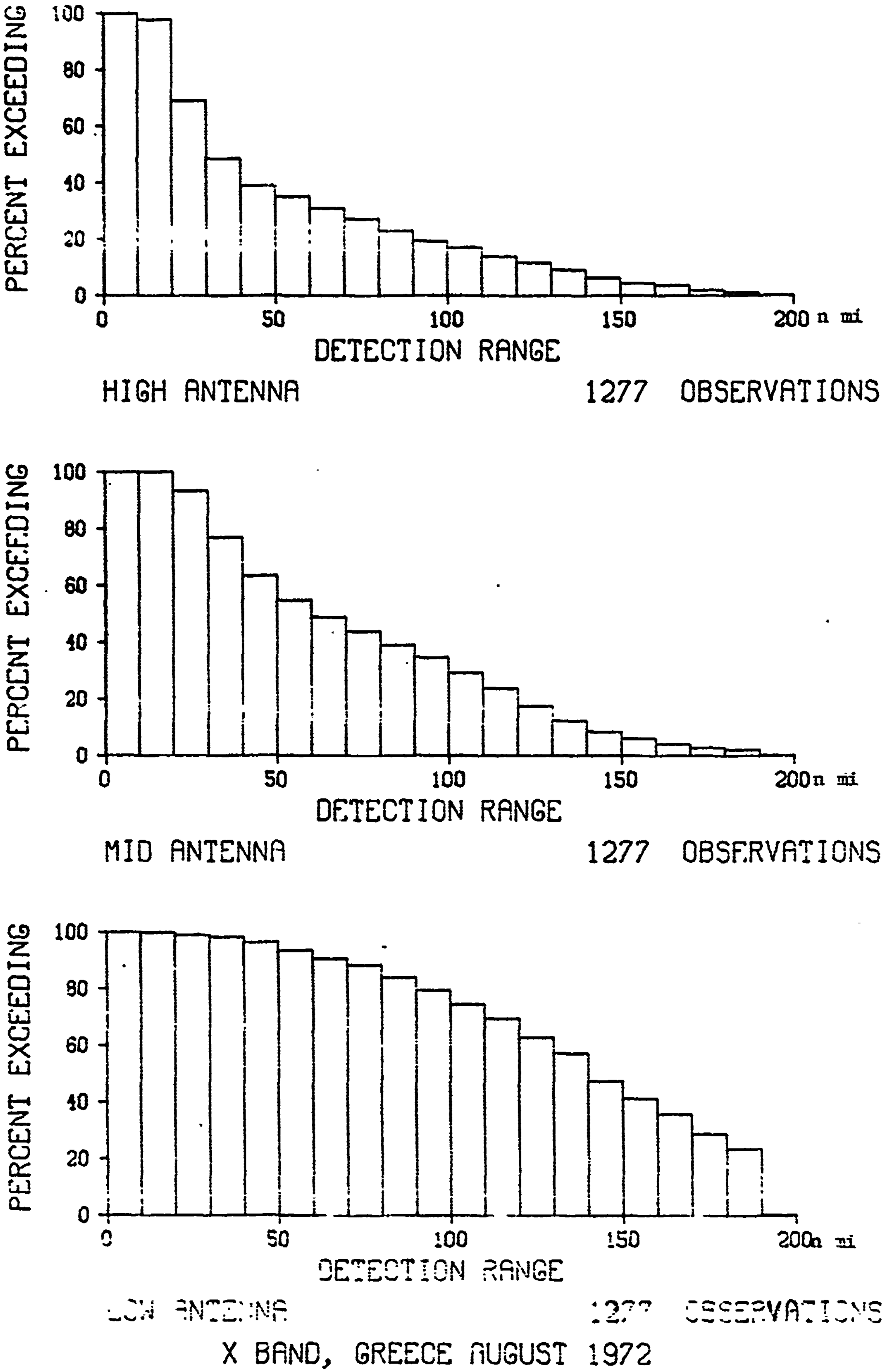

Figure 75. Cumulative distribution of detection range for X-band

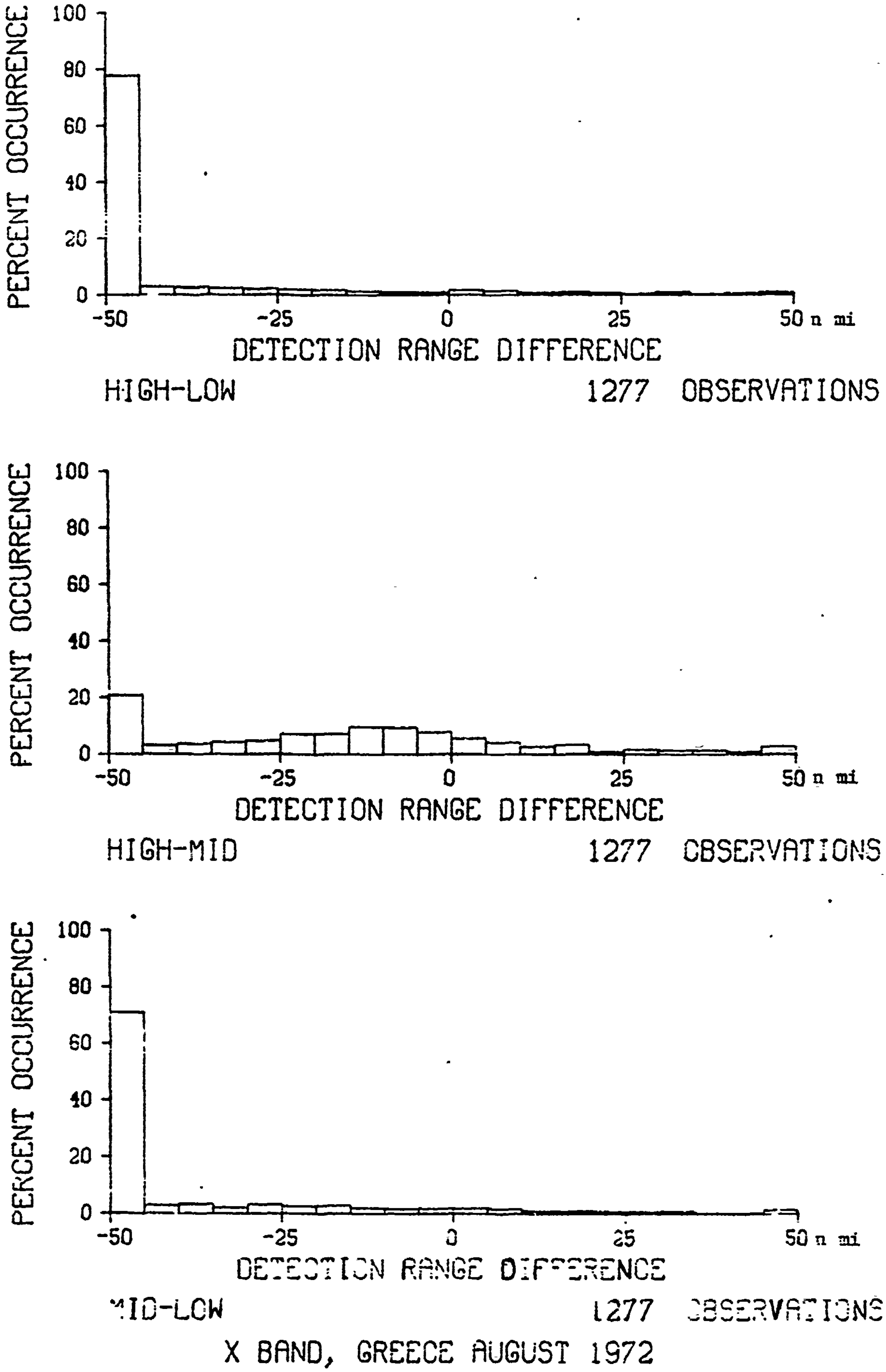

Figure 7b. Frequency distribution of detection range differences between antennas

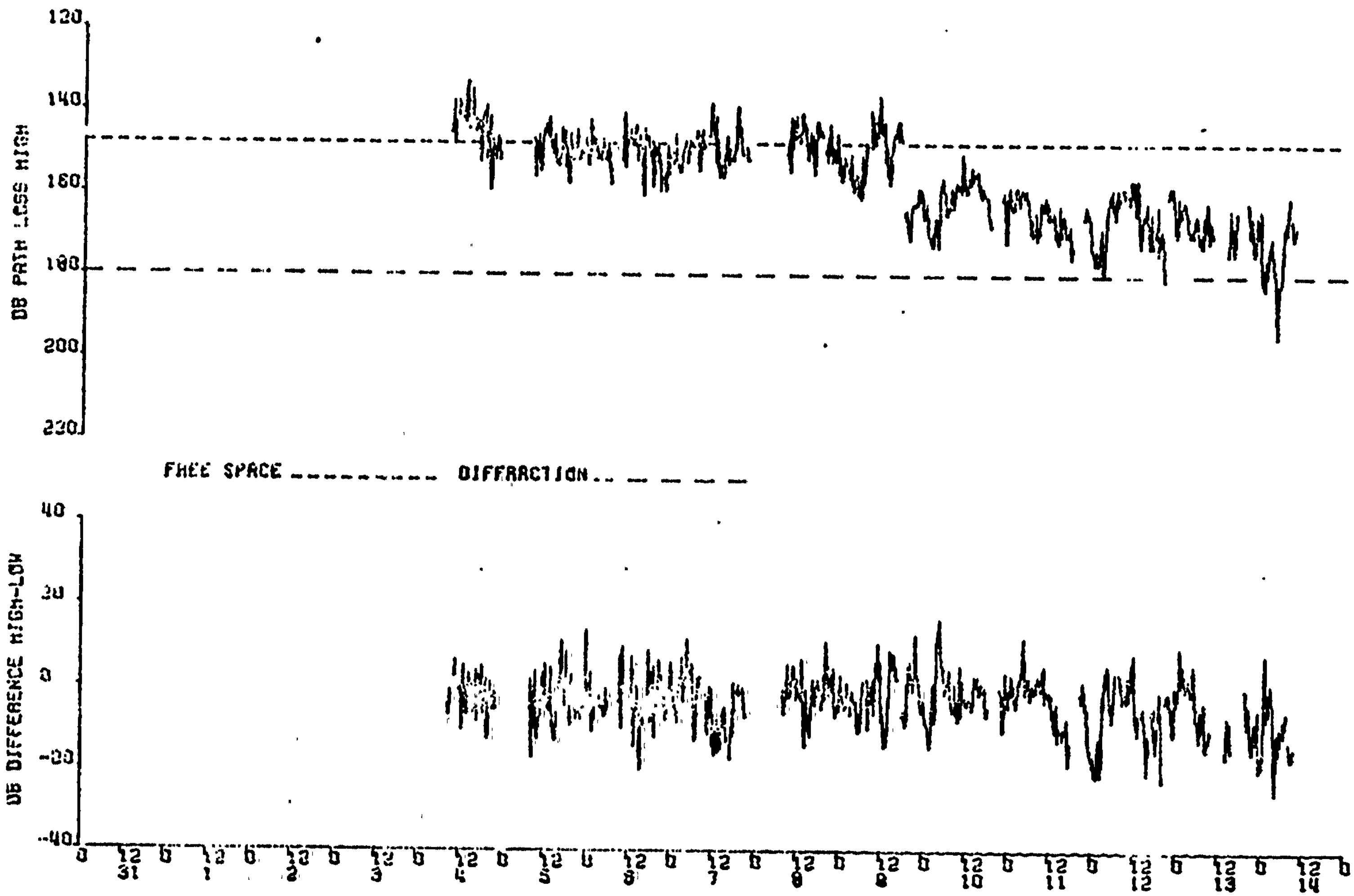

KU-BAND, NAXOS TO MYKONOS, GREECE AUGUST 1972

Figure 77. Path loss for high Ku-band antenna and path loss difference high-low antenna

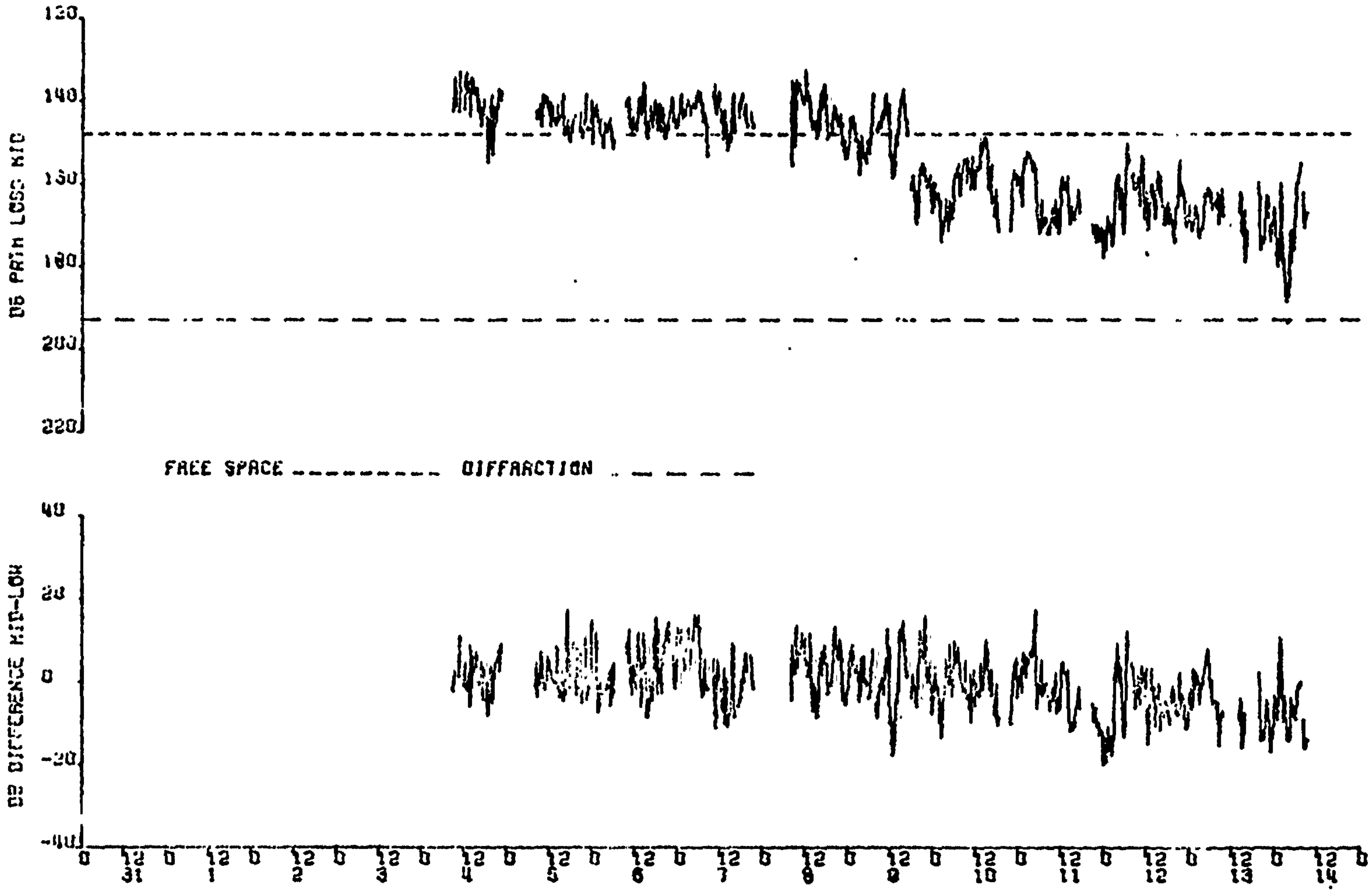

KU BAND, NAXOS TO MYKONOS, GREECE AUGUST 1972

Figure 78. Path loss for mid Ku-band antenna and path loss difference mid-low antenna

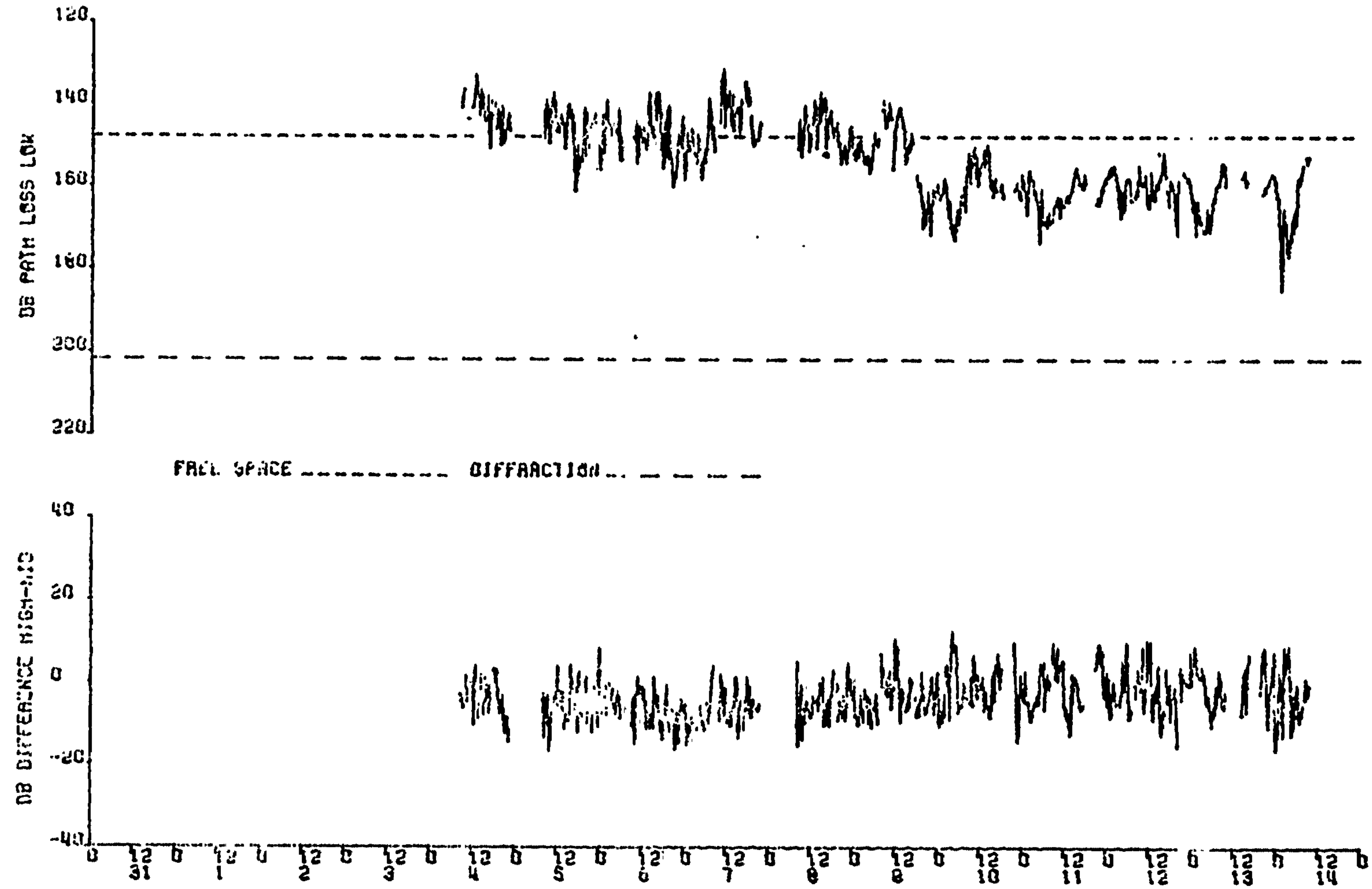

KU BAND, NAXOS TO MYKONOS, GREECE AUGUST 1972

Figure 79. Path loss for low Ku-band antenna and path loss difference high-mid antenna

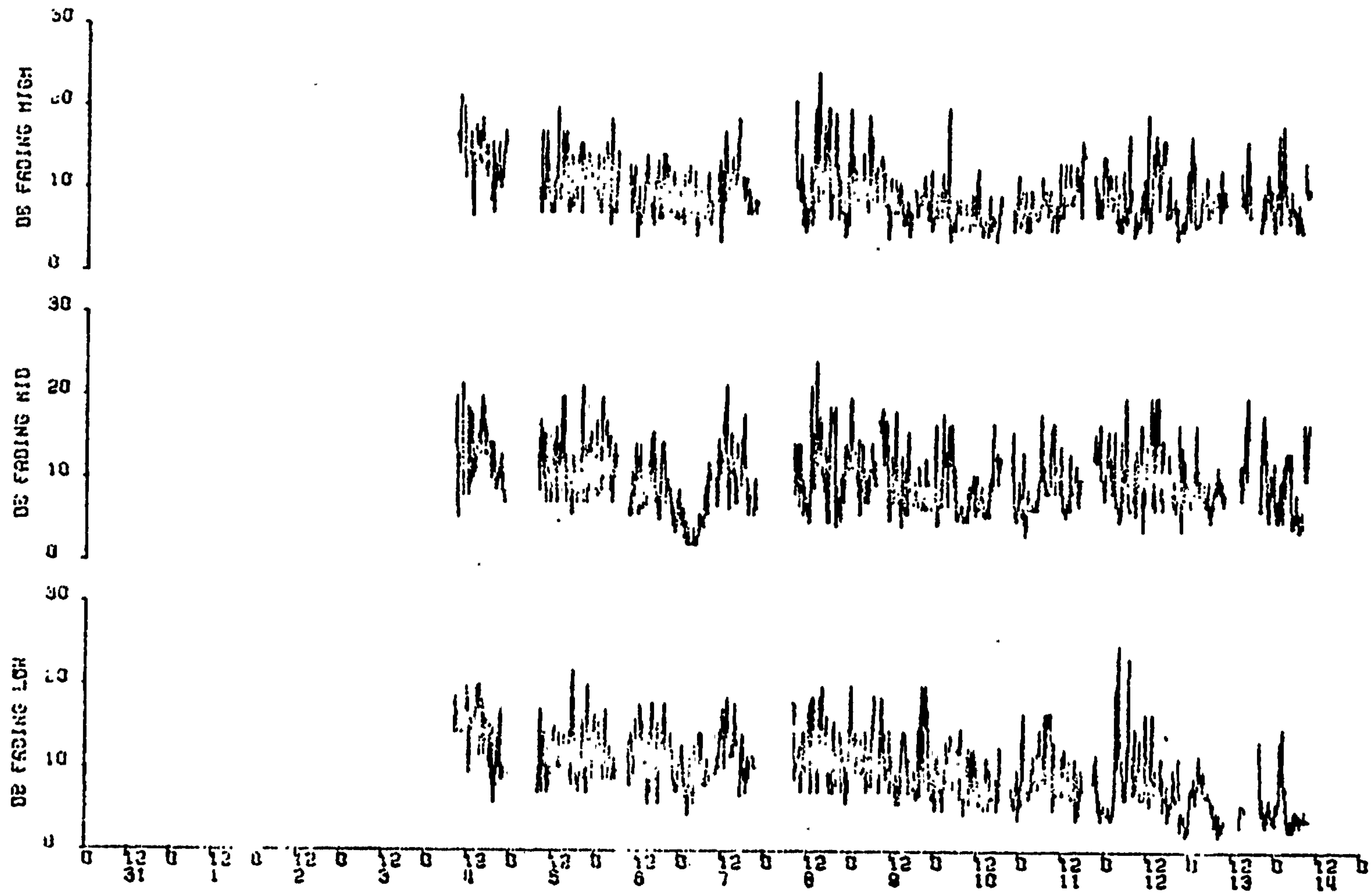

KU BAND, ... TO ..., GREECE AUGUST 1972

Figure 80. Fading Ku-band

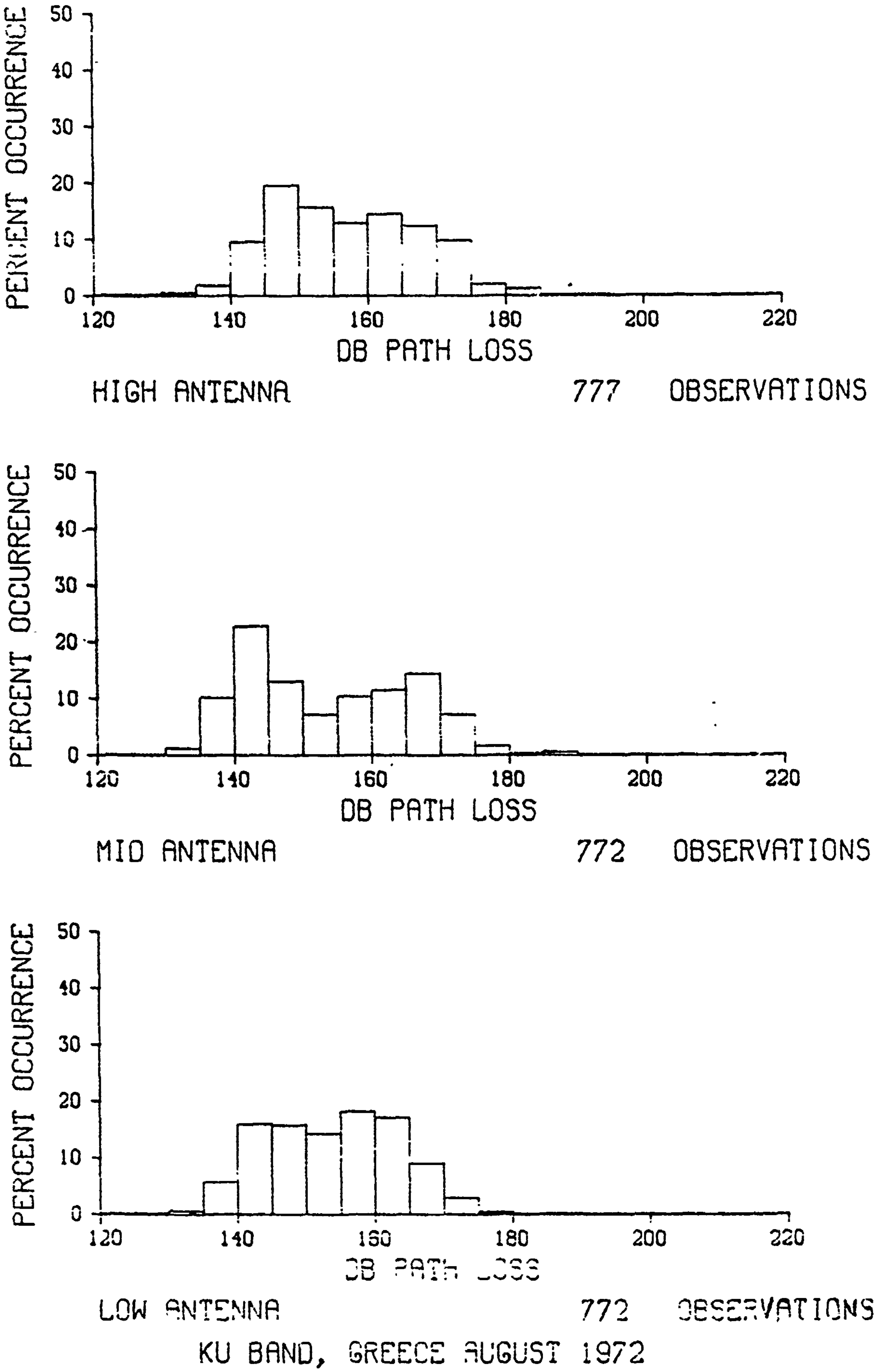

Figure 81. Frequency distributions of path loss for Ku-band

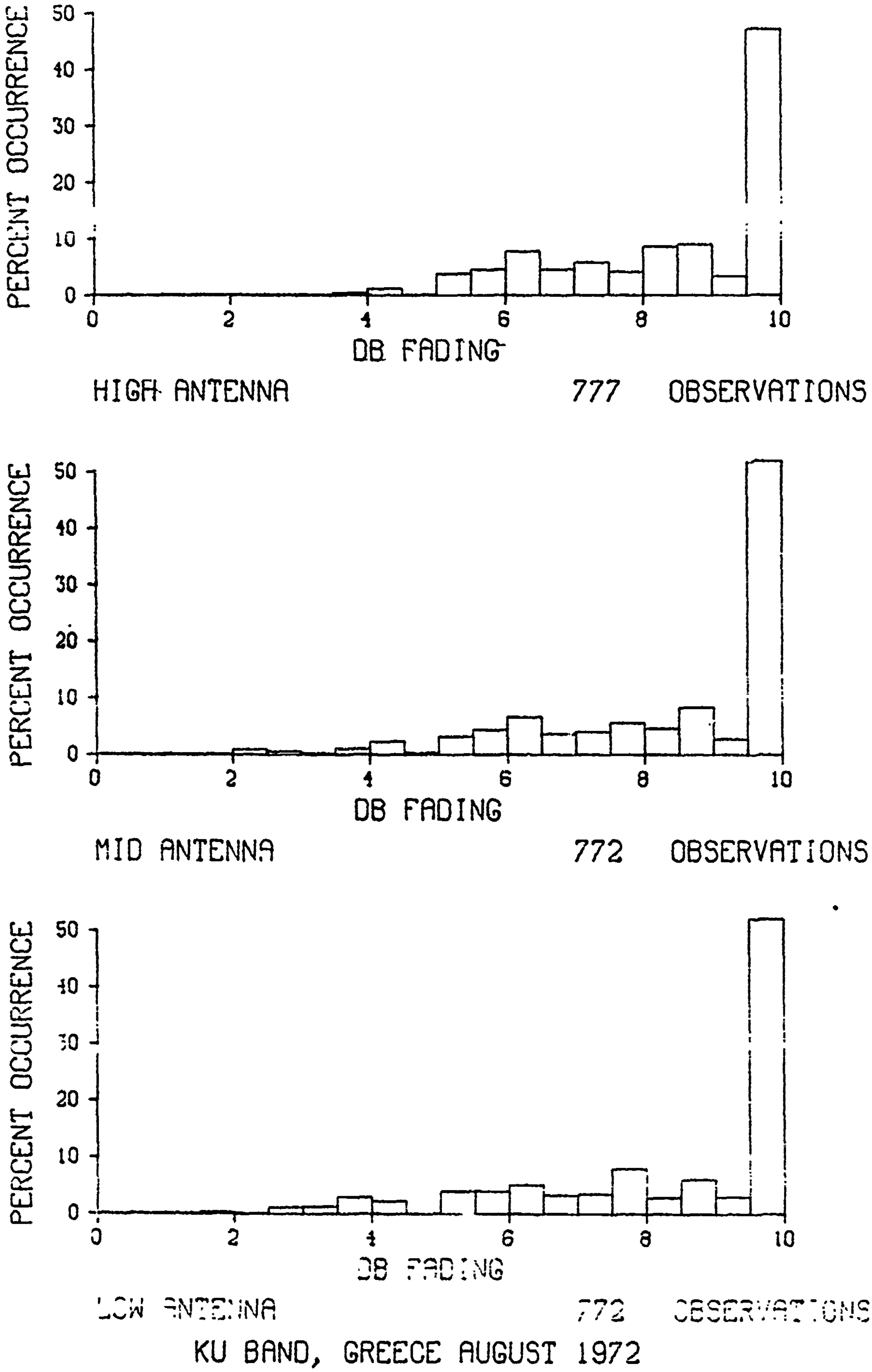

Figure 82. Frequency distributions of fading for Ku-band

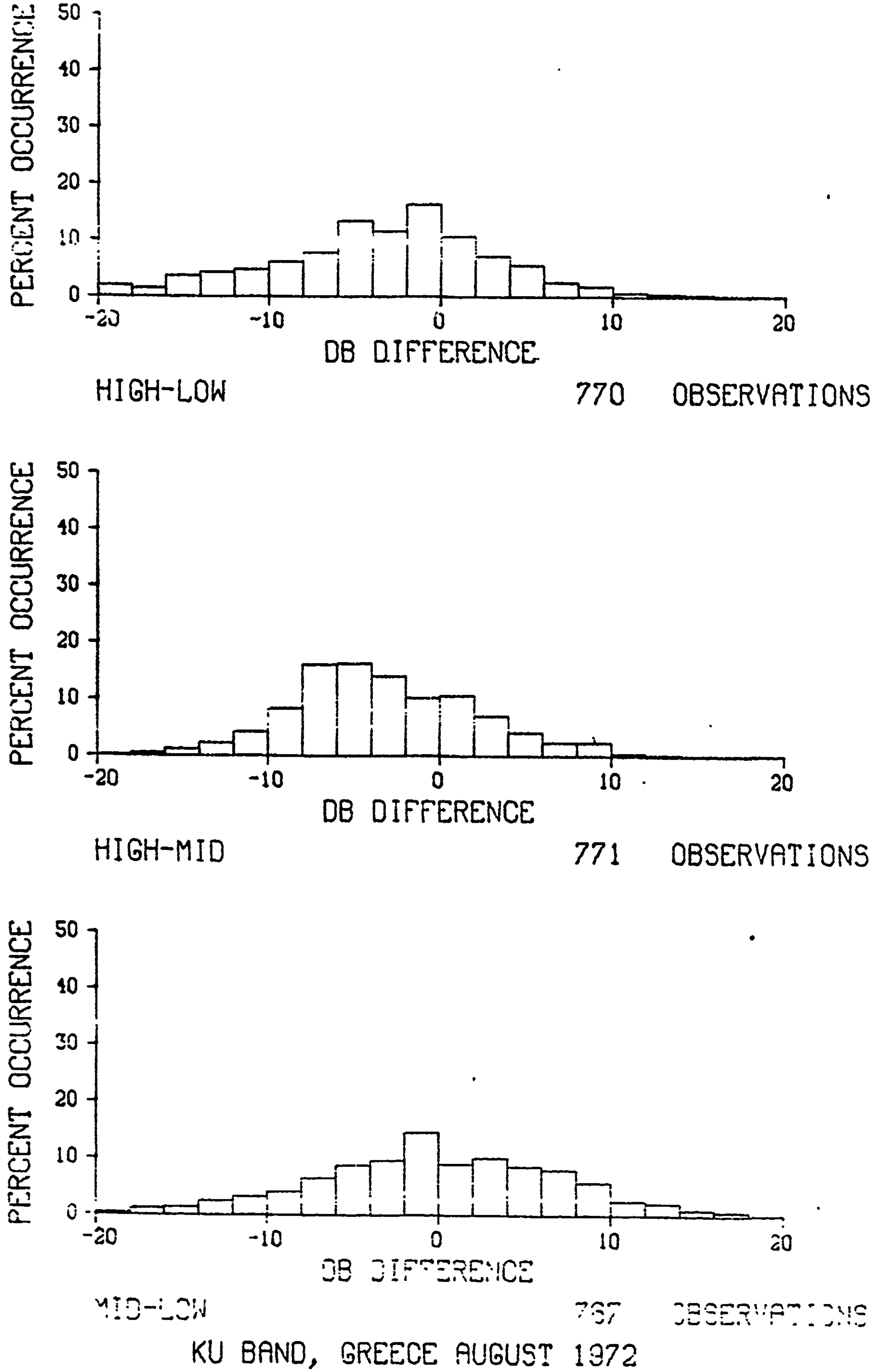

Figure 8[illegible] Frequency distributions of path loss differences between antennas for Ku-band

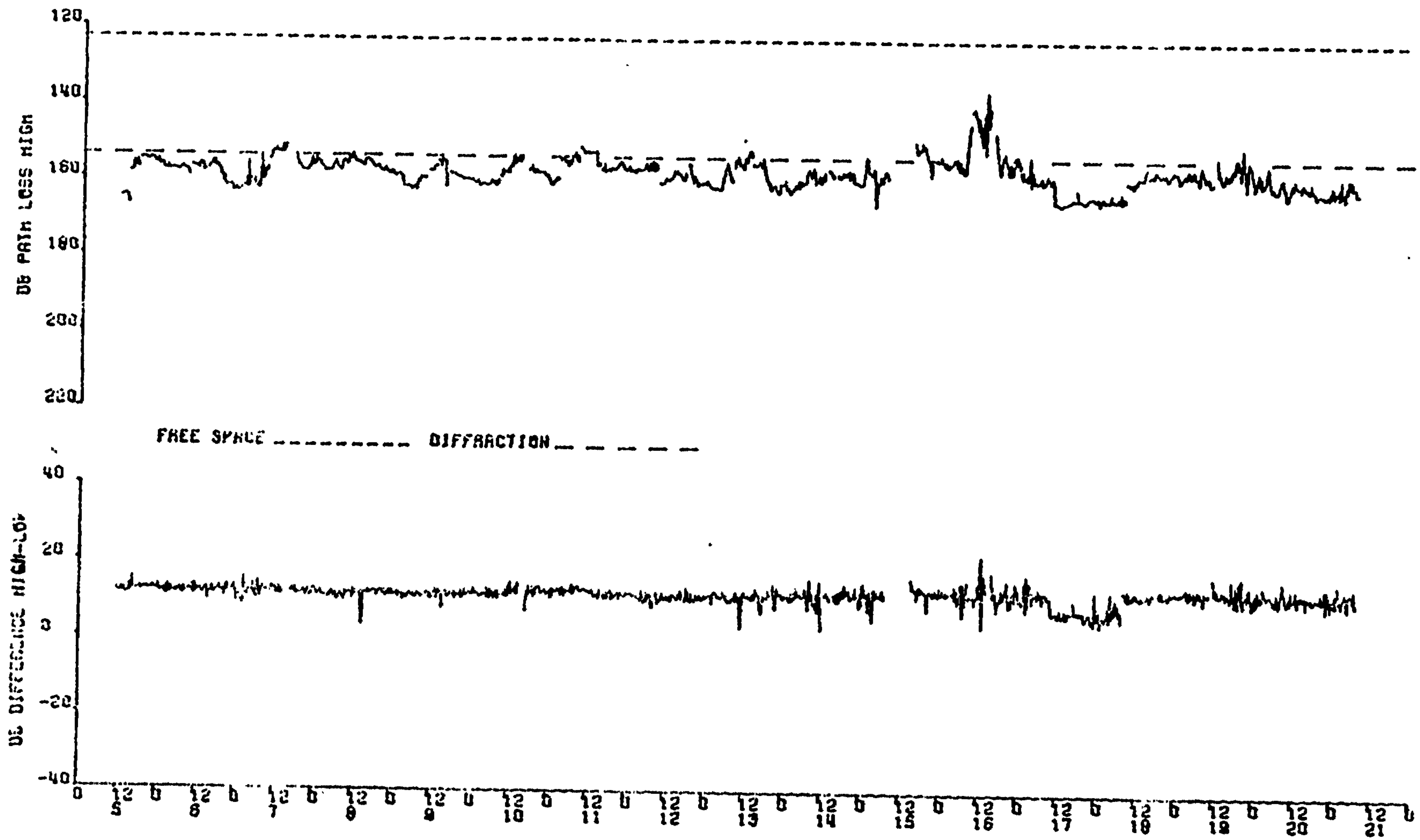

L BAND, NAXOS TO MYKONOS, GREECE NOVEMBER 1972

Figure 84. Path loss for high L-band antenna and path loss difference high-low antenna

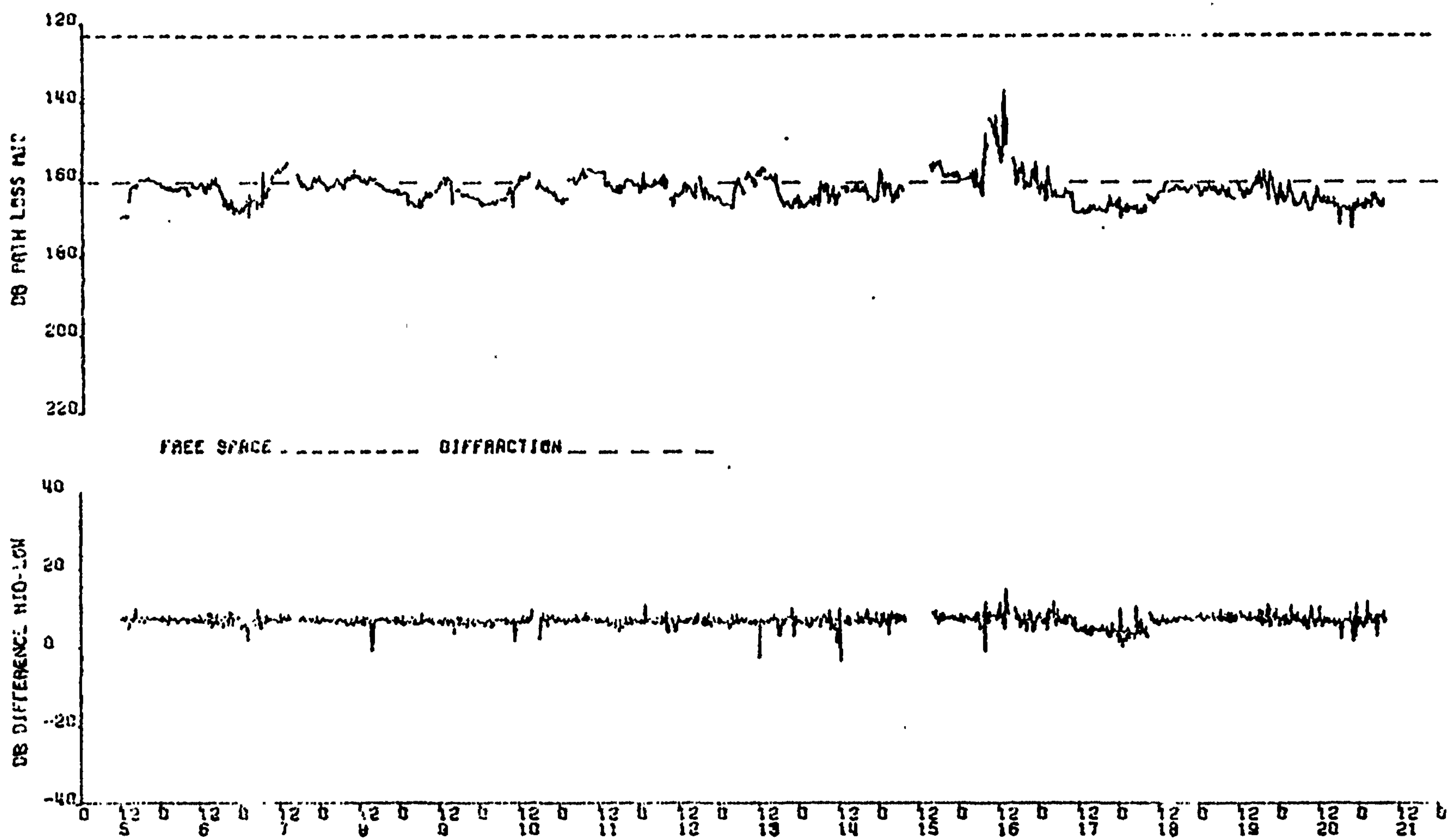

L BAND, NAXOS TO HYMETTOS, GREECE NOVEMBER 1972

Figure 85. Path loss for middle L-band antenna and path loss difference mid-low antenna

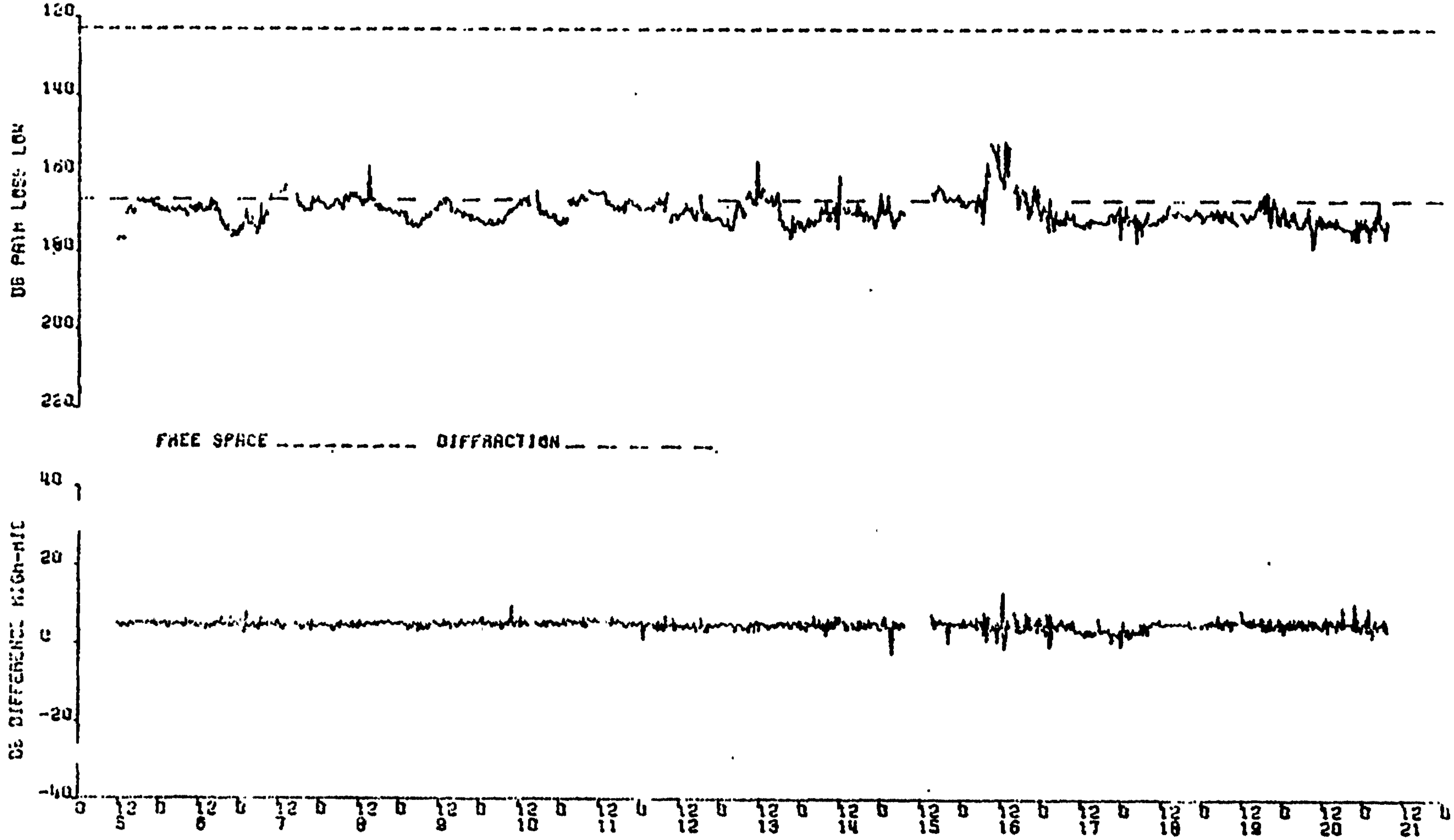

L BAND, NAXOS TO MYKONOS, GREECE   NOVEMBER 1972

Figure 86. Path loss for low L-band antenna and path loss difference high-mid antenna

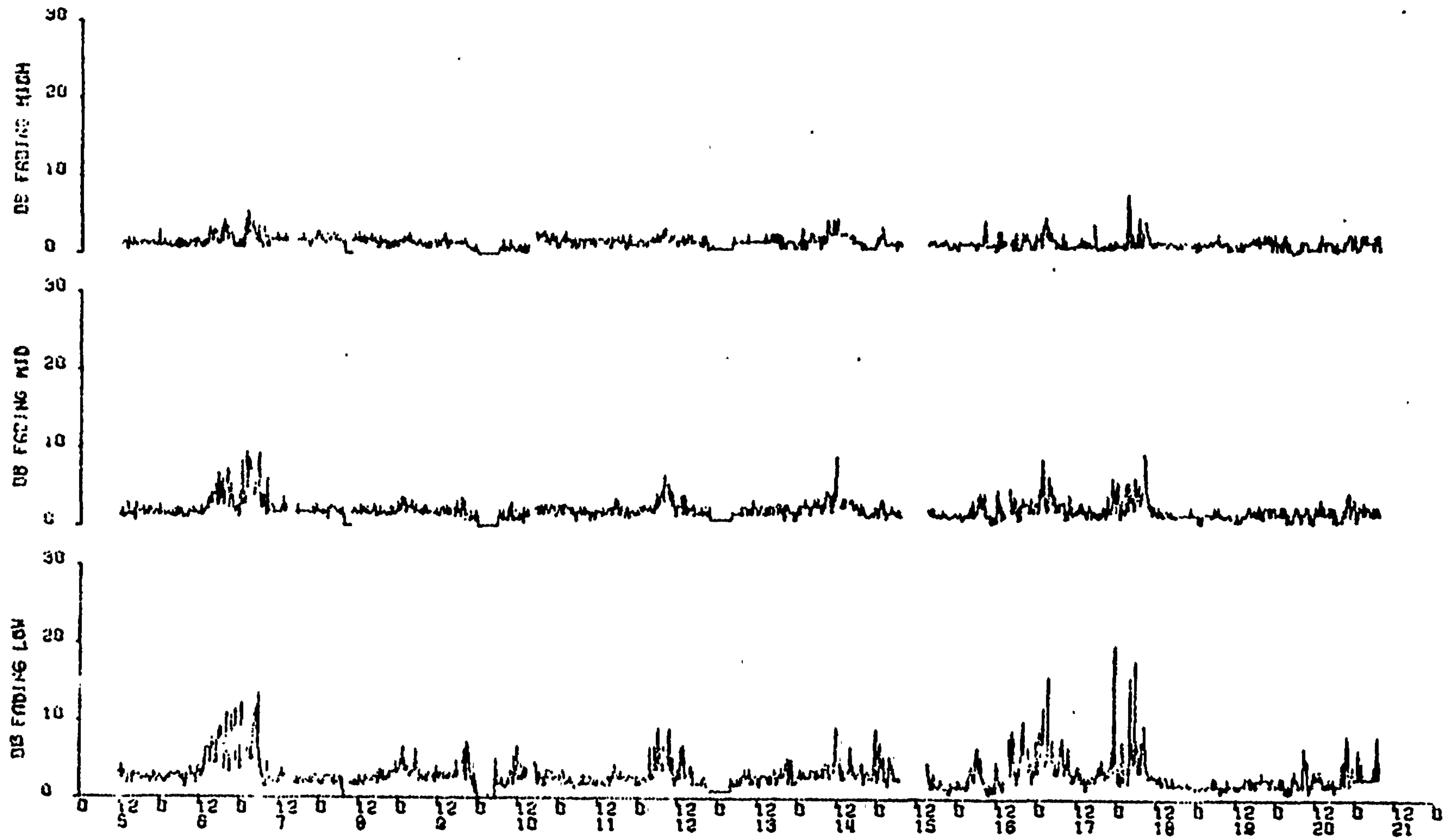

L BAND, NAXOS TO MYKONOS, GREECE NOVEMBER 1972

Figure 87. Fading L-band

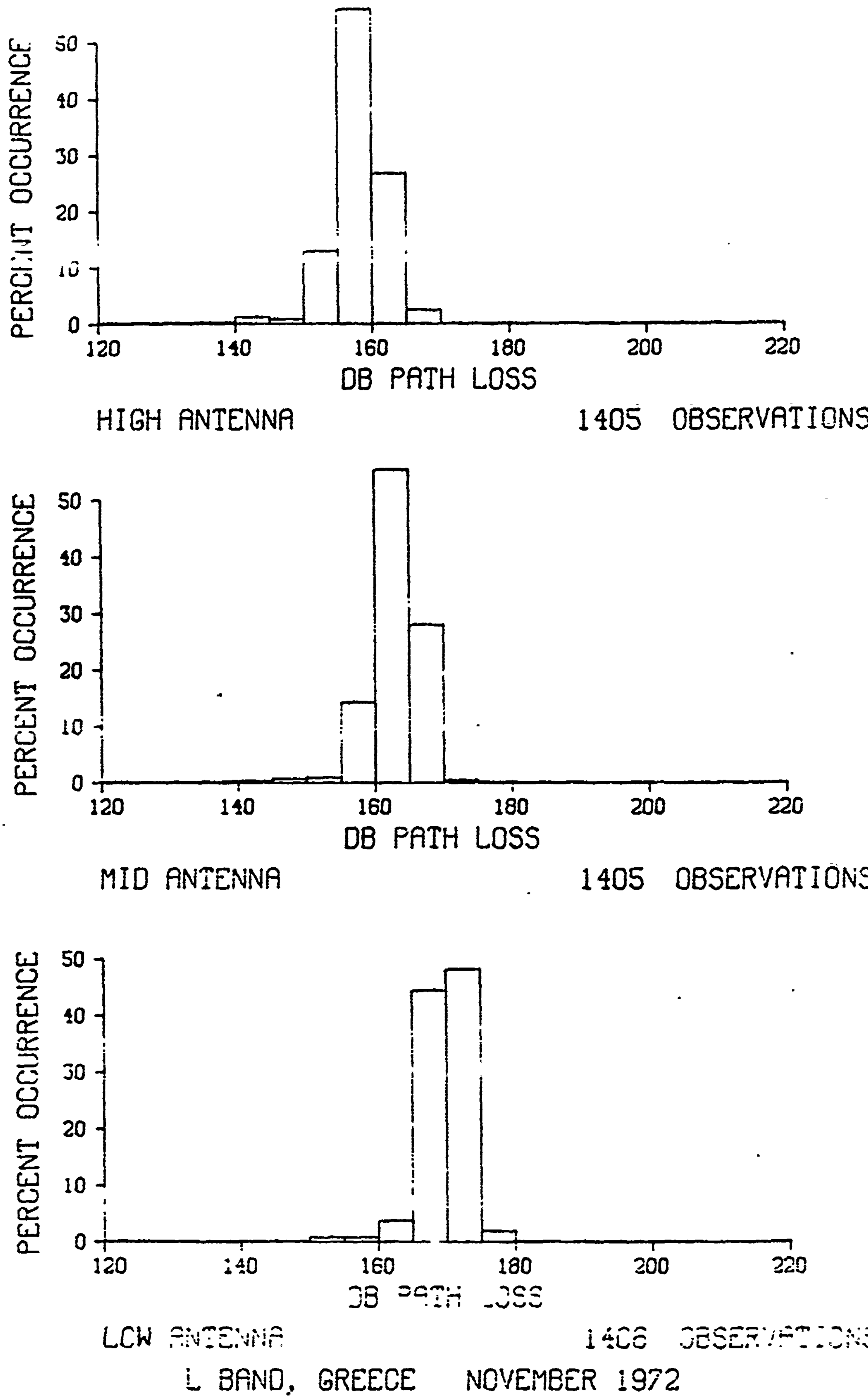

Figure 88. Frequency distributions of path loss for L-band

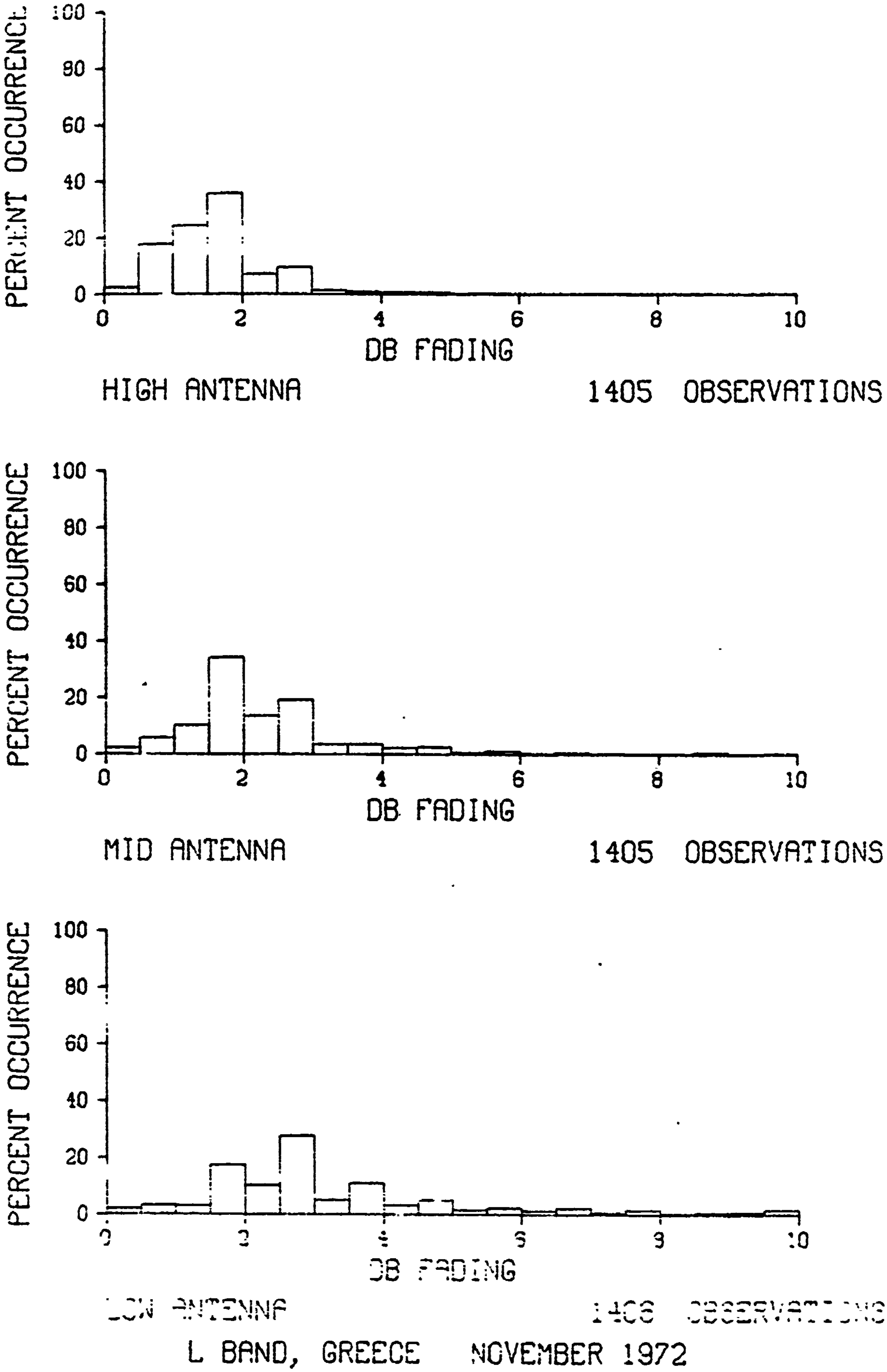

Figure 89. Frequency distributions of fading L-band

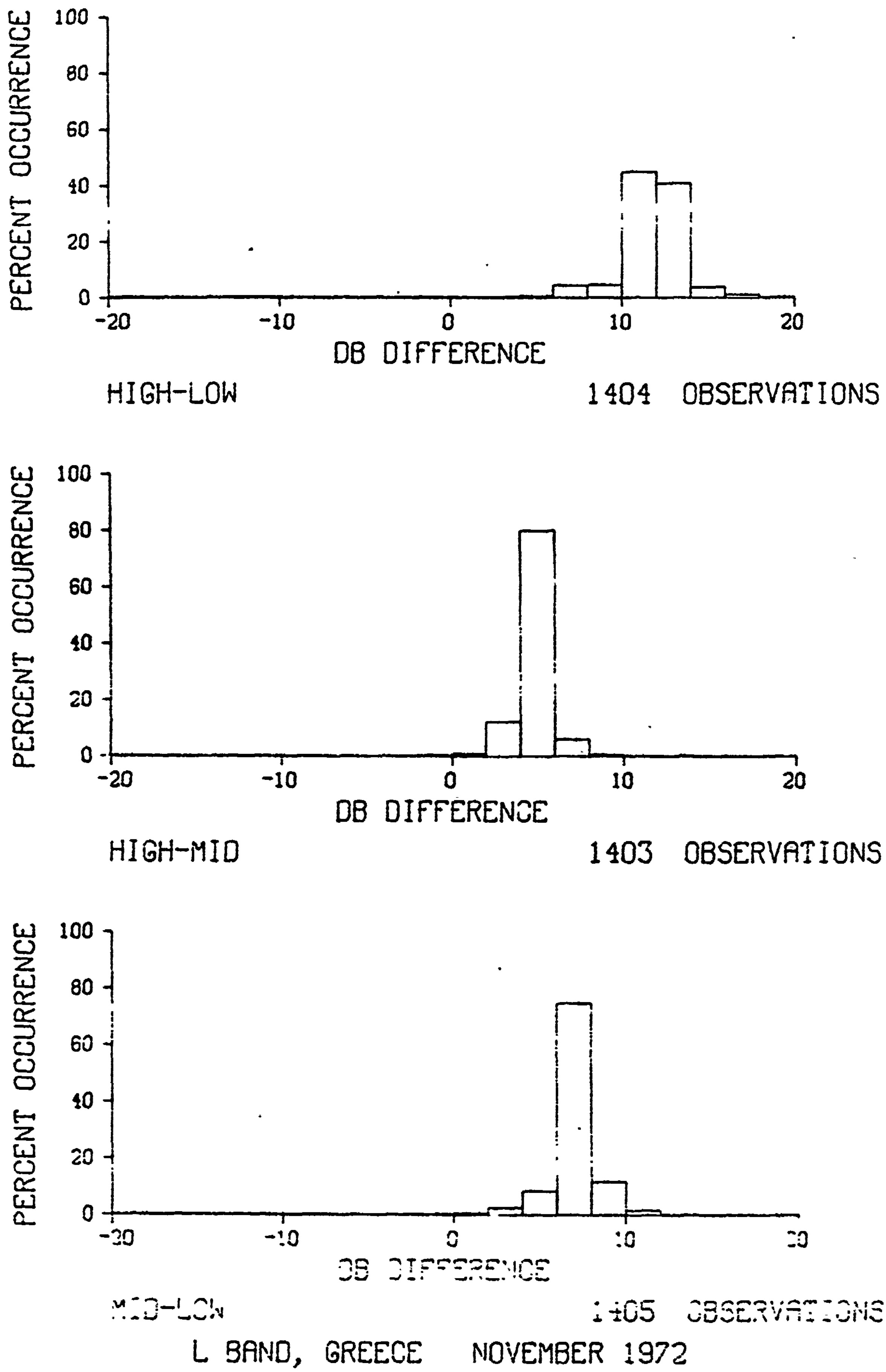

Figure 90. Frequency distributions of path loss differences between antennas for L-band

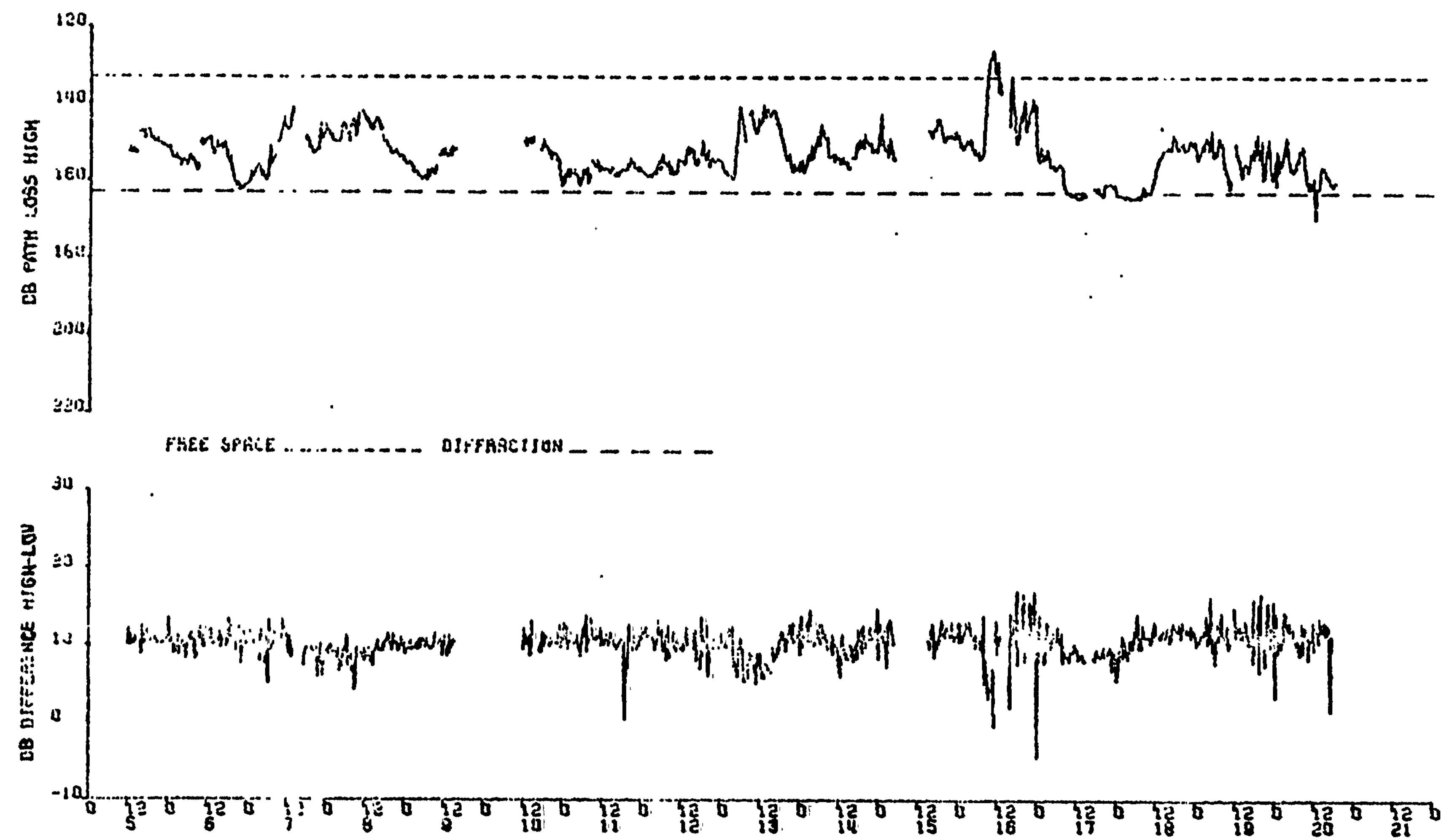

S BAND, NAXOS TO MYKENOS, GREECE   NOVEMBER 1972

Figure 91. Path loss for high S-band antenna and path loss difference high-low antenna

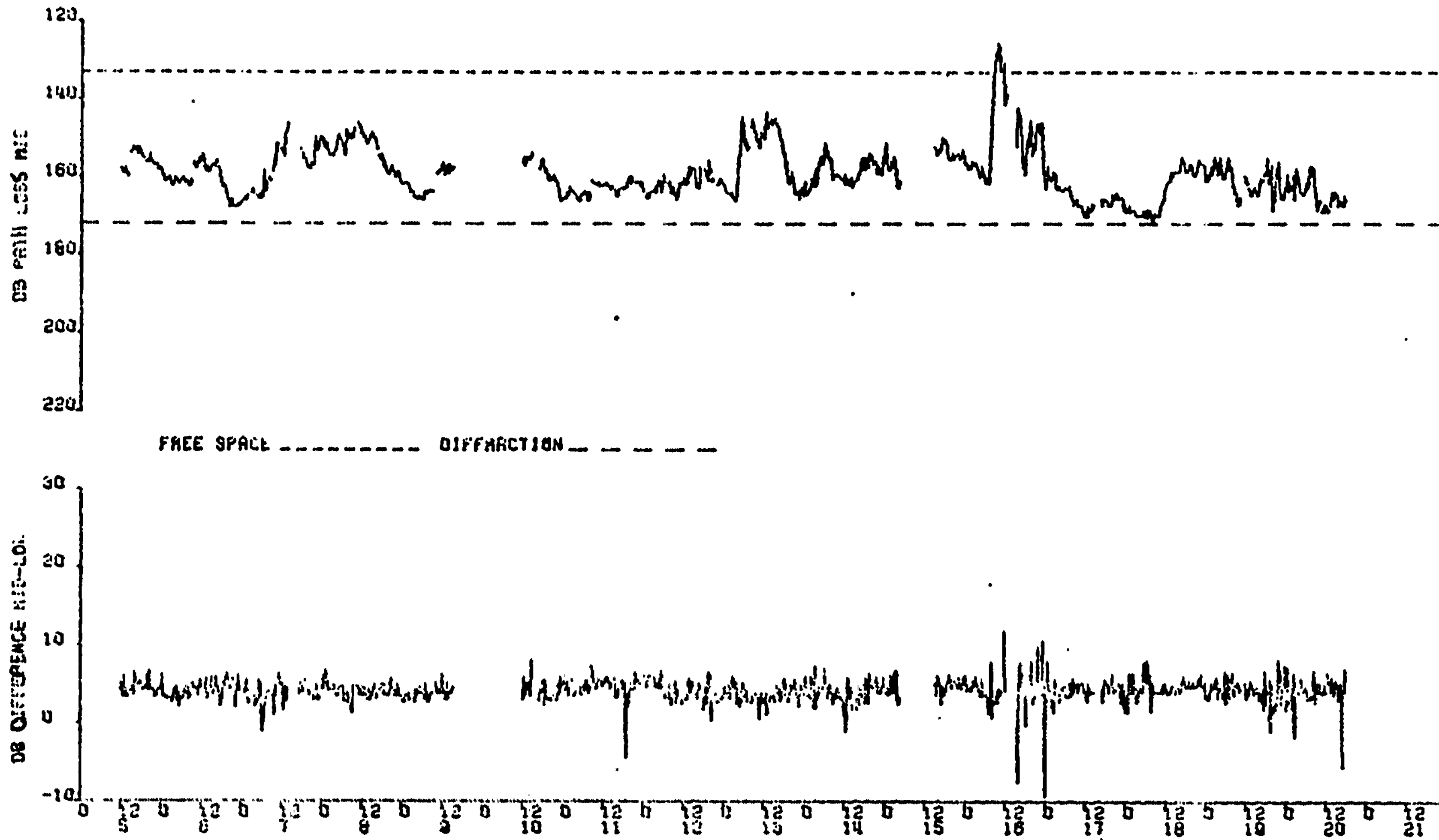

S BAND, NAXOS TO ATHENS, GREECE NOVEMBER 1972

Figure 92. Path loss for middle S-band antenna and path loss difference mid-low antenna

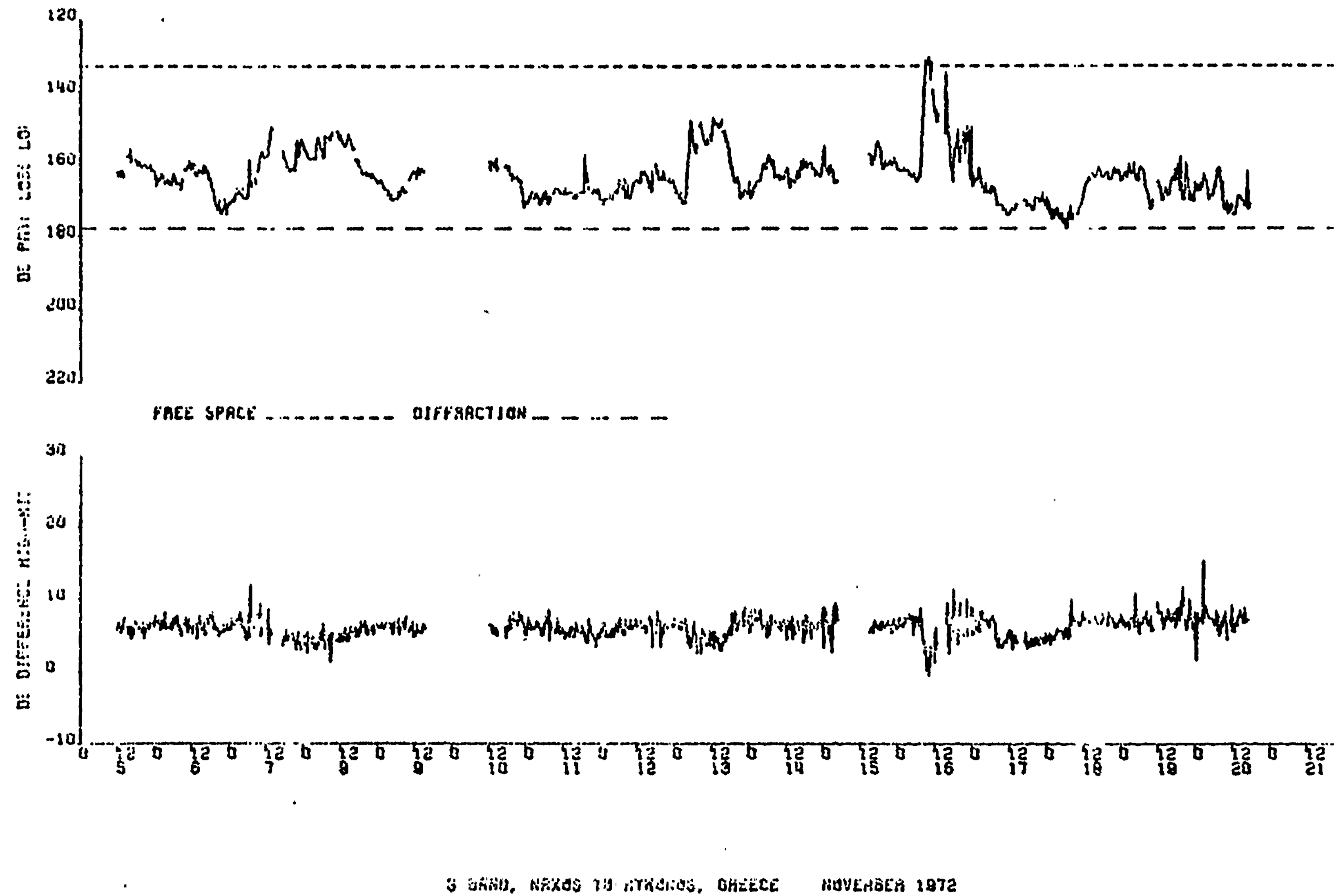

Figure 93. Path loss for low S-band antenna and path loss difference mid-low antenna

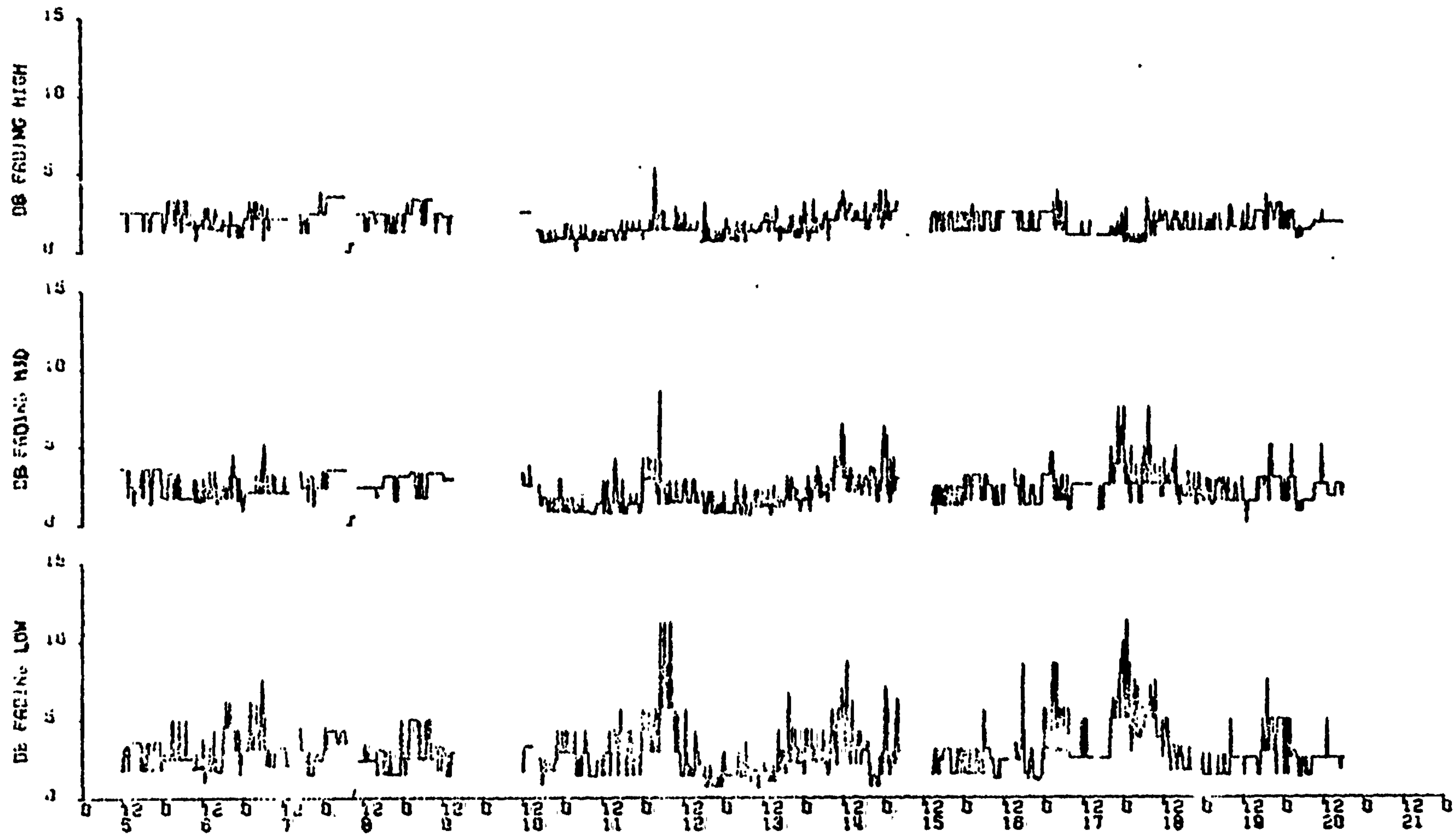

S BAND, NAXOS TO MYKONOS, GREECE NOVEMBER 1972

Figure 94. Fading S-band

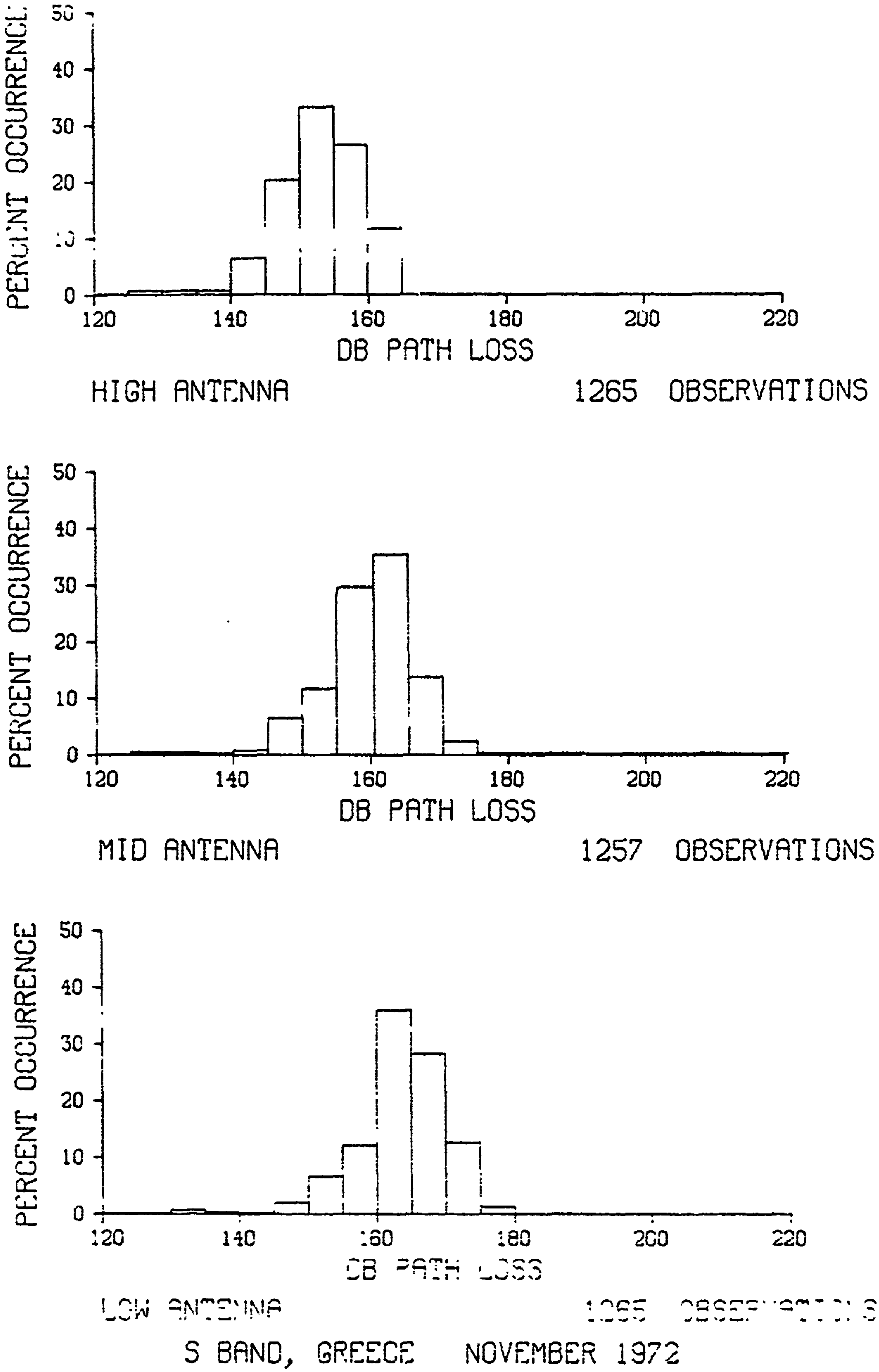

Figure 95. Frequency distributions of path loss for S-band

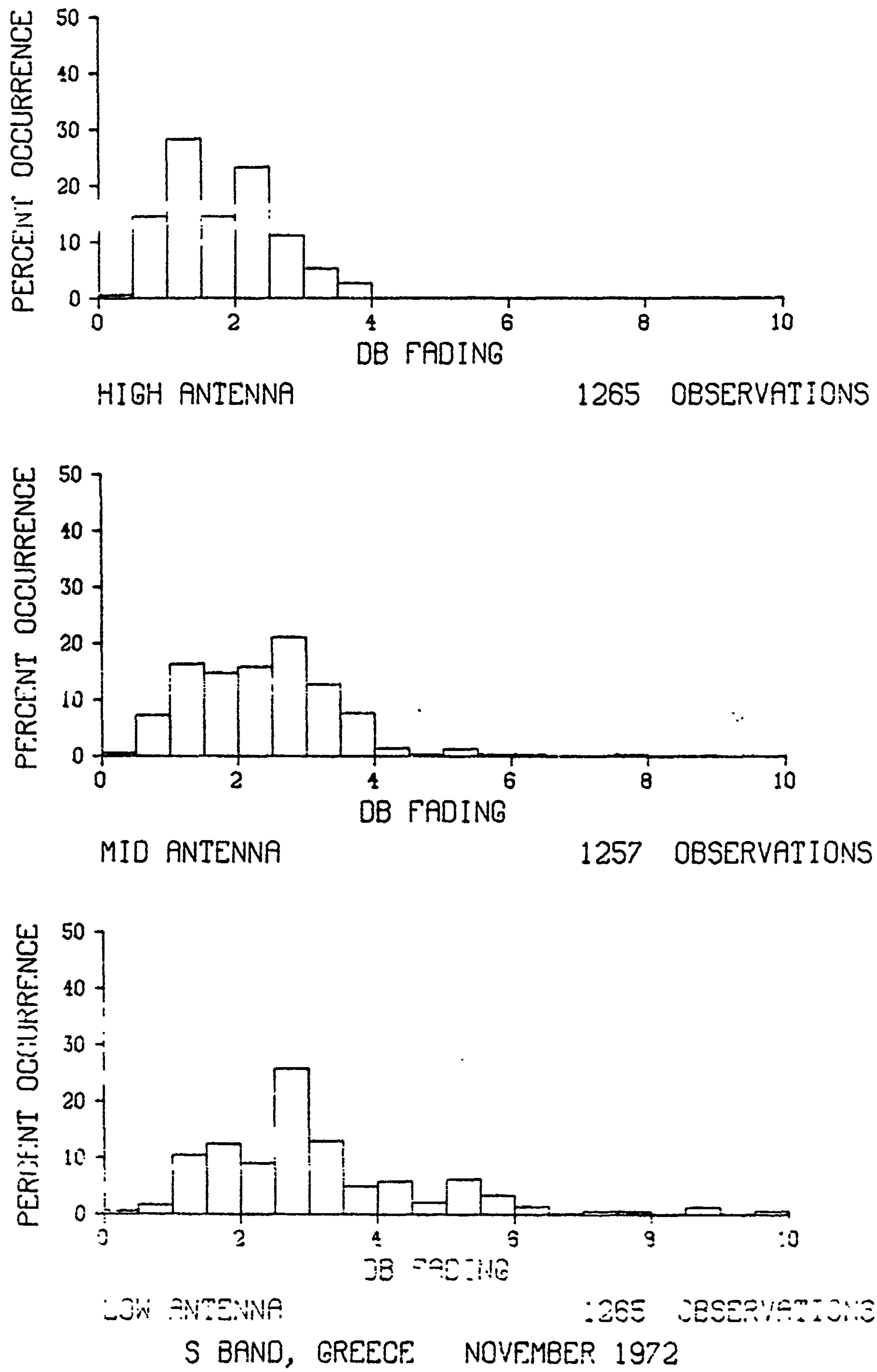

Figure 96. Frequency distributions of fading for S-band

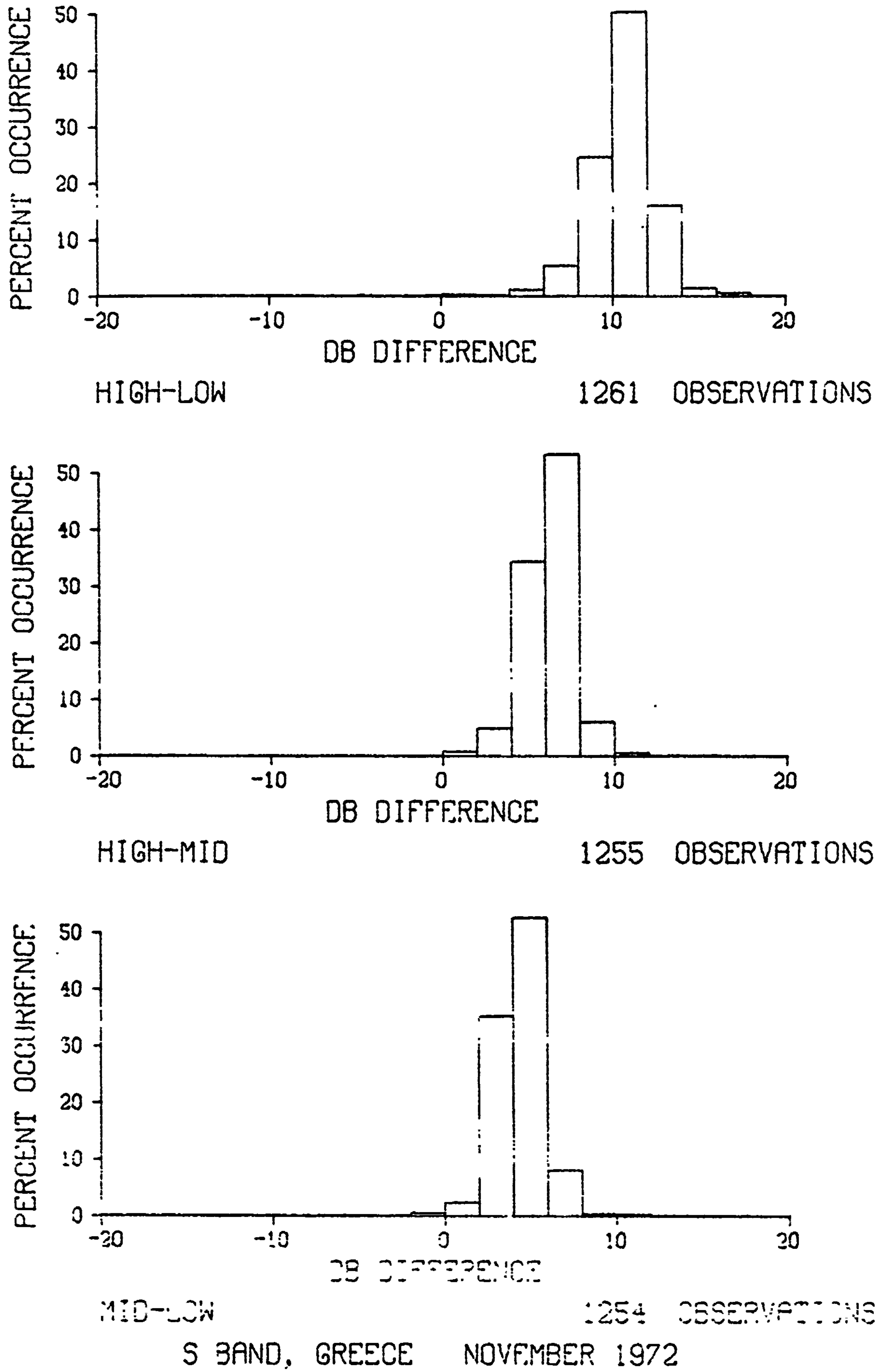

Figure 97. Frequency distributions of path loss differences between antennas for S-band

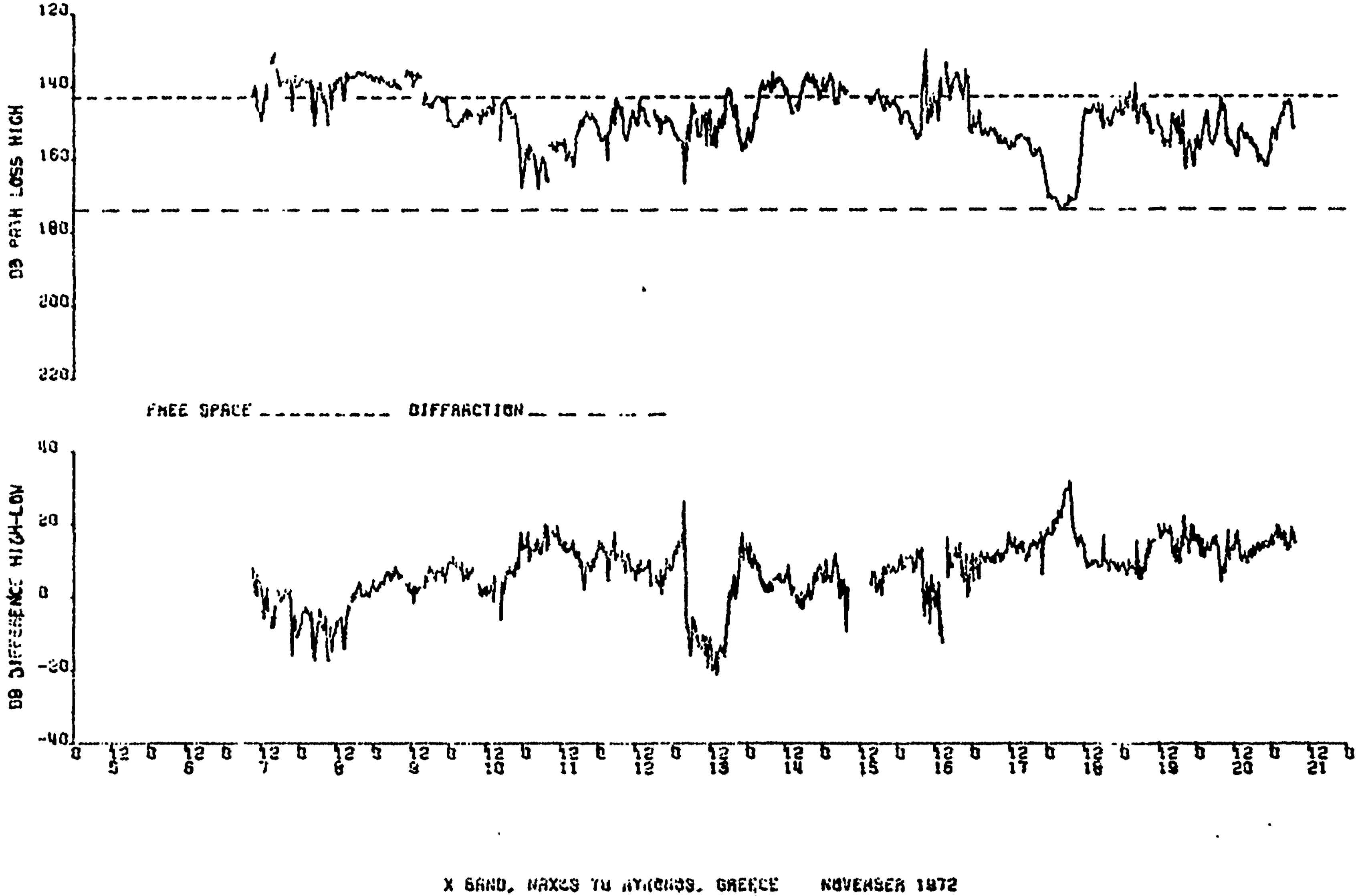

Figure 98. Path loss for high X-band antenna and path loss difference high-low antenna

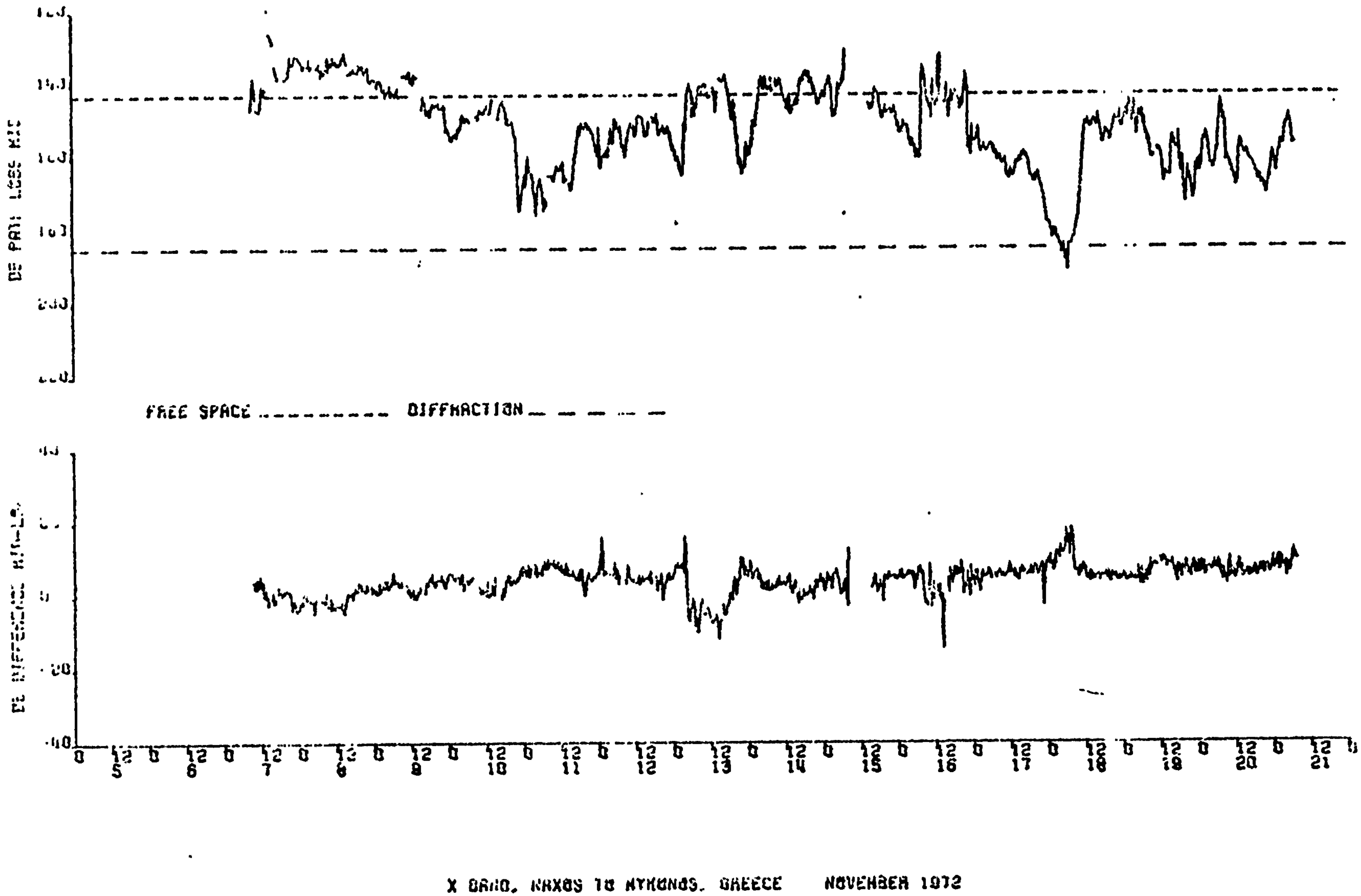

Figure 99. Path loss middle X-band antenna and path loss difference mid-low antenna

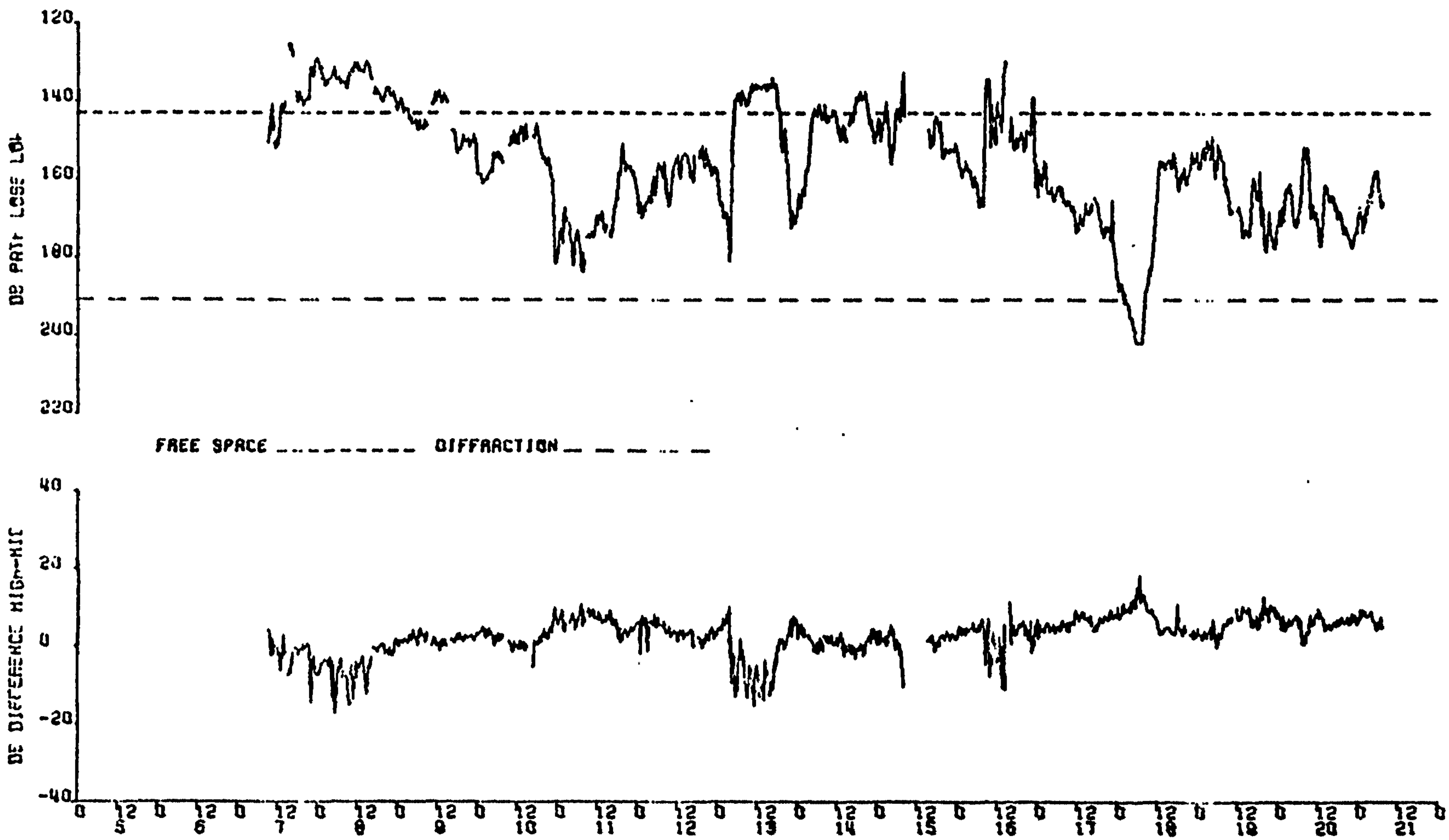

X BAND, NAXOS TO MYKONOS, GREECE NOVEMBER 1972

Figure 100. Path loss low X-band antenna and path loss difference high-mid antenna

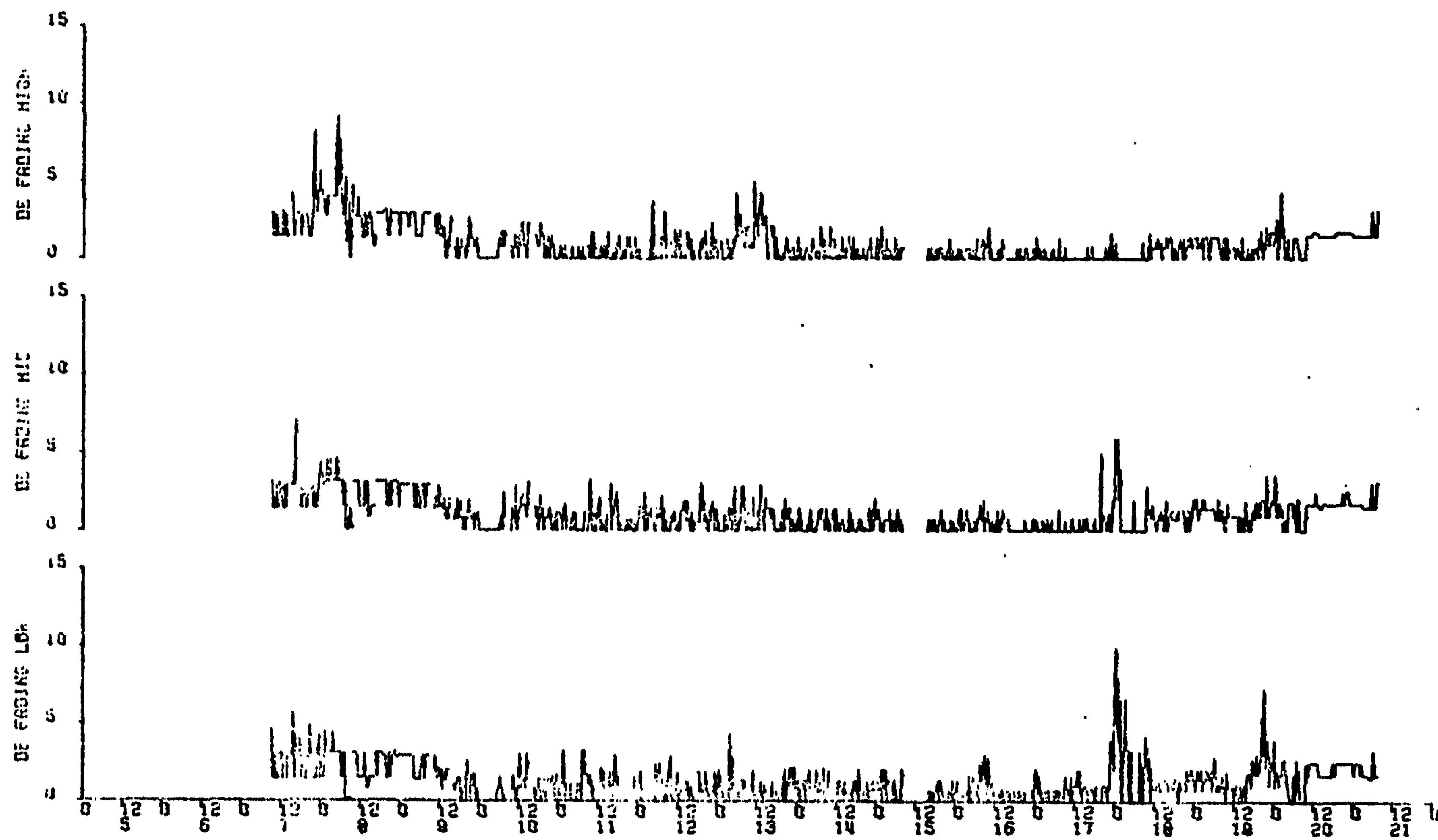

X BAND, NAXOS TO MYKONOS, GREECE NOVEMBER 1972

Figure 101. Fading X-band

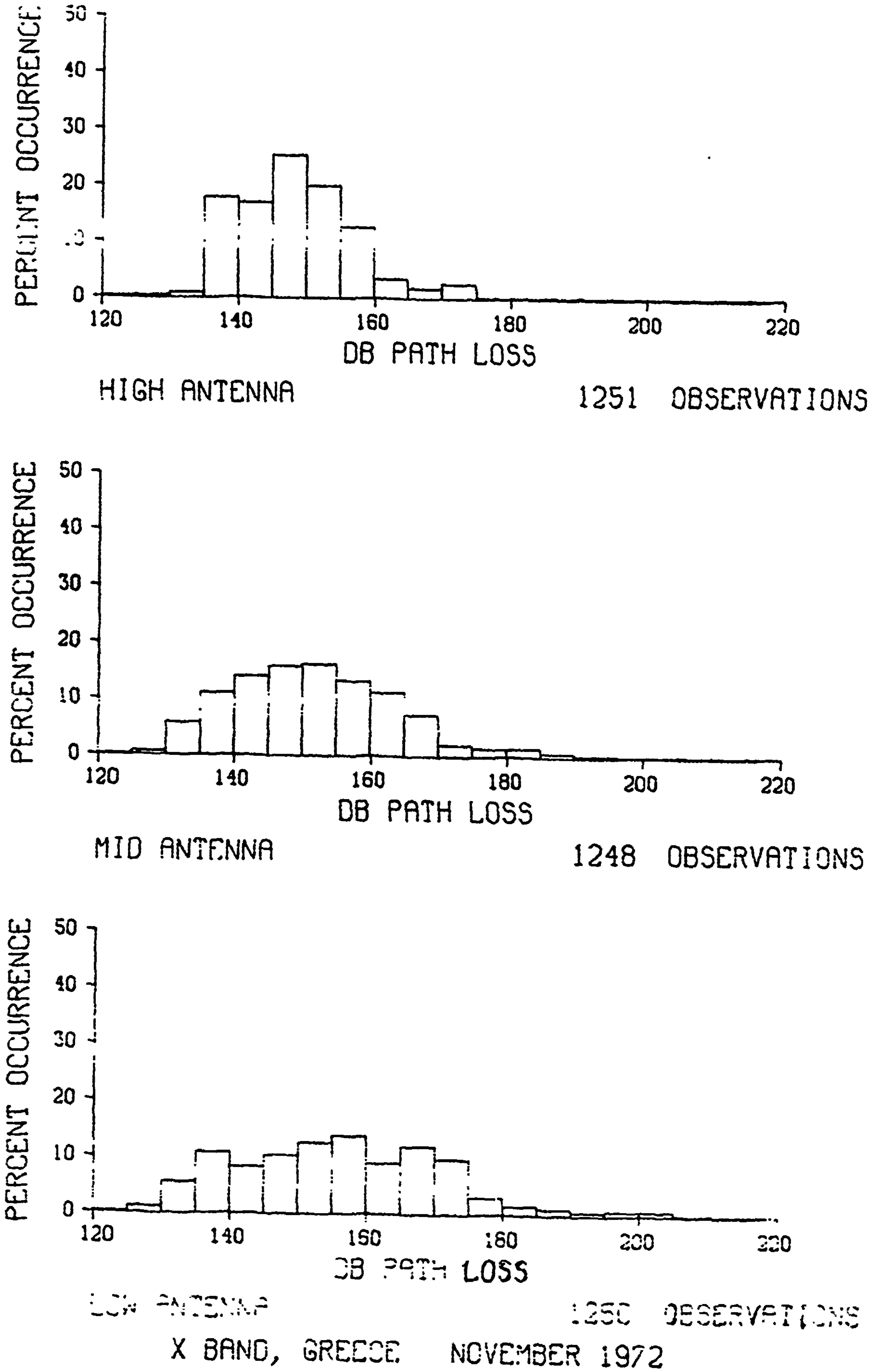

Figure 102. Frequency distribution of path loss for X-band

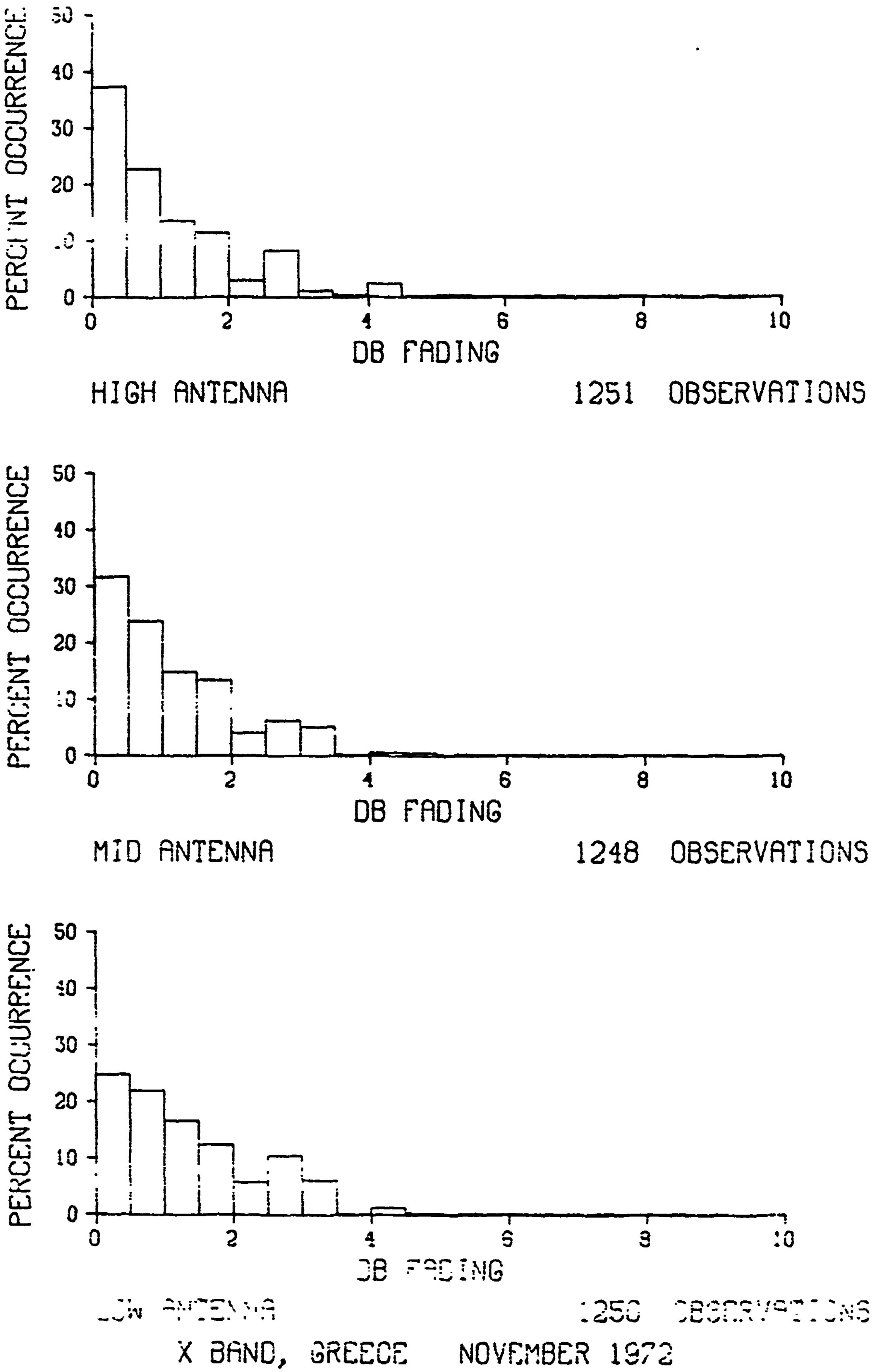

Figure 103. Frequency distribution of fading X-band

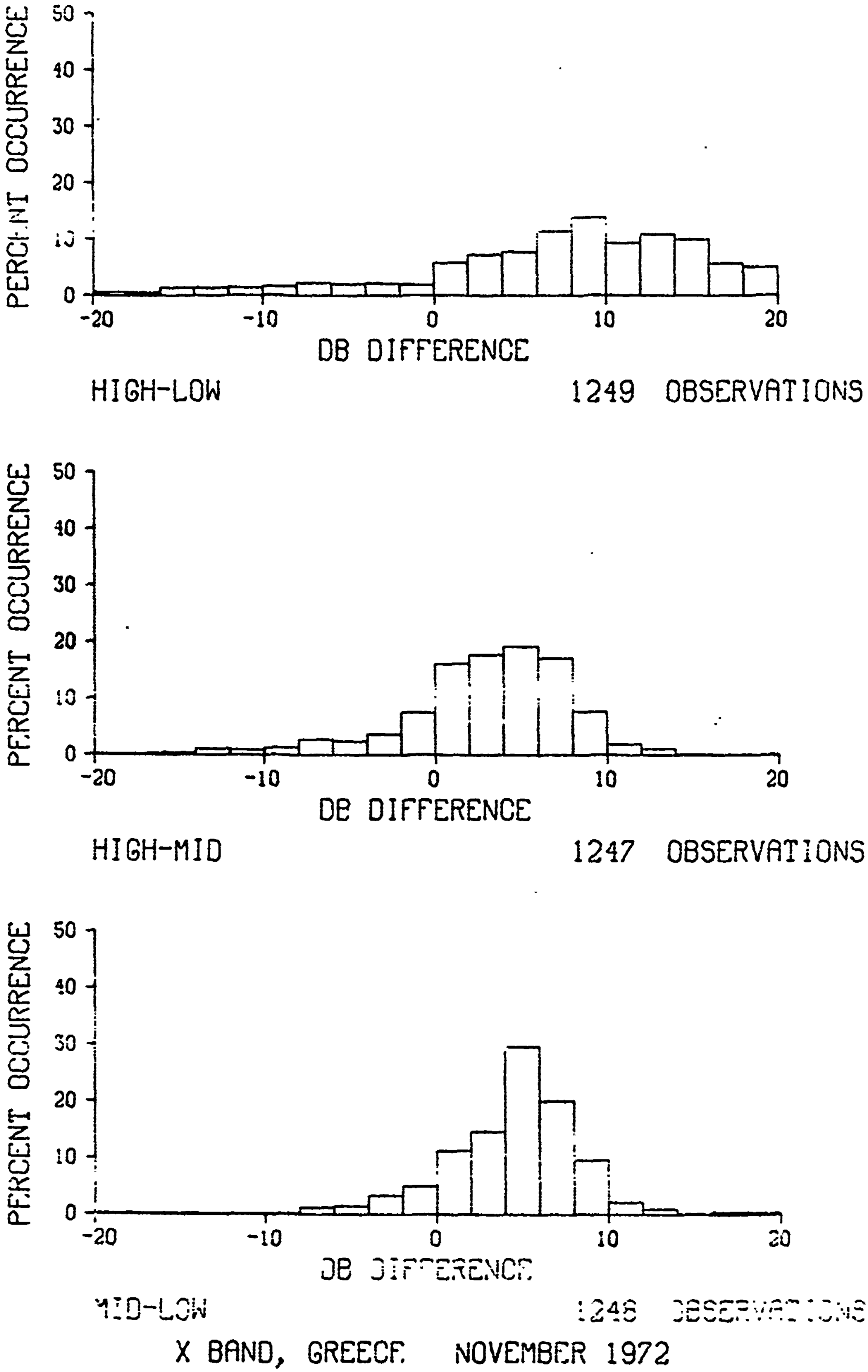

Figure 104. Frequency distribution of differences between antennas for X-band

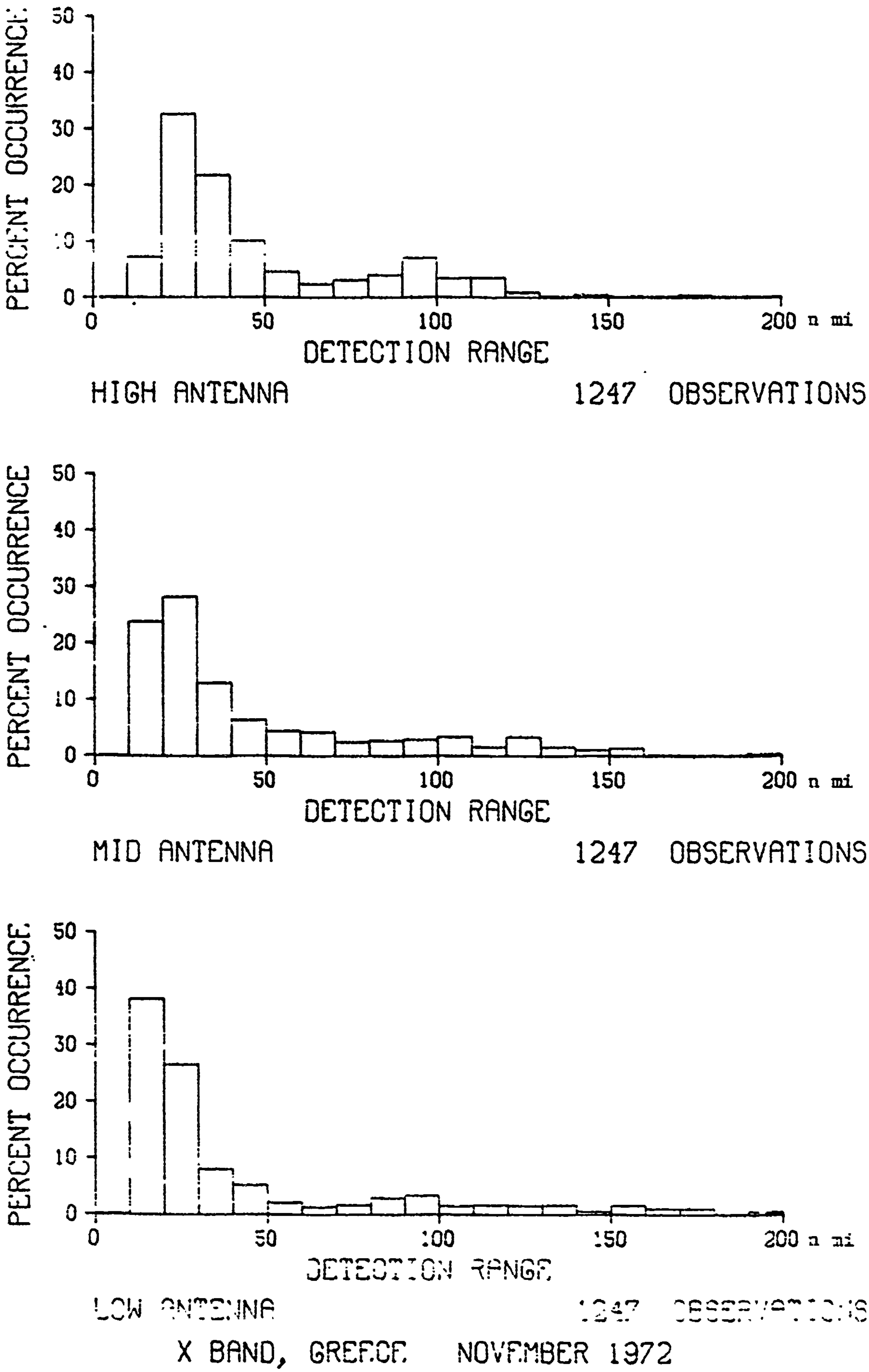

Figure 105. Frequency distribution of detection range for X-band

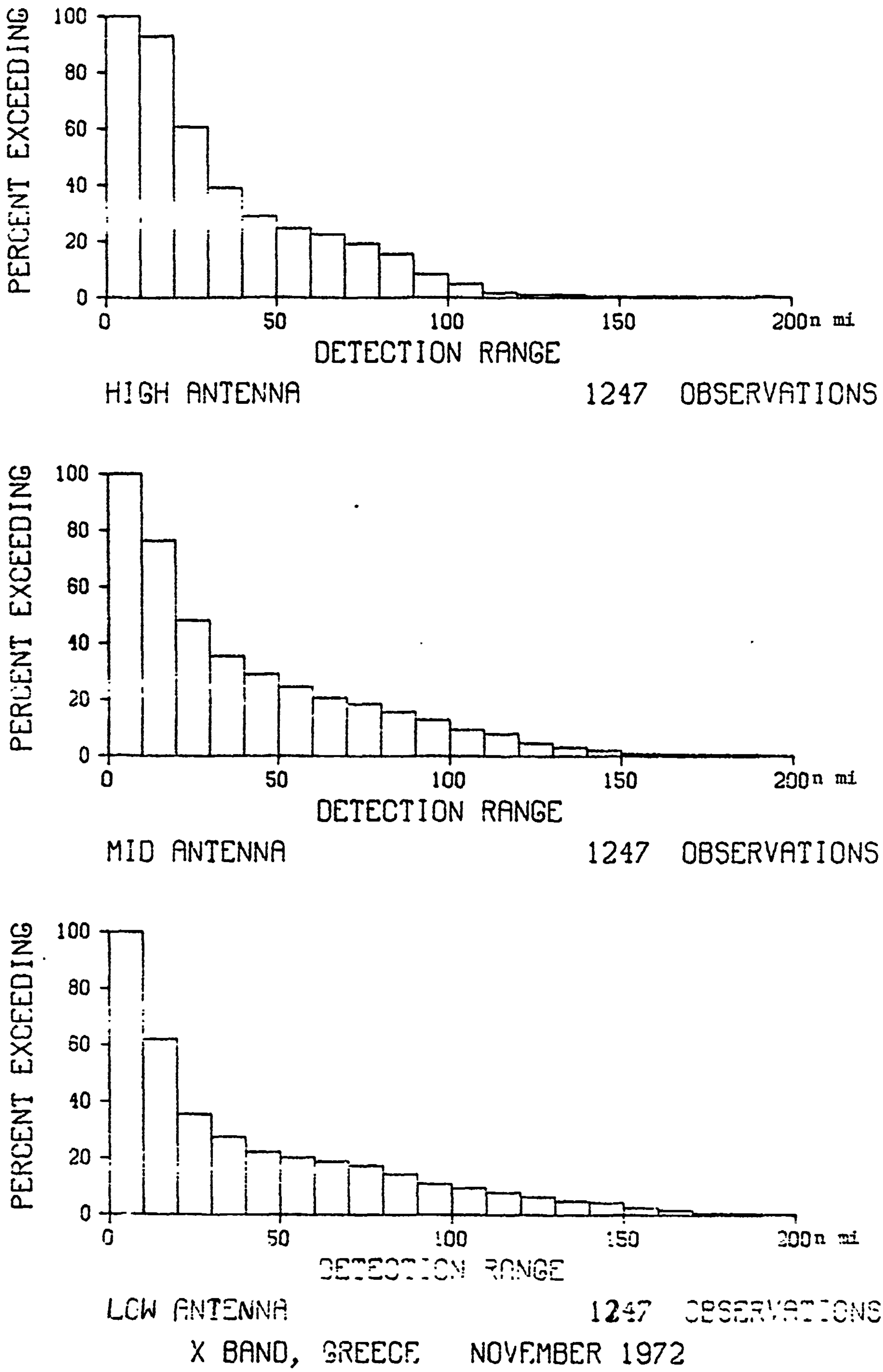

Figure 106. Cumulative distribution of detection range for X-band

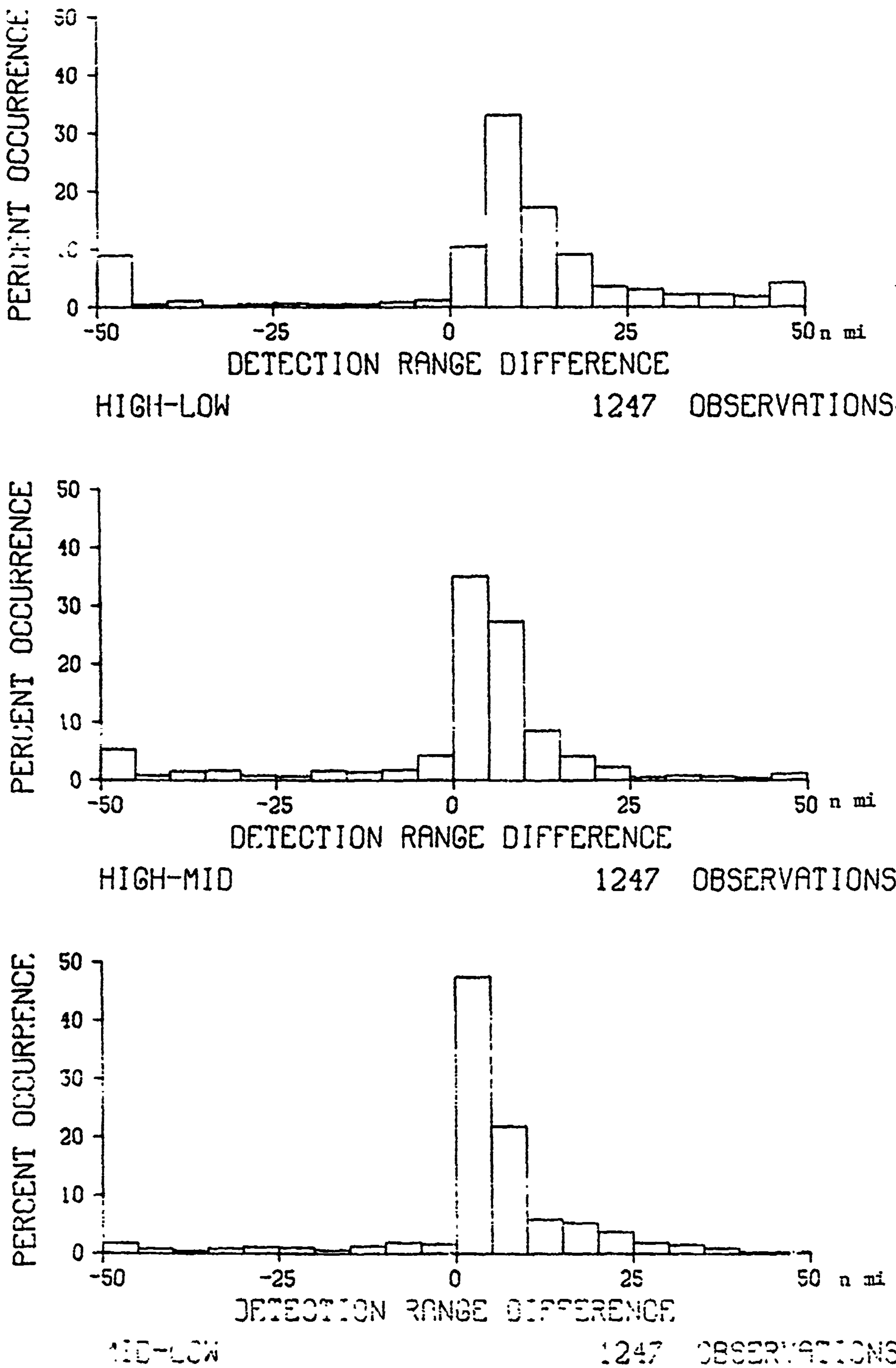

Figure 107. Frequency distribution of detection range differences between antennas for X-band

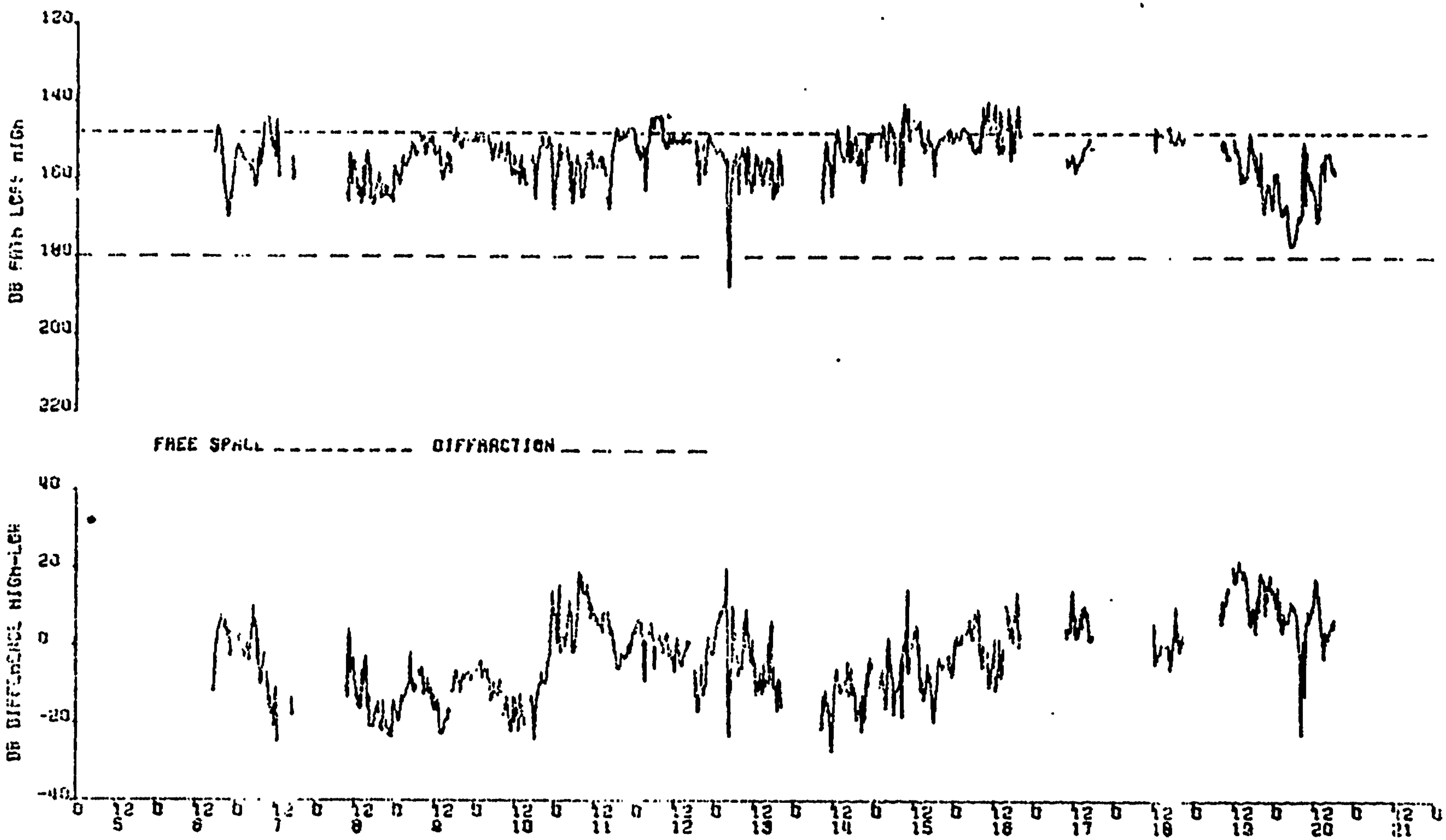

KU BAND, NAXOS TO MYKONOS, GREECE NOVEMBER 1972

Figure 108. Path loss for high Ku-band antenna and path loss difference high-low antenna

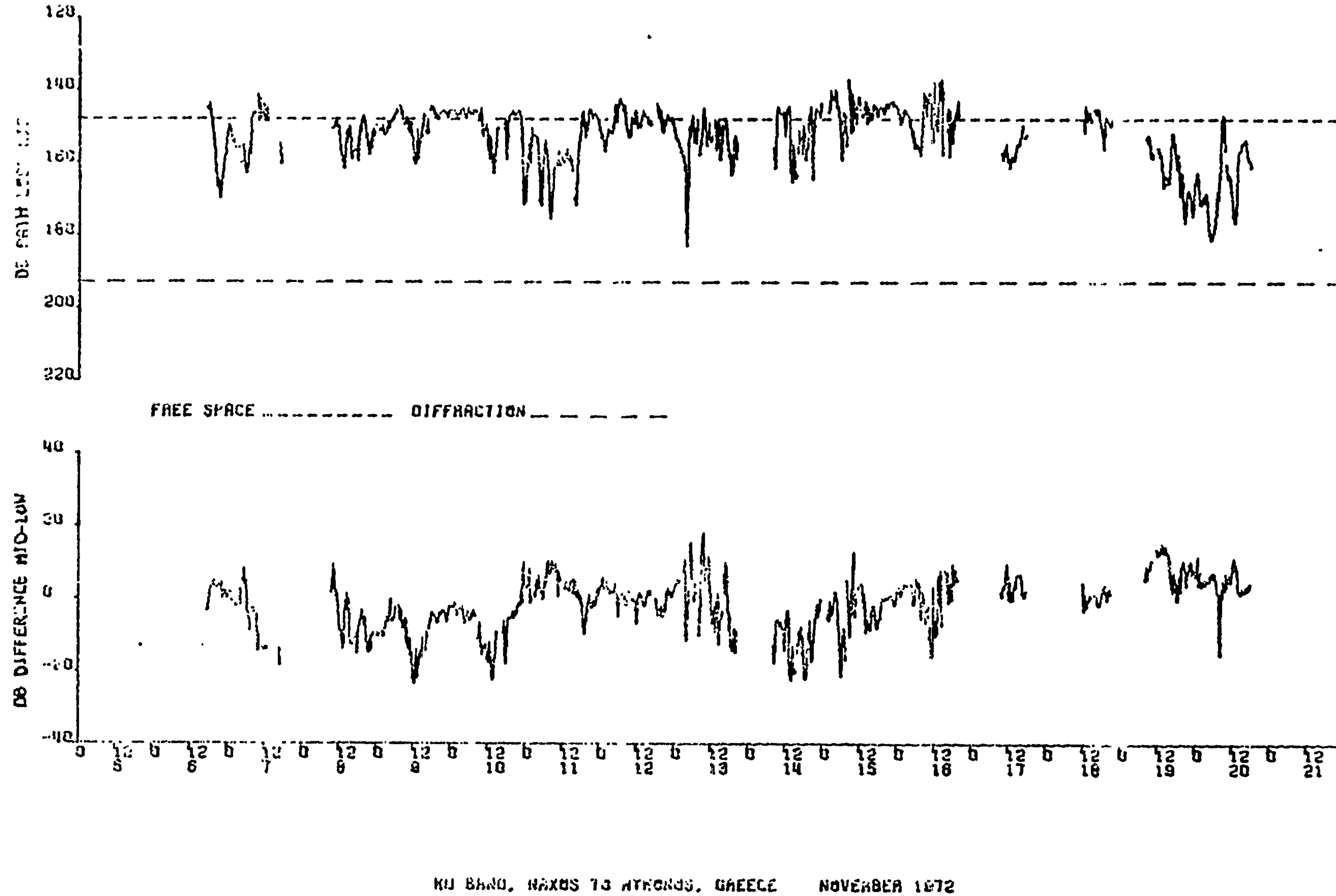

Figure 109. Path loss for mid Ku-band antenna and path loss difference mid-low antenna

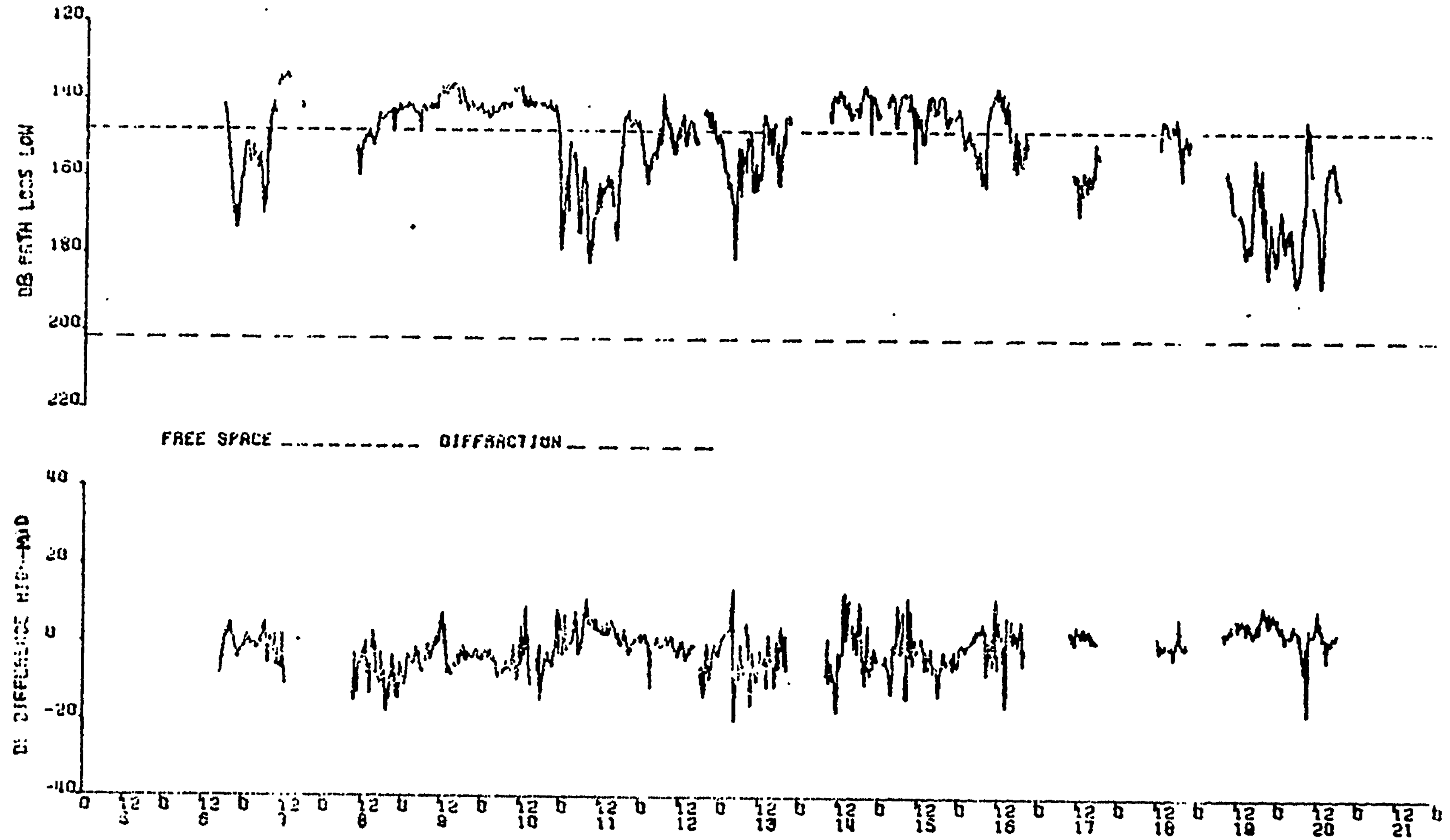

KU BAND, NAXOS TO MYKONOS, GREECE   NOVEMBER 1972

Figure 110. Path loss for low Ku-band antenna and path loss difference high-mid antenna

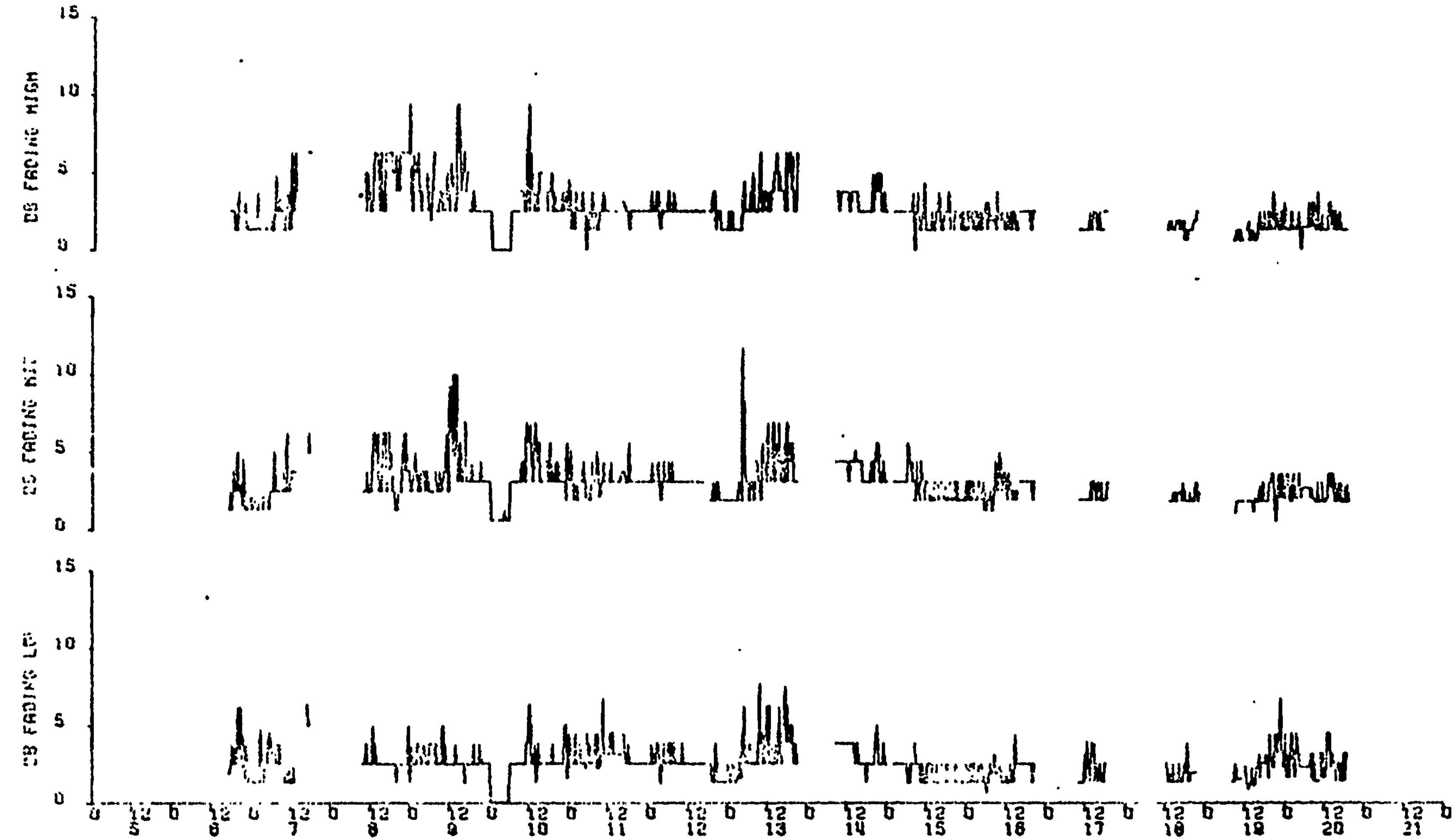

KU BAND, NAXOS TO HYMETTOS, GREECE NOVEMBER 1972

Figure 111. Fading Ku-band

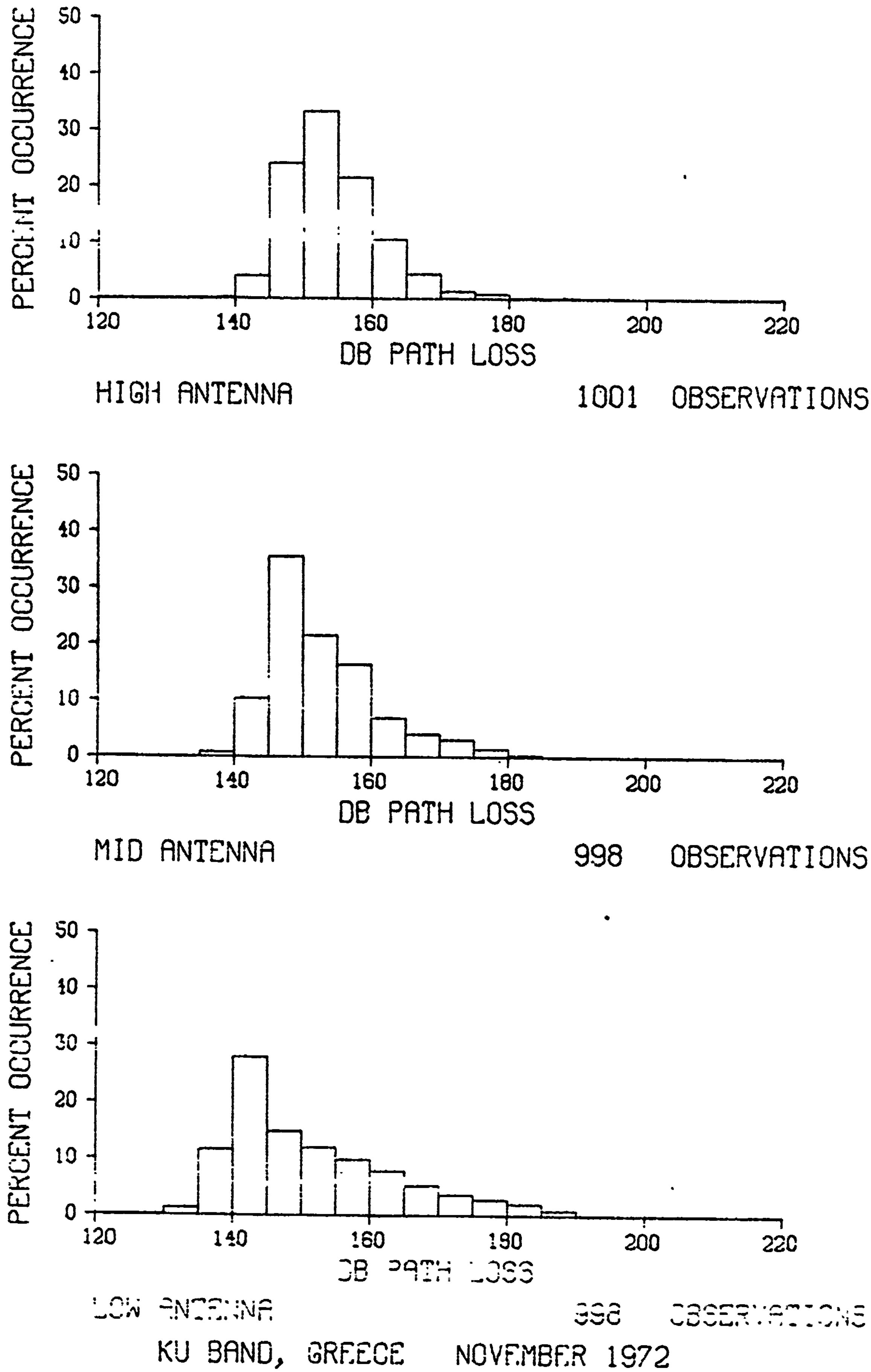

Figure 112. Frequency distributions of path loss for Ku-band

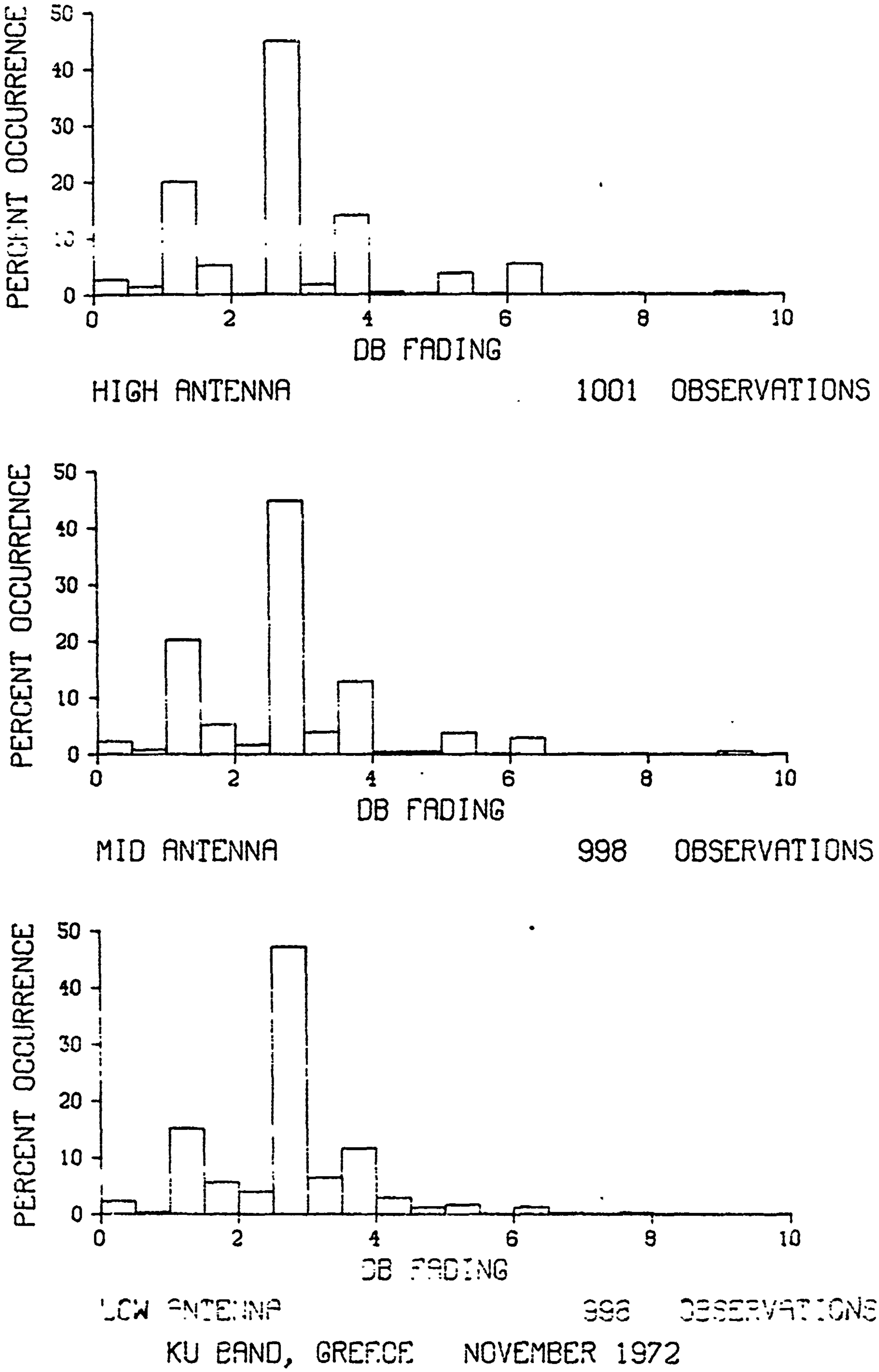

Figure 113. Frequency distributions of fading for Ku-band

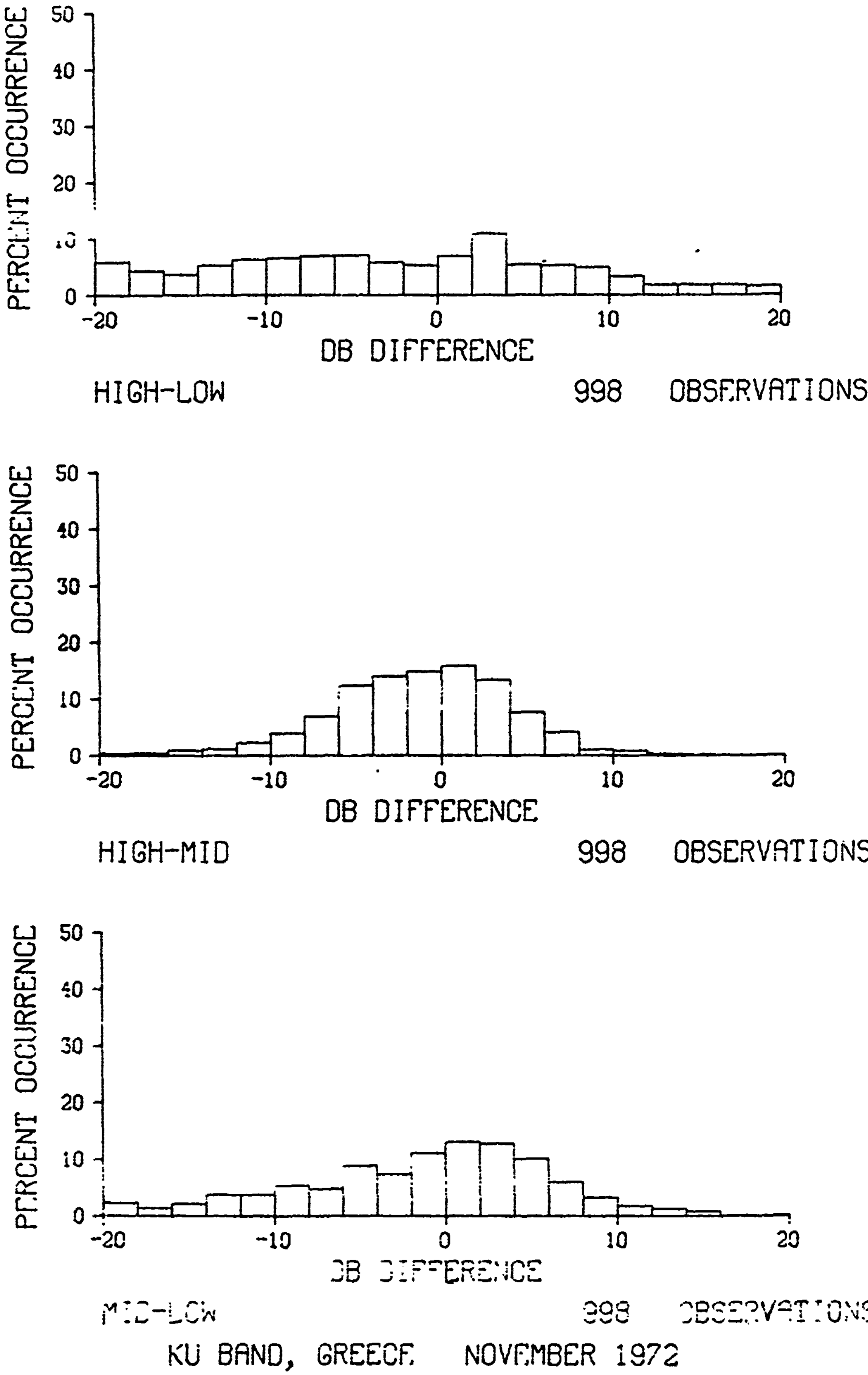

Figure 114. Frequency distributions of path loss differences between antennas for Ku-band

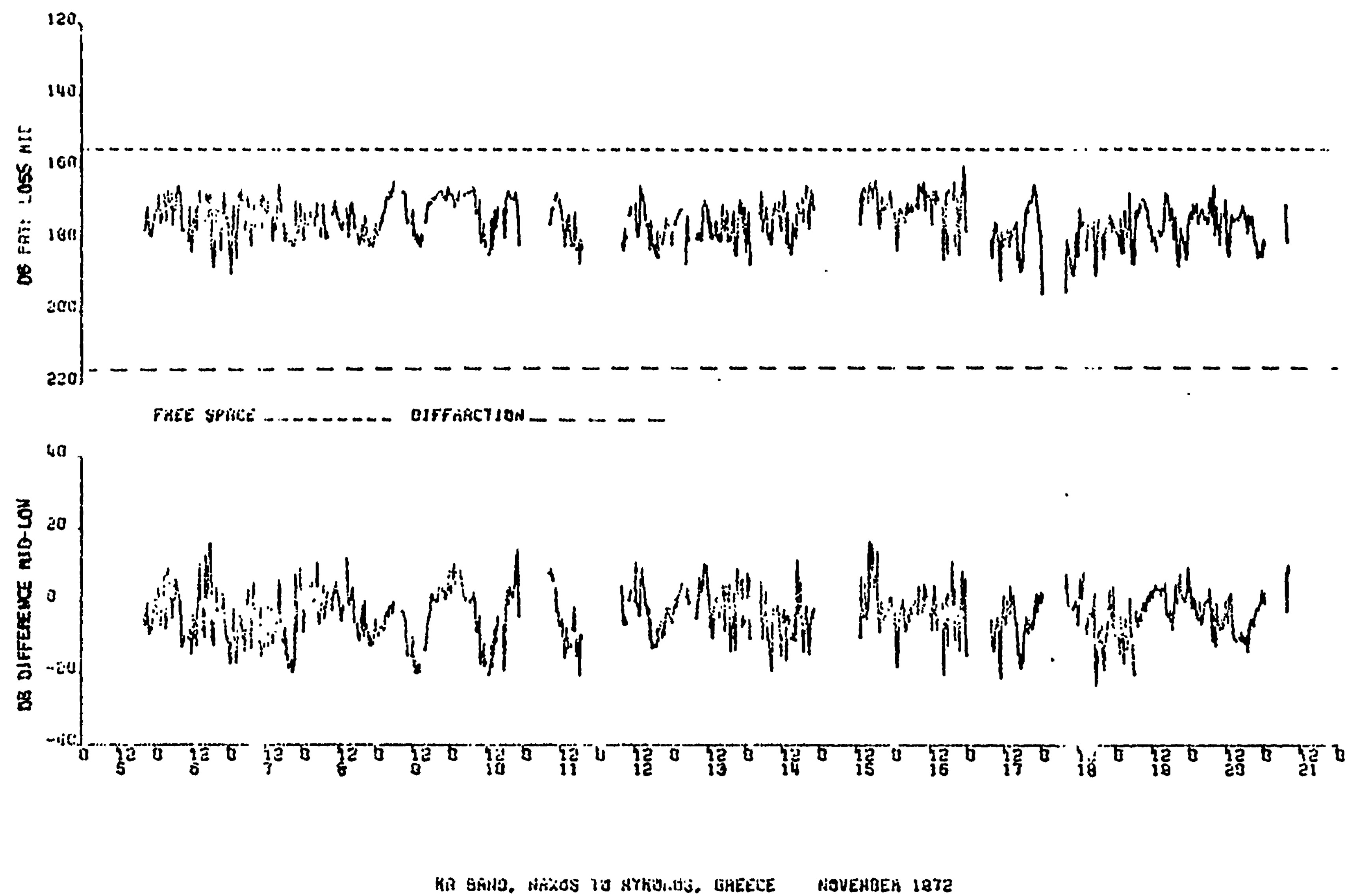

Figure 115. Path loss for middle Ka-band antenna and path loss difference mid-low antenna

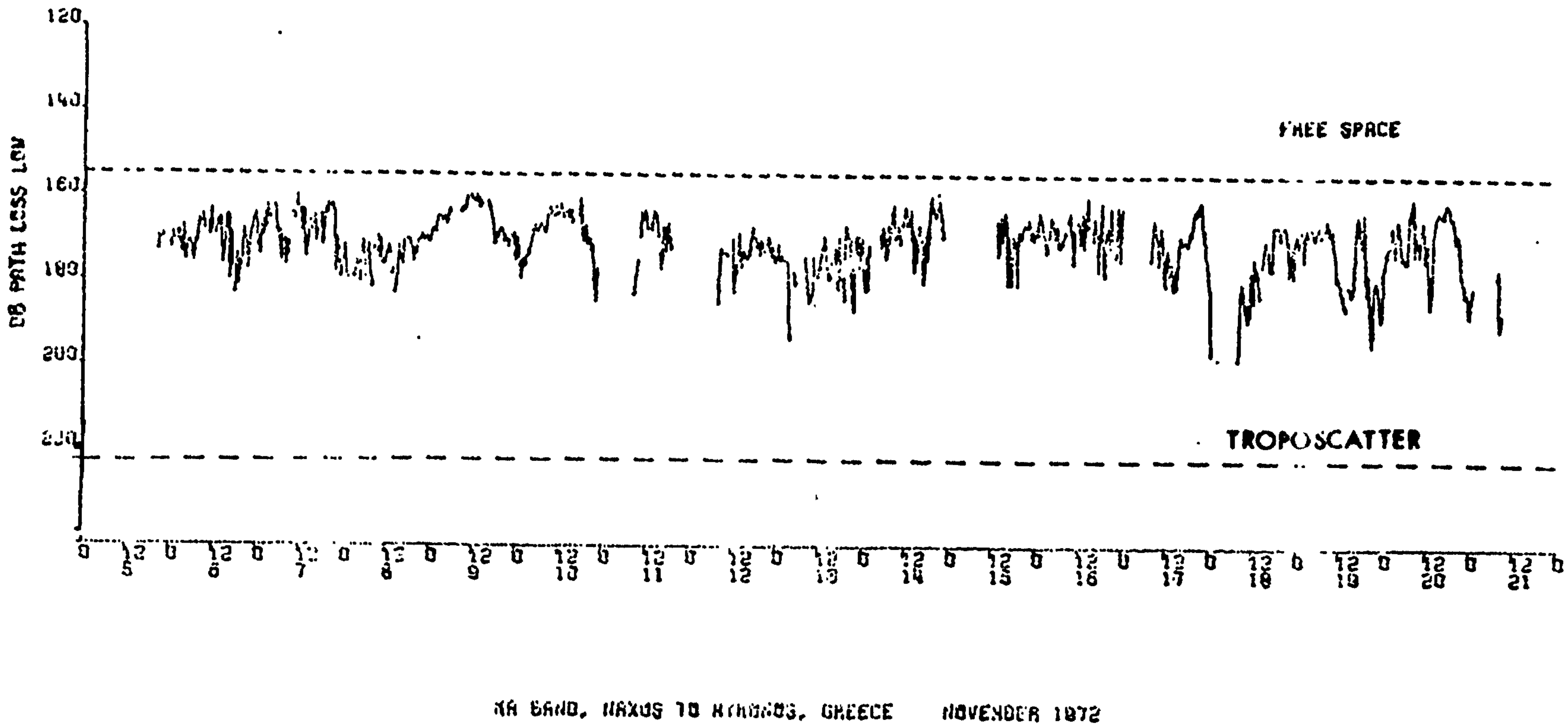

Figure 116. Path loss for low Ka-band antenna

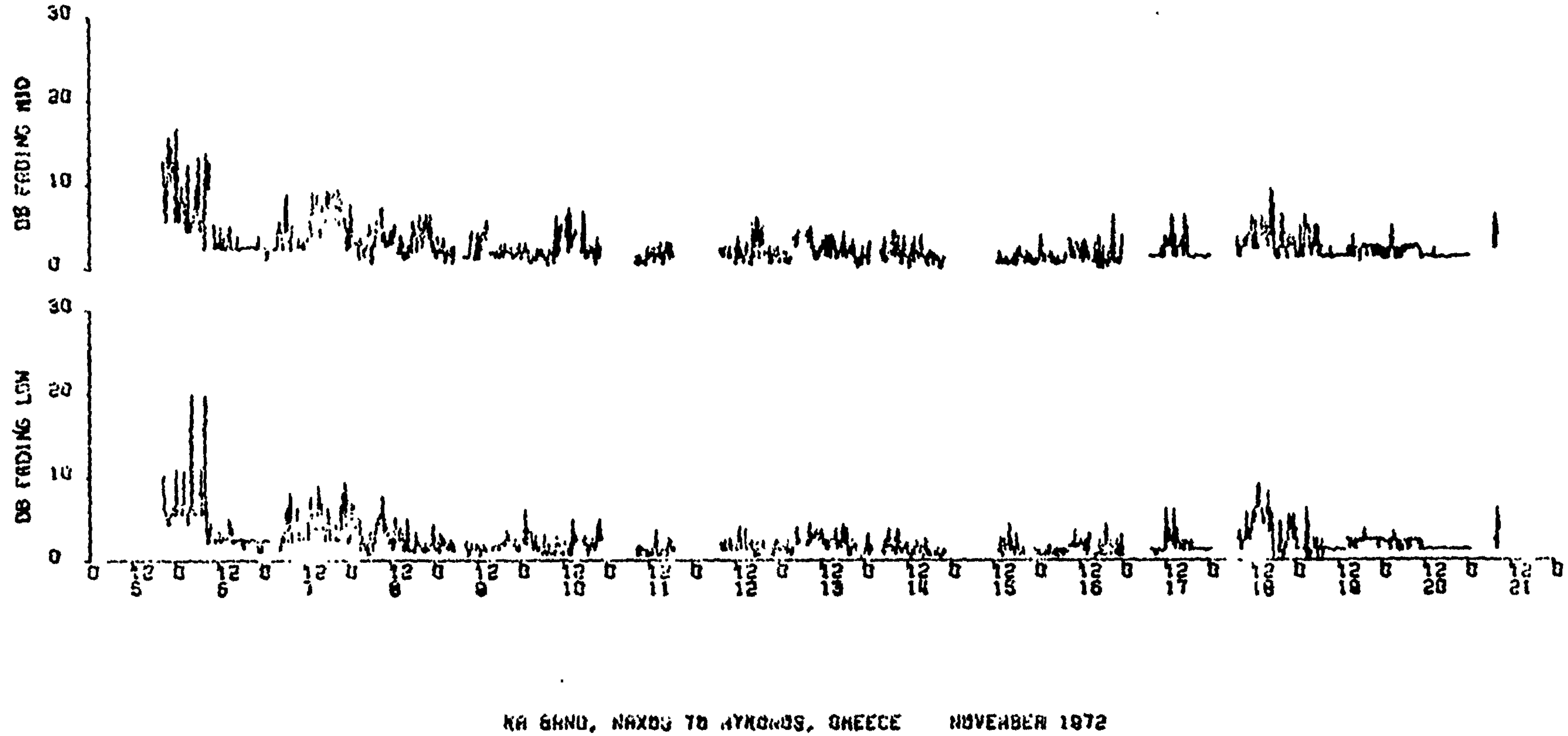

Figure 117. Fading Ka-band

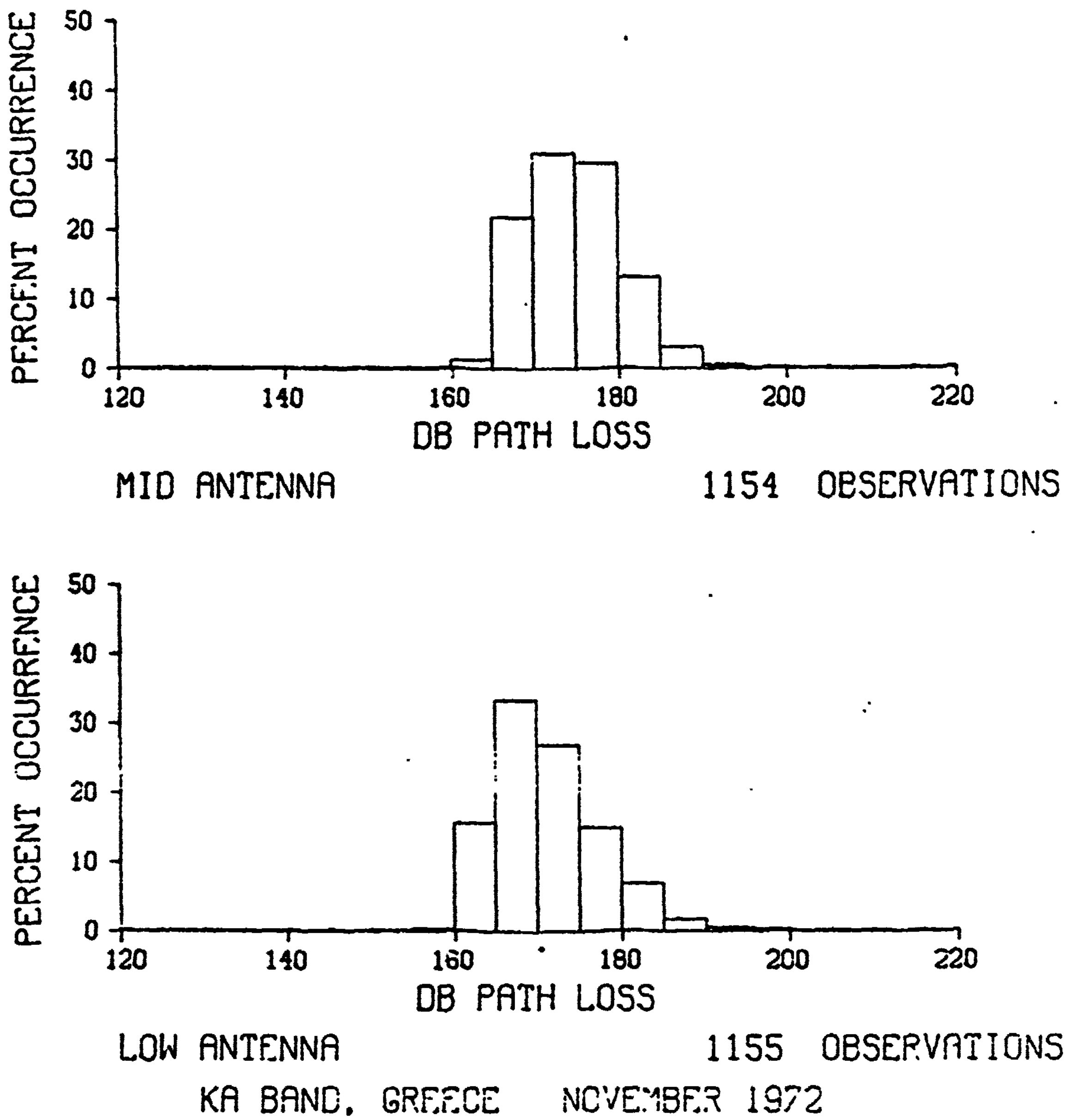

Figure 118. Frequency distribution of path loss for Ka-band

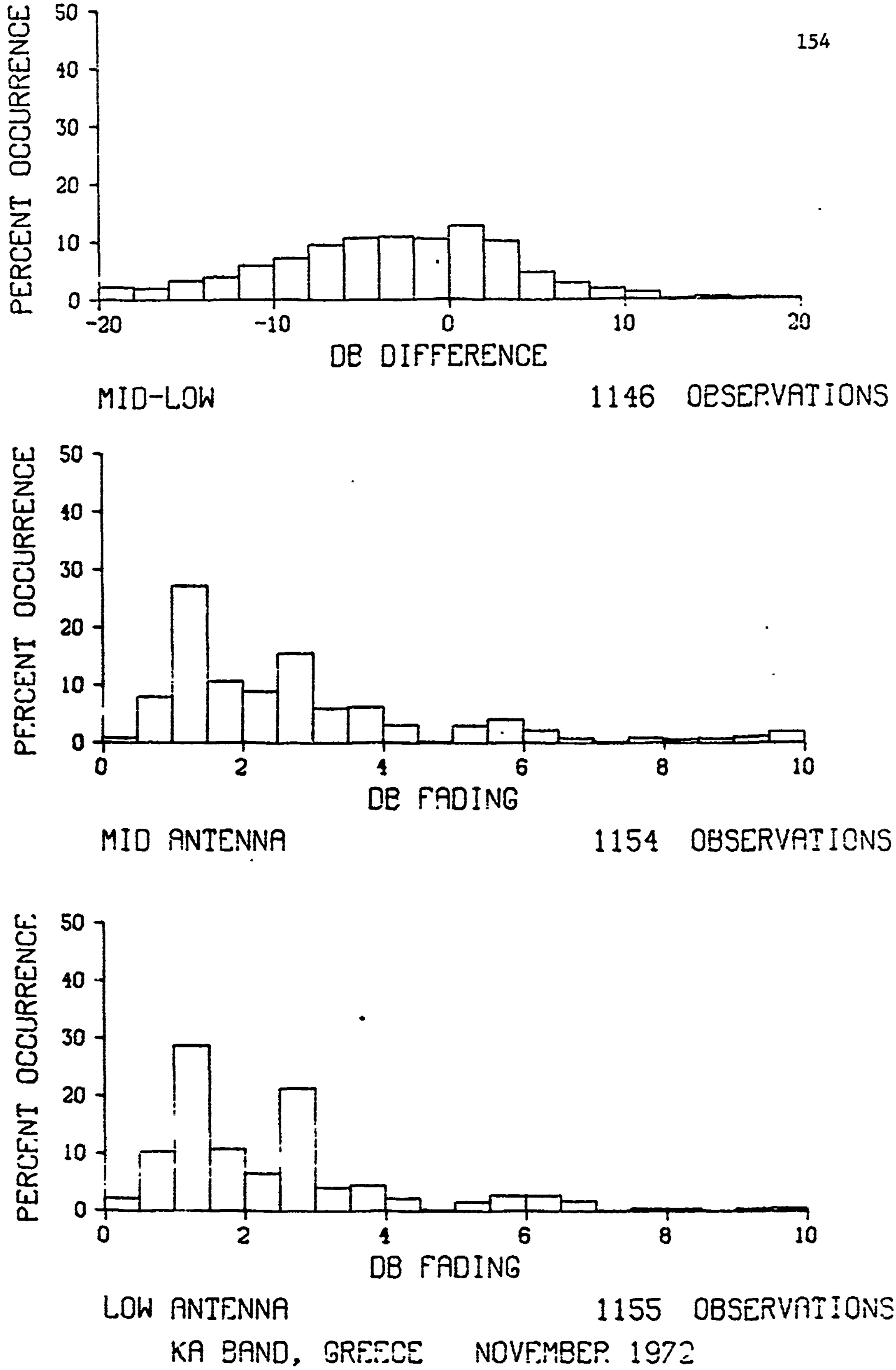

Figure 119. Frequency distributions of path loss difference between antennas and fading for Ka-band

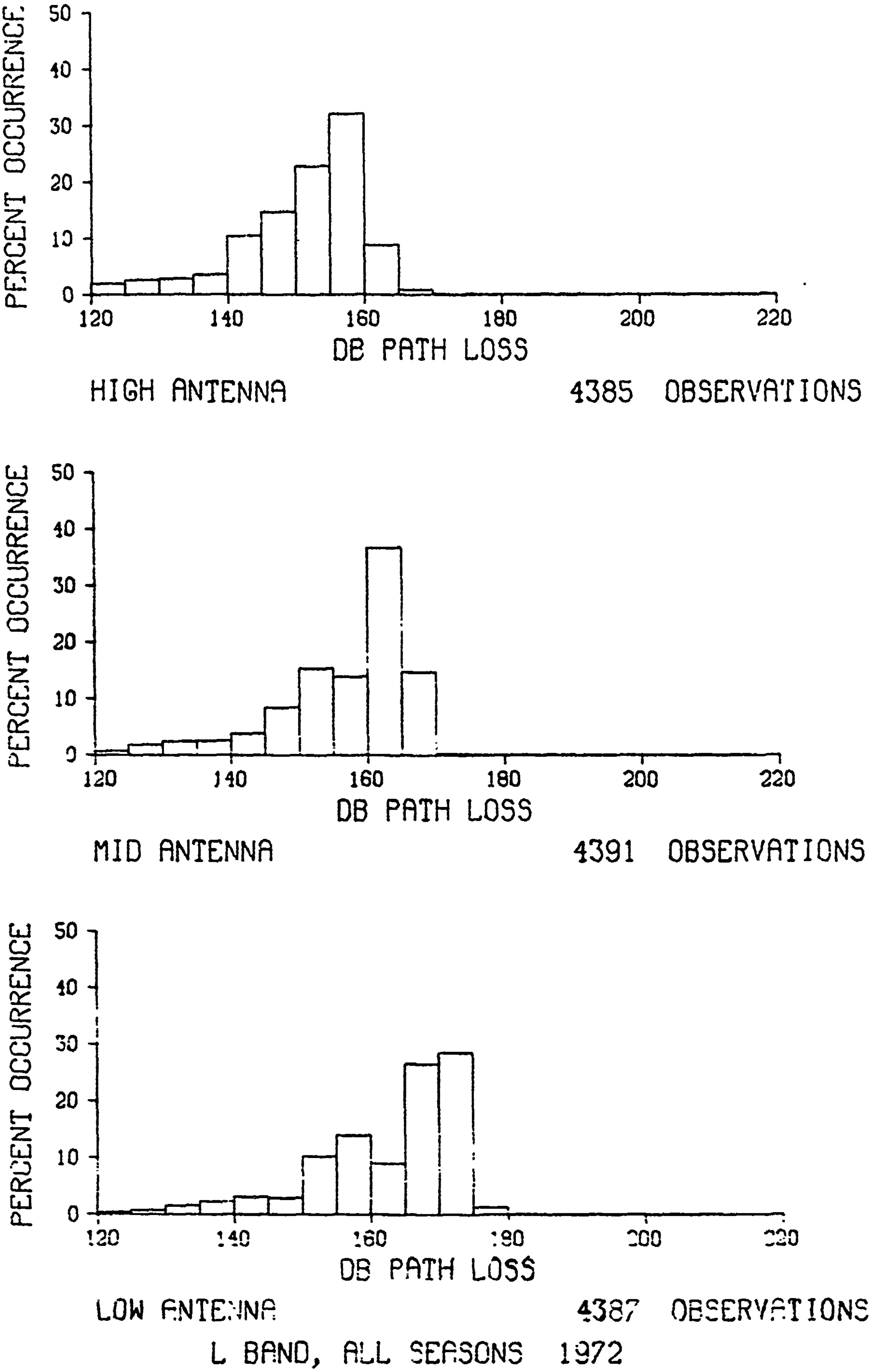

Figure 120. Frequency distributions of path loss for L-band

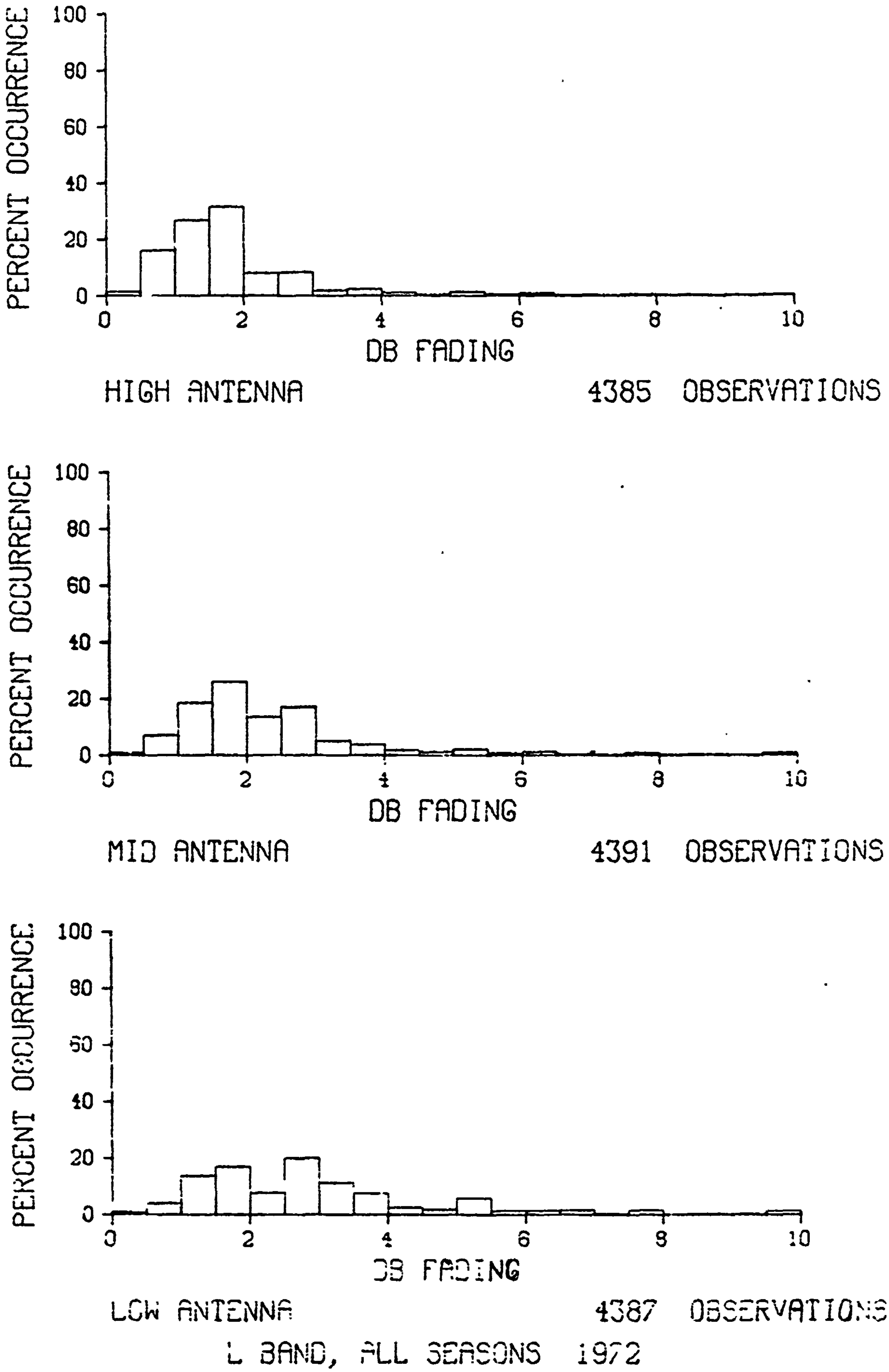

Figure 121. Frequency distributions of fading L-band

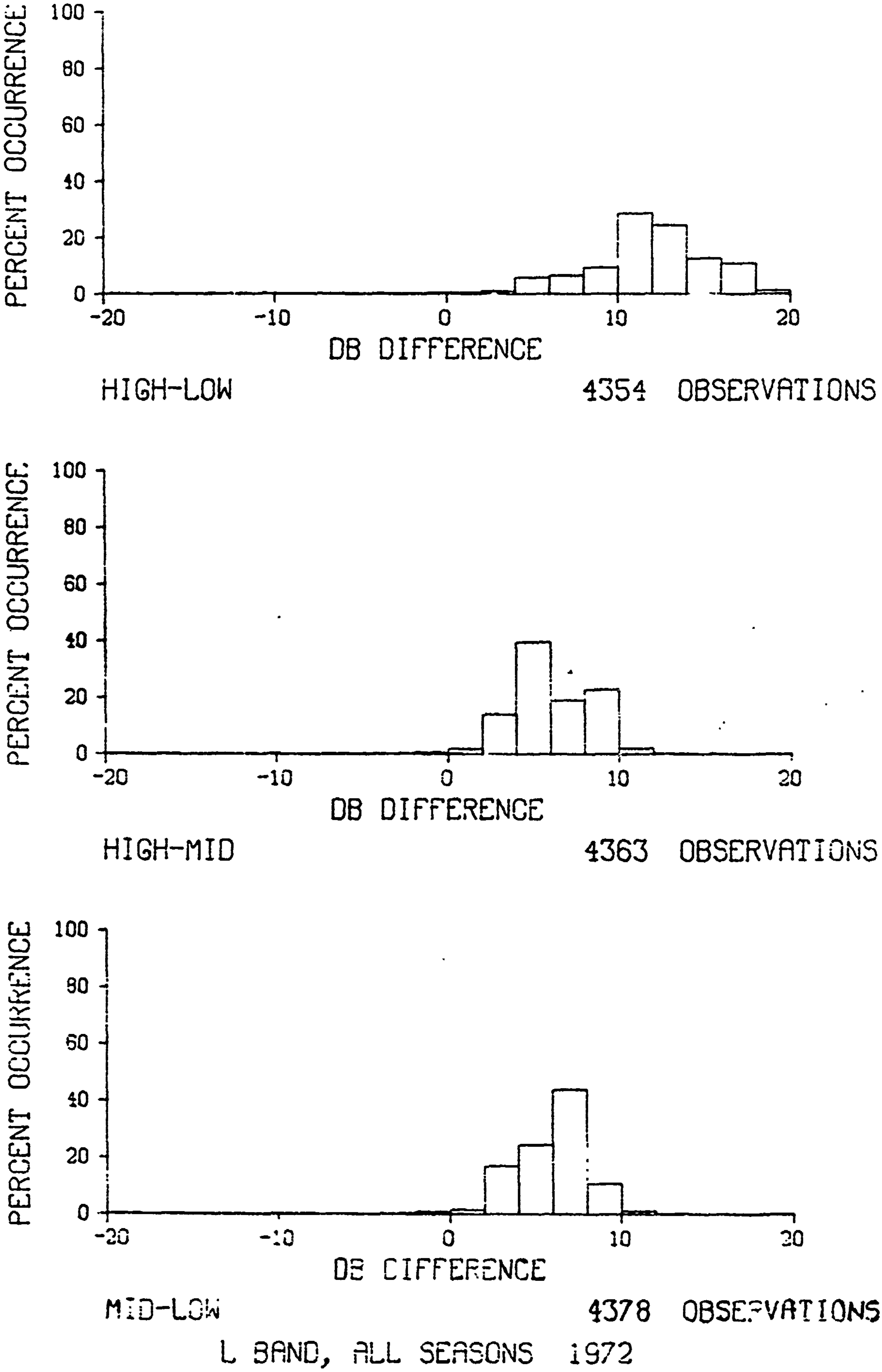

Figure 122. Frequency distributions of path loss differences between antennas for L-band

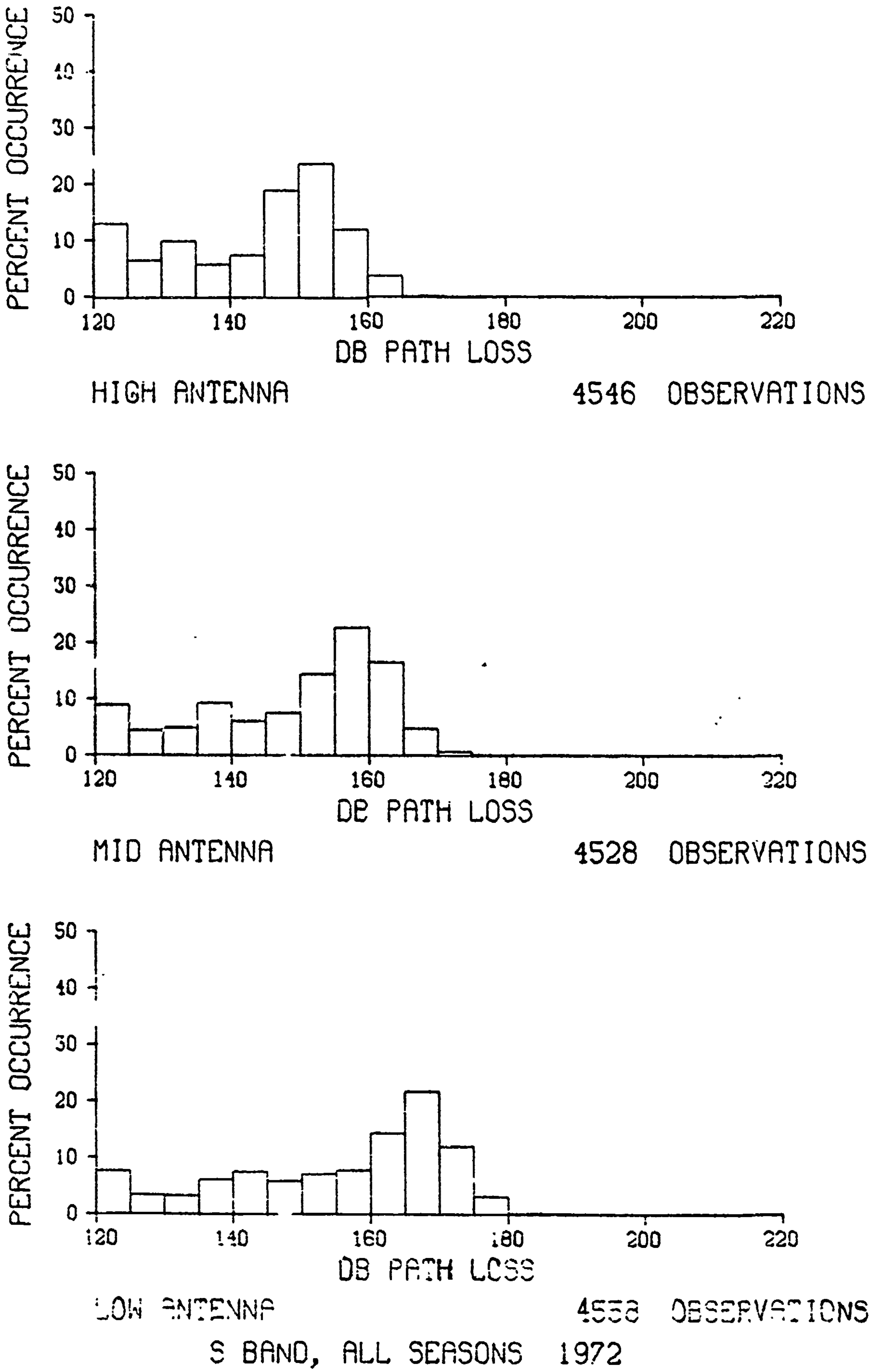

Figure 123. Frequency distributions of path loss for S-band

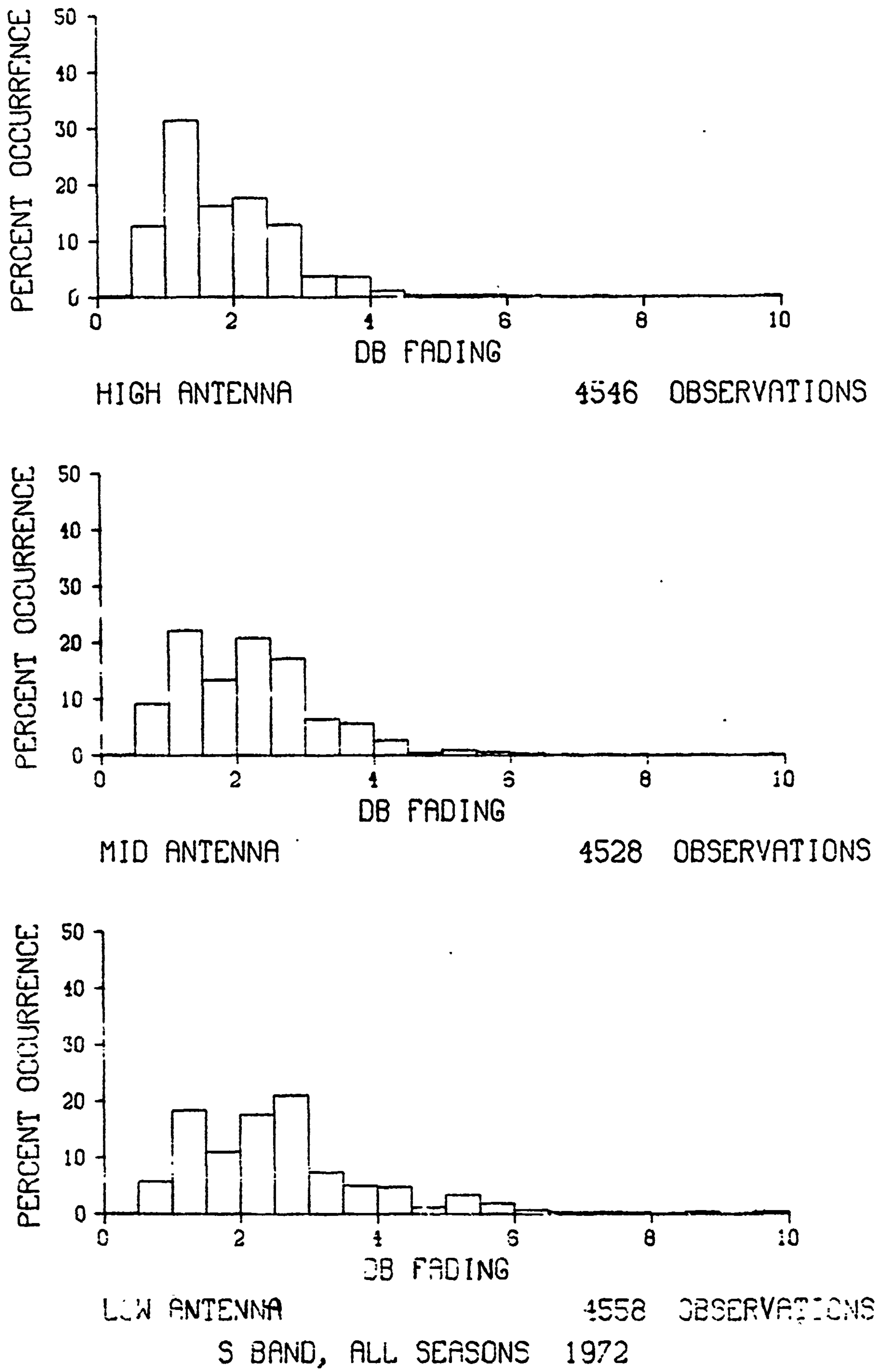

Figure 124. Frequency distributions of fading for S-band

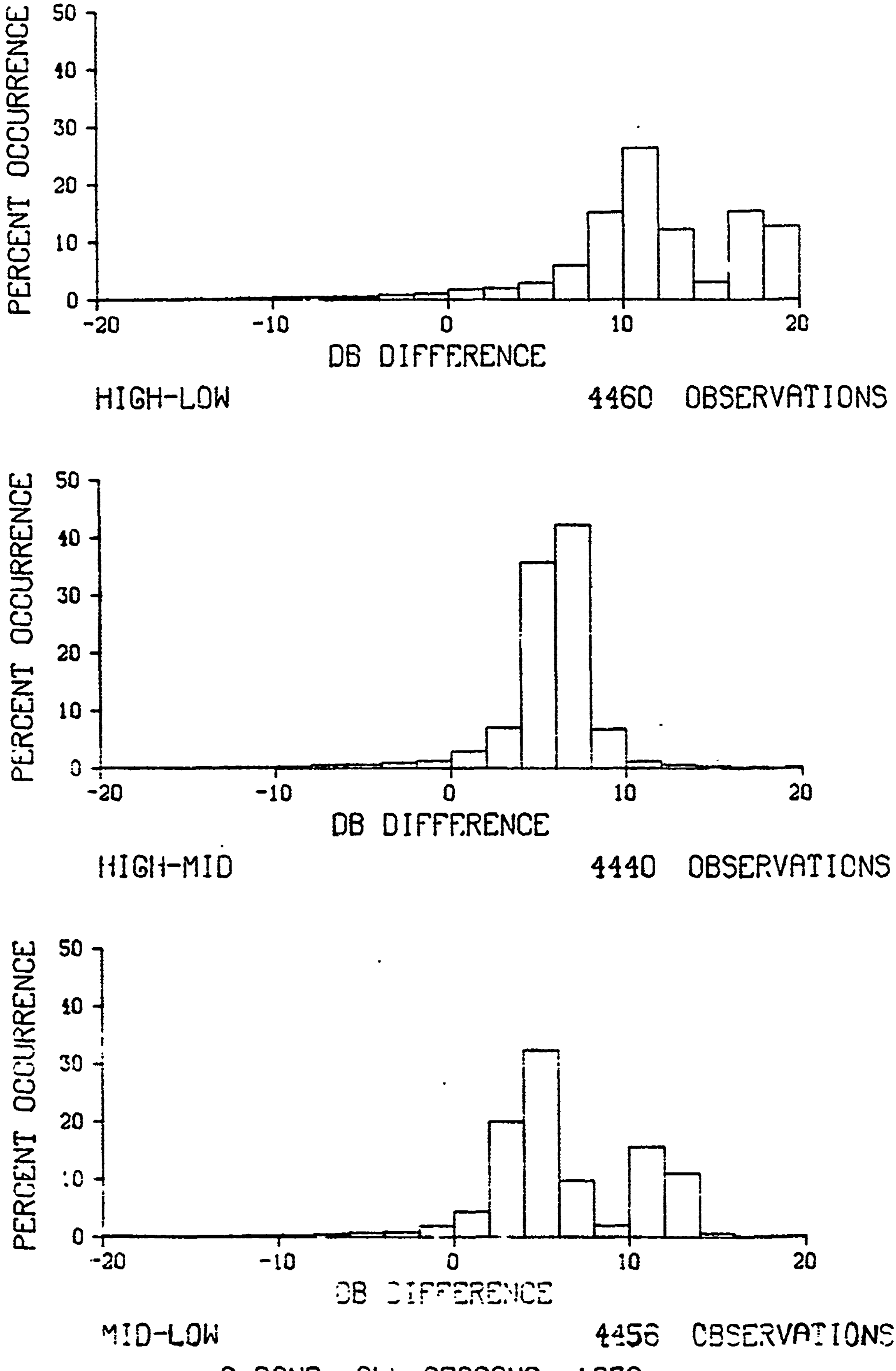

Figure 125. Frequency distributions of path loss differences between antennas for S-band

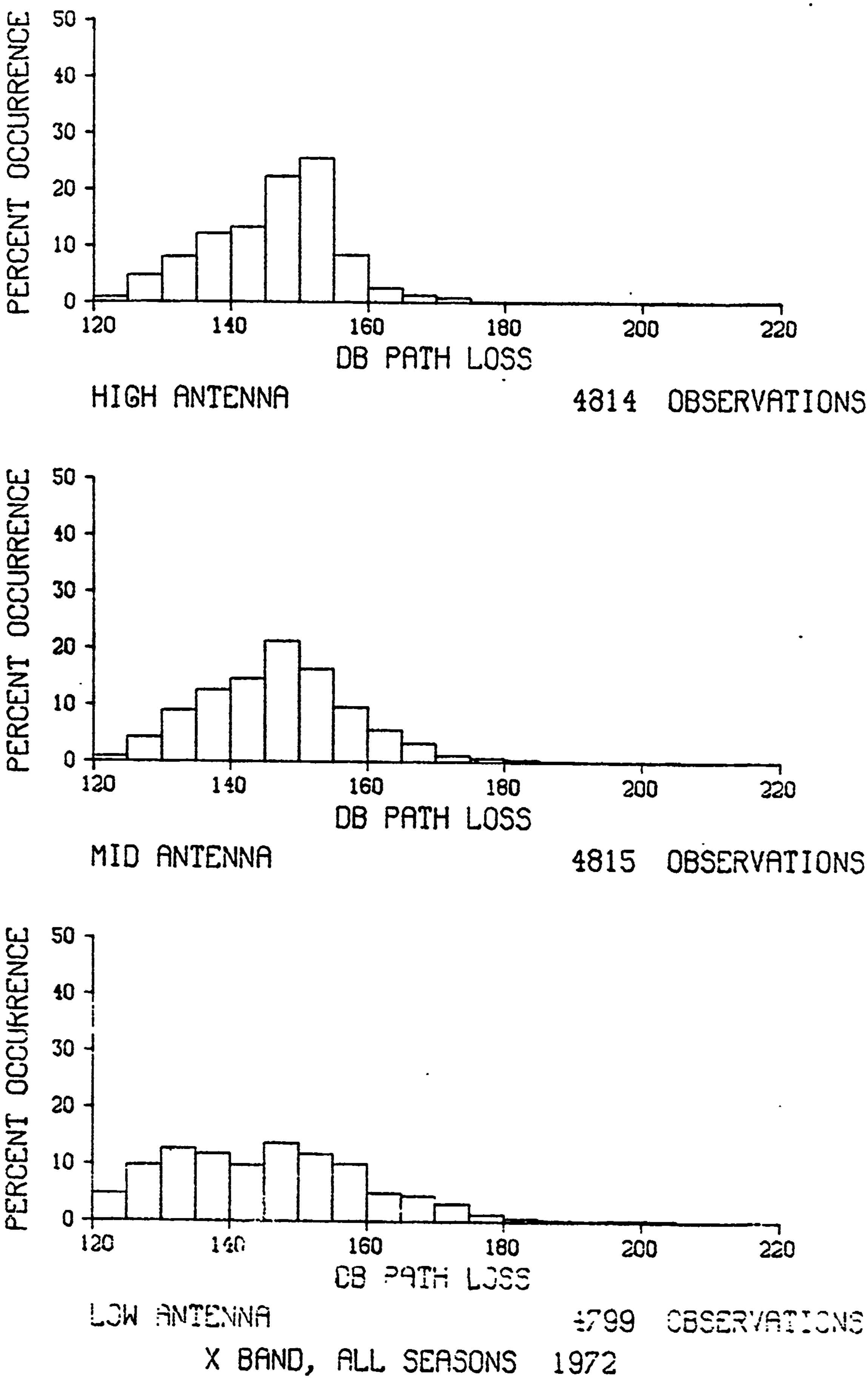

Figure 126. Frequency distribution of path loss for X-band

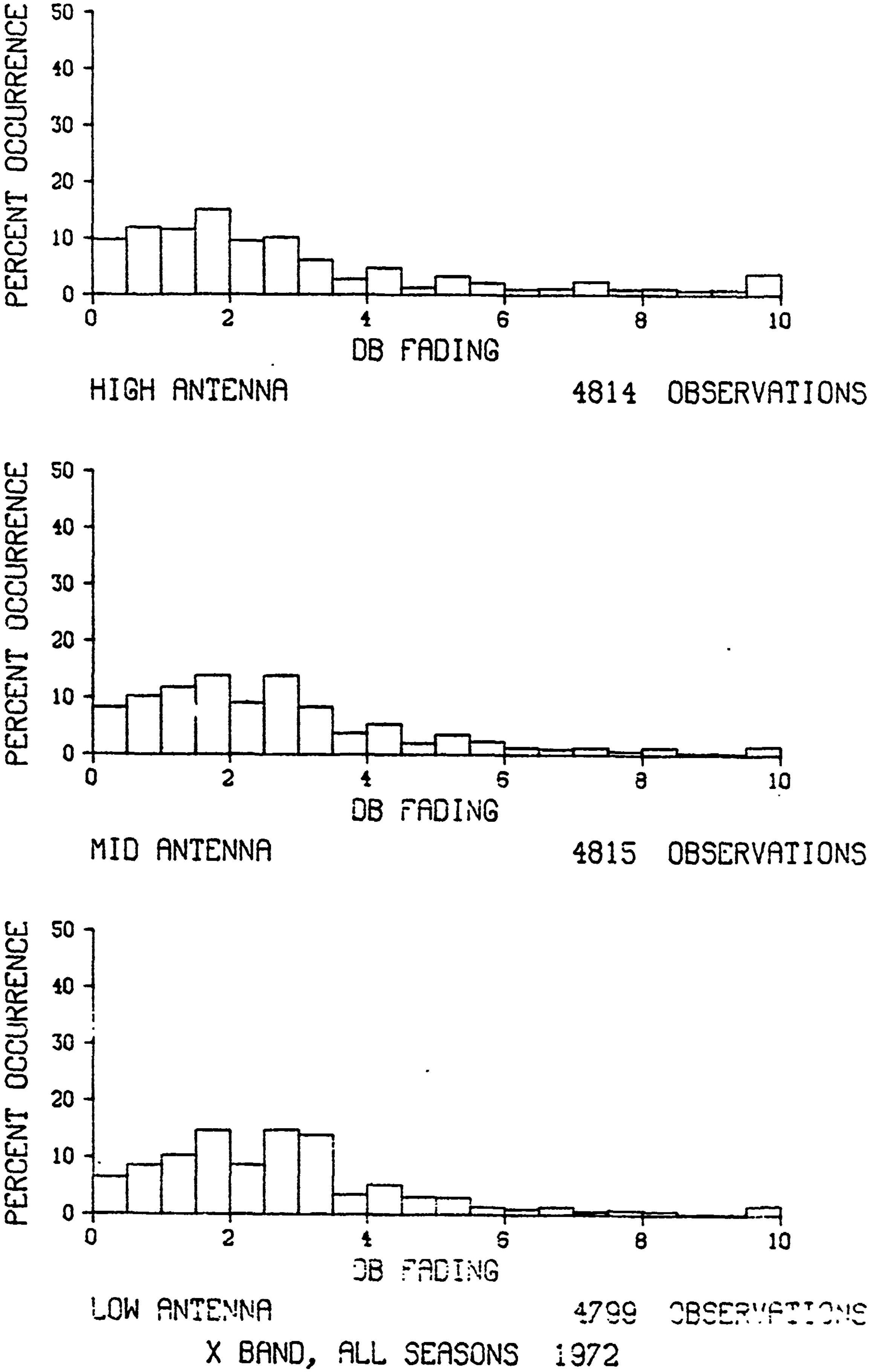

Figure 127. Frequency distribution of fading X-band

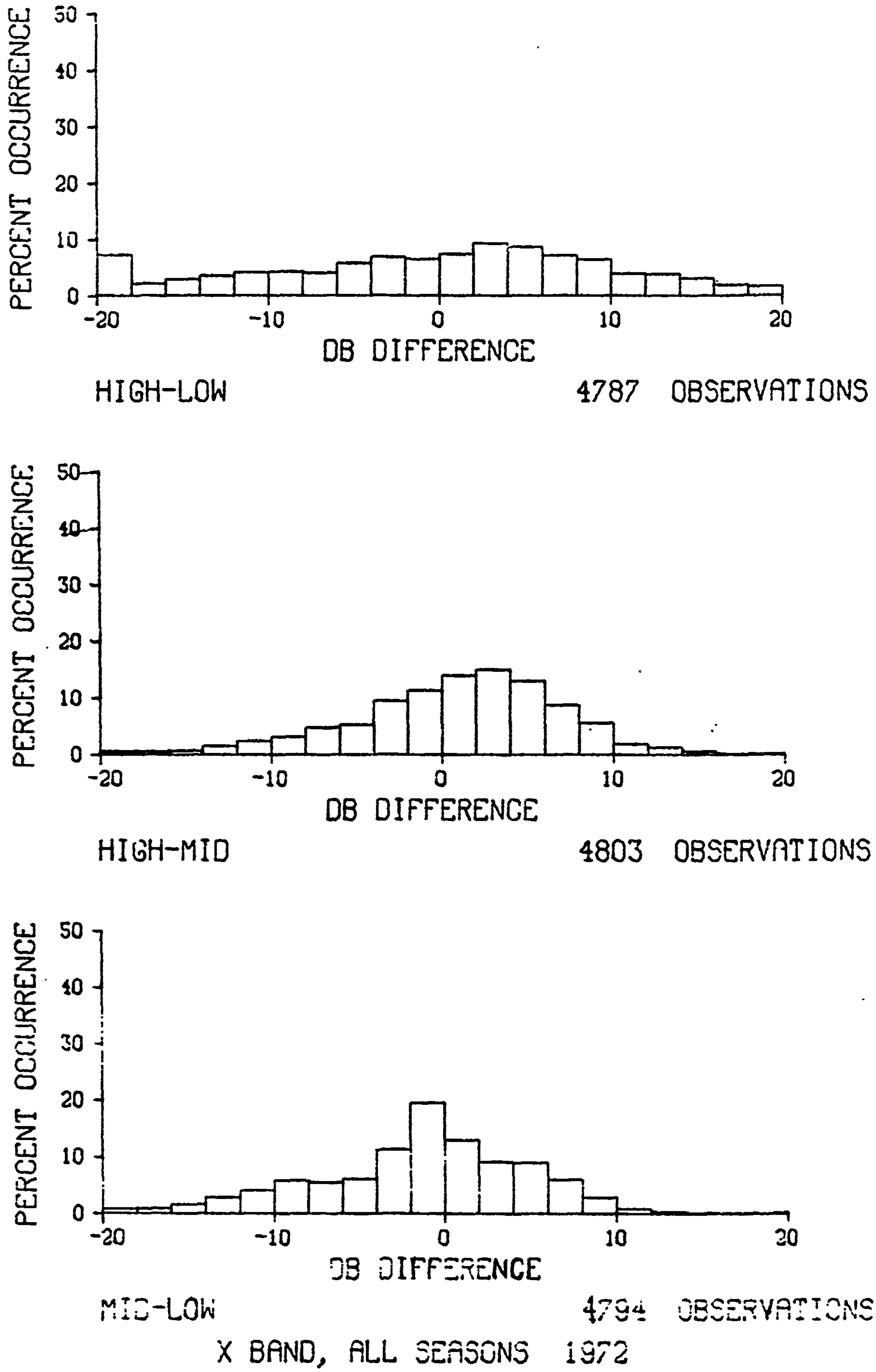

Figure 128. Frequency distribution of differences between antennas for X-band

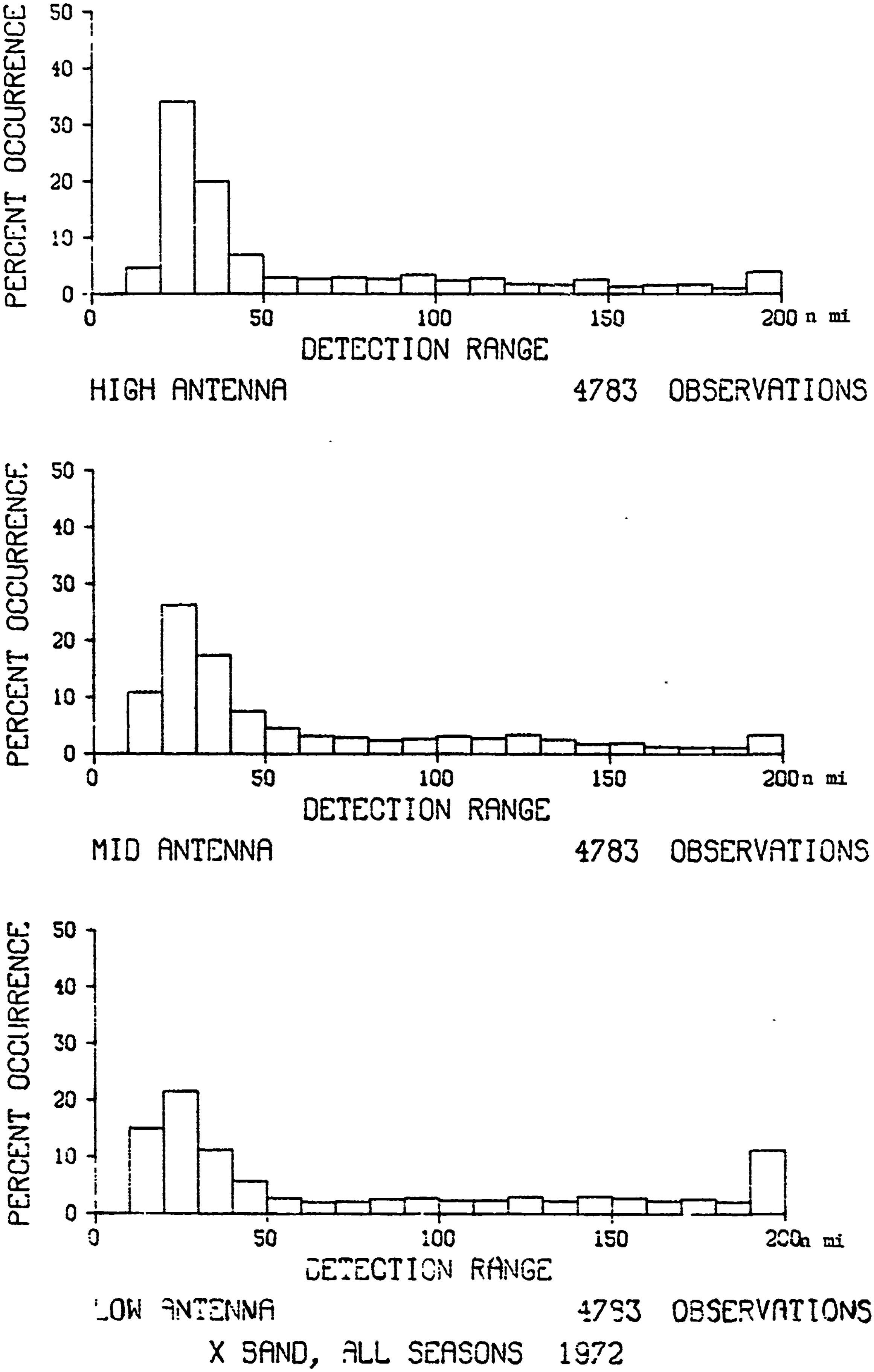

Figure 129. Frequency distribution of detection range for X-band

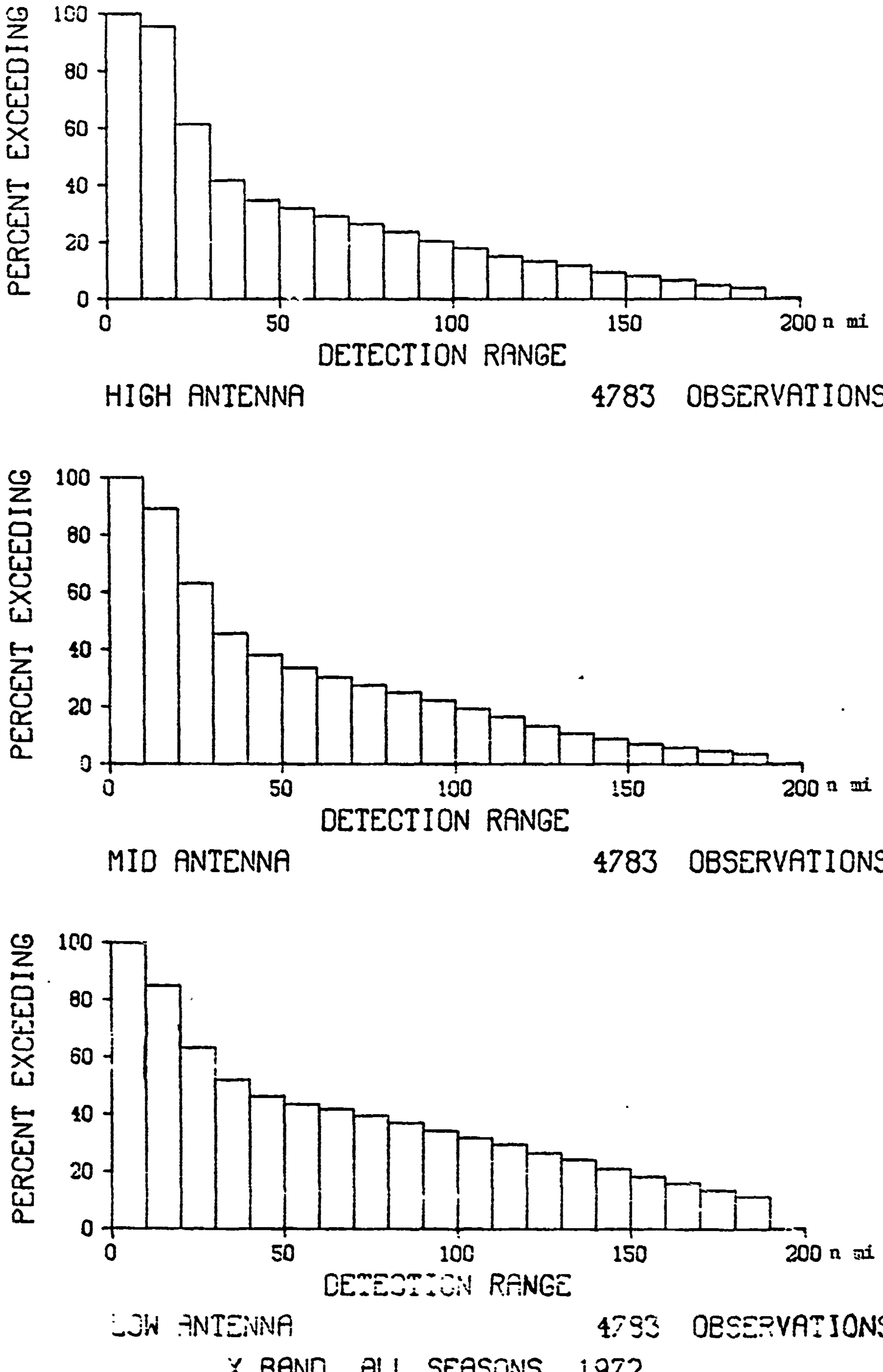

Figure 130. Cumulative distribution of detection range for X-band

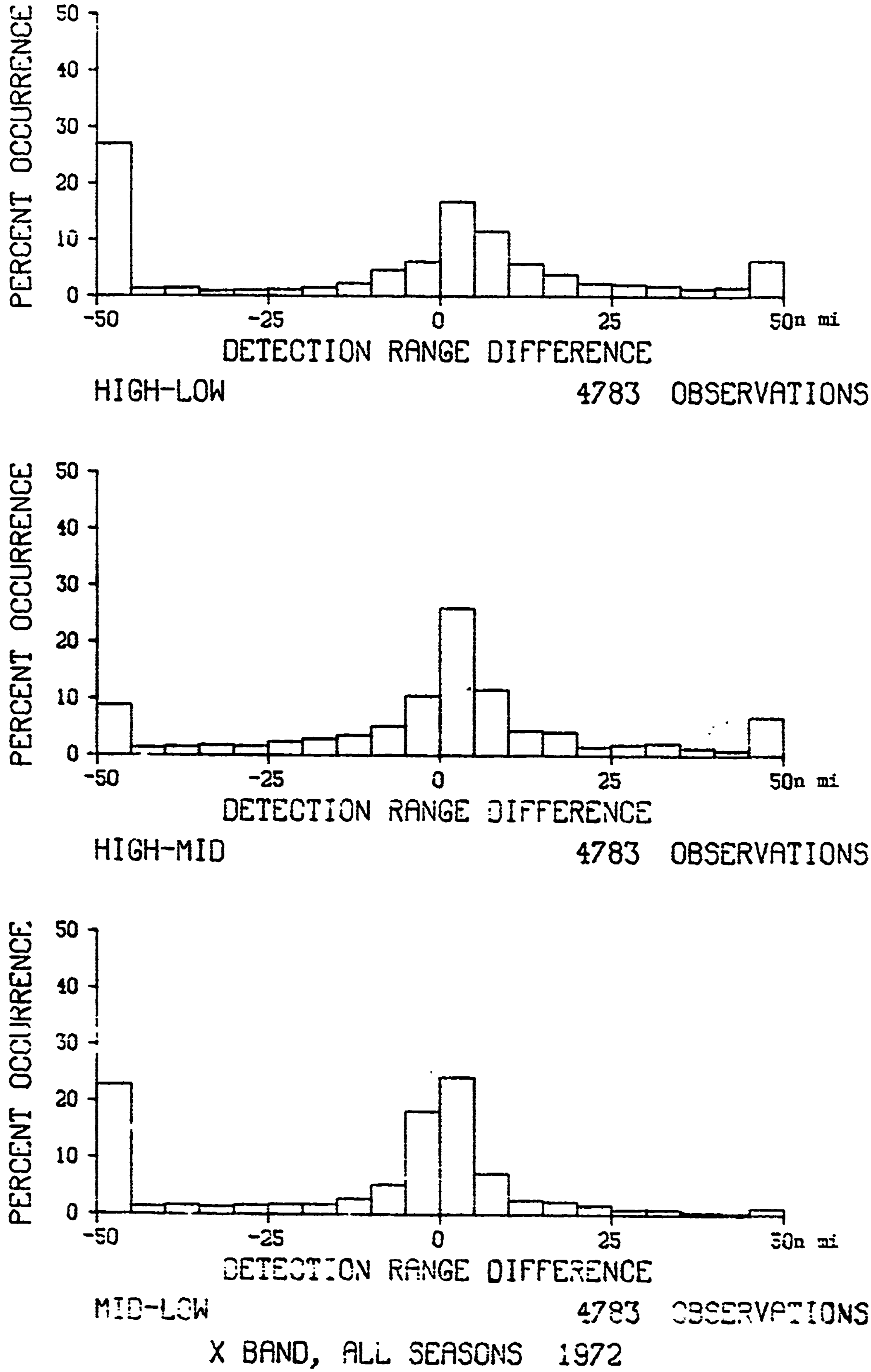

Figure 131. Frequency distribution of detection range differences between antennas for X-band

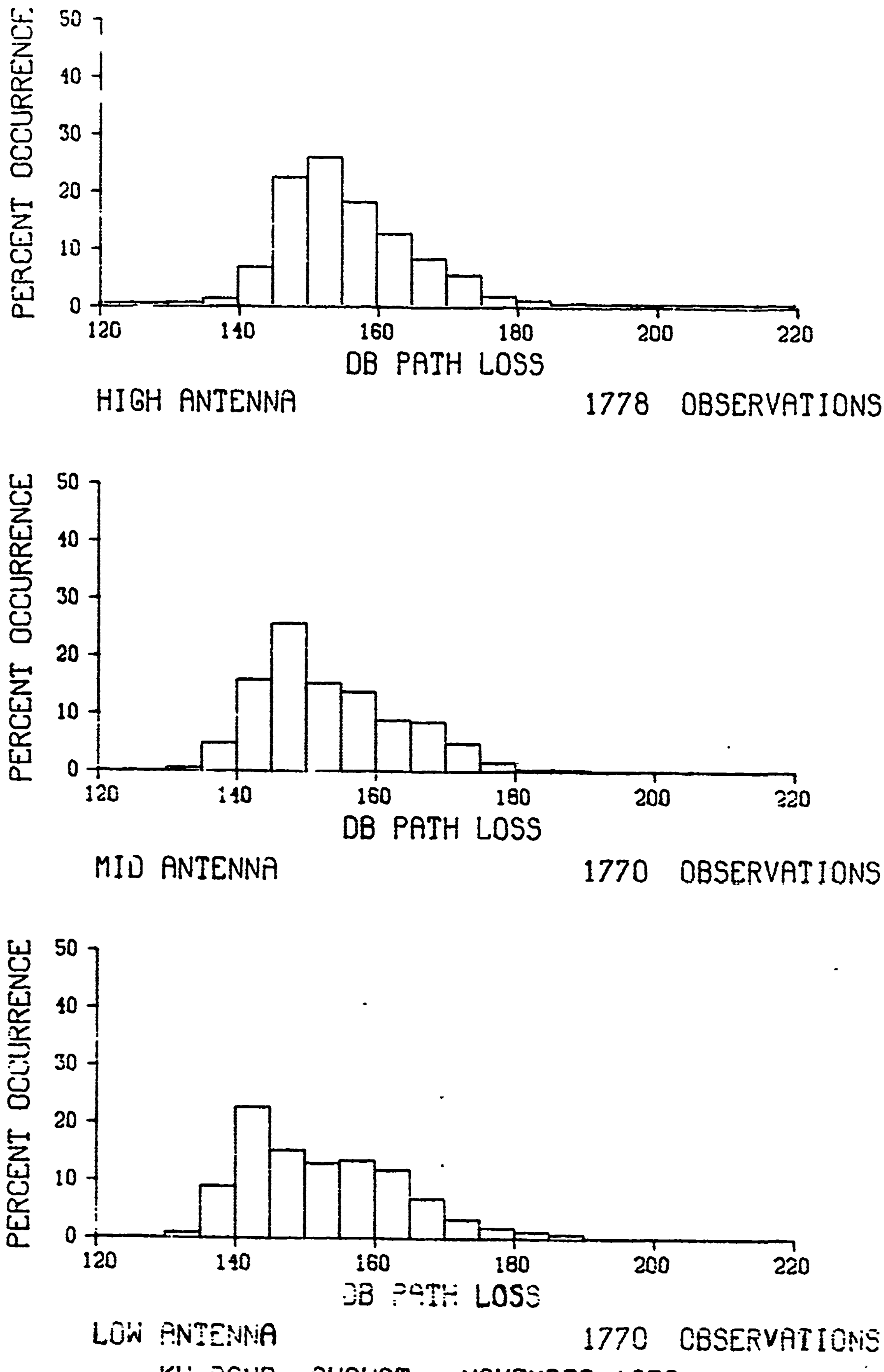

Figure 132. Frequency distributions of path loss for Ku-band

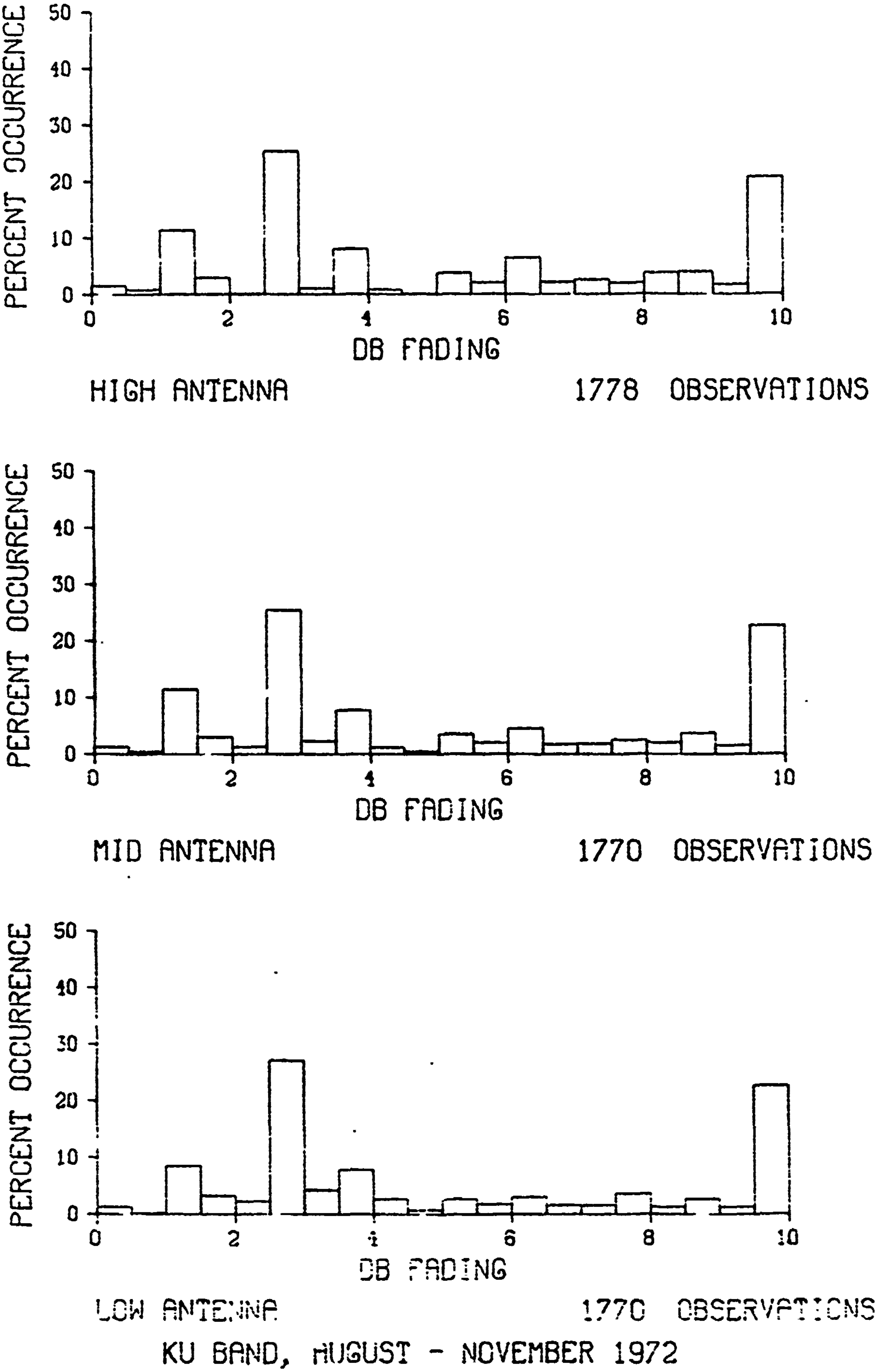

Figure 133. Frequency distributions of fading for Ku-band

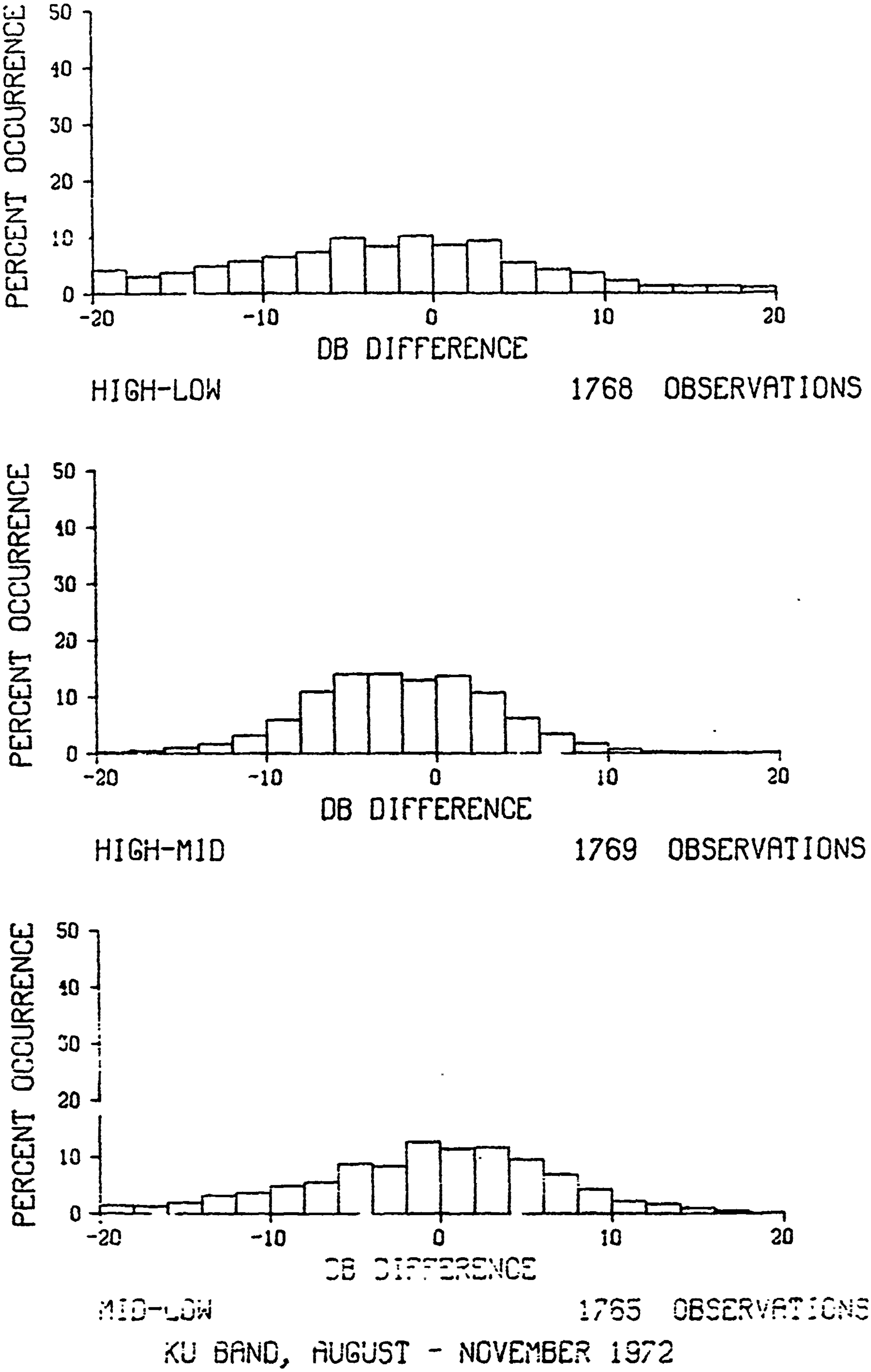

Figure 134. Frequency distributions of path loss differences between antennas for Ku-band

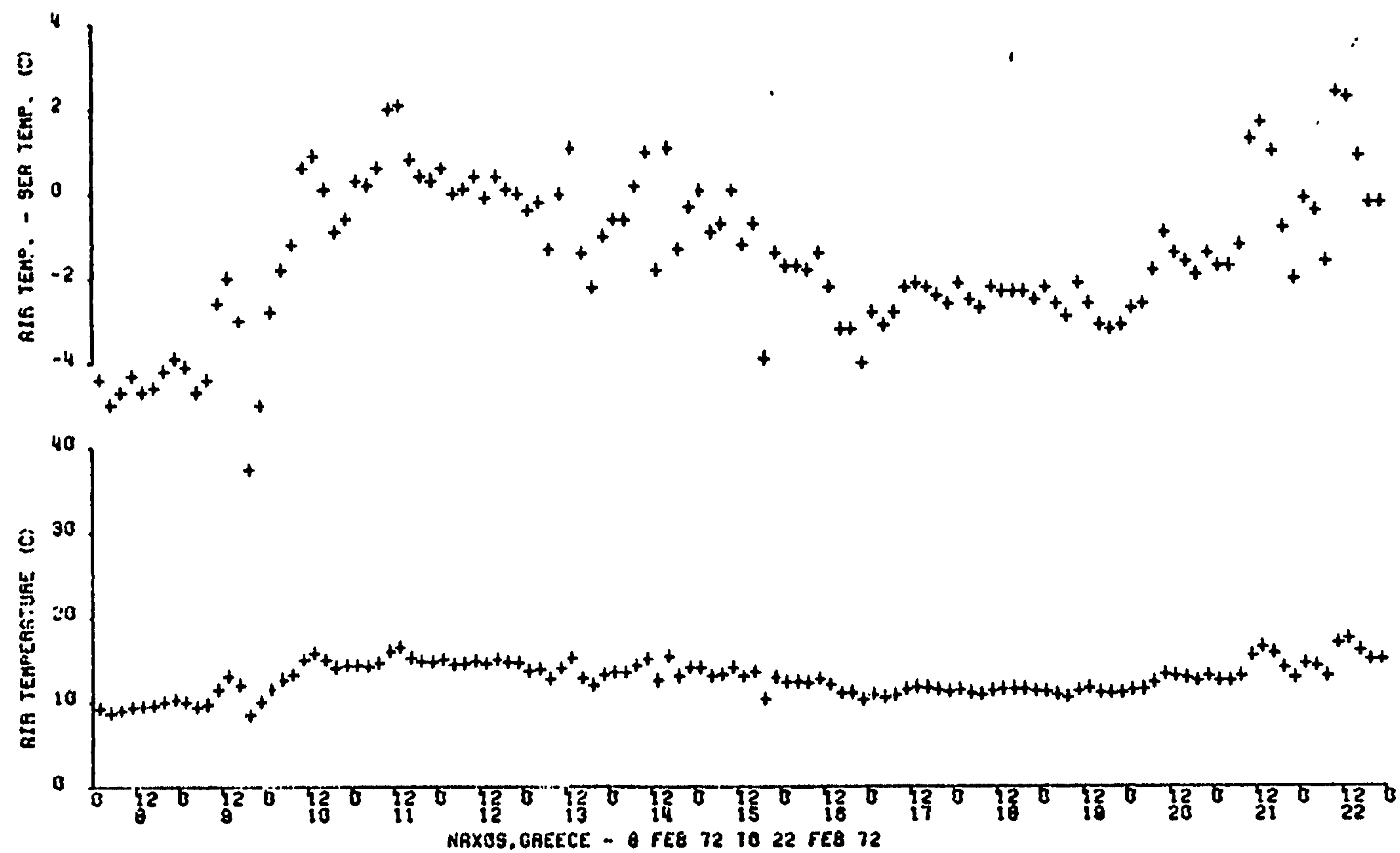

Figure 135. Meteorological measurements at Naxos, winter period

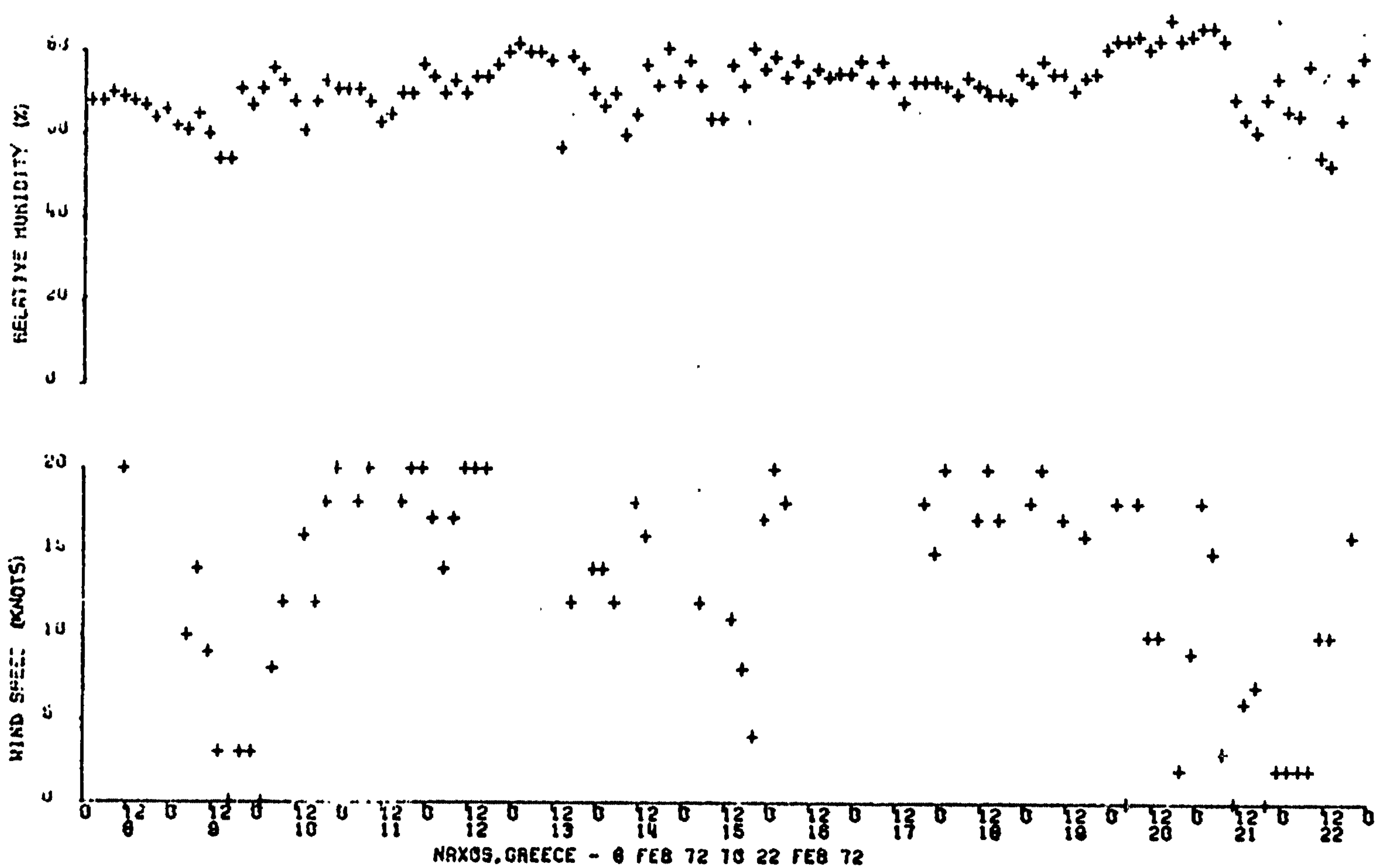

Figure 136. Meteorological measurements at Naxos, winter period

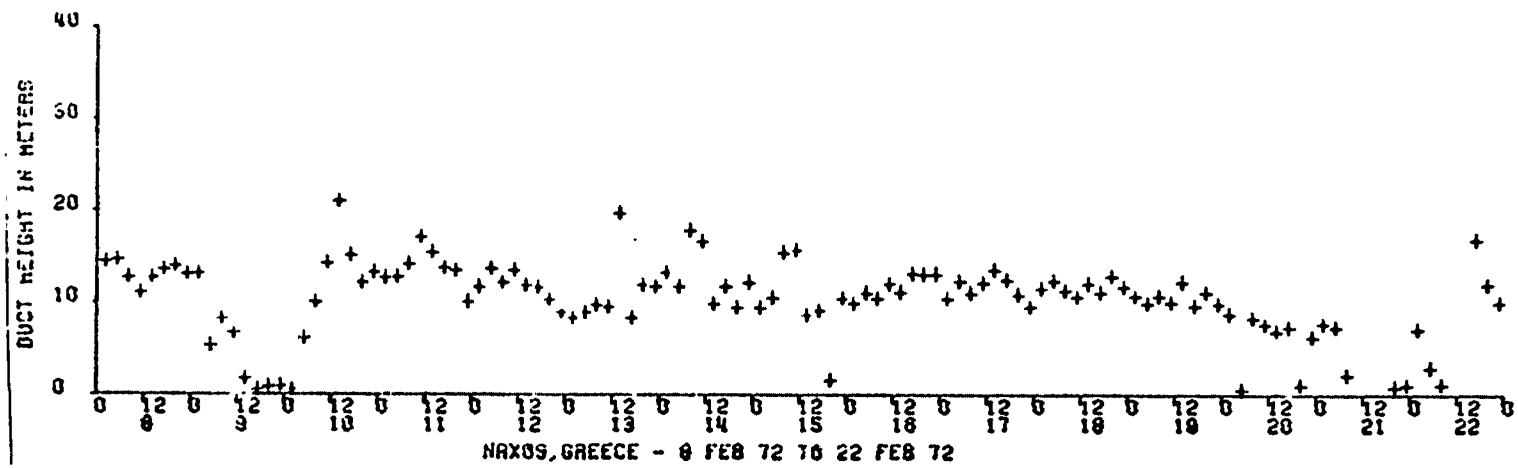

Figure 137. Duct heights calculated from meteorological measurements at Naxos, winter period

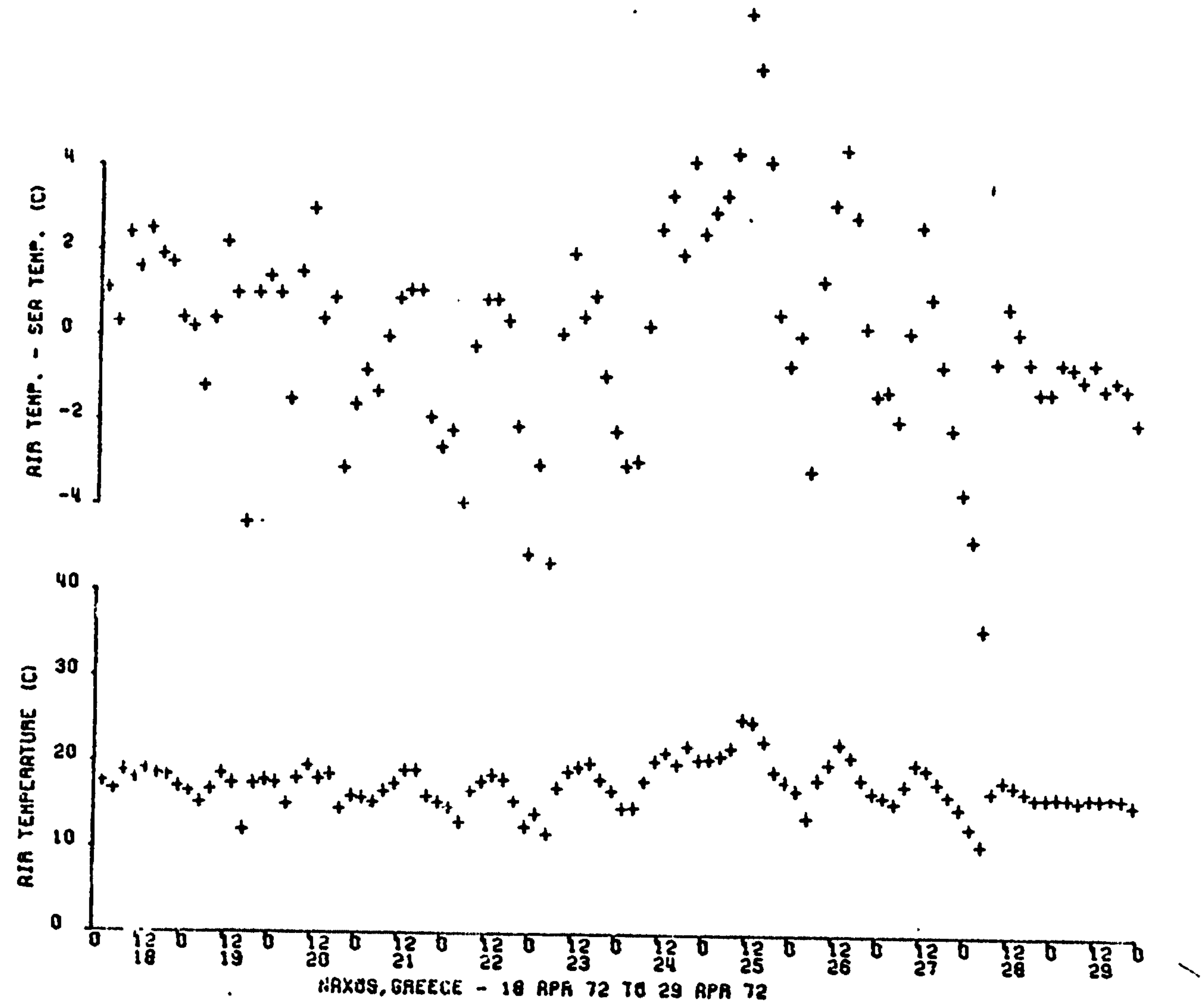

Figure 138. Meteorological measurements at Naxos, spring period

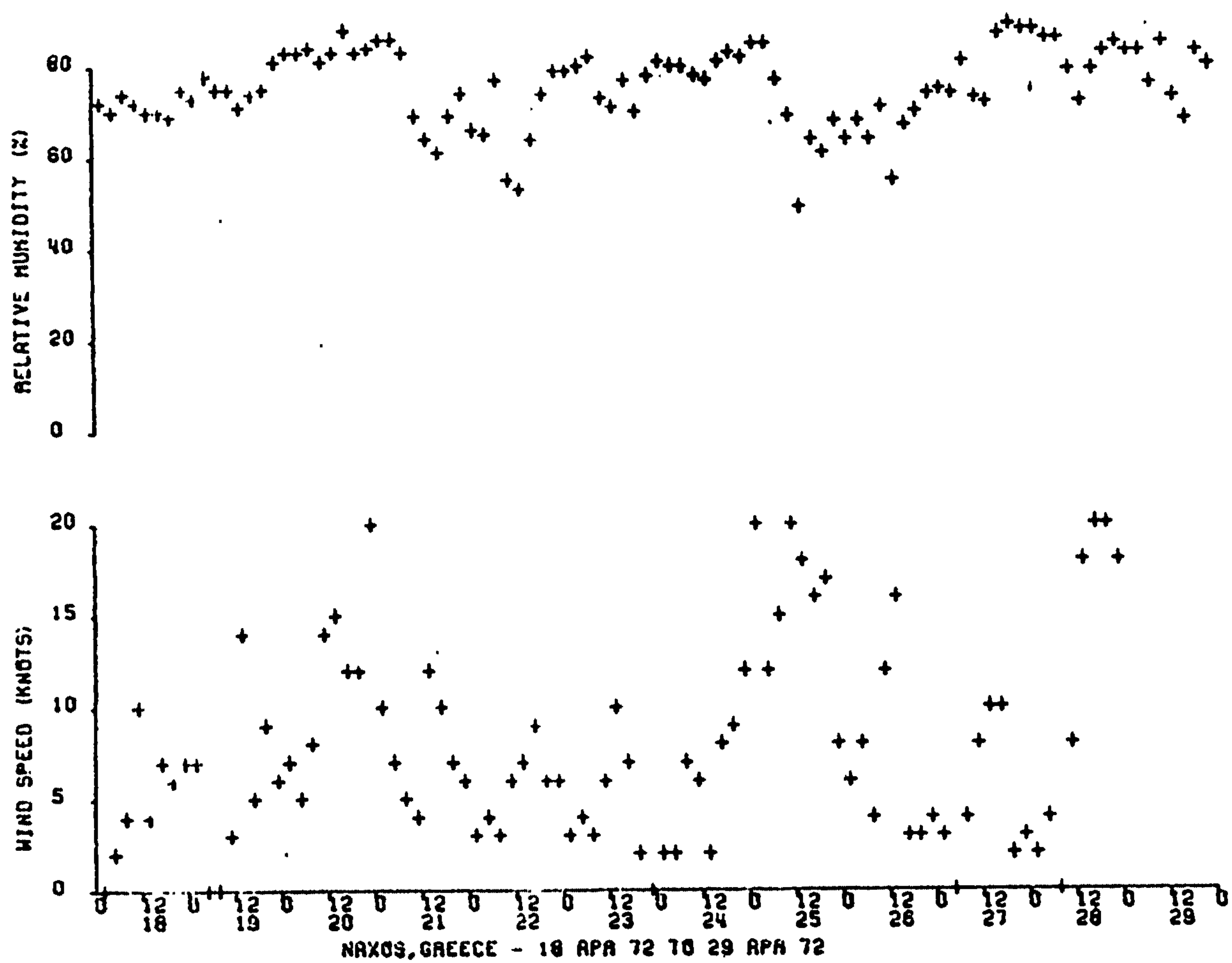

Figure 139. Meteorological measurements at Naxos, spring period

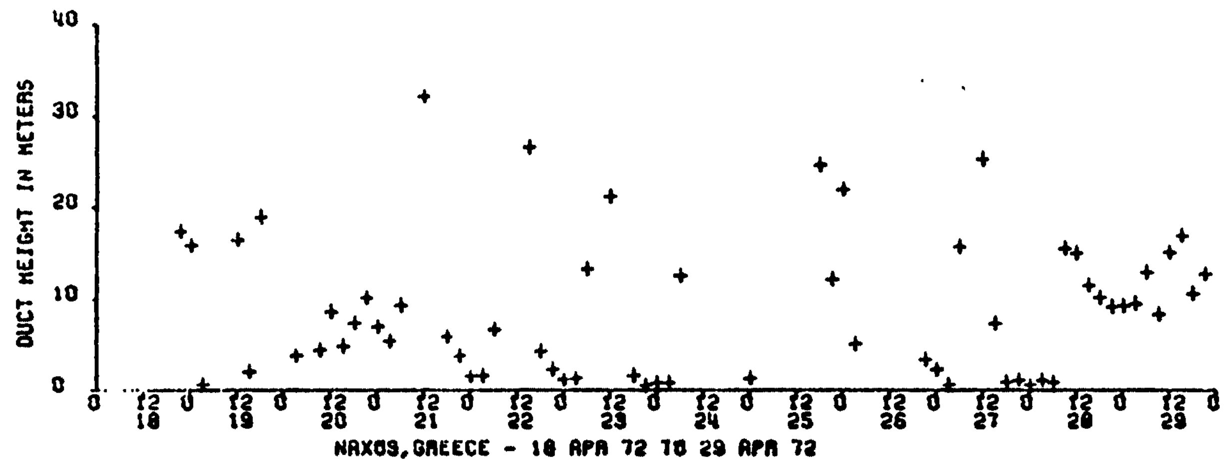

Figure 140. Duct heights calculated from meteorological measurements at Naxos, spring period

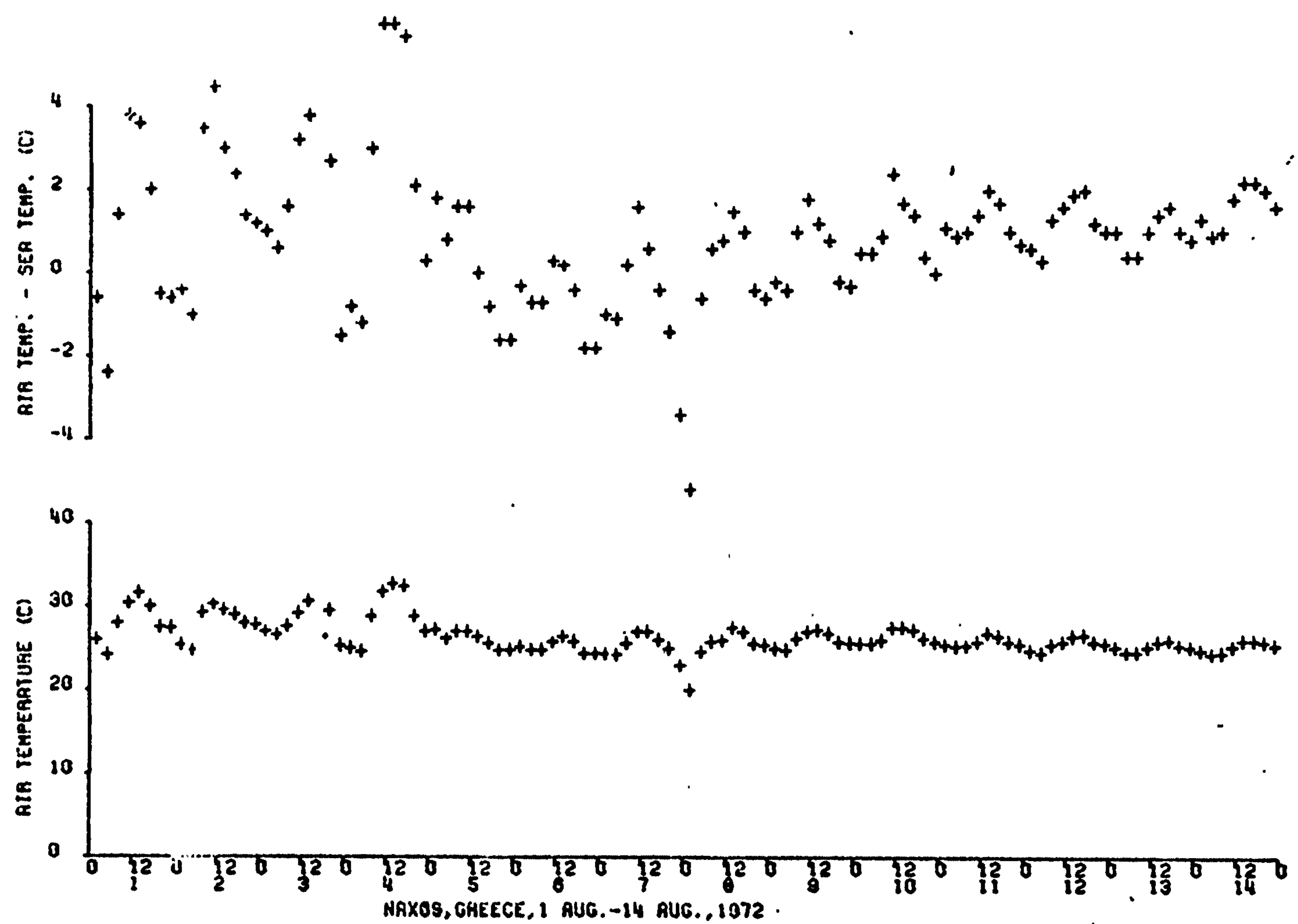

Figure 141. Meteorological measurements at Naxos, summer period

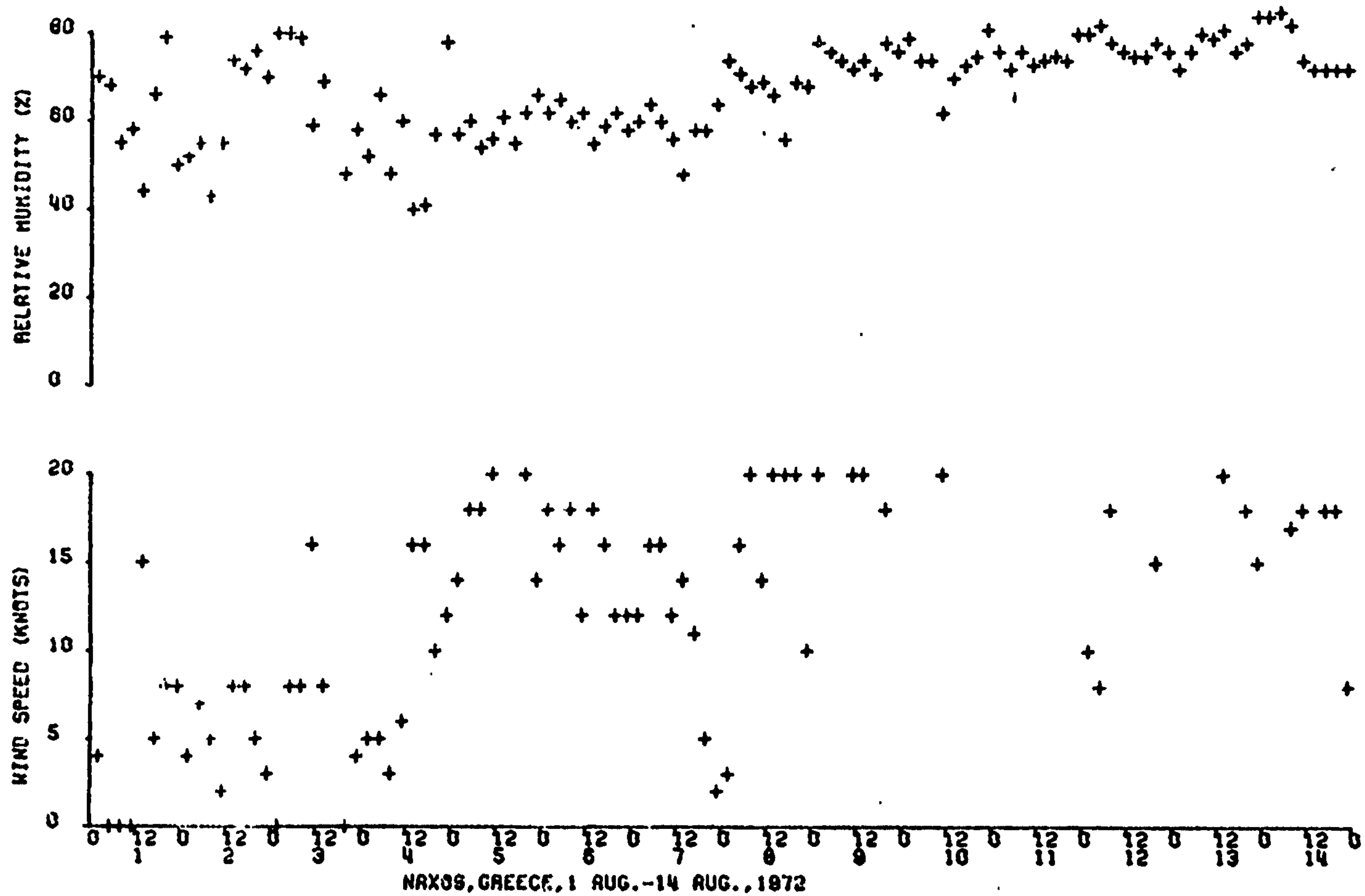

Figure 142. Meteorological measurements at Naxos, summer period

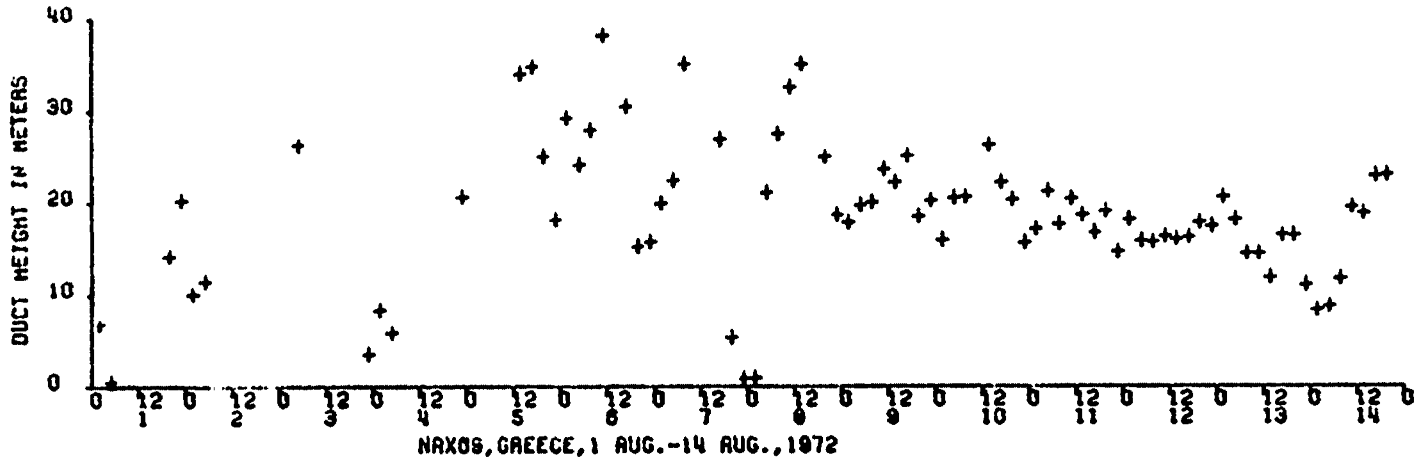

Figure 143. Duct heights calculated from meteorological measurements at Naxos, summer period

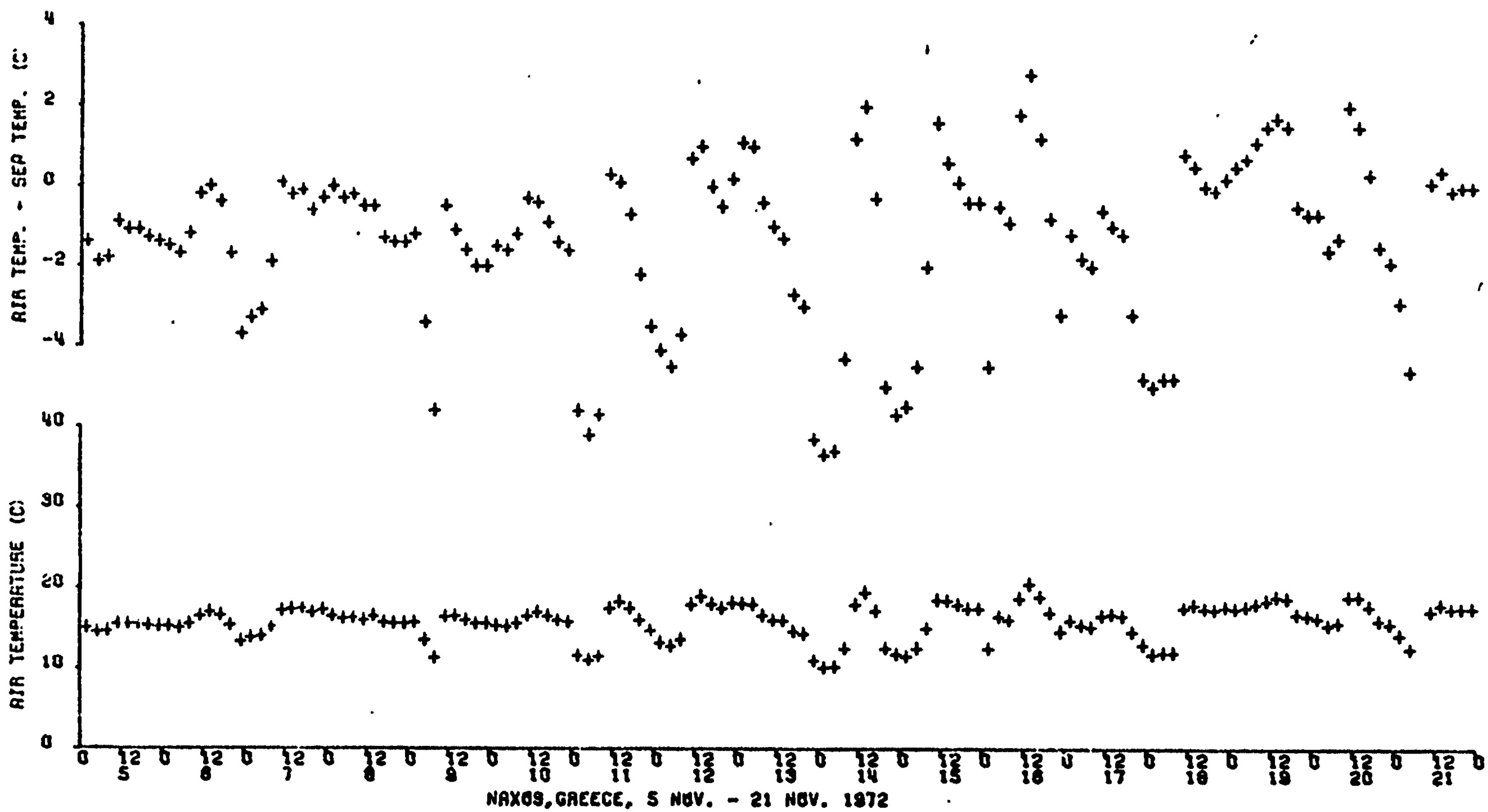

Figure 144. Meteorological measurements at Naxos, fall period

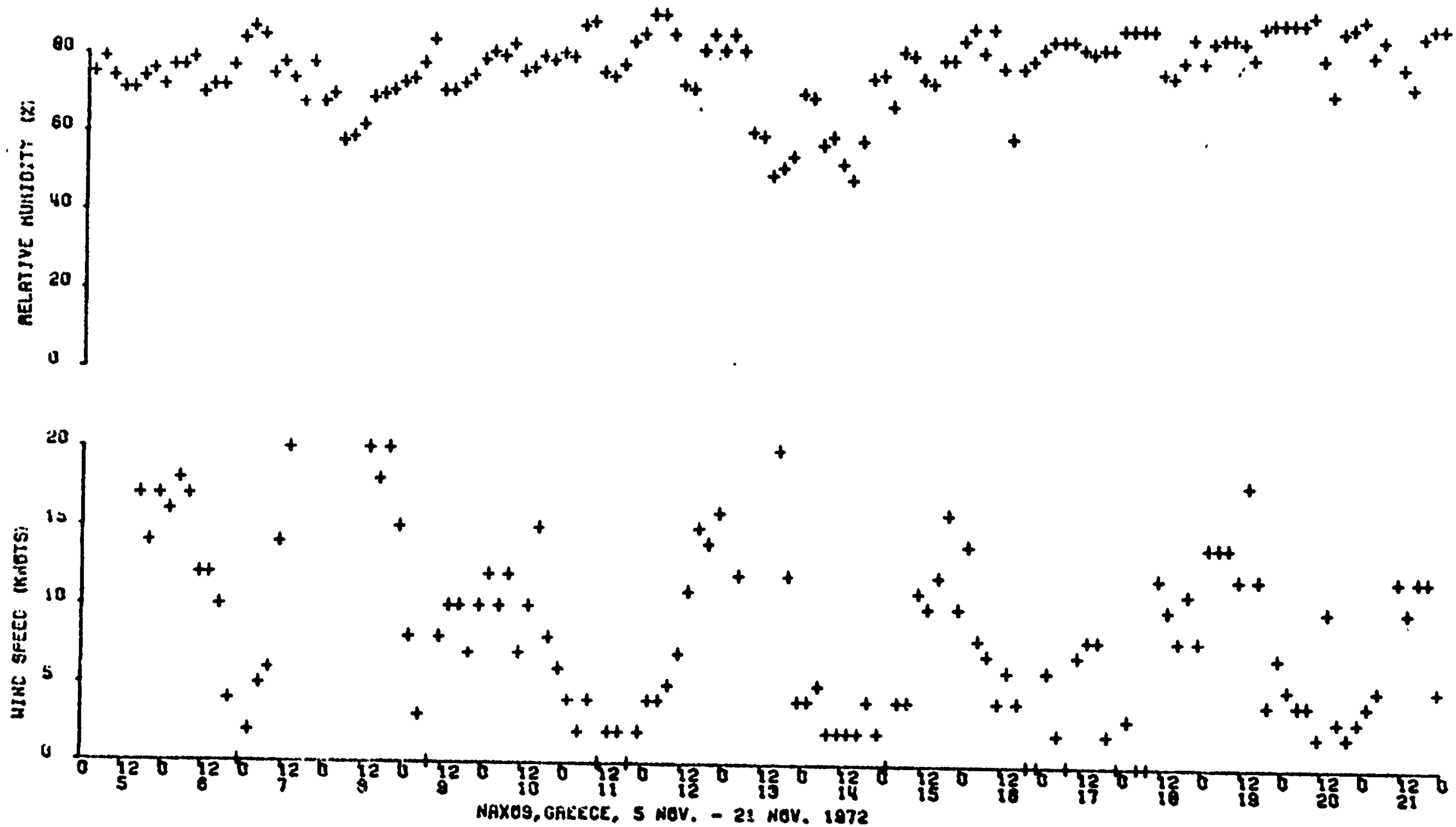

Figure 145. Meteorological measurements at Naxos, fall period

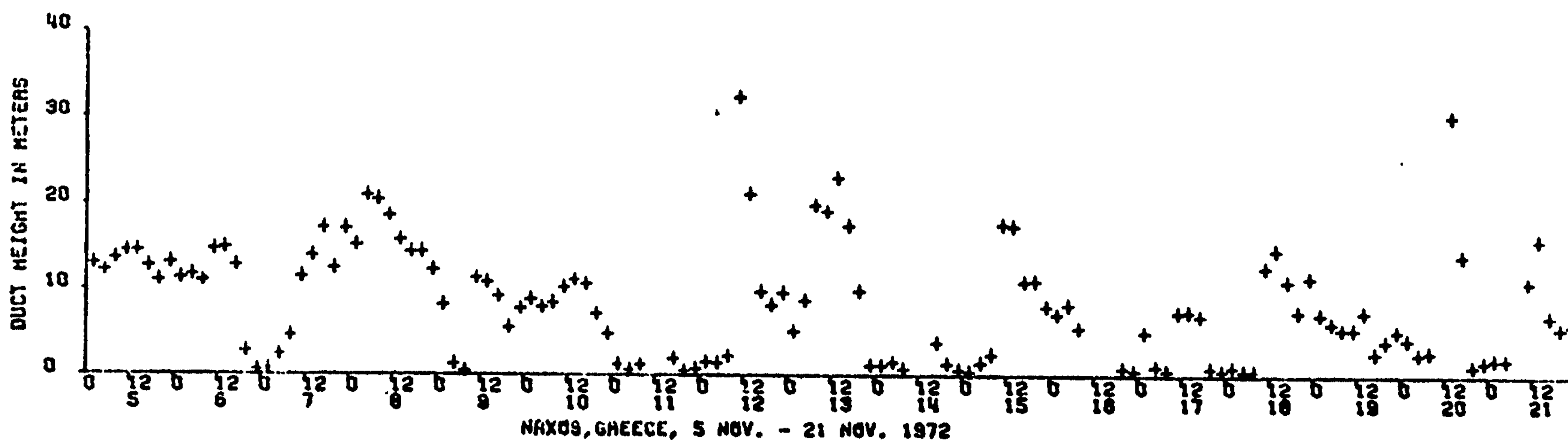

Figure 146. Duct heights calculated from meteorological measurements at Naxos, fall period

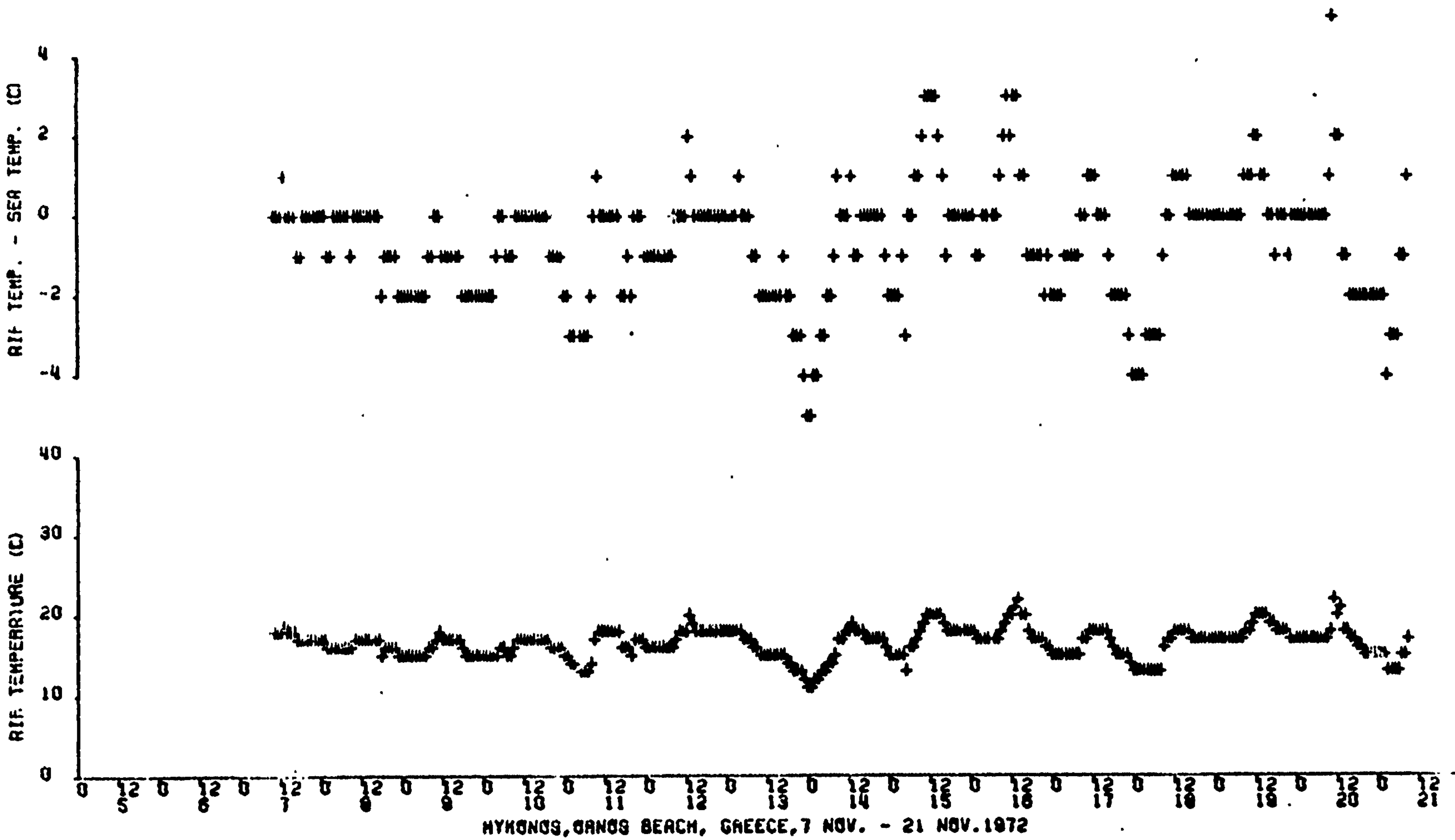

Figure 147. Meteorological measurements at Mykonos, fall period

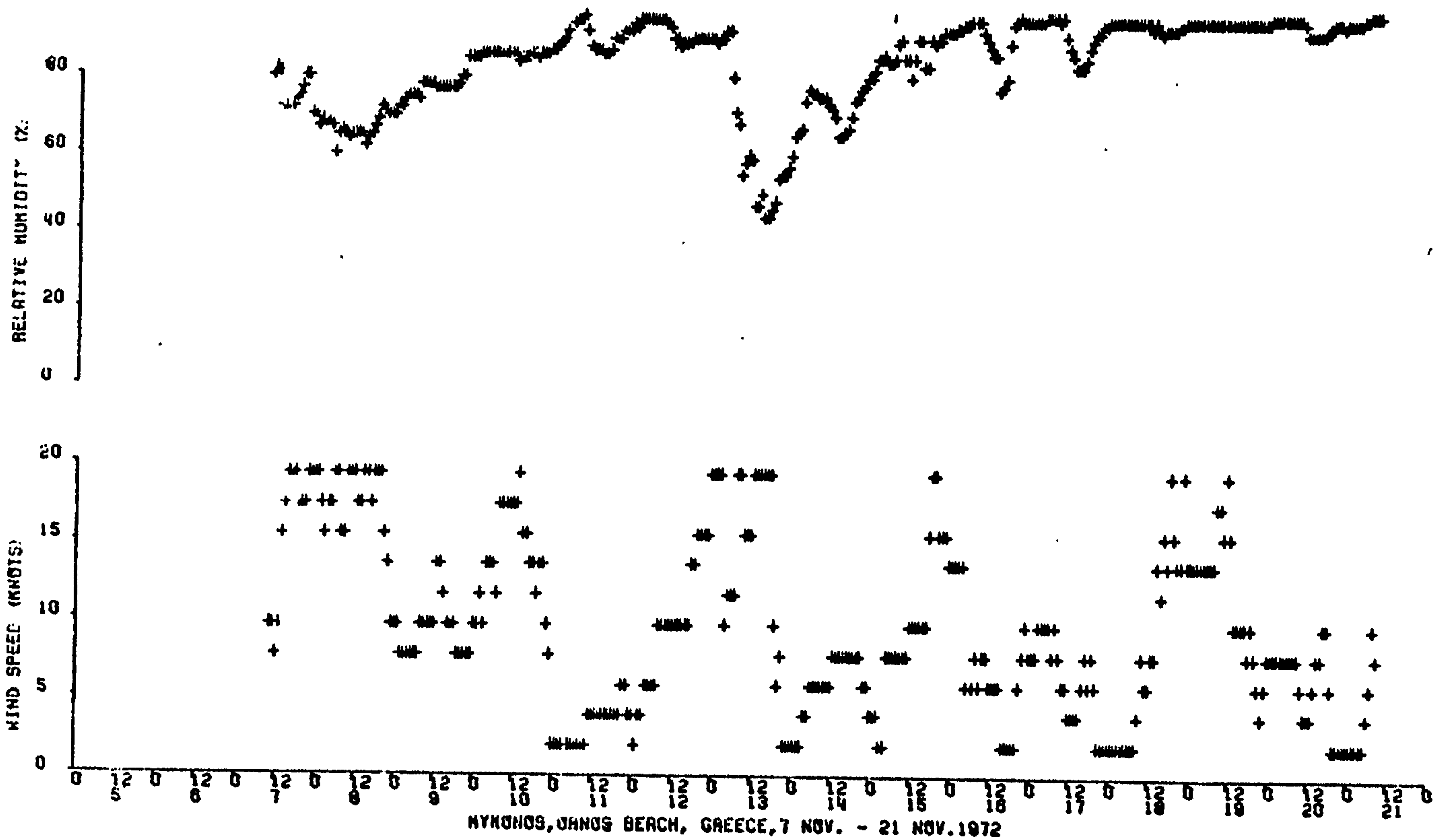

Figure 148. Meteorological measurements at Mykonos, fall period

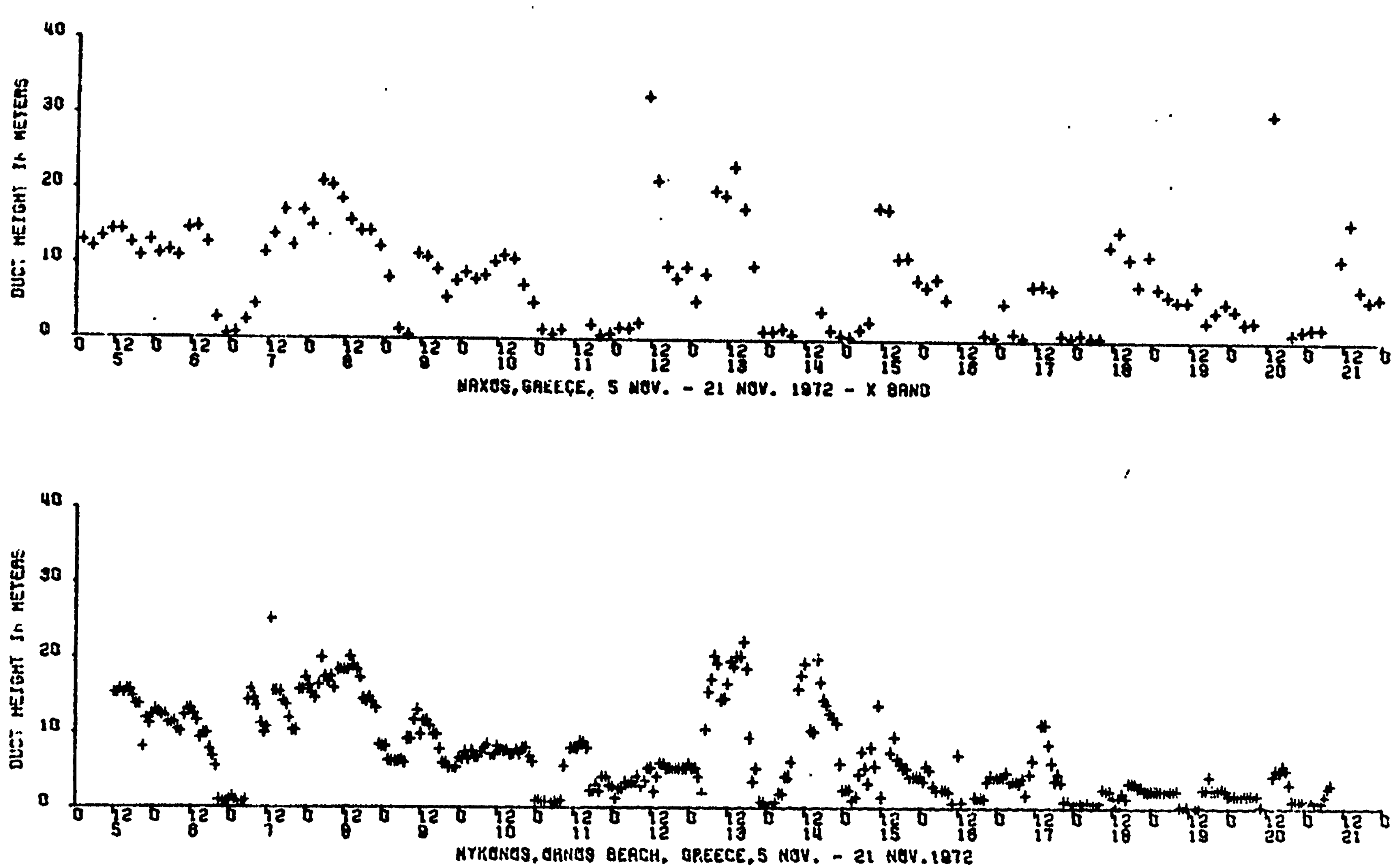

Figure 149. Duct heights calculated from meteorological measurements at Naxos and at Mykonos

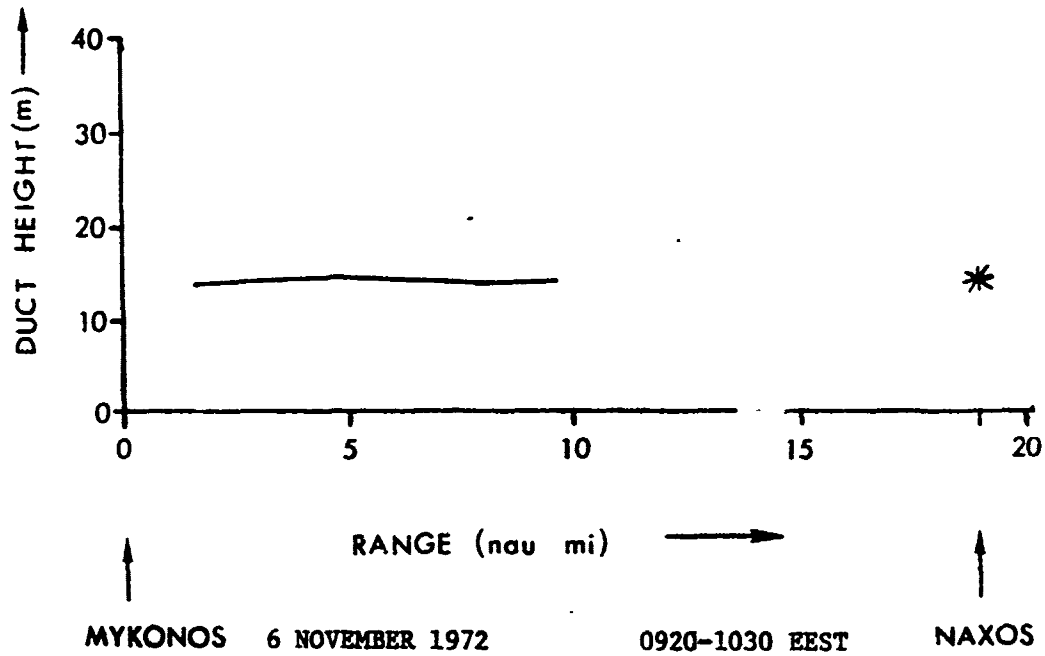

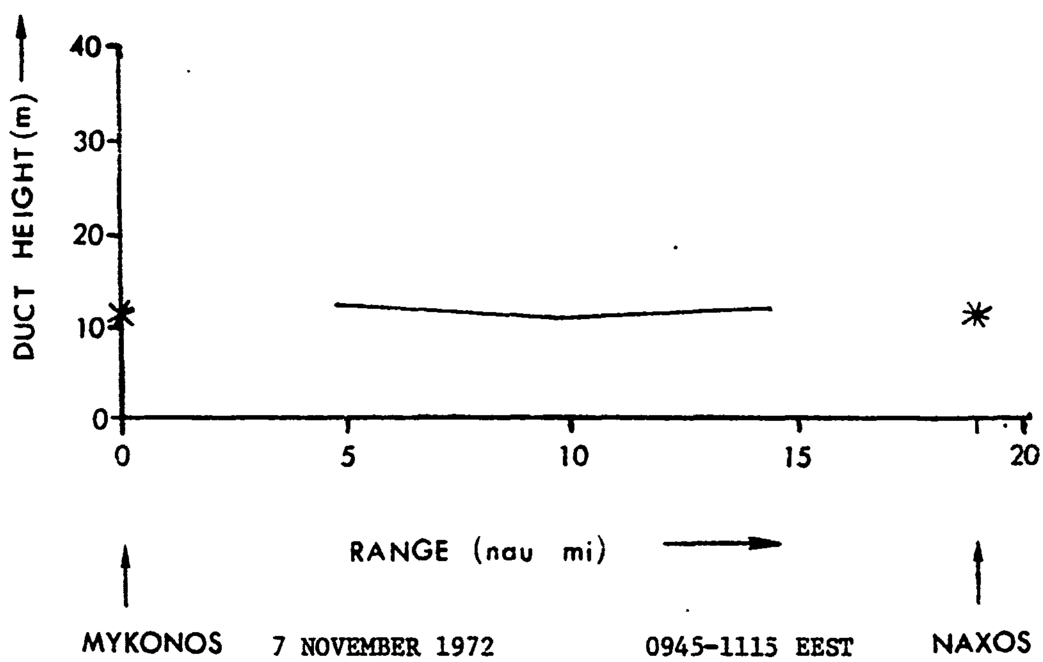

Figure 150. Duct height measurements along the propagation path

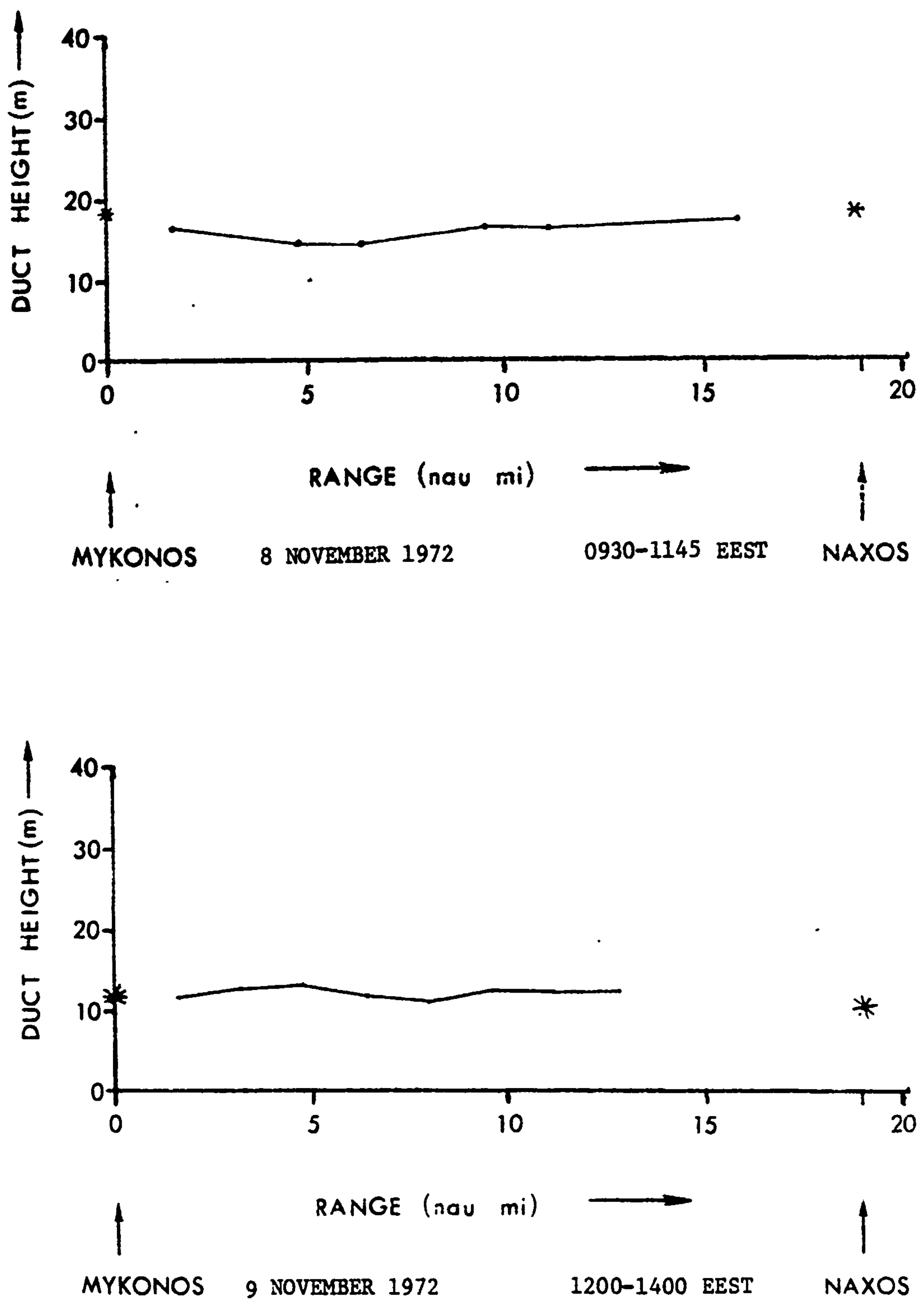

Figure 151. Duct height measurements along the propagation path

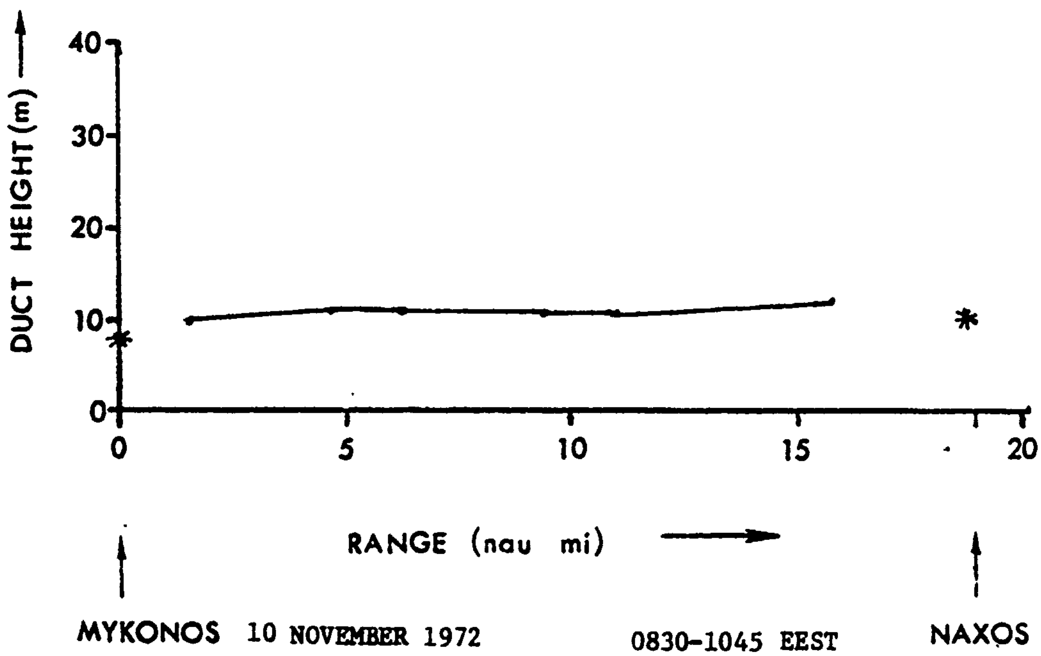

Figure 152. Duct height measurements along the propagation path

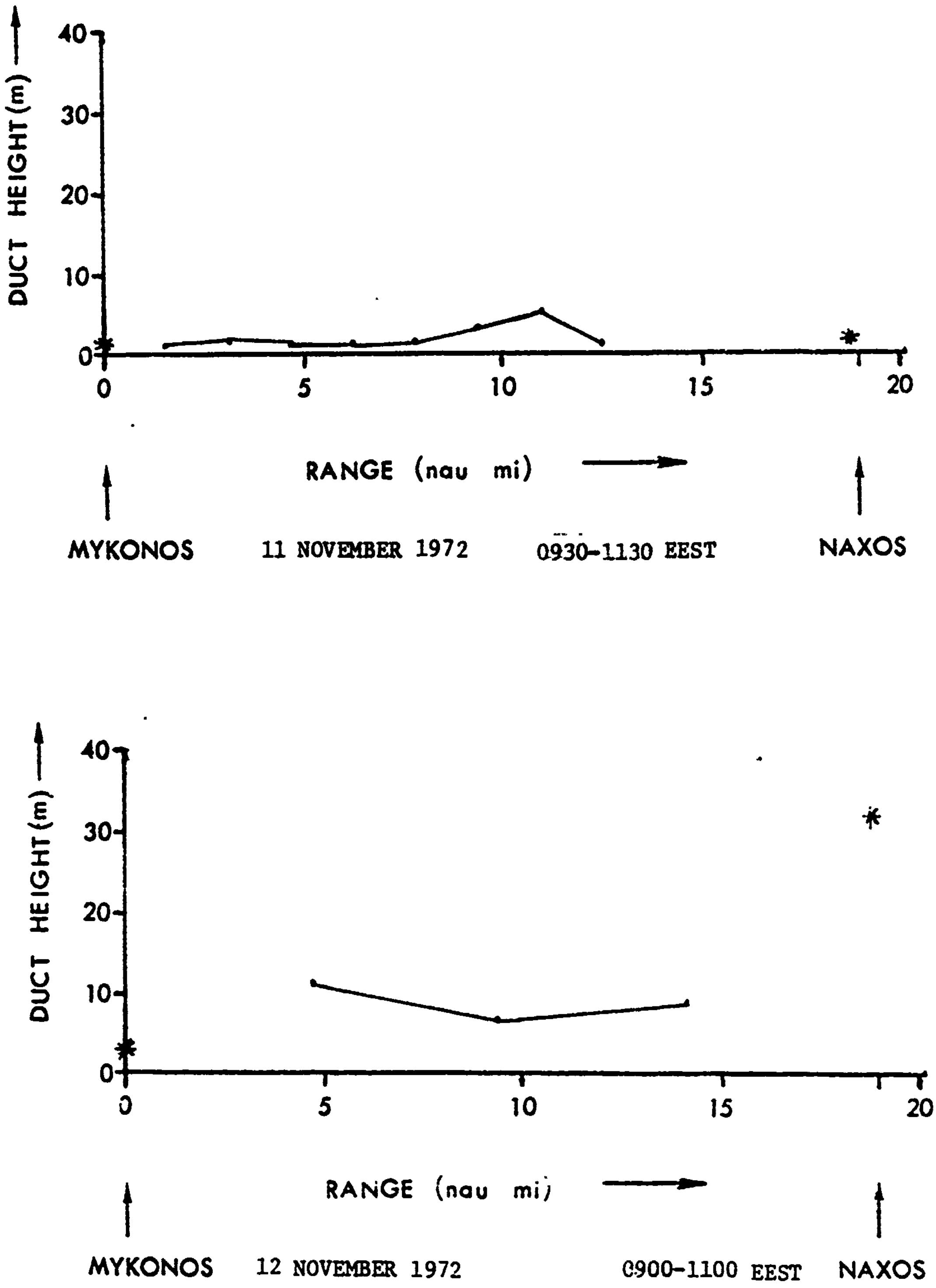

Figure 153. Duct height measurements along the propagation path

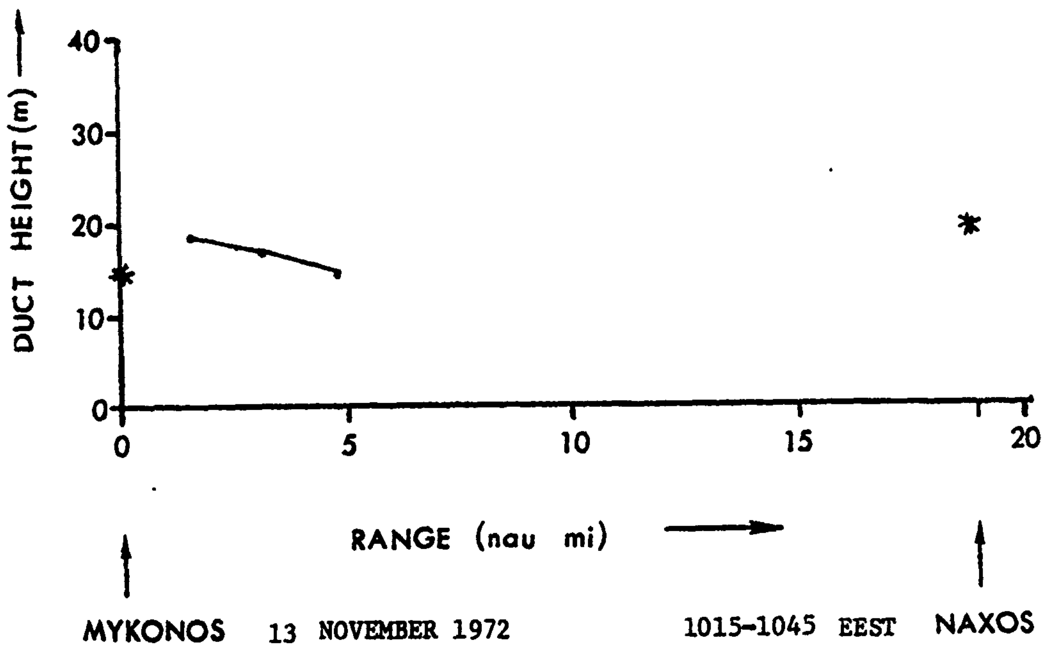

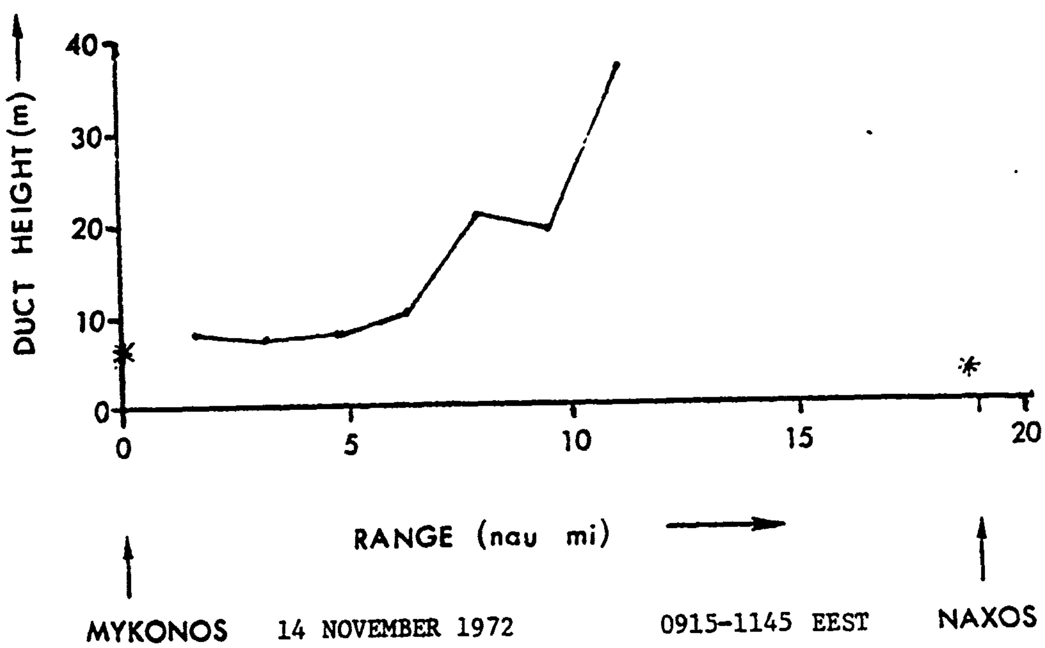

Figure 154. Duct height measurements along the propagation path

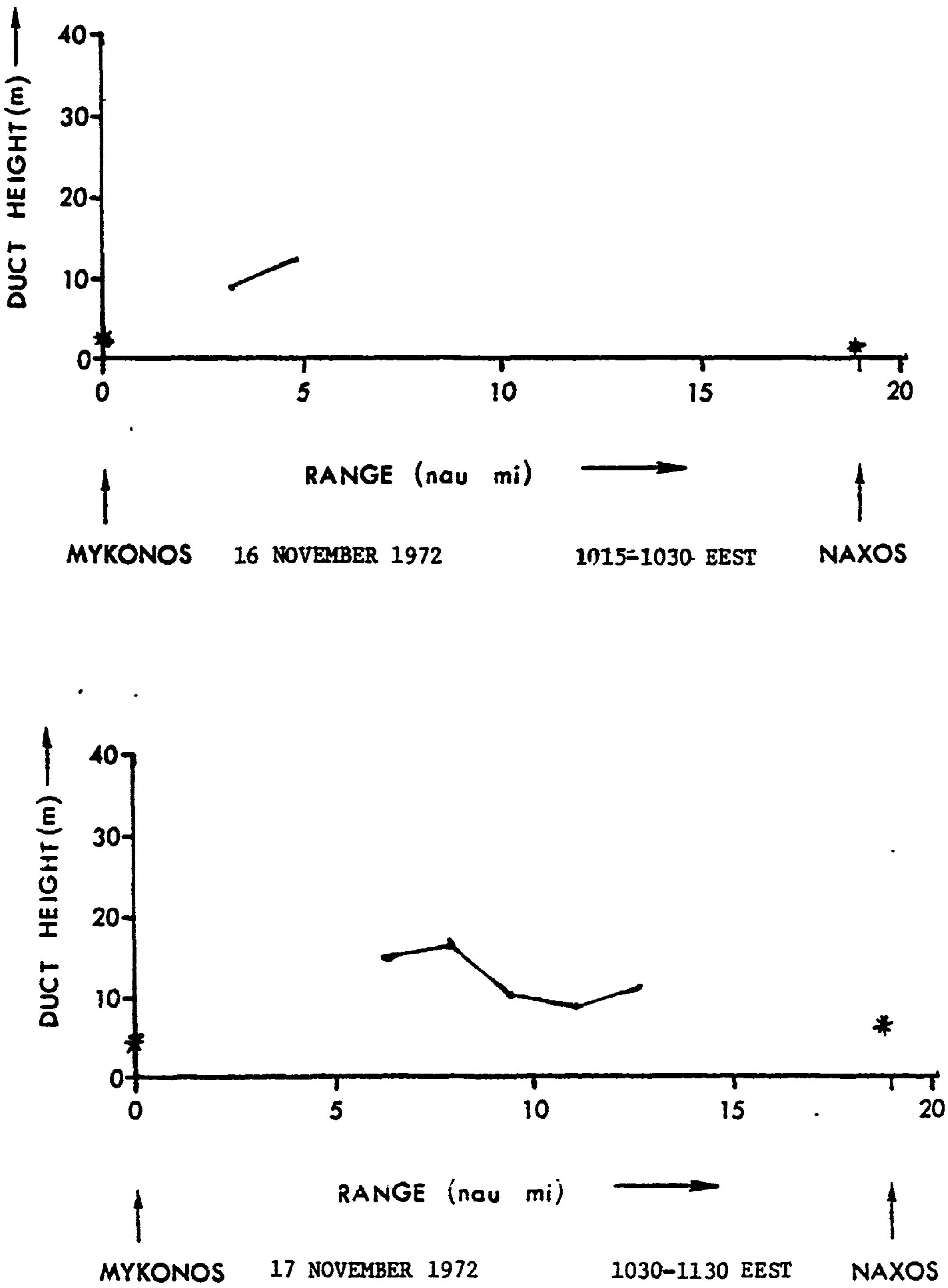

Figure 155. Duct height measurements along the propagation path

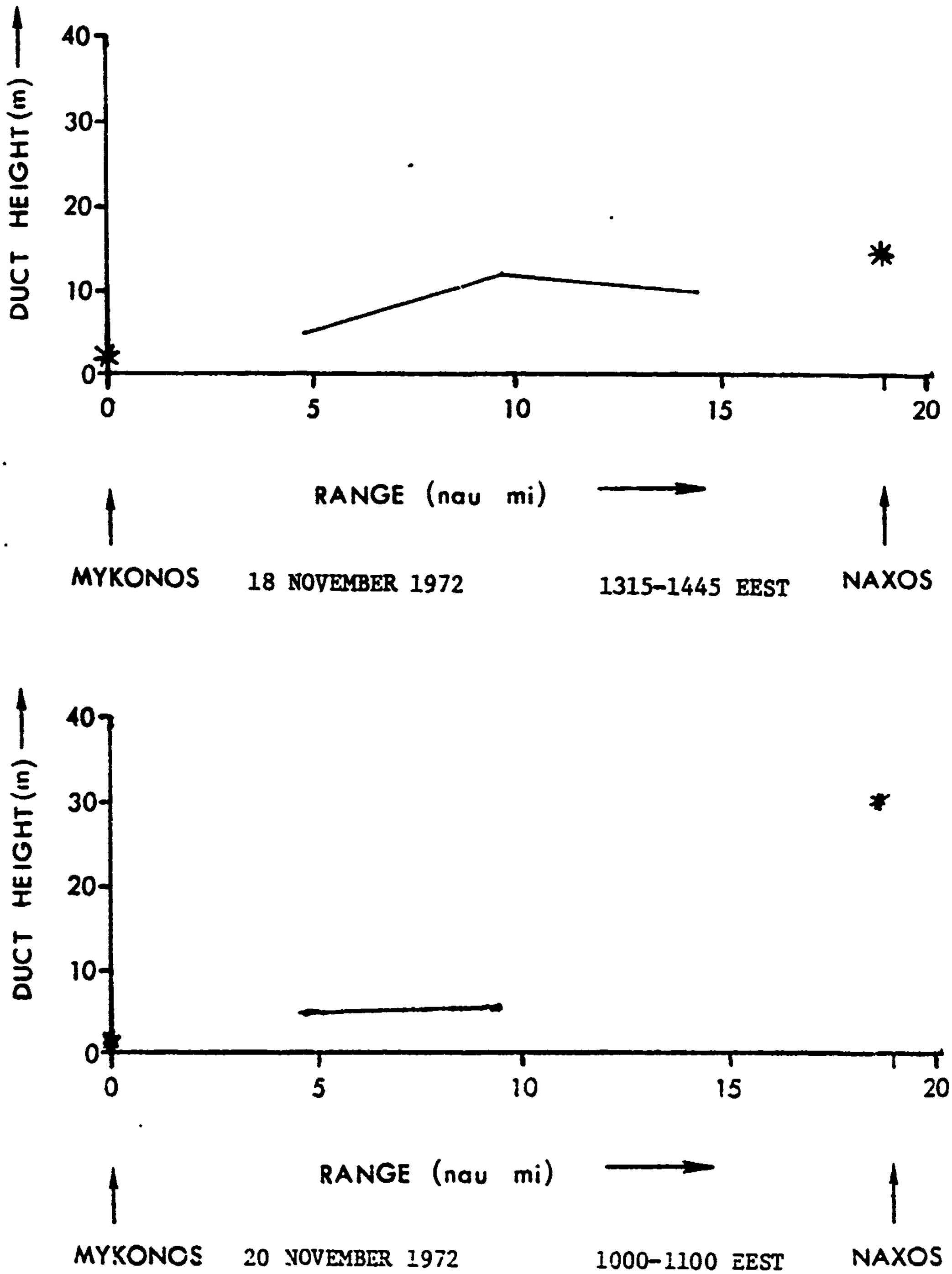

Figure 156. Duct height measurements along the propagation path

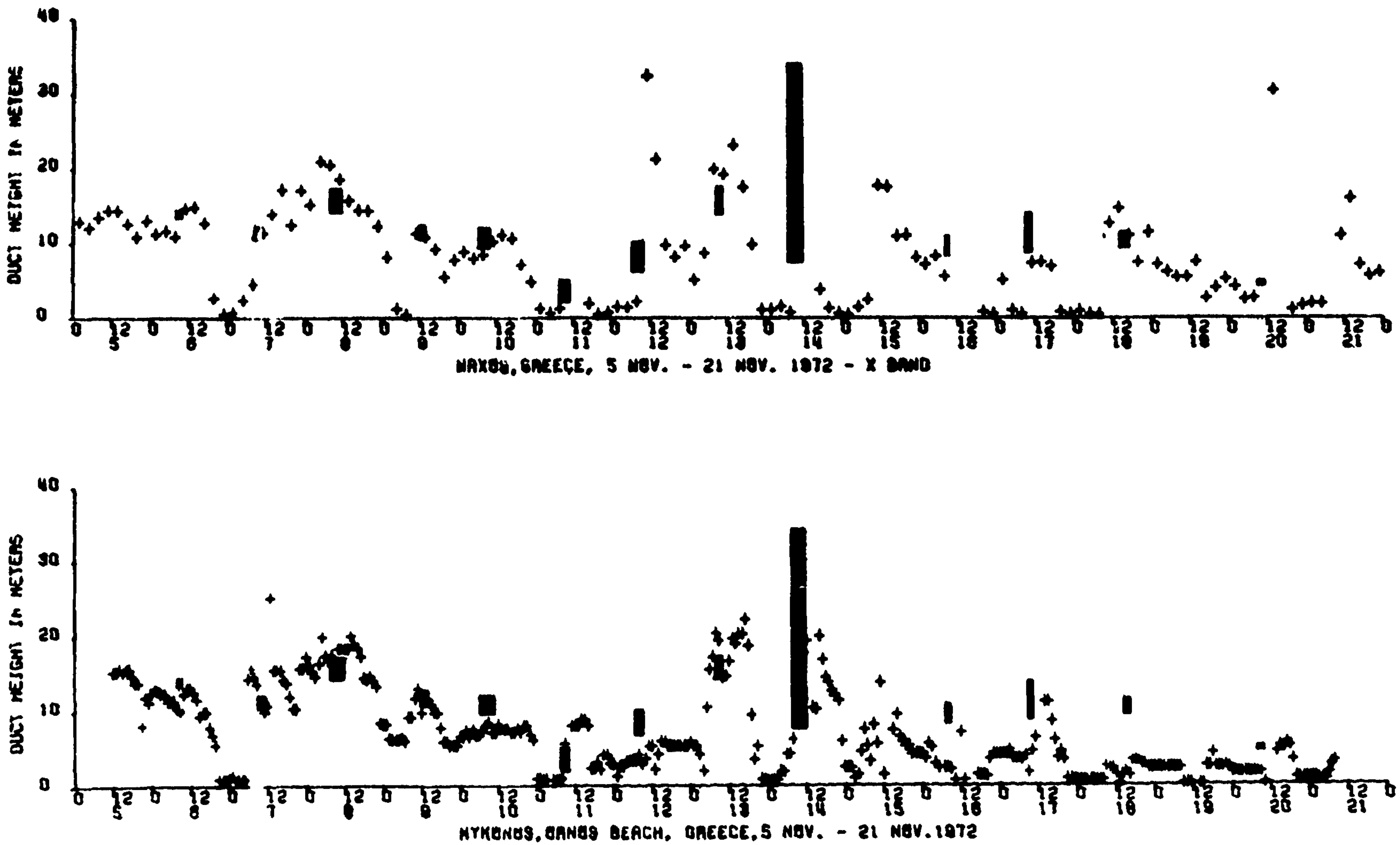

Figure 157. Duct heights calculated from meteorological measurements at Naxos and at Mykonos (crosses) and along the propagation path (shaded areas)

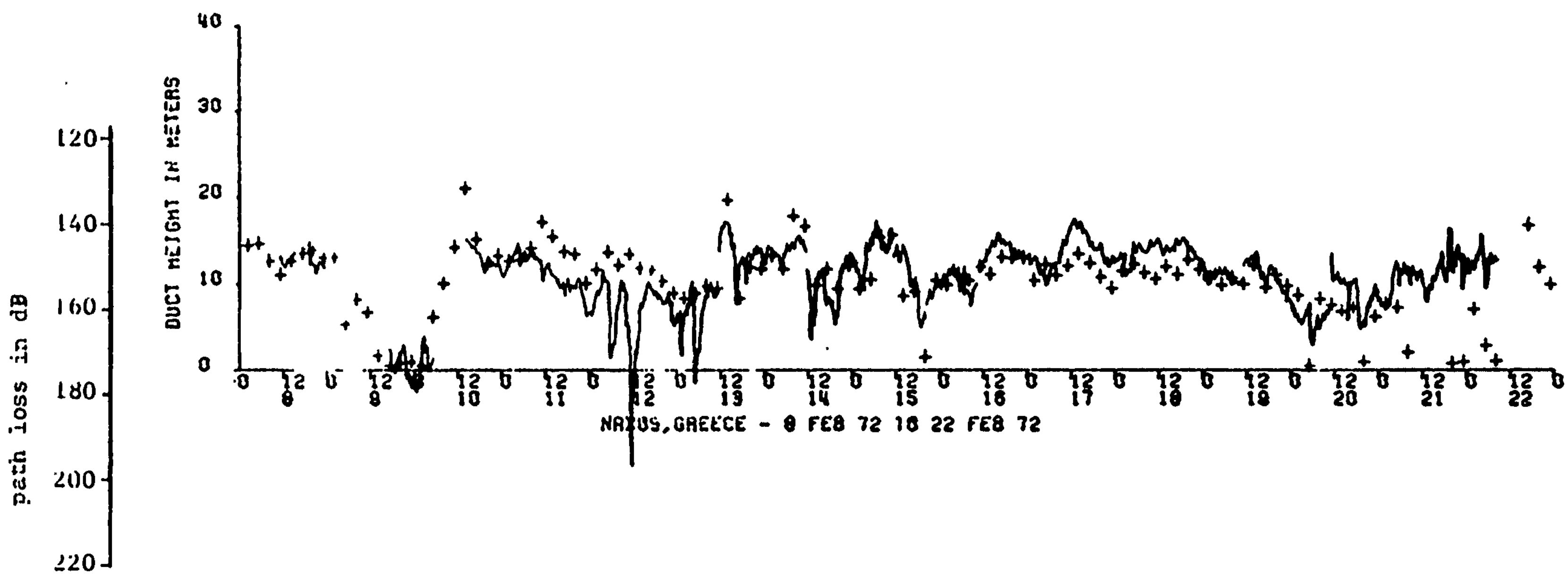

Figure 158. Path loss for low X-band antenna and duct height(+), winter period

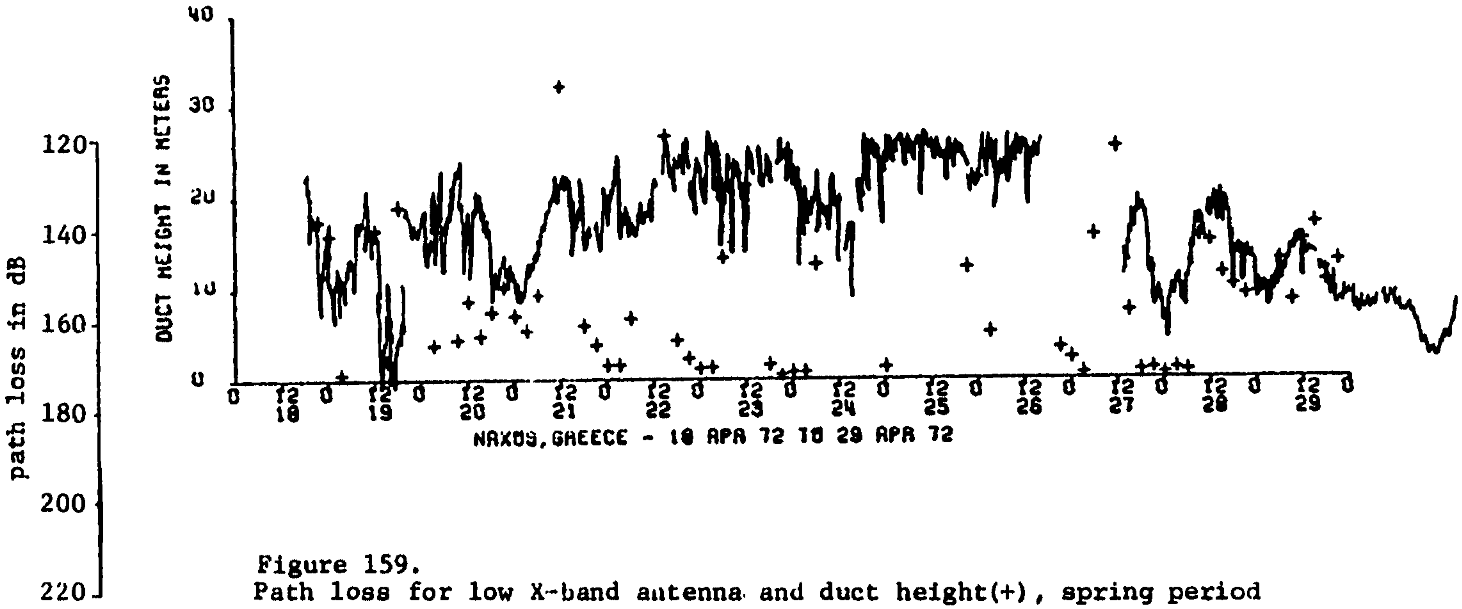

Figure 159.
Path loss for low X-band antenna and duct height(+), spring period

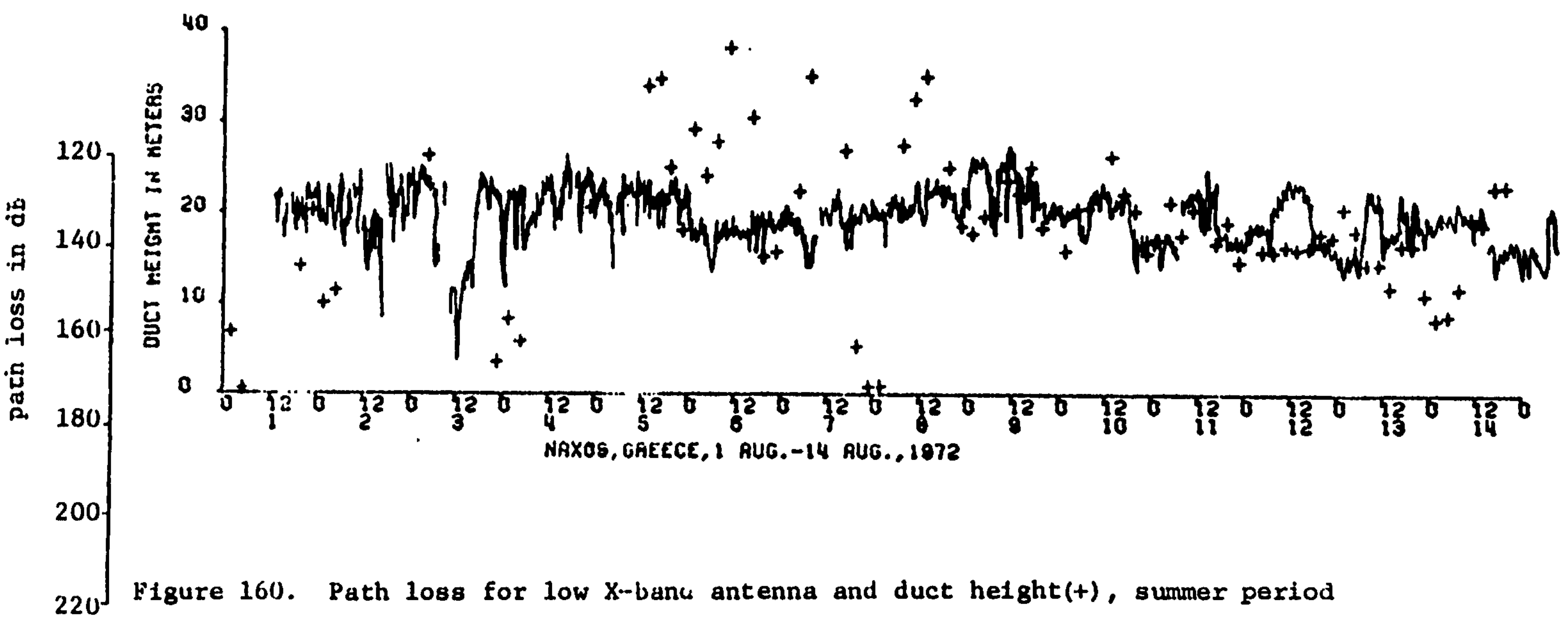

Figure 160. Path loss for low X-band antenna and duct height(+), summer period

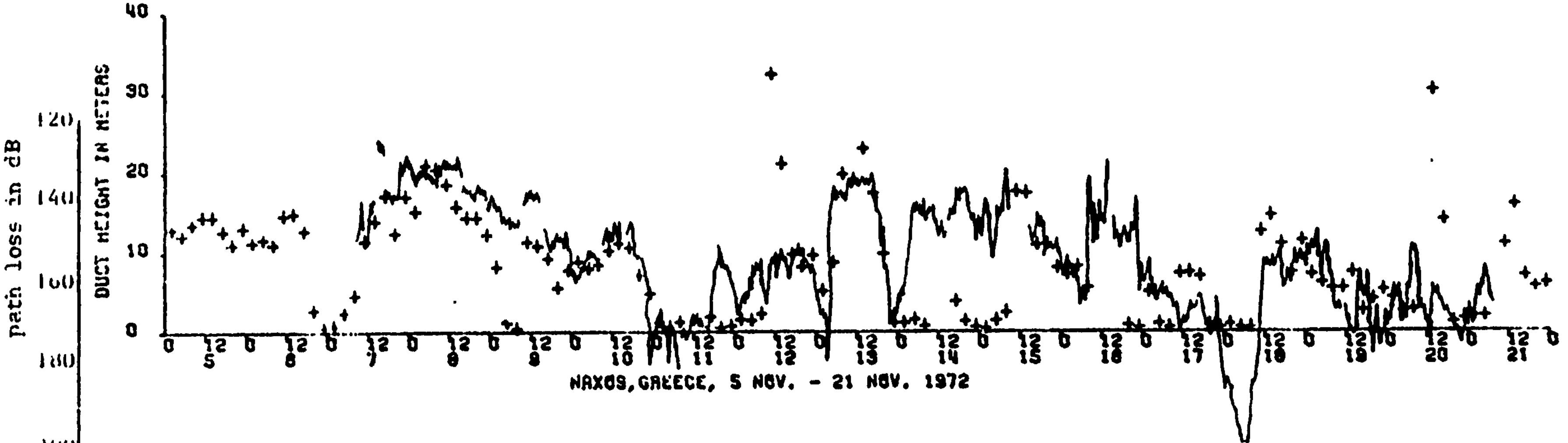

Figure 161. Path loss for low X-band antenna and duct height(+), fall period

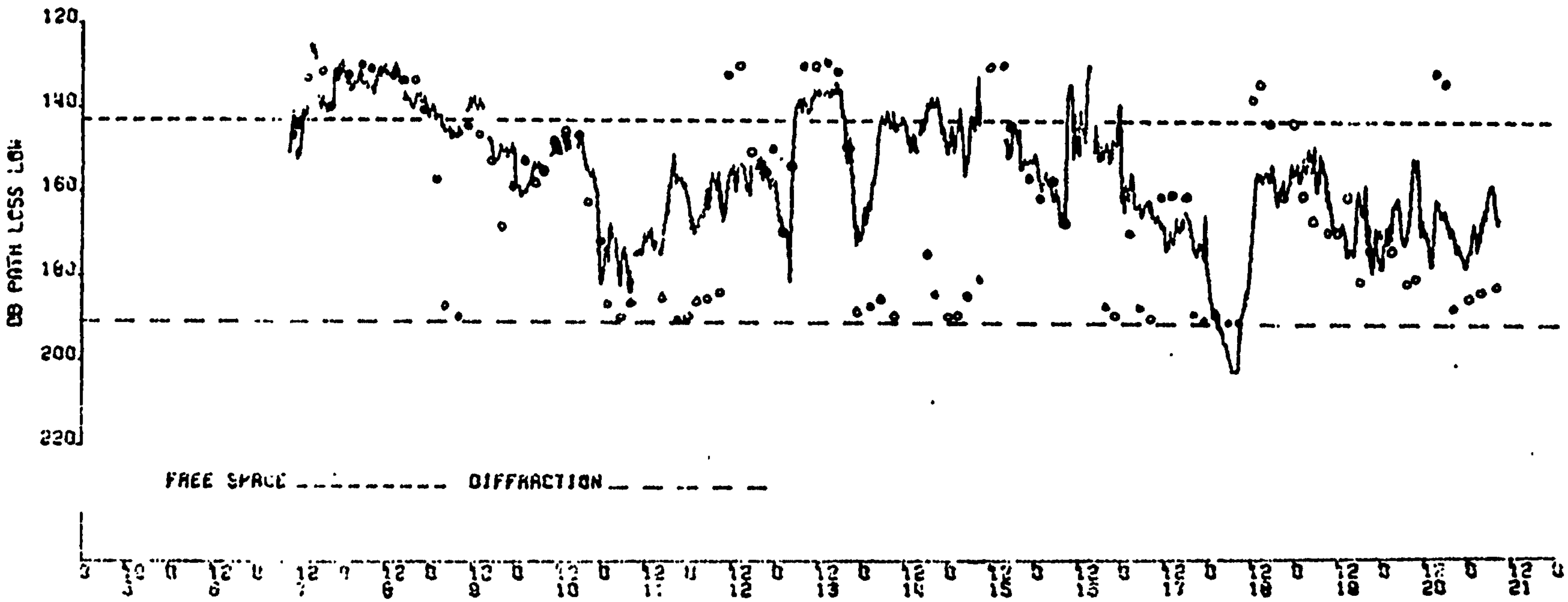

Figure 162. Measured path loss for low X-band antenna during fall period (solid line) and calculated path loss from Naxos duct heights (circles)

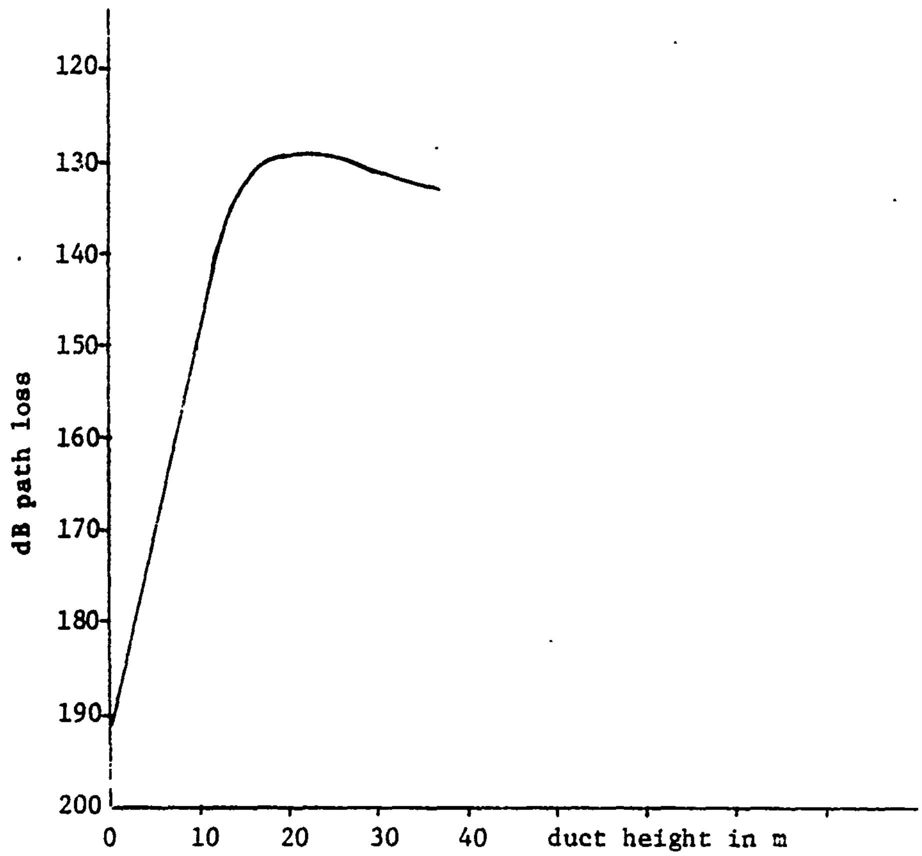

Figure 163. Duct height-path loss relationship for low X-band antenna

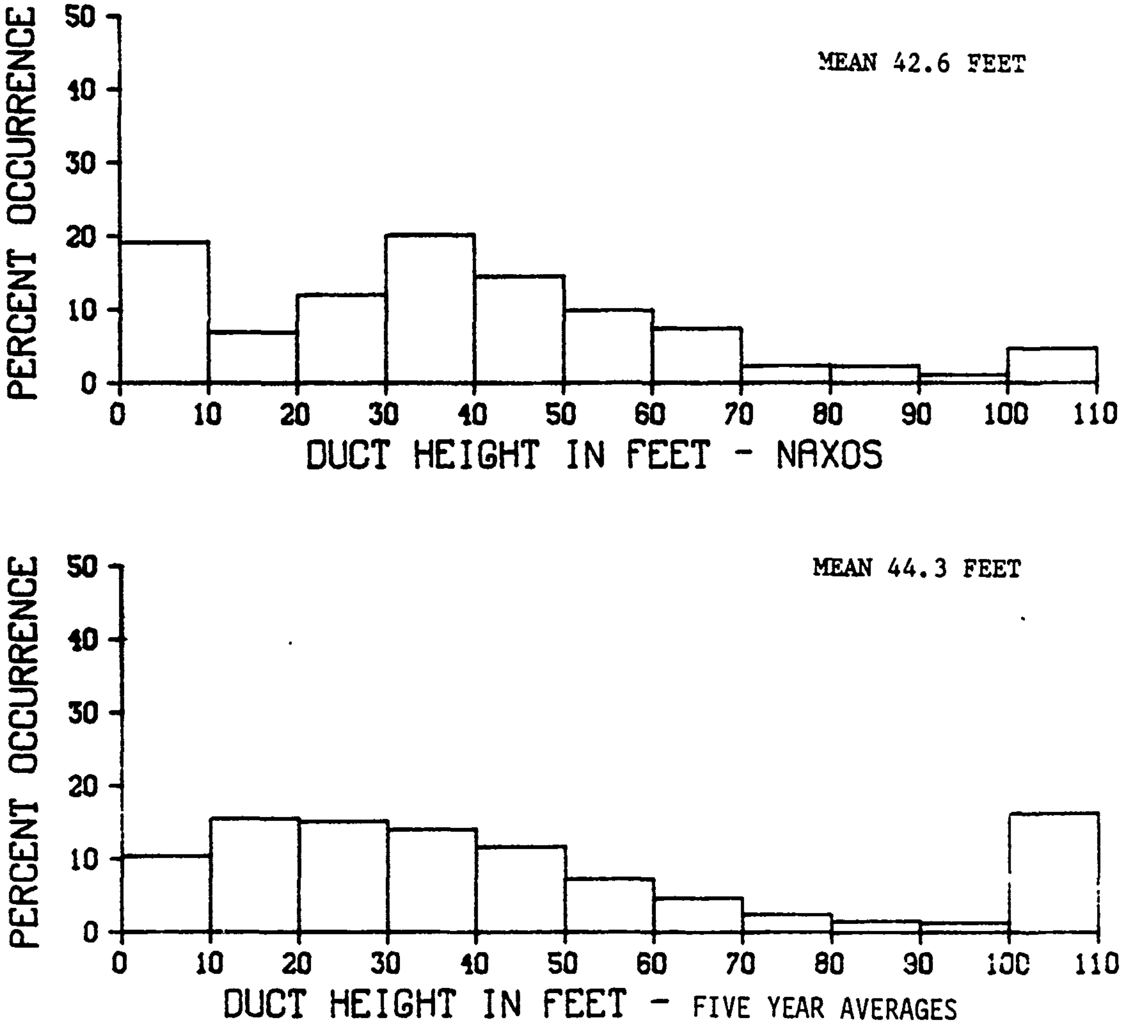

Figure 164. Duct height distribution from Naxos measurements and from five year meteorological averages for the area of the propagation path

IX. TABLES

PAGE

PAGE

PAGE

Period	Winter	Spring	Summer	Fall
Dates	8-22 February 1972	18 April - 1 May 1972	31 July - 14 August 1972	7-21 November 1972
L-band (1.0426 GHz)	5-11 (3-5)	29-35 (13-15)	53-59 (23-25)	84-90 (36-38)
S-band (3.0075 GHz)	12-18 (6-8)	36-42 (16-18)	60-66 (26-28	91-97 (39-41)
X-band (9.624 GHz)	19-28 (9-12)	43-52 (19-22)	67-76 (29-32)	98-107 (42-45)
Ku-band (17.9648 GHz)	---	---	77-83 (33-35)	108-114 (46-48)
Ka-band (37.44 GHz)	---	---	---	115-119 (49-51)

Table 1. Measurement periods and frequencies with corresponding figure and table (in parenthesis) numbers.

Frequency band		L	S	X	Ku	Ka
Frequency in GHz		1.0426	3.0075	9.624	17.9648	37.44
Path length in km		35.2	35.2	35.2	35.2	35.2
Transmitter height in m above msl		4.8	4.8	4.8	4.5	5.1
Receiving antenna heights in m above msl	high	19.2	19.2	19.2	17.8	---
	mid	10.0	10.0	10.0	9.5	8.6
	low	4.9	4.9	4.9	4.3	3.6
Max measurable path loss in dB		184	195	203	200	223
Atmospheric absorption over path in dB		.14	.32	.67	2.75	4.9
Calculated path loss for standard atmospheric conditions (absorption included) in dB	high	154	163	173	183	---
	mid	161	172	183	196	216
	low	167	178	191	205	223

Table 2. Propagation link characteristics

L BAND, NAXOS TO MYKONOS, GREECE   FEBRUARY 1972

HIGH-LOW	MID-LOW	HIGH-MID
0.0 % > 20.0 DB	0.0 % > 20.0 DB	0.1 % > 20.0 DB
54.5 % > 15.0 DB	0.0 % > 15.0 DB	0.1 % > 15.0 DB
99.9 % > 10.0 DB	0.9 % > 10.0 DB	4.8 % > 10.0 DB
100.0 % > 6.0 DB	65.1 % > 6.0 DB	99.3 % > 6.0 DB
100.0 % > 3.0 DB	97.0 % > 3.0 DB	99.4 % > 3.0 DB
100.0 % > 0.0 DB	99.8 % > 0.0 DB	100.0 % > 0.0 DB
100.0 % > -3.0 DB	99.9 % > -3.0 DB	100.0 % > -3.0 DB
100.0 % > -6.0 DB	99.9 % > -6.0 DB	100.0 % > -6.0 DB
100.0 % > -10.0 DB	100.0 % > -10.0 DB	100.0 % > -10.0 DB
100.0 % > -15.0 DB	100.0 % > -15.0 DB	100.0 % > -15.0 DB
100.0 % > -20.0 DB	100.0 % > -20.0 DB	100.0 % > -20.0 DB
TOTAL ENTRIES = 1253	TOTAL ENTRIES = 1253	TOTAL ENTRIES = 1253

FADING HIGH	FADING MIDDLE	FADING LOW
0.0 % > 20.0 DB	0.0 % > 20.0 DB	0.0 % > 20.0 DB
0.0 % > 15.0 DB	0.0 % > 15.0 DB	0.0 % > 15.0 DB
0.0 % > 10.0 DB	0.0 % > 10.0 DB	0.0 % > 10.0 DB
0.0 % > 8.0 DB	0.0 % > 8.0 DB	0.0 % > 8.0 DB
0.0 % > 6.0 DB	0.0 % > 6.0 DB	2.5 % > 6.0 DB
0.0 % > 5.0 DB	0.0 % > 5.0 DB	2.5 % > 5.0 DB
0.1 % > 4.0 DB	1.8 % > 4.0 DB	10.2 % > 4.0 DB
0.6 % > 3.0 DB	10.2 % > 3.0 DB	35.5 % > 3.0 DB
15.2 % > 2.0 DB	46.4 % > 2.0 DB	57.3 % > 2.0 DB
90.9 % > 1.0 DB	97.5 % > 1.0 DB	99.3 % > 1.0 DB
TOTAL ENTRIES = 1253	TOTAL ENTRIES = 1253	TOTAL ENTRIES = 1253

Table 3. Statistical presentation for L-band

PATH LOSS	% HIGH	% MID	% LOW
120.0 TO 125.0	0.0	0.0	0.0
125.0 TO 130.0	0.0	0.0	0.0
130.0 TO 135.0	0.0	0.0	0.0
135.0 TO 140.0	0.0	0.0	0.0
140.0 TO 145.0	0.0	0.0	0.0
145.0 TO 150.0	6.6	0.0	0.0
150.0 TO 155.0	45.1	0.2	0.0
155.0 TO 160.0	47.9	16.1	0.0
160.0 TO 165.0	0.4	63.5	11.3
165.0 TO 170.0	0.0	20.0	40.7
170.0 TO 175.0	0.0	0.0	45.8
175.0 TO 180.0	0.0	0.1	2.2
180.0 TO 185.0	0.0	0.0	0.0
185.0 TO 190.0	0.0	0.0	0.0
190.0 TO 195.0	0.0	0.0	0.0
195.0 TO 200.0	0.0	0.0	0.0
200.0 TO 205.0	0.0	0.0	0.0
205.0 TO 210.0	0.0	0.0	0.0
210.0 TO 215.0	0.0	0.0	0.0
215.0 TO 220.0	0.0	0.0	0.0
ENTRIES	1253	1253	1253

FADING	% HIGH	% MID	% LOW
0.0 TO 0.5	0.0	0.0	0.2
0.5 TO 1.0	9.1	2.5	0.2
1.0 TO 1.5	30.6	16.6	19.2
1.5 TO 2.0	45.2	30.3	19.0
2.0 TO 2.5	10.7	23.5	5.9
2.5 TO 3.0	3.8	16.9	17.9
3.0 TO 3.5	0.2	6.6	23.7
3.5 TO 4.0	0.3	1.8	3.0
4.0 TO 4.5	0.0	1.4	0.9
4.5 TO 5.0	0.1	0.0	0.0
5.0 TO 5.5	0.0	0.4	7.7
5.5 TO 6.0	0.0	0.0	0.0
6.0 TO 6.5	0.0	0.0	0.2
6.5 TO 7.0	0.0	0.0	2.3
7.0 TO 7.5	0.0	0.0	0.0
7.5 TO 8.0	0.0	0.0	0.0
8.0 TO 8.5	0.0	0.0	0.0
8.5 TO 9.0	0.0	0.0	0.0
9.0 TO 9.5	0.0	0.0	0.0
9.5 TO 10.0	0.0	0.0	0.0
ENTRIES	1253	1253	1253

Table 4. Frequency distributions of path loss and fading for L-band

DIFFERENCE	% HIGH-LOW	% HIGH-MID	% MID-LOW
-20.0 TO -18.0	0.0	0.0	0.0
-18.0 TO -16.0	0.0	0.0	0.0
-16.0 TO -14.0	0.0	0.0	0.0
-14.0 TO -12.0	0.0	0.0	0.0
-12.0 TO -10.0	0.0	0.0	0.0
-10.0 TO -8.0	0.0	0.0	0.0
-8.0 TO -6.0	0.0	0.0	0.1
-6.0 TO -4.0	0.0	0.0	0.0
-4.0 TO -2.0	0.0	0.0	0.0
-2.0 TO 0.0	0.0	0.0	0.1
0.0 TO 2.0	0.0	0.2	0.0
2.0 TO 4.0	0.0	0.3	15.2
4.0 TO 6.0	0.0	0.2	19.4
6.0 TO 8.0	0.0	21.1	43.1
8.0 TO 10.0	0.0	73.3	21.2
10.0 TO 12.0	6.9	4.6	0.7
12.0 TO 14.0	21.2	0.1	0.1
14.0 TO 16.0	34.4	0.1	0.1
16.0 TO 18.0	34.6	0.0	0.0
18.0 TO 20.0	2.9	0.1	0.0
ENTRIES	1253	1253	1253

Table 5. Frequency distributions of path loss differences between antennas for L-band

S BAND, NAXUS TO MYKONOS, GREECE FEBRUARY 1972

HIGH-LOW	MID-LOW	HIGH-MID
2.6 % > 20.0 DB	0.0 % > 20.0 DB	0.0 % > 20.0 DB
98.2 % > 15.0 DB	0.4 % > 15.0 DB	0.0 % > 15.0 DB
99.6 % > 10.0 DB	94.8 % > 10.0 DB	1.1 % > 10.0 DB
99.8 % > 6.0 DB	99.3 % > 6.0 DB	50.3 % > 6.0 DB
99.9 % > 3.0 DB	99.3 % > 3.0 DB	98.5 % > 3.0 DB
100.0 % > 0.0 DB	99.8 % > 0.0 DB	99.3 % > 0.0 DB
100.0 % > -3.0 DB	99.9 % > -3.0 DB	99.8 % > -3.0 DB
100.0 % > -6.0 DB	100.0 % > -6.0 DB	99.9 % > -6.0 DB
100.0 % > -10.0 DB	100.0 % > -10.0 DB	100.0 % > -10.0 DB
100.0 % > -15.0 DB	100.0 % > -15.0 DB	100.0 % > -15.0 DB
100.0 % > -20.0 DB	100.0 % > -20.0 DB	100.0 % > -20.0 DB
TOTAL ENTRIES = 1216	TOTAL ENTRIES = 1216	TOTAL ENTRIES = 1216

FADING HIGH	FADING MIDDLE	FADING LOW
0.0 % > 20.0 DB	0.0 % > 20.0 DB	0.0 % > 20.0 DB
0.0 % > 15.0 DB	0.0 % > 15.0 DB	0.0 % > 15.0 DB
0.0 % > 10.0 DB	0.0 % > 10.0 DB	0.0 % > 10.0 DB
0.0 % > 8.0 DB	0.0 % > 8.0 DB	0.1 % > 8.0 DB
0.0 % > 6.0 DB	0.0 % > 6.0 DB	0.8 % > 6.0 DB
0.0 % > 5.0 DB	0.2 % > 5.0 DB	1.4 % > 5.0 DB
1.5 % > 4.0 DB	3.2 % > 4.0 DB	8.5 % > 4.0 DB
10.0 % > 3.0 DB	16.9 % > 3.0 DB	26.0 % > 3.0 DB
54.0 % > 2.0 DB	70.5 % > 2.0 DB	65.8 % > 2.0 DB
98.9 % > 1.0 DB	98.7 % > 1.0 DB	93.9 % > 1.0 DB
TOTAL ENTRIES = 1216	TOTAL ENTRIES = 1216	TOTAL ENTRIES = 1216

Table 6. Statistical presentation for S-band

S BAND, GREECE FEBRUARY 1972

PATH LOSS	% HIGH	% MID	% LOW
120.0 TO 125.0	0.0	0.0	0.0
125.0 TO 130.0	0.0	0.0	0.0
130.0 TO 135.0	0.0	0.0	0.0
135.0 TO 140.0	0.0	0.0	0.0
140.0 TO 145.0	1.2	0.0	0.0
145.0 TO 150.0	31.7	0.9	0.0
150.0 TO 155.0	50.8	21.5	0.0
155.0 TO 160.0	14.0	50.2	0.7
160.0 TO 165.0	2.1	23.1	7.6
165.0 TO 170.0	0.2	3.9	49.2
170.0 TO 175.0	0.0	0.2	31.7
175.0 TO 180.0	0.0	0.0	10.6
180.0 TO 185.0	0.0	0.0	0.3
185.0 TO 190.0	0.0	0.0	0.0
190.0 TO 195.0	0.0	0.0	0.0
195.0 TO 200.0	0.0	0.0	0.0
200.0 TO 205.0	0.0	0.0	0.0
205.0 TO 210.0	0.0	0.0	0.0
210.0 TO 215.0	0.0	0.0	0.0
215.0 TO 220.0	0.0	0.0	0.0
ENTRIES	1216	1216	1216

FADING	% HIGH	% MID	% LOW
0.0 TO 0.5	0.0	0.0	0.0
0.5 TO 1.0	2.5	1.2	6.1
1.0 TO 1.5	17.8	9.5	15.9
1.5 TO 2.0	25.7	17.6	9.4
2.0 TO 2.5	21.6	26.2	11.7
2.5 TO 3.0	21.5	27.3	31.0
3.0 TO 3.5	3.9	5.5	7.4
3.5 TO 4.0	5.5	9.4	9.8
4.0 TO 4.5	1.2	2.4	2.5
4.5 TO 5.0	0.3	0.5	0.7
5.0 TO 5.5	0.0	0.2	4.1
5.5 TO 6.0	0.0	0.1	0.6
6.0 TO 6.5	0.0	0.0	0.4
6.5 TO 7.0	0.0	0.0	0.2
7.0 TO 7.5	0.0	0.0	0.0
7.5 TO 8.0	0.0	0.0	0.1
8.0 TO 8.5	0.0	0.0	0.1
8.5 TO 9.0	0.0	0.0	0.0
9.0 TO 9.5	0.0	0.0	0.0
9.5 TO 10.0	0.0	0.0	0.0
ENTRIES	1216	1216	1216

Table 7. Frequency distributions of path loss and fading for S-band

S. BAND, GREECE FEBRUARY 1972

DIFFERENCE	% HIGH-LOW	% HIGH-MID	% MID-LOW
-20.0 TO -18.0	0.0	0.0	0.0
-18.0 TO -16.0	0.0	0.0	0.0
-16.0 TO -14.0	0.0	0.0	0.0
-14.0 TO -12.0	0.0	0.0	0.0
-12.0 TO -10.0	0.0	0.0	0.0
-10.0 TO -8.0	0.0	0.0	0.0
-8.0 TO -6.0	0.0	0.1	0.0
-6.0 TO -4.0	0.0	0.0	0.1
-4.0 TO -2.0	0.0	0.1	0.0
-2.0 TO 0.0	0.0	0.3	0.1
0.0 TO 2.0	0.0	0.7	0.0
2.0 TO 4.0	0.1	1.5	0.0
4.0 TO 6.0	0.1	44.5	0.5
6.0 TO 8.0	0.1	46.5	1.2
8.0 TO 10.0	0.1	5.1	2.1
10.0 TO 12.0	0.7	1.0	54.9
12.0 TO 14.0	0.7	0.3	39.4
14.0 TO 16.0	1.0	0.0	1.3
16.0 TO 18.0	53.5	0.0	0.1
18.0 TO 20.0	43.8	0.0	0.2
ENTRIES	1216	1216	1216

Table 8. Frequency distributions of path loss differences between antennas for S-band

X BAND, NAXOS TO MYKONOS, GREECE   FEBRUARY 1972

HIGH-LOW

0.0 %	>	20.0 DB
0.2 %	>	15.0 DB
1.[illegible] %	>	10.0 DB
7.7 %	>	6.0 DB
25.1 %	>	3.0 DB
40.3 %	>	0.0 DB
72.5 %	>	-3.0 DB
[illegible] %	>	-6.0 DB
98.4 %	>	-10.0 DB
100.0 %	>	-15.0 DB
100.0 %	>	-20.0 DB

TOTAL ENTRIES = 1202

MID-LOW

0.0 %	>	20.0 DB
0.0 %	>	15.0 DB
0.1 %	>	10.0 DB
1.2 %	>	6.0 DB
5.0 %	>	3.0 DB
28.1 %	>	0.0 DB
85.0 %	>	-3.0 DB
99.3 %	>	-6.0 DB
99.9 %	>	-10.0 DB
100.0 %	>	-15.0 DB
100.0 %	>	-20.0 DB

TOTAL ENTRIES = 1202

HIGH-MID

0.0 %	>	20.0 DB
0.2 %	>	15.0 DB
0.8 %	>	10.0 DB
6.2 %	>	6.0 DB
25.9 %	>	3.0 DB
52.2 %	>	0.0 DB
92.3 %	>	-3.0 DB
98.5 %	>	-6.0 DB
100.0 %	>	-10.0 DB
100.0 %	>	-15.0 DB
100.0 %	>	-20.0 DB

TOTAL ENTRIES = 1202

FADING HIGH

0.0 %	>	20.0 DB
0.0 %	>	15.0 DB
0.1 %	>	10.0 DB
0.2 %	>	8.0 DB
0.8 %	>	6.0 DB
1.1 %	>	5.0 DB
[illegible] %	>	4.0 DB
13.6 %	>	3.0 DB
46.8 %	>	2.0 DB
97.4 %	>	1.0 DB

TOTAL ENTRIES = 1202

FADING MIDDLE

0.0 %	>	20.0 DB
0.1 %	>	15.0 DB
0.1 %	>	10.0 DB
0.2 %	>	8.0 DB
0.7 %	>	6.0 DB
1.2 %	>	5.0 DB
7.3 %	>	4.0 DB
21.6 %	>	3.0 DB
54.6 %	>	2.0 DB
91.9 %	>	1.0 DB

TOTAL ENTRIES = 1202

FADING LOW

0.0 %	>	20.0 DB
0.0 %	>	15.0 DB
0.0 %	>	10.0 DB
0.2 %	>	8.0 DB
1.2 %	>	6.0 DB
3.0 %	>	5.0 DB
11.5 %	>	4.0 DB
33.2 %	>	3.0 DB
69.3 %	>	2.0 DB
96.6 %	>	1.0 DB

TOTAL ENTRIES = 1202

Table 9. Statistical presentation for X-band

X BAND, GREECE FEBRUARY 1972

PATH LOSS	% HIGH	% MID	% LOW
120.0 TO 125.0	0.0	0.0	0.0
125.0 TO 130.0	0.0	0.0	0.0
130.0 TO 135.0	0.0	0.0	0.0
135.0 TO 140.0	0.0	0.0	0.6
140.0 TO 145.0	0.8	2.2	9.8
145.0 TO 150.0	31.1	33.0	33.6
150.0 TO 155.0	49.4	35.0	24.7
155.0 TO 160.0	12.0	17.2	16.6
160.0 TO 165.0	3.5	7.1	8.2
165.0 TO 170.0	2.3	2.5	2.6
170.0 TO 175.0	0.5	1.6	2.1
175.0 TO 180.0	0.2	1.1	1.4
180.0 TO 185.0	0.2	0.2	0.2
185.0 TO 190.0	0.0	0.1	0.0
190.0 TO 195.0	0.0	0.1	0.1
195.0 TO 200.0	0.0	0.0	0.2
200.0 TO 205.0	0.0	0.0	0.0
205.0 TO 210.0	0.0	0.0	0.0
210.0 TO 215.0	0.0	0.0	0.0
215.0 TO 220.0	0.0	0.0	0.0
ENTRIES	1202	1202	1202

FADING	% HIGH	% MID	% LOW
0.0 TO 0.5	0.0	0.0	0.0
0.5 TO 1.0	11.0	6.7	2.9
1.0 TO 1.5	18.6	17.4	8.4
1.5 TO 2.0	18.4	14.1	14.3
2.0 TO 2.5	25.0	22.4	18.4
2.5 TO 3.0	12.9	17.5	21.9
3.0 TO 3.5	7.0	9.0	13.7
3.5 TO 4.0	3.0	5.1	8.0
4.0 TO 4.5	2.0	3.2	6.0
4.5 TO 5.0	0.7	2.9	2.1
5.0 TO 5.5	0.5	0.6	1.6
5.5 TO 6.0	0.2	0.4	1.5
6.0 TO 6.5	0.2	0.4	0.4
6.5 TO 7.0	0.1	0.2	0.2
7.0 TO 7.5	0.2	0.1	0.2
7.5 TO 8.0	0.1	0.0	0.1
8.0 TO 8.5	0.1	0.0	0.0
8.5 TO 9.0	0.1	0.0	0.0
9.0 TO 9.5	0.1	0.0	0.1
9.5 TO 10.0	0.1	0.2	0.2
ENTRIES	1202	1202	1202

Table 10. Frequency distributions of path loss and fading for X-band

DIFFERENCE	% HIGH-LOW	% HIGH-MID	% MID-LOW
-20.0 TO -18.0	0.0	0.0	0.0
-18.0 TO -16.0	0.0	0.0	0.0
-16.0 TO -14.0	0.1	0.0	0.0
-14.0 TO -12.0	0.3	0.0	0.1
-12.0 TO -10.0	1.2	0.0	0.0
-10.0 TO -8.0	0.8	0.3	0.2
-8.0 TO -6.0	3.3	1.2	0.5
-6.0 TO -4.0	10.4	2.7	4.2
-4.0 TO -2.0	17.4	14.4	23.5
-2.0 TO 0.0	16.7	20.3	41.6
0.0 TO 2.0	13.2	25.2	17.7
2.0 TO 4.0	16.3	17.7	9.3
4.0 TO 6.0	11.8	11.8	1.7
6.0 TO 8.0	5.4	4.7	0.6
8.0 TO 10.0	1.4	0.8	0.6
10.0 TO 12.0	0.6	0.4	0.0
12.0 TO 14.0	0.5	0.2	0.0
14.0 TO 16.0	0.3	0.1	0.1
16.0 TO 18.0	0.2	0.1	0.0
18.0 TO 20.0	0.0	0.1	0.0
ENTRIES	1202	1202	1202

DET RANGE	% HIGH	% MID	% LOW
0.0 TO 10.0	0.0	0.0	0.0
10.0 TO 20.0	6.6	11.9	14.1
20.0 TO 30.0	61.5	52.4	39.8
30.0 TO 40.0	30.6	30.5	28.4
40.0 TO 50.0	1.0	4.8	11.5
50.0 TO 60.0	0.2	0.3	3.1
60.0 TO 70.0	0.1	0.0	1.0
70.0 TO 80.0	0.0	0.0	0.9
80.0 TO 90.0	0.0	0.0	1.2
90.0 TO 100.0	0.0	0.0	0.0
100.0 TO 110.0	0.0	0.0	0.0
110.0 TO 120.0	0.0	0.0	0.0
120.0 TO 130.0	0.0	0.0	0.0
130.0 TO 140.0	0.0	0.0	0.0
140.0 TO 150.0	0.0	0.0	0.0
150.0 TO 160.0	0.0	0.0	0.0
160.0 TO 170.0	0.0	0.0	0.0
170.0 TO 180.0	0.0	0.0	0.0
180.0 TO 190.0	0.0	0.0	0.0
190.0 TO 200.0	0.0	0.0	0.0
ENTRIES	1202	1202	1202

Table 11. Frequency distributions of path loss difference and detection range for X-band

DET RANGE	%> HIGH	%> MID	%> LOW
10.0	100.0	100.0	100.0
20.0	93.4	88.1	85.9
30.0	31.9	35.7	46.1
40.0	1.3	5.2	17.7
50.0	0.3	0.3	6.2
60.0	0.1	0.0	3.2
70.0	0.0	0.0	2.2
80.0	0.0	0.0	1.2
90.0	0.0	0.0	0.0
100.0	0.0	0.0	0.0
110.0	0.0	0.0	0.0
120.0	0.0	0.0	0.0
130.0	0.0	0.0	0.0
140.0	0.0	0.0	0.0
150.0	0.0	0.0	0.0
160.0	0.0	0.0	0.0
170.0	0.0	0.0	0.0
180.0	0.0	0.0	0.0
190.0	0.0	0.0	0.0
200.0	0.0	0.0	0.0
ENTRIES	1202	1202	1202

DET RANGE DIFF	% HIGH-LOW	% HIGH-MID	% MID-LOW
-50.0 TO -45.0	1.7	0.0	0.1
-45.0 TO -40.0	0.3	0.0	0.3
-40.0 TO -35.0	0.5	0.0	0.4
-35.0 TO -30.0	0.2	0.0	1.0
-30.0 TO -25.0	0.8	0.1	0.3
-25.0 TO -20.0	1.2	0.2	0.7
-20.0 TO -15.0	2.9	1.3	1.4
-15.0 TO -10.0	7.1	1.7	4.4
-10.0 TO -5.0	15.1	7.9	13.3
-5.0 TO 0.0	20.4	27.6	48.0
0.0 TO 5.0	42.3	50.3	29.5
5.0 TO 10.0	6.6	8.9	0.2
10.0 TO 15.0	0.7	1.6	0.0
15.0 TO 20.0	0.1	0.2	0.2
20.0 TO 25.0	0.0	0.2	0.0
25.0 TO 30.0	0.0	0.0	0.0
30.0 TO 35.0	0.0	0.0	0.0
35.0 TO 40.0	0.0	0.0	0.0
40.0 TO 45.0	0.0	0.0	0.0
45.0 TO 50.0	0.0	0.0	0.0
ENTRIES	1202	1202	1202

Table 12. Cumulative distribution of detection range and frequency distribution of detection range differences for X-band

L BAND, NAXOS TO MYKONOS, GREECE APRIL 1972

HIGH-LOW

0.5 %	>	20.0 DB
5.3 %	>	15.0 DB
73.5 %	>	10.0 DB
95.6 %	>	6.0 DB
98.9 %	>	3.0 DB
99.6 %	>	0.0 DB
99.9 %	>	-3.0 DB
100.0 %	>	-6.0 DB
100.0 %	>	-10.0 DB
100.0 %	>	-15.0 DB
100.0 %	>	-20.0 DB

TOTAL ENTRIES = 729

MID-LOW

0.0 %	>	20.0 DB
0.3 %	>	15.0 DB
1.9 %	>	10.0 DB
21.2 %	>	6.0 DB
89.2 %	>	3.0 DB
97.5 %	>	0.0 DB
99.5 %	>	-3.0 DB
99.9 %	>	-6.0 DB
100.0 %	>	-10.0 DB
100.0 %	>	-15.0 DB
100.0 %	>	-20.0 DB

TOTAL ENTRIES = 749

HIGH-MID

0.0 %	>	20.0 DB
0.0 %	>	15.0 DB
2.8 %	>	10.0 DB
57.9 %	>	6.0 DB
93.9 %	>	3.0 DB
98.1 %	>	0.0 DB
99.5 %	>	-3.0 DB
99.7 %	>	-6.0 DB
100.0 %	>	-10.0 DB
100.0 %	>	-15.0 DB
100.0 %	>	-20.0 DB

TOTAL ENTRIES = 737

FADING HIGH

0.0 %	>	20.0 DB
0.0 %	>	15.0 DB
0.7 %	>	10.0 DB
1.5 %	>	8.0 DB
3.3 %	>	6.0 DB
3.7 %	>	5.0 DB
7.2 %	>	4.0 DB
13.0 %	>	3.0 DB
29.3 %	>	2.0 DB
72.2 %	>	1.0 DB

TOTAL ENTRIES = 752

FADING MIDDLE

0.0 %	>	20.0 DB
0.0 %	>	15.0 DB
0.9 %	>	10.0 DB
4.0 %	>	8.0 DB
9.0 %	>	6.0 DB
9.8 %	>	5.0 DB
17.3 %	>	4.0 DB
23.4 %	>	3.0 DB
45.6 %	>	2.0 DB
65.8 %	>	1.0 DB

TOTAL ENTRIES = 758

FADING LOW

0.0 %	>	20.0 DB
0.1 %	>	15.0 DB
1.5 %	>	10.0 DB
4.4 %	>	8.0 DB
13.0 %	>	6.0 DB
14.5 %	>	5.0 DB
26.5 %	>	4.0 DB
36.2 %	>	3.0 DB
61.8 %	>	2.0 DB
90.8 %	>	1.0 DB

TOTAL ENTRIES = 754

Table 13. Statistical presentation for L-band

L BAND, GREECE APRIL 1972

PATH LOSS	% HIGH	% MID	% LOW
120.0 TO 125.0	4.7	0.8	0.3
125.0 TO 130.0	8.6	5.0	0.5
130.0 TO 135.0	9.3	7.8	4.8
135.0 TO 140.0	12.6	9.2	7.7
140.0 TO 145.0	21.0	11.9	10.9
145.0 TO 150.0	25.3	14.0	10.3
150.0 TO 155.0	15.6	22.6	12.7
155.0 TO 160.0	2.7	24.5	24.4
160.0 TO 165.0	0.0	4.2	25.2
165.0 TO 170.0	0.0	0.0	3.2
170.0 TO 175.0	0.0	0.0	0.0
175.0 TO 180.0	0.0	0.0	0.0
180.0 TO 185.0	0.0	0.0	0.0
185.0 TO 190.0	0.0	0.0	0.0
190.0 TO 195.0	0.0	0.0	0.0
195.0 TO 200.0	0.0	0.0	0.0
200.0 TO 205.0	0.0	0.0	0.0
205.0 TO 210.0	0.0	0.0	0.0
210.0 TO 215.0	0.0	0.0	0.0
215.0 TO 220.0	0.0	0.0	0.0
ENTRIES	752	758	754

FADING	% HIGH	% MID	% LOW
0.0 TO 0.5	1.7	0.4	0.4
0.5 TO 1.0	26.1	13.9	8.8
1.0 TO 1.5	36.0	33.0	26.0
1.5 TO 2.0	4.7	2.1	1.5
2.0 TO 2.5	7.2	9.5	9.8
2.5 TO 3.0	11.0	17.8	17.4
3.0 TO 3.5	0.7	0.3	2.4
3.5 TO 4.0	4.3	4.2	6.2
4.0 TO 4.5	2.4	3.2	3.4
4.5 TO 5.0	0.1	0.0	0.3
5.0 TO 5.5	2.4	6.5	9.4
5.5 TO 6.0	0.1	0.3	1.5
6.0 TO 6.5	0.5	1.5	2.5
6.5 TO 7.0	0.0	0.4	0.4
7.0 TO 7.5	0.0	0.1	0.5
7.5 TO 8.0	1.3	3.0	5.2
8.0 TO 8.5	0.0	0.3	0.0
8.5 TO 9.0	0.3	0.5	0.7
9.0 TO 9.5	0.0	0.3	0.3
9.5 TO 10.0	1.7	2.9	3.4
ENTRIES	752	758	754

Table 14. Frequency distributions of path loss and fading for L-band

DIFFERENCE	% HIGH-LOW	% HIGH-MID	% MID-LOW
-20.0 TO -18.0	0.0	0.0	0.0
-18.0 TO -16.0	0.0	0.0	0.0
-16.0 TO -14.0	0.0	0.0	0.0
-14.0 TO -12.0	0.0	0.0	0.0
-12.0 TO -10.0	0.0	0.0	0.0
-10.0 TO -8.0	0.0	0.1	0.0
-8.0 TO -6.0	0.0	0.1	0.1
-6.0 TO -4.0	0.1	0.0	0.4
-4.0 TO -2.0	0.0	0.3	0.3
-2.0 TO 0.0	0.3	0.1	1.7
0.0 TO 2.0	0.1	1.9	2.9
2.0 TO 4.0	1.2	9.6	18.2
4.0 TO 6.0	1.2	25.1	45.4
6.0 TO 8.0	6.1	51.3	25.4
8.0 TO 10.0	15.1	7.9	3.7
10.0 TO 12.0	36.5	2.6	0.8
12.0 TO 14.0	26.7	0.9	0.5
14.0 TO 16.0	7.5	0.0	0.4
16.0 TO 18.0	1.9	0.0	0.1
18.0 TO 20.0	1.1	0.0	0.0
ENTRIES	729	737	749

Table 15. Frequency distributions of path loss differences between antennas for L-band

S BAND, NAXOS TO MYKONOS, GREECE APRIL 1972

HIGH-LOW	MID-LOW	HIGH-MID
1.6 % > 20.0 DB	0.0 % > 20.0 DB	0.1 % > 20.0 DB
7.2 % > 15.0 DB	0.7 % > 15.0 DB	1.2 % > 15.0 DB
65.2 % > 10.0 DB	2.7 % > 10.0 DB	4.1 % > 10.0 DB
87.4 % > 6.0 DB	31.8 % > 6.0 DB	45.2 % > 6.0 DB
91.9 % > 3.0 DB	83.9 % > 3.0 DB	86.8 % > 3.0 DB
95.6 % > 0.0 DB	93.5 % > 0.0 DB	95.7 % > 0.0 DB
97.7 % > -3.0 DB	97.2 % > -3.0 DB	97.5 % > -3.0 DB
98.7 % > -6.0 DB	99.0 % > -6.0 DB	98.6 % > -6.0 DB
99.6 % > -10.0 DB	99.7 % > -10.0 DB	99.0 % > -10.0 DB
100.0 % > -15.0 DB	100.0 % > -15.0 DB	99.9 % > -15.0 DB
100.0 % > -20.0 DB	100.0 % > -20.0 DB	99.9 % > -20.0 DB
TOTAL ENTRIES = 706	TOTAL ENTRIES = 707	TOTAL ENTRIES = 691

FADING HIGH	FADING MIDDLE	FADING LOW
0.0 % > 20.0 DB	0.0 % > 20.0 DB	0.0 % > 20.0 DB
0.0 % > 15.0 DB	0.0 % > 15.0 DB	0.0 % > 15.0 DB
0.1 % > 10.0 DB	0.4 % > 10.0 DB	0.4 % > 10.0 DB
0.3 % > 8.0 DB	0.8 % > 8.0 DB	1.1 % > 8.0 DB
0.9 % > 6.0 DB	1.6 % > 6.0 DB	3.1 % > 6.0 DB
2.7 % > 5.0 DB	5.2 % > 5.0 DB	8.0 % > 5.0 DB
5.1 % > 4.0 DB	9.3 % > 4.0 DB	15.3 % > 4.0 DB
14.9 % > 3.0 DB	19.8 % > 3.0 DB	27.1 % > 3.0 DB
34.6 % > 2.0 DB	45.1 % > 2.0 DB	59.3 % > 2.0 DB
79.9 % > 1.0 DB	83.5 % > 1.0 DB	90.6 % > 1.0 DB
TOTAL ENTRIES = 786	TOTAL ENTRIES = 774	TOTAL ENTRIES = 796

Table 16. Statistical presentation for S-band

PATH LOSS	% HIGH	% MID	% LOW
120.0 TO 125.0	15.6	9.7	8.2
125.0 TO 130.0	5.0	4.3	3.0
130.0 TO 135.0	5.3	4.7	4.3
135.0 TO 140.0	14.5	4.7	4.8
140.0 TO 145.0	24.0	12.7	5.4
145.0 TO 150.0	26.7	25.5	10.9
150.0 TO 155.0	4.1	29.5	23.4
155.0 TO 160.0	4.6	6.1	22.4
160.0 TO 165.0	0.0	3.1	13.4
165.0 TO 170.0	0.0	0.0	4.3
170.0 TO 175.0	0.1	0.0	0.0
175.0 TO 180.0	0.0	0.0	0.0
180.0 TO 185.0	0.0	0.0	0.0
185.0 TO 190.0	0.0	0.0	0.0
190.0 TO 195.0	0.0	0.0	0.0
195.0 TO 200.0	0.0	0.0	0.0
200.0 TO 205.0	0.0	0.0	0.0
205.0 TO 210.0	0.0	0.0	0.0
210.0 TO 215.0	0.0	0.0	0.0
215.0 TO 220.0	0.0	0.0	0.0
ENTRIES	786	774	796

FADING	% HIGH	% MID	% LOW
0.0 TO 0.5	0.0	0.0	0.0
0.5 TO 1.0	19.8	16.5	8.9
1.0 TO 1.5	33.7	22.4	14.2
1.5 TO 2.0	8.8	8.3	10.2
2.0 TO 2.5	13.5	27.5	26.1
2.5 TO 3.0	8.1	5.0	13.1
3.0 TO 3.5	3.8	3.2	3.4
3.5 TO 4.0	4.5	3.4	3.8
4.0 TO 4.5	3.3	6.2	8.4
4.5 TO 5.0	0.5	0.9	1.5
5.0 TO 5.5	1.7	2.3	3.3
5.5 TO 6.0	0.8	1.9	3.6
6.0 TO 6.5	1.0	0.8	0.8
6.5 TO 7.0	0.0	0.1	0.4
7.0 TO 7.5	0.3	0.3	0.5
7.5 TO 8.0	0.0	0.3	0.8
8.0 TO 8.5	0.1	0.1	0.0
8.5 TO 9.0	0.0	0.3	0.1
9.0 TO 9.5	0.0	0.1	0.5
9.5 TO 10.0	0.1	0.4	0.5
ENTRIES	786	774	796

Table 17. Frequency distributions of path loss and fading for S-band

DIFFERENCE	% HIGH-LOW	% HIGH-MID	% MID-LOW
-20.0 TO -18.0	0.0	0.1	0.0
-18.0 TO -16.0	0.0	0.0	0.0
-16.0 TO -14.0	0.1	0.1	0.0
-14.0 TO -12.0	0.0	0.1	0.0
-12.0 TO -10.0	0.3	0.6	0.3
-10.0 TO -8.0	0.6	0.1	0.4
-8.0 TO -6.0	0.3	0.3	0.3
-6.0 TO -4.0	0.3	0.6	0.8
-4.0 TO -2.0	1.1	0.7	1.1
-2.0 TO 0.0	1.6	1.4	2.7
0.0 TO 2.0	1.8	4.2	4.5
2.0 TO 4.0	3.7	12.0	13.4
4.0 TO 6.0	2.4	29.7	38.0
6.0 TO 8.0	6.7	38.6	29.7
8.0 TO 10.0	14.7	7.1	5.1
10.0 TO 12.0	27.2	1.9	2.3
12.0 TO 14.0	25.8	1.2	0.3
14.0 TO 16.0	8.5	0.7	0.4
16.0 TO 18.0	2.3	0.3	0.1
18.0 TO 20.0	2.7	0.1	0.4
ENTRIES	706	691	707

Table 18. Frequency distributions of path loss differences between antennas for S-band

X BAND, NAXOS TO MYKONOS, GREECE APRIL 1972

HIGH-LOW

0.5 %	>	20.0 DB
3.4 %	>	15.0 DB
13.2 %	>	10.0 DB
36.5 %	>	6.0 DB
57.2 %	>	3.0 DB
72.1 %	>	0.0 DB
79.5 %	>	-3.0 DB
85.7 %	>	-6.0 DB
91.1 %	>	-10.0 DB
96.4 %	>	-15.0 DB
98.6 %	>	-20.0 DB

TOTAL ENTRIES = 1058

MID-LOW

0.0 %	>	20.0 DB
0.2 %	>	15.0 DB
1.0 %	>	10.0 DB
3.7 %	>	6.0 DB
9.1 %	>	3.0 DB
37.4 %	>	0.0 DB
73.6 %	>	-3.0 DB
86.9 %	>	-6.0 DB
94.9 %	>	-10.0 DB
98.6 %	>	-15.0 DB
99.7 %	>	-20.0 DB

TOTAL ENTRIES = 1063

HIGH-MID

0.4 %	>	20.0 DB
2.1 %	>	15.0 DB
12.9 %	>	10.0 DB
38.9 %	>	6.0 DB
64.1 %	>	3.0 DB
80.6 %	>	0.0 DB
87.5 %	>	-3.0 DB
92.8 %	>	-6.0 DB
96.6 %	>	-10.0 DB
98.6 %	>	-15.0 DB
99.6 %	>	-20.0 DB

TOTAL ENTRIES = 1065

FADING HIGH

0.1 %	>	20.0 DB
1.7 %	>	15.0 DB
3.2 %	>	10.0 DB
7.2 %	>	8.0 DB
12.5 %	>	6.0 DB
14.1 %	>	5.0 DB
20.2 %	>	4.0 DB
27.9 %	>	3.0 DB
41.5 %	>	2.0 DB
95.2 %	>	1.0 DB

TOTAL ENTRIES = 1069

FADING MIDDLE

0.0 %	>	20.0 DB
0.2 %	>	15.0 DB
1.8 %	>	10.0 DB
4.1 %	>	8.0 DB
7.3 %	>	6.0 DB
10.4 %	>	5.0 DB
16.6 %	>	4.0 DB
26.3 %	>	3.0 DB
46.8 %	>	2.0 DB
88.0 %	>	1.0 DB

TOTAL ENTRIES = 1071

FADING LOW

0.0 %	>	20.0 DB
0.4 %	>	15.0 DB
1.1 %	>	10.0 DB
2.3 %	>	8.0 DB
6.2 %	>	6.0 DB
7.5 %	>	5.0 DB
15.8 %	>	4.0 DB
32.7 %	>	3.0 DB
47.7 %	>	2.0 DB
90.7 %	>	1.0 DB

TOTAL ENTRIES = 1065

Table 19. Statistical presentation for X-band

PATH LOSS	% HIGH	% MID	% LOW
120.0 TO 125.0	3.9	3.6	14.4
125.0 TO 130.0	18.7	15.0	11.5
130.0 TO 135.0	23.7	15.6	11.7
135.0 TO 140.0	17.1	15.2	13.1
140.0 TO 145.0	16.5	14.0	11.4
145.0 TO 150.0	6.9	11.1	10.7
150.0 TO 155.0	7.6	8.5	10.0
155.0 TO 160.0	3.2	7.5	10.4
160.0 TO 165.0	2.1	4.4	2.8
165.0 TO 170.0	0.3	3.6	3.1
170.0 TO 175.0	0.0	1.0	0.6
175.0 TO 180.0	0.0	0.2	0.3
180.0 TO 185.0	0.0	0.0	0.0
185.0 TO 190.0	0.0	0.0	0.0
190.0 TO 195.0	0.0	0.0	0.0
195.0 TO 200.0	0.0	0.0	0.0
200.0 TO 205.0	0.0	0.0	0.0
205.0 TO 210.0	0.0	0.0	0.0
210.0 TO 215.0	0.0	0.0	0.0
215.0 TO 220.0	0.0	0.0	0.0
ENTRIES	1069	1071	1065

FADING	% HIGH	% MID	% LOW
0.0 TO 0.5	0.5	0.2	0.2
0.5 TO 1.0	14.3	10.7	9.1
1.0 TO 1.5	14.3	13.6	12.5
1.5 TO 2.0	29.2	27.9	30.2
2.0 TO 2.5	6.5	7.3	5.4
2.5 TO 3.0	7.3	11.7	9.9
3.0 TO 3.5	6.1	9.5	15.4
3.5 TO 4.0	1.6	2.1	1.3
4.0 TO 4.5	2.1	2.7	3.7
4.5 TO 5.0	1.1	1.1	2.5
5.0 TO 5.5	3.1	2.9	2.4
5.5 TO 6.0	1.5	2.9	1.1
6.0 TO 6.5	0.3	0.7	0.6
6.5 TO 7.0	1.1	0.7	1.7
7.0 TO 7.5	2.2	1.1	1.1
7.5 TO 8.0	0.7	0.6	0.5
8.0 TO 8.5	1.7	1.5	1.1
8.5 TO 9.0	0.2	0.0	0.1
9.0 TO 9.5	1.8	0.6	0.0
9.5 TO 10.0	3.9	2.1	1.1
ENTRIES	1069	1071	1065

Table 10. Frequency distributions of path loss and fading for X-band

DIFFERENCE	% HIGH-LOW	% HIGH-MID	% MID-LOW
-20.0 TO -18.0	2.1	0.8	0.7
-18.0 TO -16.0	0.9	0.2	0.3
-16.0 TO -14.0	1.7	0.7	0.8
-14.0 TO -12.0	1.4	0.6	0.7
-12.0 TO -10.0	2.6	1.1	2.7
-10.0 TO -8.0	2.7	1.2	2.5
-8.0 TO -6.0	2.6	2.7	5.0
-6.0 TO -4.0	3.5	3.4	7.5
-4.0 TO -2.0	4.2	3.8	12.5
-2.0 TO 0.0	5.7	5.0	28.9
0.0 TO 2.0	7.8	5.0	21.1
2.0 TO 4.0	13.0	17.7	10.4
4.0 TO 6.0	14.8	18.7	3.0
6.0 TO 8.0	12.8	11.9	2.1
8.0 TO 10.0	10.3	14.3	0.6
10.0 TO 12.0	5.3	5.4	0.6
12.0 TO 14.0	3.5	4.2	0.3
14.0 TO 16.0	1.6	2.0	0.1
16.0 TO 18.0	1.5	0.7	0.1
18.0 TO 20.0	1.3	0.7	0.0
ENTRIES	1058	1055	1063

DET RANGE	% HIGH	% MID	% LOW
0.0 TO 10.0	0.0	0.0	0.0
10.0 TO 20.0	2.4	7.7	5.5
20.0 TO 30.0	10.9	17.9	20.7
30.0 TO 40.0	5.0	9.2	3.4
40.0 TO 50.0	7.0	4.8	4.4
50.0 TO 60.0	2.7	4.3	2.8
60.0 TO 70.0	4.2	2.1	2.5
70.0 TO 80.0	4.7	4.5	3.8
80.0 TO 90.0	2.1	1.8	2.2
90.0 TO 100.0	2.6	3.4	3.1
100.0 TO 110.0	4.3	3.4	2.9
110.0 TO 120.0	4.3	3.8	2.6
120.0 TO 130.0	4.5	4.3	3.4
130.0 TO 140.0	4.3	3.2	1.8
140.0 TO 150.0	7.4	2.2	1.7
150.0 TO 160.0	3.2	4.2	3.2
160.0 TO 170.0	5.7	3.0	2.2
170.0 TO 180.0	4.5	3.7	2.4
180.0 TO 190.0	4.1	4.0	2.3
190.0 TO 200.0	16.0	12.7	22.3
ENTRIES	1057	1057	1057

Table 21. Frequency distributions of path loss difference and detection range for X-band

X BAND, GREECE APRIL 1972

DET RANGE	%> HIGH	%> MID	%> LOW
10.0	100.0	100.0	100.0
20.0	97.6	92.3	93.4
30.0	86.8	74.5	72.7
40.0	81.7	65.3	64.2
50.0	74.7	60.5	59.9
60.0	72.0	56.2	57.0
70.0	67.3	54.1	54.5
80.0	63.1	49.6	50.7
90.0	61.0	47.8	48.5
100.0	58.5	44.4	45.4
110.0	54.2	41.0	42.5
120.0	50.0	37.2	39.8
130.0	45.4	32.9	36.4
140.0	40.9	29.7	34.6
150.0	33.5	27.5	32.9
160.0	30.3	23.4	29.7
170.0	24.6	20.3	27.5
180.0	20.1	16.7	25.2
190.0	16.0	12.7	22.3
200.0	-0.0	-0.0	-0.0
ENTRIES	1057	1057	1057

DET RANGE DIFF	% HIGH-LOW	% HIGH-MID	% MID-LOW
-50.0 TO -45.0	15.7	8.3	15.9
-45.0 TO -40.0	1.2	1.4	1.5
-40.0 TO -35.0	1.7	0.7	2.4
-35.0 TO -30.0	1.0	0.7	1.8
-30.0 TO -25.0	0.9	0.9	2.0
-25.0 TO -20.0	0.9	1.3	3.1
-20.0 TO -15.0	1.0	1.5	2.5
-15.0 TO -10.0	0.7	1.0	4.0
-10.0 TO -5.0	2.1	1.2	4.5
-5.0 TO 0.0	2.2	2.0	24.1
0.0 TO 5.0	13.8	12.2	17.9
5.0 TO 10.0	4.1	5.5	4.7
10.0 TO 15.0	4.7	5.1	3.4
15.0 TO 20.0	5.9	9.7	2.8
20.0 TO 25.0	5.1	3.3	2.2
25.0 TO 30.0	5.0	6.1	1.0
30.0 TO 35.0	4.7	7.1	1.2
35.0 TO 40.0	2.6	3.4	0.6
40.0 TO 45.0	4.1	2.3	0.8
45.0 TO 50.0	22.6	25.6	3.6
ENTRIES	1057	1057	1057

Table [illegible]. Cumulative distribution of detection range and frequency distribution of detection range differences for X-band

L BAND, NAXOS TO MYKONOS, GREECE AUGUST 1972

HIGH-LOW	MID-LOW	HIGH-MID
0.0 % > 20.0 DB	0.0 % > 20.0 DB	0.0 % > 20.0 DB
0.6 % > 15.0 DB	0.0 % > 15.0 DB	0.0 % > 15.0 DB
30.5 % > 10.0 DB	0.7 % > 10.0 DB	0.9 % > 10.0 DB
70.9 % > 6.0 DB	8.9 % > 6.0 DB	11.9 % > 6.0 DB
96.8 % > 3.0 DB	67.9 % > 3.0 DB	68.1 % > 3.0 DB
99.0 % > 0.0 DB	97.0 % > 0.0 DB	96.4 % > 0.0 DB
99.7 % > -3.0 DB	99.4 % > -3.0 DB	98.8 % > -3.0 DB
100.0 % > -6.0 DB	99.7 % > -6.0 DB	99.9 % > -6.0 DB
100.0 % > -10.0 DB	100.0 % > -10.0 DB	100.0 % > -10.0 DB
100.0 % > -15.0 DB	100.0 % > -15.0 DB	100.0 % > -15.0 DB
100.0 % > -20.0 DB	100.0 % > -20.0 DB	100.0 % > -20.0 DB
TOTAL ENTRIES = 968	TOTAL ENTRIES = 971	TOTAL ENTRIES = 970

FADING HIGH	FADING MIDDLE	FADING LOW
0.0 % > 20.0 DB	0.0 % > 20.0 DB	0.0 % > 20.0 DB
0.0 % > 15.0 DB	0.0 % > 15.0 DB	0.0 % > 15.0 DB
0.1 % > 10.0 DB	0.4 % > 10.0 DB	0.6 % > 10.0 DB
0.7 % > 8.0 DB	1.0 % > 8.0 DB	1.5 % > 8.0 DB
4.0 % > 6.0 DB	4.8 % > 6.0 DB	4.6 % > 6.0 DB
5.1 % > 5.0 DB	5.2 % > 5.0 DB	5.3 % > 5.0 DB
10.6 % > 4.0 DB	9.5 % > 4.0 DB	15.0 % > 4.0 DB
20.9 % > 3.0 DB	24.2 % > 3.0 DB	33.9 % > 3.0 DB
37.0 % > 2.0 DB	41.8 % > 2.0 DB	54.4 % > 2.0 DB
63.9 % > 1.0 DB	90.1 % > 1.0 DB	93.4 % > 1.0 DB
TOTAL ENTRIES - 975	TOTAL ENTRIES = 975	TOTAL ENTRIES = 974

Table 23. Statistical presentation for L-band

L BAND, GREECE AUGUST 1972

PATH LOSS	% HIGH	% MID	% LOW
120.0 TO 125.0	5.0	2.1	0.8
125.0 TO 130.0	4.3	4.0	2.3
130.0 TO 135.0	4.9	4.9	3.3
135.0 TO 140.0	6.1	4.2	4.4
140.0 TO 145.0	28.8	7.1	5.4
145.0 TO 150.0	36.5	26.1	4.7
150.0 TO 155.0	14.1	49.4	35.1
155.0 TO 160.0	0.3	1.9	42.9
160.0 TO 165.0	0.0	0.3	1.0
165.0 TO 170.0	0.0	0.0	0.0
170.0 TO 175.0	0.0	0.0	0.0
175.0 TO 180.0	0.0	0.0	0.0
180.0 TO 185.0	0.0	0.0	0.0
185.0 TO 190.0	0.0	0.0	0.0
190.0 TO 195.0	0.0	0.0	0.0
195.0 TO 200.0	0.0	0.0	0.0
200.0 TO 205.0	0.0	0.0	0.0
205.0 TO 210.0	0.0	0.0	0.0
210.0 TO 215.0	0.0	0.0	0.0
215.0 TO 220.0	0.0	0.0	0.0
ENTRIES	975	975	974

FADING	% HIGH	% MID	% LOW
0.0 TO 0.5	1.1	0.2	0.0
0.5 TO 1.0	15.0	9.6	6.6
1.0 TO 1.5	18.2	21.6	13.0
1.5 TO 2.0	28.6	26.7	26.0
2.0 TO 2.5	6.1	3.9	5.5
2.5 TO 3.0	10.1	13.1	14.1
3.0 TO 3.5	5.5	9.2	10.8
3.5 TO 4.0	4.9	6.1	9.0
4.0 TO 4.5	1.3	0.8	3.3
4.5 TO 5.0	0.3	0.6	0.4
5.0 TO 5.5	3.8	2.9	6.0
5.5 TO 6.0	1.1	0.4	0.7
6.0 TO 6.5	2.5	3.0	2.1
6.5 TO 7.0	0.3	0.0	0.3
7.0 TO 7.5	0.0	0.0	0.0
7.5 TO 8.0	0.5	0.8	0.7
8.0 TO 8.5	0.1	0.0	0.0
8.5 TO 9.0	0.3	0.5	0.3
9.0 TO 9.5	0.0	0.1	0.0
9.5 TO 10.0	0.3	0.4	1.2
ENTRIES	975	975	974

Table 24. Frequency distributions of path loss and fading for L-band

L BAND, GREECE AUGUST 1972

DIFFERENCE	% HIGH-LOW	% HIGH-MID	% MID-LOW
-20.0 TO -18.0	0.0	0.0	0.0
-18.0 TO -16.0	0.0	0.0	0.0
-16.0 TO -14.0	0.0	0.0	0.0
-14.0 TO -12.0	0.0	0.0	0.0
-12.0 TO -10.0	0.0	0.0	0.0
-10.0 TO -8.0	0.0	0.1	0.1
-8.0 TO -6.0	0.0	0.0	0.2
-6.0 TO -4.0	0.1	0.6	0.1
-4.0 TO -2.0	0.3	0.6	0.3
-2.0 TO 0.0	0.6	1.3	2.3
0.0 TO 2.0	1.5	5.4	3.3
2.0 TO 4.0	1.8	38.0	39.1
4.0 TO 6.0	24.5	42.0	37.3
6.0 TO 8.0	16.8	10.1	14.3
8.0 TO 10.0	23.6	0.8	1.8
10.0 TO 12.0	27.0	0.7	0.5
12.0 TO 14.0	2.7	0.3	0.2
14.0 TO 16.0	0.7	0.0	0.0
16.0 TO 18.0	0.3	0.0	0.0
18.0 TO 20.0	0.1	0.0	0.0
ENTRIES	968	970	971

Table 25. Frequency distributions of path loss differences between antennas for L-band

S BAND, NAXOS TO MYKONOS, GREECE   AUGUST 1972

HIGH-LOW	MID-LOW	HIGH-MID
0.3 % > 20.0 DB	0.2 % > 20.0 DB	0.2 % > 20.0 DB
2.2 % > 15.0 DB	0.2 % > 15.0 DB	0.6 % > 15.0 DB
42.5 % > 10.0 DB	1.6 % > 10.0 DB	2.7 % > 10.0 DB
74.5 % > 6.0 DB	10.2 % > 6.0 DB	39.7 % > 6.0 DB
84.0 % > 3.0 DB	66.3 % > 3.0 DB	76.8 % > 3.0 DB
91.4 % > 0.0 DB	86.8 % > 0.0 DB	90.0 % > 0.0 DB
95.5 % > -3.0 DB	94.6 % > -3.0 DB	95.2 % > -3.0 DB
97.0 % > -6.0 DB	97.1 % > -6.0 DB	97.3 % > -6.0 DB
98.9 % > -10.0 DB	98.7 % > -10.0 DB	99.3 % > -10.0 DB
99.9 % > -15.0 DB	99.8 % > -15.0 DB	99.8 % > -15.0 DB
100.0 % > -20.0 DB	99.9 % > -20.0 DB	100.0 % > -20.0 DB
TOTAL ENTRIES = 1277	TOTAL ENTRIES = 1279	TOTAL ENTRIES = 1278

FADING HIGH	FADING MIDDLE	FADING LOW
0.0 % > 20.0 DB	0.0 % > 20.0 DB	0.0 % > 20.0 DB
0.1 % > 15.0 DB	0.0 % > 15.0 DB	0.2 % > 15.0 DB
0.1 % > 10.0 DB	0.2 % > 10.0 DB	0.5 % > 10.0 DB
0.3 % > 8.0 DB	0.3 % > 8.0 DB	0.8 % > 8.0 DB
0.5 % > 6.0 DB	0.8 % > 6.0 DB	1.2 % > 6.0 DB
0.9 % > 5.0 DB	1.3 % > 5.0 DB	2.0 % > 5.0 DB
1.6 % > 4.0 DB	3.1 % > 4.0 DB	5.6 % > 4.0 DB
5.5 % > 3.0 DB	8.0 % > 3.0 DB	11.6 % > 3.0 DB
23.6 % > 2.0 DB	33.2 % > 2.0 DB	48.6 % > 2.0 DB
35.7 % > 1.0 DB	66.0 % > 1.0 DB	92.3 % > 1.0 DB
TOTAL ENTRIES = 1279	TOTAL ENTRIES = 1261	TOTAL ENTRIES = 1281

Table 26. Statistical presentation for S-band

S BAND, GREECE AUGUST 1972

PATH LOSS	% HIGH	% MID	% LOW
120.0 TO 125.0	36.4	25.4	21.9
125.0 TO 130.0	19.1	12.5	9.9
130.0 TO 135.0	30.6	14.1	8.4
135.0 TO 140.0	10.5	29.7	13.7
140.0 TO 145.0	3.3	13.0	23.3
145.0 TO 150.0	0.2	4.0	12.0
150.0 TO 155.0	0.0	1.2	4.4
155.0 TO 160.0	0.0	0.0	1.1
160.0 TO 165.0	0.0	0.0	0.1
165.0 TO 170.0	0.0	0.0	0.1
170.0 TO 175.0	0.0	0.0	0.1
175.0 TO 180.0	0.0	0.0	0.0
180.0 TO 185.0	0.0	0.0	0.0
185.0 TO 190.0	0.0	0.0	0.0
190.0 TO 195.0	0.0	0.0	0.0
195.0 TO 200.0	0.0	0.0	0.0
200.0 TO 205.0	0.0	0.0	0.0
205.0 TO 210.0	0.0	0.0	0.0
210.0 TO 215.0	0.0	0.0	0.0
215.0 TO 220.0	0.0	0.0	0.0
ENTRIES	1279	1281	1281

FADING	% HIGH	% MID	% LOW
0.0 TO 0.5	0.2	0.0	0.1
0.5 TO 1.0	16.2	14.0	7.6
1.0 TO 1.5	45.7	39.7	31.3
1.5 TO 2.0	13.3	11.2	11.6
2.0 TO 2.5	10.3	16.4	26.5
2.5 TO 3.0	9.0	10.7	11.4
3.0 TO 3.5	1.8	2.9	4.4
3.5 TO 4.0	1.7	1.5	1.3
4.0 TO 4.5	0.6	1.9	3.6
4.5 TO 5.0	0.2	0.2	0.2
5.0 TO 5.5	0.0	0.2	0.1
5.5 TO 6.0	0.5	0.5	0.5
6.0 TO 6.5	0.0	0.1	0.2
6.5 TO 7.0	0.1	0.2	0.2
7.0 TO 7.5	0.1	0.2	0.2
7.5 TO 8.0	0.0	0.0	0.0
8.0 TO 8.5	0.1	0.2	0.2
8.5 TO 9.0	0.0	0.0	0.0
9.0 TO 9.5	0.1	0.0	0.0
9.5 TO 10.0	0.2	0.2	0.7
ENTRIES	1279	1281	1281

Table 27. Frequency distributions of path loss and fading for S-band

DIFFERENCE	% HIGH-LOW	% HIGH-MID	% MID-LOW
-20.0 TO -18.0	0.1	0.0	0.2
-18.0 TO -16.0	0.0	0.2	0.0
-16.0 TO -14.0	0.2	0.1	0.2
-14.0 TO -12.0	0.3	0.2	0.2
-12.0 TO -10.0	0.5	0.2	0.7
-10.0 TO -8.0	0.9	0.7	0.5
-8.0 TO -6.0	0.9	1.3	1.2
-6.0 TO -4.0	0.9	1.3	1.6
-4.0 TO -2.0	1.8	2.5	2.0
-2.0 TO 0.0	2.5	3.4	4.5
0.0 TO 2.0	4.9	6.3	10.2
2.0 TO 4.0	4.2	11.7	27.5
4.0 TO 6.0	7.7	31.7	39.4
6.0 TO 8.0	11.6	28.8	8.4
8.0 TO 10.0	20.5	9.0	1.8
10.0 TO 12.0	26.3	1.5	0.8
12.0 TO 14.0	11.7	0.5	0.5
14.0 TO 16.0	3.6	0.2	0.2
16.0 TO 18.0	0.6	0.1	0.0
18.0 TO 20.0	0.7	0.3	0.2
ENTRIES	1277	1278	1279

Table 28. Frequency distributions of path loss differences between antennas for S-band

X BAND, NAXOS TO MYKONOS, GREECE AUGUST 1972

HIGH-LOW

0.0	% >	20.0	DB
0.0	% >	15.0	DB
0.6	% >	10.0	DB
0.9	% >	6.0	DB
3.1	% >	3.0	DB
7.0	% >	0.0	DB
10.8	% >	-3.0	DB
19.2	% >	-6.0	DB
38.5	% >	-10.0	DB
63.9	% >	-15.0	DB
82.9	% >	-20.0	DB

TOTAL ENTRIES = 1278

MID-LOW

0.0	% >	20.0	DB
0.1	% >	15.0	DB
0.2	% >	10.0	DB
1.1	% >	6.0	DB
3.0	% >	3.0	DB
7.7	% >	0.0	DB
16.4	% >	-3.0	DB
31.2	% >	-6.0	DB
65.5	% >	-10.0	DB
92.0	% >	-15.0	DB
99.1	% >	-20.0	DB

TOTAL ENTRIES = 1281

HIGH-MID

0.0	% >	20.0	DB
0.0	% >	15.0	DB
0.5	% >	10.0	DB
3.4	% >	6.0	DB
8.9	% >	3.0	DB
23.0	% >	0.0	DB
42.4	% >	-3.0	DB
62.1	% >	-6.0	DB
83.9	% >	-10.0	DB
96.8	% >	-15.0	DB
99.1	% >	-20.0	DB

TOTAL ENTRIES = 1289

FADING HIGH

2.2	% >	20.0	DB
3.3	% >	15.0	DB
9.7	% >	10.0	DB
17.7	% >	8.0	DB
33.1	% >	6.0	DB
41.4	% >	5.0	DB
60.5	% >	4.0	DB
78.9	% >	3.0	DB
94.3	% >	2.0	DB
99.9	% >	1.0	DB

TOTAL ENTRIES = 1292

FADING MIDDLE

0.2	% >	20.0	DB
0.2	% >	15.0	DB
2.8	% >	10.0	DB
7.8	% >	8.0	DB
20.0	% >	6.0	DB
29.8	% >	5.0	DB
50.1	% >	4.0	DB
71.6	% >	3.0	DB
94.1	% >	2.0	DB
100.0	% >	1.0	DB

TOTAL ENTRIES = 1294

FADING LOW

0.1	% >	20.0	DB
0.4	% >	15.0	DB
3.7	% >	10.0	DB
6.3	% >	8.0	DB
15.4	% >	6.0	DB
19.8	% >	5.0	DB
38.7	% >	4.0	DB
68.0	% >	3.0	DB
87.8	% >	2.0	DB
99.6	% >	1.0	DB

TOTAL ENTRIES = 1282

Table 29. Statistical presentation for X-band

PATH LOSS	% HIGH	% MID	% LOW
120.0 TO 125.0	0.2	0.2	6.5
125.0 TO 130.0	2.2	3.1	26.4
130.0 TO 135.0	9.8	14.8	32.7
135.0 TO 140.0	14.0	23.9	22.4
140.0 TO 145.0	18.7	27.1	10.2
145.0 TO 150.0	24.0	24.1	0.9
150.0 TO 155.0	23.8	5.8	0.5
155.0 TO 160.0	5.2	0.9	0.2
160.0 TO 165.0	1.2	0.1	0.1
165.0 TO 170.0	0.9	0.0	0.1
170.0 TO 175.0	0.1	0.0	0.0
175.0 TO 180.0	0.1	0.0	0.0
180.0 TO 185.0	0.0	0.0	0.0
185.0 TO 190.0	0.0	0.0	0.0
190.0 TO 195.0	0.0	0.0	0.0
195.0 TO 200.0	0.0	0.0	0.0
200.0 TO 205.0	0.0	0.0	0.0
205.0 TO 210.0	0.0	0.0	0.0
210.0 TO 215.0	0.0	0.0	0.0
215.0 TO 220.0	0.0	0.0	0.0
ENTRIES	1292	1294	1282

FADING	% HIGH	% MID	% LOW
0.0 TO 0.5	0.0	0.0	0.0
0.5 TO 1.0	0.1	0.0	0.4
1.0 TO 1.5	1.0	2.6	4.7
1.5 TO 2.0	3.9	2.0	4.6
2.0 TO 2.5	4.2	3.4	5.3
2.5 TO 3.0	11.8	19.9	17.0
3.0 TO 3.5	10.1	10.2	20.9
3.5 TO 4.0	6.0	7.3	4.7
4.0 TO 4.5	11.7	14.1	9.6
4.5 TO 5.0	2.8	3.6	7.2
5.0 TO 5.5	8.9	10.2	7.7
5.5 TO 6.0	6.2	5.9	2.5
6.0 TO 6.5	2.7	3.4	2.7
6.5 TO 7.0	3.1	2.9	3.4
7.0 TO 7.5	6.8	3.5	0.4
7.5 TO 8.0	2.7	1.9	2.5
8.0 TO 8.5	2.8	3.4	1.2
8.5 TO 9.0	2.6	1.0	0.2
9.0 TO 9.5	1.7	0.6	0.3
9.5 TO 10.0	10.8	3.6	4.8
ENTRIES	1292	1294	1282

Table 30. Frequency distributions of path loss and fading for X-band

DIFFERENCE	% HIGH-LOW	% HIGH-MID	% MID-LOW
-20.0 TO -18.0	25.0	1.1	2.1
-18.0 TO -16.0	6.7	1.5	3.1
-16.0 TO -14.0	8.0	1.8	5.5
-14.0 TO -12.0	10.6	4.2	10.1
-12.0 TO -10.0	10.8	7.3	13.2
-10.0 TO -8.0	11.2	9.0	19.7
-8.0 TO -6.0	7.5	12.0	14.5
-6.0 TO -4.0	7.0	11.9	11.3
-4.0 TO -2.0	3.9	15.4	6.8
-2.0 TO 0.0	2.2	12.2	5.7
0.0 TO 2.0	3.2	9.0	3.5
2.0 TO 4.0	1.5	7.7	2.7
4.0 TO 6.0	1.5	3.5	0.7
6.0 TO 8.0	0.1	2.1	0.7
8.0 TO 10.0	0.2	0.9	0.2
10.0 TO 12.0	0.4	0.3	0.1
12.0 TO 14.0	0.2	0.2	0.0
14.0 TO 16.0	0.1	0.0	0.0
16.0 TO 18.0	0.0	0.0	0.0
18.0 TO 20.0	0.0	0.0	0.1
ENTRIES	1278	1289	1281

DET RANGE	% HIGH	% MID	% LOW
0.0 TO 10.0	0.0	0.0	0.0
10.0 TO 20.0	2.2	0.1	0.2
20.0 TO 30.0	23.3	6.5	0.8
30.0 TO 40.0	20.6	16.3	0.7
40.0 TO 50.0	9.5	13.5	1.9
50.0 TO 60.0	3.3	8.8	2.9
60.0 TO 70.0	4.3	6.1	3.1
70.0 TO 80.0	3.8	4.8	2.3
80.0 TO 90.0	4.4	4.9	4.2
90.0 TO 100.0	3.4	4.2	4.4
100.0 TO 110.0	2.1	5.4	5.2
110.0 TO 120.0	3.3	5.6	4.9
120.0 TO 130.0	2.3	6.1	5.7
130.0 TO 140.0	2.4	5.2	5.5
140.0 TO 150.0	2.7	3.8	9.9
150.0 TO 160.0	2.0	2.4	6.1
160.0 TO 170.0	0.7	2.0	5.5
170.0 TO 180.0	2.0	1.2	7.0
180.0 TO 190.0	0.5	0.9	5.4
190.0 TO 200.0	1.1	1.9	23.4
ENTRIES	1277	1277	1277

Table 31. Frequency distributions of path loss difference and detection range for X-band

X BAND, GREECE AUGUST 1972

DET RANGE	%> HIGH	%> MID	%> LOW
10.0	100.0	100.0	100.0
20.0	97.8	99.9	99.8
30.0	69.0	93.3	99.1
40.0	48.4	77.1	98.4
50.0	38.9	63.6	96.5
60.0	35.1	54.7	93.6
70.0	30.3	48.6	90.4
80.0	27.0	43.9	88.2
90.0	22.6	38.9	83.9
100.0	19.2	34.7	79.6
110.0	17.1	29.3	74.4
120.0	13.8	23.6	69.5
130.0	11.5	17.5	62.8
140.0	9.1	12.3	57.3
150.0	6.3	8.5	47.4
160.0	4.3	6.0	41.3
170.0	3.6	4.0	35.8
180.0	1.6	2.8	29.8
190.0	1.1	1.9	23.4
200.0	-0.0	-0.0	-0.0
ENTRIES	1277	1277	1277

DET RANGE DIFF	% HIGH-LOW	% HIGH-MID	% MID-LOW
-50.0 TO -45.0	77.3	20.8	70.9
-45.0 TO -40.0	2.7	3.1	2.8
-40.0 TO -35.0	2.4	3.6	3.2
-35.0 TO -30.0	2.2	4.2	2.0
-30.0 TO -25.0	2.0	4.7	3.1
-25.0 TO -20.0	1.8	6.9	2.4
-20.0 TO -15.0	1.6	6.9	2.7
-15.0 TO -10.0	1.1	9.6	1.8
-10.0 TO -5.0	0.6	9.2	1.4
-5.0 TO 0.0	0.6	7.7	1.6
0.0 TO 5.0	1.6	5.6	1.6
5.0 TO 10.0	1.3	4.0	1.5
10.0 TO 15.0	0.5	2.4	0.9
15.0 TO 20.0	0.5	3.3	0.6
20.0 TO 25.0	0.8	0.6	0.6
25.0 TO 30.0	0.2	1.4	0.4
30.0 TO 35.0	0.3	1.3	0.6
35.0 TO 40.0	0.2	1.2	0.2
40.0 TO 45.0	0.4	0.9	0.2
45.0 TO 50.0	0.9	2.7	1.2
ENTRIES	1277	1277	1277

Table 32. Cumulative distribution of detection range and frequency distribution of detection range differences for X-band

KU BAND, NAXOS TO MYKONOS, GREECE AUGUST 1972

HIGH-LOW		MID-LOW		HIGH-MID	
0.0 % >	20.0 DB	0.0 % >	20.0 DB	0.0 % >	20.0 DB
0.3 % >	15.0 DB	0.8 % >	15.0 DB	0.0 % >	15.0 DB
1.4 % >	10.0 DB	6.3 % >	10.0 DB	0.5 % >	10.0 DB
5.6 % >	6.0 DB	19.4 % >	6.0 DB	4.4 % >	6.0 DB
13.6 % >	3.0 DB	33.8 % >	3.0 DB	11.8 % >	3.0 DB
28.8 % >	0.0 DB	47.7 % >	0.0 DB	25.7 % >	0.0 DB
49.1 % >	-3.0 DB	66.1 % >	-3.0 DB	44.5 % >	-3.0 DB
67.7 % >	-6.0 DB	80.2 % >	-6.0 DB	67.4 % >	-6.0 DB
84.[illegible] % >	-10.0 DB	91.4 % >	-10.0 DB	90.4 % >	-10.0 DB
94.9 % >	-15.0 DB	98.0 % >	-15.0 DB	99.1 % >	-15.0 DB
98.7 % >	-20.0 DB	99.9 % >	-20.0 DB	100.0 % >	-20.0 DB
TOTAL ENTRIES = 770		TOTAL ENTRIES = 767		TOTAL ENTRIES = 771	

FADING HIGH		FADING MIDDLE		FADING LOW	
0.4 % >	20.0 DB	0.6 % >	20.0 DB	0.4 % >	20.0 DB
[illegible].8 % >	15.0 DB	10.5 % >	15.0 DB	9.3 % >	15.0 DB
35.0 % >	10.0 DB	39.0 % >	10.0 DB	40.7 % >	10.0 DB
63.2 % >	8.0 DB	66.8 % >	8.0 DB	64.0 % >	8.0 DB
89.[illegible] % >	6.0 DB	86.9 % >	6.0 DB	83.9 % >	6.0 DB
94.7 % >	5.0 DB	92.0 % >	5.0 DB	88.1 % >	5.0 DB
99.[illegible] % >	4.0 DB	97.4 % >	4.0 DB	94.0 % >	4.0 DB
100.0 % >	3.0 DB	98.6 % >	3.0 DB	98.4 % >	3.0 DB
100.0 % >	2.0 DB	100.0 % >	2.0 DB	99.7 % >	2.0 DB
100.0 % >	1.0 DB	100.0 % >	1.0 DB	100.0 % >	1.0 DB
TOTAL ENTRIES = 77[illegible]		TOTAL ENTRIES = 772		TOTAL ENTRIES = 772	

Table 33. Statistical presentation Ku-band

KU BAND, GREECE AUGUST 1972

PATH LOSS	% HIGH	% MID	% LOW
120.0 TO 125.0	0.0	0.0	0.0
125.0 TO 130.0	0.0	0.0	0.0
130.0 TO 135.0	0.4	1.2	0.5
135.0 TO 140.0	1.8	10.1	5.7
140.0 TO 145.0	9.5	22.8	16.1
145.0 TO 150.0	19.6	13.0	15.8
150.0 TO 155.0	15.6	7.1	14.2
155.0 TO 160.0	12.9	10.4	18.3
160.0 TO 165.0	14.5	11.5	17.1
165.0 TO 170.0	12.4	14.4	8.9
170.0 TO 175.0	9.8	7.1	2.8
175.0 TO 180.0	2.1	1.7	0.4
180.0 TO 185.0	1.3	0.3	0.0
185.0 TO 190.0	0.1	0.5	0.1
190.0 TO 195.0	0.1	0.0	0.0
195.0 TO 200.0	0.0	0.0	0.0
200.0 TO 205.0	0.0	0.0	0.0
205.0 TO 210.0	0.0	0.0	0.0
210.0 TO 215.0	0.0	0.0	0.0
215.0 TO 220.0	0.0	0.0	0.0
ENTRIES	777	772	772

FADING	% HIGH	% MID	% LOW
0.0 TO 0.5	0.0	0.0	0.0
0.5 TO 1.0	0.0	0.0	0.0
1.0 TO 1.5	0.0	0.0	0.0
1.[illegible] TO 2.0	0.0	0.0	0.3
2.0 TO 2.5	0.0	0.9	0.0
2.5 TO 3.0	0.0	0.5	1.2
3.0 TO 3.5	0.0	0.1	1.3
3.5 TO 4.0	0.4	1.0	3.0
4.0 TO 4.5	1.2	2.2	2.2
4.5 TO 5.0	0.0	0.3	0.0
5.0 TO 5.5	3.7	3.1	4.0
5.5 TO 6.0	4.5	4.4	4.0
6.0 TO 6.5	7.7	6.6	5.2
6.5 TO 7.0	4.5	3.6	3.2
7.0 TO 7.5	5.8	4.0	3.5
7.5 TO 8.0	4.1	5.6	8.0
8.0 TO 8.5	8.6	4.7	2.8
8.5 TO 9.0	9.0	8.4	6.1
9.0 TO 9.5	3.3	2.7	3.0
9.5 TO 10.0	47.1	51.8	52.2
ENTRIES	777	772	772

Table 34. Frequency distributions of path loss and fading for Ku-band

DIFFERENCE	% HIGH-LOW	% HIGH-MID	% MID-LOW
-20.0 TO -18.0	1.8	0.0	0.3
-18.0 TO -16.0	1.4	0.4	1.2
-16.0 TO -14.0	3.6	1.2	1.4
-14.0 TO -12.0	4.3	2.2	2.5
-12.0 TO -10.0	4.8	4.3	3.3
-10.0 TO -8.0	6.1	8.4	4.2
-8.0 TO -6.0	7.8	16.1	6.5
-6.0 TO -4.0	13.4	16.2	8.7
-4.0 TO -2.0	11.6	14.0	9.6
-2.0 TO 0.0	16.4	10.2	14.6
0.0 TO 2.0	10.6	10.6	9.0
2.0 TO 4.0	7.1	7.0	10.2
4.0 TO 6.0	5.5	4.2	8.6
6.0 TO 8.0	2.5	2.3	8.0
8.0 TO 10.0	1.7	2.3	5.7
10.0 TO 12.0	0.6	0.4	2.5
12.0 TO 14.0	0.4	0.1	2.1
14.0 TO 16.0	0.3	0.0	1.0
16.0 TO 18.0	0.1	0.0	0.7
18.0 TO 20.0	0.0	0.0	0.0
ENTRIES	770	771	767

Table 35. Frequency distributions of path loss differences between antennas for Ku-band

L BAND, NAXOS TO MYKONOS, GREECE   NOVEMBER 1972

HIGH-LOW

0.1	% >	20.0	DB
2.1	% >	15.0	DB
90.2	% >	10.0	DB
98.9	% >	6.0	DB
[illegible]	% >	3.0	DB
100.0	% >	0.0	DB
100.0	% >	-3.0	DB
100.0	% >	-6.0	DB
100.0	% >	-10.0	DB
100.0	% >	-15.0	DB
100.0	% >	-20.0	DB

TOTAL ENTRIES = 1[illegible]04

MID-LOW

0.0	% >	20.0	DB
0.0	% >	15.0	DB
1.1	% >	10.0	DB
85.1	% >	6.0	DB
98.3	% >	3.0	DB
99.7	% >	0.0	DB
99.9	% >	-3.0	DB
100.0	% >	-6.0	DB
100.0	% >	-10.0	DB
100.0	% >	-15.0	DB
100.0	% >	-20.0	DB

TOTAL ENTRIES = 1405

HIGH-MID

0.0	% >	20.0	DB
0.0	% >	15.0	DB
0.2	% >	10.0	DB
6.0	% >	6.0	DB
95.6	% >	3.0	DB
99.6	% >	0.0	DB
100.0	% >	-3.0	DB
100.0	% >	-6.0	DB
100.0	% >	-10.0	DB
100.0	% >	-15.0	DB
100.0	% >	-20.0	DB

TOTAL ENTRIES = 1403

FADING HIGH

0.0	% >	20.0	DB
0.0	% >	15.0	DB
0.0	% >	10.0	DB
[illegible]	% >	[illegible]	DB
0.1	% >	[illegible]	DB
[illegible]	% >	5.0	DB
1.1	% >	4.0	DB
[illegible]	% >	3.0	DB
[illegible]	% >	2.0	DB
[illegible]	% >	1.0	DB

TOTAL ENTRIES = 1[illegible]

FADING MIDDLE

0.0	% >	20.0	DB
0.0	% >	15.0	DB
0.0	% >	10.0	DB
0.8	% >	8.0	DB
1.9	% >	6.0	DB
3.1	% >	5.0	DB
7.2	% >	4.0	DB
[illegible]	% >	3.0	DB
46.5	% >	2.0	DB
91.1	% >	1.0	DB

TOTAL ENTRIES = 1405

FADING LOW

0.0	% >	20.0	DB
0.3	% >	15.0	DB
1.1	% >	10.0	DB
2.9	% >	8.0	DB
8.3	% >	6.0	DB
10.9	% >	5.0	DB
20.0	% >	4.0	DB
36.3	% >	3.0	DB
74.0	% >	2.0	DB
94.6	% >	1.0	DB

TOTAL ENTRIES = 1406

Table 36. Statistical presentation for L-band

L BAND, GREECE NOVEMBER 1972

PATH LOSS	% HIGH	% MID	% LOW
120.0 TO 125.0	0.0	0.0	0.0
125.0 TO 130.0	0.0	0.0	0.0
130.0 TO 135.0	0.0	0.0	0.0
135.0 TO 140.0	0.1	0.1	0.0
140.0 TO 145.0	1.1	0.3	0.0
145.0 TO 150.0	0.8	0.6	0.0
150.0 TO 155.0	12.9	0.9	0.7
155.0 TO 160.0	55.9	14.3	0.8
160.0 TO 165.0	26.8	55.4	3.8
165.0 TO 170.0	2.4	28.0	44.5
170.0 TO 175.0	0.0	0.4	48.3
175.0 TO 180.0	0.0	0.0	1.9
180.0 TO 185.0	0.0	0.0	0.0
185.0 TO 190.0	0.0	0.0	0.0
190.0 TO 195.0	0.0	0.0	0.0
195.0 TO 200.0	0.0	0.0	0.0
200.0 TO 205.0	0.0	0.0	0.0
205.0 TO 210.0	0.0	0.0	0.0
210.0 TO 215.0	0.0	0.0	0.0
215.0 TO 220.0	0.0	0.0	0.0
ENTRIES	1405	1405	1406

FADING	% HIGH	% MID	% LOW
0.0 TO 0.5	2.2	2.2	1.9
0.5 TO 1.0	17.7	5.7	3.1
1.0 TO 1.5	24.2	10.2	2.9
1.5 TO 2.0	35.7	34.3	17.6
2.0 TO 2.5	7.1	13.5	10.2
2.5 TO 3.0	9.5	19.1	27.7
3.0 TO 3.5	1.4	3.6	5.0
3.5 TO 4.0	0.9	3.6	11.0
4.0 TO 4.5	0.6	2.1	3.3
4.5 TO 5.0	0.6	2.4	5.1
5.0 TO 5.5	0.2	0.5	1.5
5.5 TO 6.0	0.1	1.0	2.3
6.0 TO 6.5	0.0	0.3	1.1
6.5 TO 7.0	0.0	0.5	2.2
7.0 TO 7.5	0.0	0.2	0.5
7.5 TO 8.0	0.0	0.0	1.5
8.0 TO 8.5	0.1	0.0	0.3
8.5 TO 9.0	0.0	0.4	0.4
9.0 TO 9.5	0.0	0.1	0.7
9.5 TO 10.0	0.0	0.3	1.5
ENTRIES	1405	1405	1406

Table 37. Frequency distributions of path loss and fading for L-band

DIFFERENCE	% HIGH-LOW	% HIGH-MID	% MID-LOW
-20.0 TO -18.0	0.0	0.0	0.0
-18.0 TO -16.0	0.0	0.0	0.0
-16.0 TO -14.0	0.0	0.0	0.0
-14.0 TO -12.0	0.0	0.0	0.0
-12.0 TO -10.0	0.0	0.0	0.0
-10.0 TO -8.0	0.0	0.0	0.0
-8.0 TO -6.0	0.0	0.0	0.0
-6.0 TO -4.0	0.0	0.0	0.0
-4.0 TO -2.0	0.0	0.1	0.1
-2.0 TO 0.0	0.0	0.3	0.1
0.0 TO 2.0	0.0	0.6	0.6
2.0 TO 4.0	0.3	12.2	2.4
4.0 TO 6.0	0.5	80.1	8.5
6.0 TO 8.0	4.3	5.9	74.9
8.0 TO 10.0	4.5	0.6	11.7
10.0 TO 12.0	44.9	0.1	1.4
12.0 TO 14.0	40.7	0.1	0.1
14.0 TO 16.0	3.6	0.0	0.1
16.0 TO 18.0	1.0	0.0	0.0
18.0 TO 20.0	0.1	0.0	0.0
ENTRIES	1404	1403	1405

Table 38. Frequency distributions of path loss differences between antennas for L-band

S BAND, NAXOS TO SYROS, GREECE   NOVEMBER 1972

HIGH-LOW	MID-LOW	HIGH-MID
0.0 % > 20.0 DB	0.0 % > 20.0 DB	0.0 % > 20.0 DB
1.0 % > 15.0 DB	0.0 % > 15.0 DB	0.1 % > 15.0 DB
65.7 % > 10.0 DB	0.2 % > 10.0 DB	0.6 % > 10.0 DB
97.9 % > 6.0 DB	0.7 % > 6.0 DB	56.7 % > 6.0 DB
[illegible] % > 3.0 DB	[illegible] % > 3.0 DB	98.2 % > 3.0 DB
[illegible] % > 0.0 DB	99.2 % > 0.0 DB	99.9 % > 0.0 DB
99.7 % > -3.0 DB	99.7 % > -3.0 DB	100.0 % > -3.0 DB
100.0 % > -6.0 DB	99.8 % > -6.0 DB	100.0 % > -6.0 DB
100.0 % > -10.0 DB	100.0 % > -10.0 DB	100.0 % > -10.0 DB
100.0 % > -15.0 DB	100.0 % > -15.0 DB	100.0 % > -15.0 DB
100.0 % > -20.0 DB	100.0 % > -20.0 DB	100.0 % > -20.0 DB
TOTAL ENTRIES = 1261	TOTAL ENTRIES = 1254	TOTAL ENTRIES = 1255

FADING HIGH	FADING MIDDLE	FADING LOW
0.0 % > 20.0 DB	0.0 % > 20.0 DB	0.0 % > 20.0 DB
0.0 % > 15.0 DB	0.0 % > 15.0 DB	0.0 % > 15.0 DB
0.0 % > 10.0 DB	0.0 % > 10.0 DB	0.4 % > 10.0 DB
[illegible] % > 8.0 DB	0.1 % > 8.0 DB	1.7 % > 8.0 DB
0.0 % > 6.0 DB	0.6 % > 6.0 DB	4.2 % > 6.0 DB
0.1 % > 5.0 DB	0.9 % > 5.0 DB	7.7 % > 5.0 DB
0.1 % > 4.0 DB	3.7 % > 4.0 DB	21.9 % > 4.0 DB
[illegible] % > 3.0 DB	25.0 % > 3.0 DB	39.9 % > 3.0 DB
41.7 % > 2.0 DB	60.8 % > 2.0 DB	74.9 % > 2.0 DB
[illegible] % > 1.0 DB	92.3 % > 1.0 DB	97.9 % > 1.0 DB
TOTAL ENTRIES = [illegible]	TOTAL ENTRIES = 1257	TOTAL ENTRIES = 1265

Table 39. Statistical presentation for S-band

S BAND, GREECE NOVEMBER 1972

PATH LOSS	% HIGH	% MID	% LOW
120.0 TO 125.0	0.0	0.0	0.0
125.0 TO 130.0	0.6	0.4	0.0
130.0 TO 135.0	0.6	0.4	0.6
135.0 TO 140.0	0.6	0.2	0.2
140.0 TO 145.0	6.4	0.7	0.2
145.0 TO 150.0	20.2	6.5	2.1
150.0 TO 155.0	33.2	11.7	6.6
155.0 TO 160.0	26.5	29.4	12.1
160.0 TO 165.0	11.7	35.1	36.0
165.0 TO 170.0	0.1	13.4	28.3
170.0 TO 175.0	0.0	2.1	12.6
175.0 TO 180.0	0.0	0.0	1.3
180.0 TO 185.0	0.0	0.0	0.0
185.0 TO 190.0	0.0	0.0	0.0
190.0 TO 195.0	0.0	0.0	0.0
195.0 TO 200.0	0.0	0.0	0.0
200.0 TO 205.0	0.0	0.0	0.0
205.0 TO 210.0	0.0	0.0	0.0
210.0 TO 215.0	0.0	0.0	0.0
215.0 TO 220.0	0.0	0.0	0.0
ENTRIES	1265	1257	1265

FADING	% HIGH	% MID	% LOW
0.0 TO 0.5	0.6	0.5	0.5
0.5 TO 1.0	14.5	7.2	1.6
1.0 TO 1.5	28.3	16.4	10.5
1.5 TO 2.0	14.5	14.3	12.5
2.0 TO 2.5	23.2	15.8	9.1
2.5 TO 3.0	11.1	21.2	25.9
3.0 TO 3.5	5.2	12.8	13.0
3.5 TO 4.0	2.6	7.6	5.1
4.0 TO 4.5	0.0	1.4	5.9
4.5 TO 5.0	0.0	0.2	2.1
5.0 TO 5.5	0.1	1.2	6.2
5.5 TO 6.0	0.0	0.2	3.4
6.0 TO 6.5	0.0	0.2	1.3
6.5 TO 7.0	0.0	0.0	0.1
7.0 TO 7.5	0.0	0.0	0.5
7.5 TO 8.0	0.0	0.2	0.6
8.0 TO 8.5	0.0	0.0	0.0
8.5 TO 9.0	0.0	0.1	1.3
9.0 TO 9.5	0.0	0.0	0.0
9.5 TO 10.0	0.0	0.0	0.5
ENTRIES	1265	1257	1265

Table 40. Frequency distributions of path loss and fading for S-band

DIFFERENCE	% HIGH-LOW	% HIGH-MID	% MID-LOW
-20.0 TO -18.0	0.0	0.0	0.0
-18.0 TO -16.0	0.0	0.0	0.0
-16.0 TO -14.0	0.0	0.0	0.0
-14.0 TO -12.0	0.0	0.0	0.0
-12.0 TO -10.0	0.0	0.0	0.0
-10.0 TO -8.0	0.0	0.0	0.1
-8.0 TO -6.0	0.0	0.0	0.1
-6.0 TO -4.0	0.1	0.0	0.2
-4.0 TO -2.0	0.0	0.0	0.0
-2.0 TO 0.0	0.1	0.1	0.5
0.0 TO 2.0	0.2	0.7	2.4
2.0 TO 4.0	0.2	4.9	35.3
4.0 TO 6.0	1.1	34.3	52.8
6.0 TO 8.0	5.4	53.3	8.1
8.0 TO 10.0	24.6	6.1	0.3
10.0 TO 12.0	50.4	0.5	0.2
12.0 TO 14.0	16.0	0.1	0.0
14.0 TO 16.0	1.4	0.1	0.0
16.0 TO 18.0	0.6	0.0	0.0
18.0 TO 20.0	0.0	0.0	0.0
ENTRIES	1261	1255	1254

Table 41. Frequency distributions of path loss differences between antennas for S-band

X BAND, NAXOS TO MYKONOS, GREECE   NOVEMBER 1972

HIGH-LOW

2.5 %	>	20.0	DB
14.7 %	>	15.0	DB
40.5 %	>	10.0	DB
65.3 %	>	6.0	DB
75.3 %	>	3.0	DB
85.8 %	>	0.0	DB
89.6 %	>	-3.0	DB
91.7 %	>	-6.0	DB
95.4 %	>	-10.0	DB
98.4 %	>	-15.0	DB
99.8 %	>	-20.0	DB

TOTAL ENTRIES - 1249

MID-LOW

0.0 %	>	20.0	DB
0.7 %	>	15.0	DB
3.4 %	>	10.0	DB
33.1 %	>	6.0	DB
71.1 %	>	3.0	DB
88.9 %	>	0.0	DB
95.5 %	>	-3.0	DB
98.4 %	>	-6.0	DB
99.8 %	>	-10.0	DB
100.0 %	>	-15.0	DB
100.0 %	>	-20.0	DB

TOTAL ENTRIES = 1248

HIGH-MID

0.0 %	>	20.0	DB
0.2 %	>	15.0	DB
3.1 %	>	10.0	DB
27.7 %	>	6.0	DB
56.5 %	>	3.0	DB
80.6 %	>	0.0	DB
88.9 %	>	-3.0	DB
93.7 %	>	-6.0	DB
97.8 %	>	-10.0	DB
99.8 %	>	-15.0	DB
100.0 %	>	-20.0	DB

TOTAL ENTRIES = 1247

FADING HIGH

0.0 %	>	20.0	DB
0.0 %	>	15.0	DB
0.0 %	>	10.0	DB
0.2 %	>	8.0	DB
0.5 %	>	6.0	DB
0.7 %	>	5.0	DB
2.0 %	>	4.0	DB
4.6 %	>	3.0	DB
15.3 %	>	2.0	DB
34.7 %	>	1.0	DB

TOTAL ENTRIES = 1251

FADING MIDDLE

0.0 %	>	20.0	DB
0.0 %	>	15.0	DB
0.0 %	>	10.0	DB
0.0 %	>	8.0	DB
0.1 %	>	6.0	DB
0.2 %	>	5.0	DB
1.0 %	>	4.0	DB
6.3 %	>	3.0	DB
14.7 %	>	2.0	DB
43.3 %	>	1.0	DB

TOTAL ENTRIES = 1248

FADING LOW

0.0 %	>	20.0	DB
0.0 %	>	15.0	DB
0.0 %	>	10.0	DB
0.1 %	>	8.0	DB
0.5 %	>	6.0	DB
0.8 %	>	5.0	DB
1.6 %	>	4.0	DB
7.4 %	>	3.0	DB
22.2 %	>	2.0	DB
48.6 %	>	1.0	DB

TOTAL ENTRIES = 1250

Table 42. Statistical presentation for X-band

PATH LOSS	% HIGH	% MID	% LOW
120.0 TO 125.0	0.0	0.0	0.0
125.0 TO 130.0	0.1	0.5	1.0
130.0 TO 135.0	0.6	5.6	5.4
135.0 TO 140.0	17.6	11.1	10.8
140.0 TO 145.0	16.8	14.0	8.2
145.0 TO 150.0	25.2	15.7	10.2
150.0 TO 155.0	19.7	16.2	12.6
155.0 TO 160.0	12.5	13.2	13.3
160.0 TO 165.0	3.4	11.2	9.0
165.0 TO 170.0	1.6	7.2	11.9
170.0 TO 175.0	2.5	1.9	9.7
175.0 TO 180.0	0.0	1.4	3.0
180.0 TO 185.0	0.0	1.4	1.4
185.0 TO 190.0	0.0	0.6	1.0
190.0 TO 195.0	0.0	0.1	0.5
195.0 TO 200.0	0.0	0.0	0.8
200.0 TO 205.0	0.0	0.0	0.7
205.0 TO 210.0	0.0	0.0	0.0
210.0 TO 215.0	0.0	0.0	0.0
215.0 TO 220.0	0.0	0.0	0.0
ENTRIES	1251	1248	1250

FADING	% HIGH	% MID	% LOW
0.0 TO 0.5	37.3	31.6	24.8
0.5 TO 1.0	22.6	23.8	21.9
1.0 TO 1.5	13.3	14.7	16.5
1.5 TO 2.0	11.2	13.4	12.4
2.0 TO 2.5	2.9	4.0	5.8
2.5 TO 3.0	8.2	6.2	10.3
3.0 TO 3.5	1.0	5.0	6.0
3.5 TO 4.0	0.2	0.2	0.0
4.0 TO 4.5	2.3	0.6	1.2
4.5 TO 5.0	0.2	0.3	0.2
5.0 TO 5.5	0.2	0.1	0.1
5.5 TO 6.0	0.1	0.0	0.2
6.0 TO 6.5	0.1	0.2	0.2
6.5 TO 7.0	0.1	0.0	0.2
7.0 TO 7.5	0.0	0.1	0.1
7.5 TO 8.0	0.2	0.0	0.0
8.0 TO 8.5	0.1	0.0	0.2
8.5 TO 9.0	0.0	0.0	0.0
9.0 TO 9.5	0.1	0.0	0.0
9.5 TO 10.0	0.0	0.0	0.1
ENTRIES	1251	1243	1250

Table 43. Frequency distributions of path loss and fading for X-band

DIFFERENCE	% HIGH-LOW	% HIGH-MID	% MID-LOW
-20.0 TO -18.0	0.5	0.0	0.0
-18.0 TO -16.0	0.4	0.1	0.0
-16.0 TO -14.0	1.2	0.2	0.1
-14.0 TO -12.0	1.2	1.0	0.0
-12.0 TO -10.0	1.4	0.9	0.1
-10.0 TO -8.0	1.6	1.3	0.2
-8.0 TO -6.0	2.1	2.6	1.1
-6.0 TO -4.0	1.8	2.2	1.4
-4.0 TO -2.0	2.0	3.4	3.3
-2.0 TO 0.0	1.8	7.5	5.0
0.0 TO 2.0	5.8	16.1	11.2
2.0 TO 4.0	7.1	17.6	14.6
4.0 TO 6.0	7.6	19.1	29.6
6.0 TO 8.0	11.2	17.0	20.0
8.0 TO 10.0	13.7	7.6	9.6
10.0 TO 12.0	9.2	1.9	2.1
12.0 TO 14.0	10.7	1.0	0.9
14.0 TO 16.0	9.9	0.2	0.2
16.0 TO 18.0	5.7	0.0	0.4
18.0 TO 20.0	5.0	0.1	0.3
ENTRIES	1249	1247	1248

DET RANGE	% HIGH	% MID	% LOW
0.0 TO 10.0	0.0	0.0	0.0
10.0 TO 20.0	7.1	23.7	33.1
20.0 TO 30.0	32.5	28.1	25.5
30.0 TO 40.0	21.6	12.8	8.0
40.0 TO 50.0	9.9	6.3	5.2
50.0 TO 60.0	4.5	4.3	2.1
60.0 TO 70.0	2.2	4.1	1.3
70.0 TO 80.0	3.0	2.3	1.6
80.0 TO 90.0	3.9	2.6	2.9
90.0 TO 100.0	7.1	2.9	3.4
100.0 TO 110.0	3.4	3.4	1.4
110.0 TO 120.0	3.4	1.5	1.7
120.0 TO 130.0	0.7	3.2	1.5
130.0 TO 140.0	0.0	1.5	1.7
140.0 TO 150.0	0.4	1.0	0.5
150.0 TO 160.0	0.1	1.4	1.6
160.0 TO 170.0	0.0	0.2	1.0
170.0 TO 180.0	0.2	0.0	1.0
180.0 TO 190.0	0.0	0.1	0.1
190.0 TO 200.0	0.0	0.4	0.5
ENTRIES	1247	1247	1247

Table [illegible]. Frequency distributions of path loss difference and detection range for X-band

DET RANGE	% > HIGH	% > MID	% > LOW
10.0	100.0	100.0	100.0
20.0	92.9	76.3	61.9
30.0	60.4	48.1	35.4
40.0	38.8	35.3	27.4
50.0	28.9	28.9	22.2
60.0	24.4	24.6	20.1
70.0	22.1	20.5	18.8
80.0	19.1	18.2	17.2
90.0	15.2	15.6	14.4
100.0	8.2	12.7	11.0
110.0	4.8	9.3	9.5
120.0	1.4	7.8	7.9
130.0	0.7	4.6	6.3
140.0	0.7	3.0	4.7
150.0	0.3	2.0	4.2
160.0	0.2	0.6	2.6
170.0	0.2	0.5	1.6
180.0	0.0	0.5	0.6
190.0	0.0	0.4	0.5
200.0	0.0	0.0	0.0
ENTRIES	1247	1247	1247

DET RANGE DIFF	% HIGH-LOW	% HIGH-MID	% MID-LOW
-50.0 TO -45.0	8.9	5.2	1.8
-45.0 TO -40.0	0.4	0.8	0.7
-40.0 TO -35.0	1.0	1.4	0.3
-35.0 TO -30.0	0.2	1.6	0.9
-30.0 TO -25.0	0.4	0.7	1.1
-25.0 TO -20.0	0.6	0.6	1.0
-20.0 TO -15.0	0.3	1.6	0.5
-15.0 TO -10.0	0.3	1.4	1.3
-10.0 TO -5.0	0.7	1.8	1.9
-5.0 TO 0.0	1.1	4.3	1.6
0.0 TO 5.0	10.3	35.0	47.5
5.0 TO 10.0	33.0	27.3	21.9
10.0 TO 15.0	17.1	8.5	5.9
15.0 TO 20.0	[illegible]	4.1	5.2
20.0 TO 25.0	3.4	2.2	[illegible]
25.0 TO 30.0	3.0	0.6	[illegible]
30.0 TO 35.0	2.1	0.8	1.4
35.0 TO 40.0	2.2	0.6	0.9
40.0 TO 45.0	1.8	0.3	0.2
45.0 TO 50.0	4.1	1.1	0.2
ENTRIES	1247	1247	1247

Table -5. Cumulative distribution of detection range and frequency distribution of detection range differences for X-band

KU BAND, NAXOS TO MYKONOS, GREECE   NOVEMBER 1972

HIGH-LOW

0.2 %	>	20.0 DB
4.0 %	>	15.0 DB
10.1 %	>	10.0 DB
20.3 %	>	6.0 DB
31.4 %	>	3.0 DB
43.5 %	>	0.0 DB
51.4 %	>	-3.0 DB
60.9 %	>	-6.0 DB
74.3 %	>	-10.0 DB
88.9 %	>	-15.0 DB
96.3 %	>	-20.0 DB

TOTAL ENTRIES = 998

MID-LOW

0.0 %	>	20.0 DB
0.4 %	>	15.0 DB
3.8 %	>	10.0 DB
13.1 %	>	6.0 DB
27.9 %	>	3.0 DB
49.1 %	>	0.0 DB
62.9 %	>	-3.0 DB
75.5 %	>	-6.0 DB
86.7 %	>	-10.0 DB
95.2 %	>	-15.0 DB
98.4 %	>	-20.0 DB

TOTAL ENTRIES = 998

HIGH-MID

0.0 %	>	20.0 DB
0.0 %	>	15.0 DB
1.1 %	>	10.0 DB
5.6 %	>	6.0 DB
18.0 %	>	3.0 DB
43.1 %	>	0.0 DB
66.2 %	>	-3.0 DB
84.1 %	>	-6.0 DB
95.1 %	>	-10.0 DB
99.0 %	>	-15.0 DB
99.9 %	>	-20.0 DB

TOTAL ENTRIES = 998

FADING HIGH

0.1 %	>	20.0 DB
0.1 %	>	15.0 DB
0.1 %	>	10.0 DB
0.5 %	>	8.0 DB
6.0 %	>	6.0 DB
9.1 %	>	5.0 DB
10.4 %	>	4.0 DB
26.1 %	>	3.0 DB
70.9 %	>	2.0 DB
98.0 %	>	1.0 DB

TOTAL ENTRIES = [illegible]

FADING MIDDLE

0.0 %	>	20.0 DB
0.0 %	>	15.0 DB
0.1 %	>	10.0 DB
0.6 %	>	8.0 DB
[illegible] %	>	6.0 DB
3.7 %	>	5.0 DB
8.3 %	>	4.0 DB
[illegible] %	>	3.0 DB
71.4 %	>	2.0 DB
97.0 %	>	1.0 DB

TOTAL ENTRIES = 998

FADING LOW

0.0 %	>	20.0 DB
0.0 %	>	15.0 DB
0.0 %	>	10.0 DB
0.0 %	>	8.0 DB
1.6 %	>	6.0 DB
1.6 %	>	5.0 DB
7.2 %	>	4.0 DB
25.4 %	>	3.0 DB
76.7 %	>	2.0 DB
97.4 %	>	1.0 DB

TOTAL ENTRIES = 998

Table 46. Statistical presentation Ku-band

PATH LOSS	% HIGH	% MID	% LOW
120.0 TO 125.0	0.0	0.0	0.0
125.0 TO 130.0	0.0	0.0	0.0
130.0 TO 135.0	0.0	0.0	1.2
135.0 TO 140.0	0.1	0.8	11.6
140.0 TO 145.0	4.0	10.4	28.0
145.0 TO 150.0	24.0	35.5	14.9
150.0 TO 155.0	33.3	21.4	12.0
155.0 TO 160.0	21.5	16.3	9.9
160.0 TO 165.0	10.5	6.8	7.8
165.0 TO 170.0	4.4	4.0	5.2
170.0 TO 175.0	1.3	3.0	3.6
175.0 TO 180.0	0.8	1.4	2.8
180.0 TO 185.0	0.1	0.3	2.0
185.0 TO 190.0	0.1	0.0	0.9
190.0 TO 195.0	0.0	0.0	0.0
195.0 TO 200.0	0.0	0.0	0.0
200.0 TO 205.0	0.0	0.0	0.0
205.0 TO 210.0	0.0	0.0	0.0
210.0 TO 215.0	0.0	0.0	0.0
215.0 TO 220.0	0.0	0.0	0.0
ENTRIES	1001	998	998

FADING	% HIGH	% MID	% LOW
0.0 TO 0.5	2.6	2.3	2.3
0.5 TO 1.0	1.4	0.7	0.3
1.0 TO 1.5	20.0	20.2	15.1
1.5 TO 2.0	5.1	5.3	5.6
2.0 TO 2.5	0.0	1.6	4.0
2.5 TO 3.0	44.9	44.7	47.3
3.0 TO 3.5	1.8	3.9	6.5
3.5 TO 4.0	14.0	12.9	11.6
4.0 TO 4.5	0.4	0.4	2.9
4.5 TO 5.0	0.1	0.4	1.1
5.0 TO 5.5	3.8	3.8	1.6
5.5 TO 6.0	0.1	0.1	0.0
6.0 TO 6.5	5.4	2.9	1.2
6.5 TO 7.0	0.0	0.0	0.2
7.0 TO 7.5	0.0	0.0	0.0
7.5 TO 8.0	0.1	0.1	0.2
8.0 TO 8.5	0.0	0.0	0.0
8.5 TO 9.0	0.0	0.0	0.0
9.0 TO 9.5	0.4	0.5	0.0
9.5 TO 10.0	0.0	0.1	0.0
ENTRIES	1001	998	998

Table 47. Frequency distributions of path loss and fading for Ku-band

DIFFERENCE	% HIGH-LOW	% HIGH-MID	% MID-LOW
-20.0 TO -18.0	5.9	0.3	2.3
-18.0 TO -16.0	4.2	0.4	1.4
-16.0 TO -14.0	3.6	0.9	2.1
-14.0 TO -12.0	5.2	1.1	3.7
-12.0 TO -10.0	6.2	2.2	3.8
-10.0 TO -8.0	6.5	3.9	5.4
-8.0 TO -6.0	6.8	6.3	4.8
-6.0 TO -4.0	7.0	12.3	8.8
-4.0 TO -2.0	5.7	14.0	7.4
-2.0 TO 0.0	5.3	14.9	11.1
0.0 TO 2.0	6.8	15.9	13.1
2.0 TO 4.0	10.9	13.3	12.7
4.0 TO 6.0	5.4	7.6	10.1
6.0 TO 8.0	5.3	4.1	6.0
8.0 TO 10.0	4.9	1.0	3.2
10.0 TO 12.0	3.3	0.8	1.8
12.0 TO 14.0	1.7	0.2	1.2
14.0 TO 16.0	1.9	0.1	0.7
16.0 TO 18.0	1.8	0.0	0.1
18.0 TO 20.0	1.5	0.0	0.1
ENTRIES	998	998	998

Table 48. Frequency distributions of path loss differences between antennas for Ku-band

KA BAND, NAXOS TO MYKONOS, GREECE NOVEMBER 1972

A. MID-LOW

0.0 %	>	20.0 DB
0.3 %	>	15.0 DB
1.3 %	>	10.0 DB
6.7 %	>	6.0 DB
17.1 %	>	3.0 DB
34.3 %	>	0.0 DB
49.6 %	>	-3.0 DB
66.1 %	>	-6.0 DB
83.0 %	>	-10.0 DB
94.8 %	>	-15.0 DB
99.4 %	>	-20.0 DB

TOTAL ENTRIES = 1146

B. FADING MIDDLE

0.0 %	>	20.0 DB
0.2 %	>	15.0 DB
1.6 %	>	10.0 DB
3.9 %	>	8.0 DB
7.4 %	>	6.0 DB
11.4 %	>	5.0 DB
17.2 %	>	4.0 DB
29.3 %	>	3.0 DB
53.6 %	>	2.0 DB
91.0 %	>	1.0 DB

TOTAL ENTRIES = 1154

C. FADING LOW

0.0 %	>	20.0 DB
0.2 %	>	15.0 DB
0.4 %	>	10.0 DB
1.2 %	>	8.0 DB
5.9 %	>	6.0 DB
8.6 %	>	5.0 DB
12.5 %	>	4.0 DB
20.6 %	>	3.0 DB
48.1 %	>	2.0 DB
86.6 %	>	1.0 DB

TOTAL ENTRIES = 1155

Table 49. Statistical presentation for Ka-band

KA BAND, GREECE NOVEMBER 1972

PATH LOSS	% MID	% LOW
120.0 TO 125.0	0.0	0.0
125.0 TO 130.0	0.0	0.0
130.0 TO 135.0	0.0	0.0
135.0 TO 140.0	0.0	0.0
140.0 TO 145.0	0.0	0.0
145.0 TO 150.0	0.0	0.0
150.0 TO 155.0	0.0	0.0
155.0 TO 160.0	0.1	0.3
160.0 TO 165.0	1.2	15.7
165.0 TO 170.0	21.6	33.2
170.0 TO 175.0	30.8	26.8
175.0 TO 180.0	29.5	14.9
180.0 TO 185.0	13.1	6.8
185.0 TO 190.0	3.0	1.6
190.0 TO 195.0	0.3	0.4
195.0 TO 200.0	0.1	0.3
200.0 TO 205.0	0.0	0.0
205.0 TO 210.0	0.0	0.0
210.0 TO 215.0	0.0	0.0
215.0 TO 220.0	0.0	0.0
ENTRIES	1154	1155

Table 50. Frequency distribution of path loss for Ka-band

DIFFERENCE	% MID-LOW
-20.0 TO -18.0	2.1
-18.0 TO -16.0	1.8
-16.0 TO -14.0	3.2
-14.0 TO -12.0	3.9
-12.0 TO -10.0	5.8
-10.0 TO -8.0	7.2
-8.0 TO -6.0	9.5
-6.0 TO -4.0	10.8
-4.0 TO -2.0	10.9
-2.0 TO 0.0	10.6
0.0 TO 2.0	12.7
2.0 TO 4.0	10.1
4.0 TO 6.0	4.7
6.0 TO 8.0	2.9
8.0 TO 10.0	1.9
10.0 TO 12.0	1.2
12.0 TO 14.0	0.2
14.0 TO 16.0	0.3
16.0 TO 18.0	0.2
18.0 TO 20.0	0.0
ENTRIES	1146

FADING	% MID	% LOW
0.0 TO 0.5	0.7	2.2
0.5 TO 1.0	7.9	10.2
1.0 TO 1.5	27.1	28.6
1.5 TO 2.0	10.6	10.7
2.0 TO 2.5	8.9	6.5
2.5 TO 3.0	15.5	21.2
3.0 TO 3.5	5.9	4.0
3.5 TO 4.0	6.2	4.3
4.0 TO 4.5	3.0	2.2
4.5 TO 5.0	0.0	0.0
5.0 TO 5.5	2.9	1.6
5.5 TO 6.0	4.0	2.7
6.0 TO 6.5	2.2	2.7
6.5 TO 7.0	0.6	1.6
7.0 TO 7.5	0.0	0.0
7.5 TO 8.0	0.7	0.3
8.0 TO 8.5	0.5	0.3
8.5 TO 9.0	0.6	0.0
9.0 TO 9.5	1.0	0.3
9.5 TO 10.0	1.8	0.5
ENTRIES	1154	1155

Table 31. Frequency distributions of path loss difference and fading for Ka-band

L BAND, ALL SEASONS 1972

PATH LOSS	% HIGH	% MID	% LOW
120.0 TO 125.0	1.9	0.6	0.2
125.0 TO 130.0	2.4	1.3	0.6
130.0 TO 135.0	2.7	2.4	1.6
135.0 TO 140.0	3.6	2.6	2.3
140.0 TO 145.0	10.4	3.7	3.1
145.0 TO 150.0	14.6	8.4	2.8
150.0 TO 155.0	22.8	15.2	10.2
155.0 TO 160.0	32.2	13.8	14.0
160.0 TO 165.0	8.7	36.6	9.0
165.0 TO 170.0	0.8	14.7	26.4
170.0 TO 175.0	0.0	0.1	28.6
175.0 TO 180.0	0.0	0.0	1.2
180.0 TO 185.0	0.0	0.0	0.0
185.0 TO 190.0	0.0	0.0	0.0
190.0 TO 195.0	0.0	0.0	0.0
195.0 TO 200.0	0.0	0.0	0.0
200.0 TO 205.0	0.0	0.0	0.0
205.0 TO 210.0	0.0	0.0	0.0
210.0 TO 215.0	0.0	0.0	0.0
215.0 TO 220.0	0.0	0.0	0.0
ENTRIES	4385	4391	4387

FADING	% HIGH	% MID	% LOW
0.0 TO 0.5	1.3	0.8	0.7
0.5 TO 1.0	16.1	7.1	4.0
1.0 TO 1.5	26.7	18.5	13.0
1.5 TO 2.0	31.5	25.9	17.1
2.0 TO 2.5	7.9	13.5	7.9
2.5 TO 3.0	8.3	16.9	20.1
3.0 TO 3.5	1.8	5.1	11.2
3.5 TO 4.0	2.2	3.7	7.5
4.0 TO 4.5	0.9	1.3	2.6
4.5 TO 5.0	0.3	0.9	1.3
5.0 TO 5.5	1.3	2.0	5.6
5.5 TO 6.0	0.3	0.5	1.2
6.0 TO 6.5	0.6	1.0	1.3
6.5 TO 7.0	0.1	0.3	[illegible]
7.0 TO 7.5	[illegible]	0.1	0.3
7.5 TO 8.0	0.3	0.7	1.5
8.0 TO 8.5	0.0	0.0	0.1
8.5 TO 9.0	0.1	0.3	0.3
9.0 TO 9.5	0.0	0.1	0.3
9.5 TO 10.0	0.3	0.7	1.3
ENTRIES	4385	4391	4387

Table 52. Frequency distributions of path loss and fading for L-band

DIFFERENCE	% HIGH-LOW	% HIGH-MID	% MID-LOW
-20.0 TO -18.0	0.0	0.0	0.0
-18.0 TO -16.0	0.0	0.0	0.0
-16.0 TO -14.0	0.0	0.0	0.0
-14.0 TO -12.0	0.0	0.0	0.0
-12.0 TO -10.0	0.0	0.0	0.0
-10.0 TO -8.0	0.0	0.0	0.0
-8.0 TO -6.0	0.0	0.0	0.1
-6.0 TO -4.0	0.0	0.1	0.1
-4.0 TO -2.0	0.1	0.2	0.2
-2.0 TO 0.0	0.2	0.4	0.9
0.0 TO 2.0	0.4	1.8	1.4
2.0 TO 4.0	0.7	14.1	16.9
4.0 TO 6.0	5.8	39.4	24.4
6.0 TO 8.0	6.5	18.9	43.9
8.0 TO 10.0	9.2	22.7	10.9
10.0 TO 12.0	28.6	1.9	0.9
12.0 TO 14.0	24.3	0.3	0.2
14.0 TO 16.0	12.5	0.0	0.1
16.0 TO 18.0	10.7	0.0	0.0
18.0 TO 20.0	1.1	0.0	0.0
ENTRIES	4354	4363	4373

Table 53. Frequency distributions of path loss differences between antennas for L-band

PATH LOSS	% HIGH	% MID	% LOW
120.0 TO 125.0	12.9	8.9	7.6
125.0 TO 130.0	6.4	4.4	3.3
130.0 TO 135.0	9.7	4.9	3.3
135.0 TO 140.0	5.6	9.3	6.2
140.0 TO 145.0	7.2	6.1	7.5
145.0 TO 150.0	18.8	7.5	5.9
150.0 TO 155.0	23.5	14.4	7.2
155.0 TO 160.0	11.9	22.7	7.7
160.0 TO 165.0	3.8	16.5	14.4
165.0 TO 170.0	0.1	4.8	21.7
170.0 TO 175.0	0.0	0.7	12.0
175.0 TO 180.0	0.0	0.0	3.2
180.0 TO 185.0	0.0	0.0	0.1
185.0 TO 190.0	0.0	0.0	0.0
190.0 TO 195.0	0.0	0.0	0.0
195.0 TO 200.0	0.0	0.0	0.0
200.0 TO 205.0	0.0	0.0	0.0
205.0 TO 210.0	0.0	0.0	0.0
210.0 TO 215.0	0.0	0.0	0.0
215.0 TO 220.0	0.0	0.0	0.0
ENTRIES	4546	4528	4558

FADING	% HIGH	% MID	% LOW
0.0 TO 0.5	0.2	0.1	0.2
0.5 TO 1.0	12.7	9.1	5.7
1.0 TO 1.5	31.3	22.2	18.4
1.5 TO 2.0	16.1	13.4	11.0
2.0 TO 2.5	17.5	20.8	17.6
2.5 TO 3.0	12.8	17.1	21.0
3.0 TO 3.5	3.7	6.4	7.4
3.5 TO 4.0	3.5	5.6	5.0
4.0 TO 4.5	1.1	2.6	4.8
4.5 TO 5.0	0.2	0.4	1.1
5.0 TO 5.5	0.3	0.9	3.4
5.5 TO 6.0	0.3	0.6	1.9
6.0 TO 6.5	0.2	0.2	0.7
6.5 TO 7.0	0.0	0.1	0.2
7.0 TO 7.5	0.1	0.1	0.3
7.5 TO 8.0	0.0	0.1	0.3
8.0 TO 8.5	0.0	0.1	0.1
8.5 TO 9.0	0.0	0.1	0.4
9.0 TO 9.5	0.0	0.0	0.1
9.5 TO 10.0	0.1	0.1	0.4
ENTRIES	4546	4528	4558

Table 54. Frequency distributions of path loss and fading for S-band

S BAND, ALL SEASONS 1972

DIFFERENCE	% HIGH-LOW	% HIGH-MID	% MID-LOW
-20.0 TO -18.0	0.0	0.0	0.0
-18.0 TO -16.0	0.0	0.0	0.0
-16.0 TO -14.0	0.1	0.0	0.0
-14.0 TO -12.0	0.1	0.1	0.1
-12.0 TO -10.0	0.2	0.2	0.2
-10.0 TO -8.0	0.4	0.2	0.2
-8.0 TO -6.0	0.3	0.5	0.4
-6.0 TO -4.0	0.3	0.5	0.7
-4.0 TO -2.0	0.7	0.9	0.8
-2.0 TO 0.0	1.0	1.3	1.9
0.0 TO 2.0	1.7	2.8	4.3
2.0 TO 4.0	1.8	7.0	20.0
4.0 TO 6.0	2.9	35.6	32.3
6.0 TO 8.0	5.9	42.1	9.8
8.0 TO 10.0	15.2	6.8	2.0
10.0 TO 12.0	26.3	1.1	15.6
12.0 TO 14.0	12.2	0.5	11.0
14.0 TO 16.0	3.0	0.2	0.5
16.0 TO 18.0	15.3	0.1	0.0
18.0 TO 20.0	12.6	0.1	0.2
ENTRIES	4460	4440	4456

Table 55. Frequency distributions of path loss differences between antennas for S-band

% > dB	February	April	August	November	Total
20	0.0	0.5	0.0	2.5	0.8
15	0.2	3.4	0.0	14.7	4.6
10	1.2	13.2	0.6	40.5	13.9
6	7.7	36.5	0.9	65.3	27.2
3	25.1	57.2	3.1	75.3	39.4
0	49.3	72.1	7.0	85.8	52.6
-3	72.5	79.5	10.8	88.6	61.8
-6	93.9	85.7	19.2	91.7	71.6
-10	98.4	91.1	38.5	95.4	80.0
-15	100.0	96.4	63.9	98.4	89.1
-20	100.0	98.6	82.9	99.8	95.1
Number of Observations	1202	1058	1278	1249	4787

Table 56. Percentage of time path loss differences between high and low X-band antennas exceed certain dB values

PATH LOSS	% HIGH	% MID	% LOW
120.0 TO 125.0	0.9	0.9	4.9
125.0 TO 130.0	4.3	4.3	9.9
130.0 TO 135.0	9.1	9.0	12.7
135.0 TO 140.0	12.1	12.7	11.9
140.0 TO 145.0	13.3	14.6	9.9
145.0 TO 150.0	22.3	21.3	13.7
150.0 TO 155.0	25.5	16.4	11.3
155.0 TO 160.0	8.3	9.6	10.1
160.0 TO 165.0	2.5	5.7	5.0
165.0 TO 170.0	1.3	3.3	4.5
170.0 TO 175.0	0.8	1.1	3.2
175.0 TO 180.0	0.1	0.7	1.2
180.0 TO 185.0	0.0	0.4	0.4
185.0 TO 190.0	0.0	0.2	0.3
190.0 TO 195.0	0.0	0.0	0.1
195.0 TO 200.0	0.0	0.0	0.3
200.0 TO 205.0	0.0	0.0	0.2
205.0 TO 210.0	0.0	0.0	0.0
210.0 TO 215.0	0.0	0.0	0.0
215.0 TO 220.0	0.0	0.0	0.0
ENTRIES	4814	4815	4799

FADING	% HIGH	% MID	% LOW
0.0 TO 0.5	9.8	8.2	6.5
0.5 TO 1.0	11.3	10.2	8.6
1.0 TO 1.5	11.5	11.9	10.4
1.5 TO 2.0	15.0	13.9	14.8
2.0 TO 2.5	9.5	9.2	8.7
2.5 TO 3.0	10.1	13.9	14.9
3.0 TO 3.5	6.1	8.4	14.0
3.5 TO 4.0	2.8	3.8	3.5
4.0 TO 4.5	4.7	5.4	5.2
4.5 TO 5.0	1.2	2.0	3.1
5.0 TO 5.5	3.3	3.6	3.0
5.5 TO 6.0	2.1	2.3	1.3
6.0 TO 6.5	1.0	1.2	1.0
6.5 TO 7.0	1.1	[illegible]	1.4
7.0 TO 7.5	2.4	1.2	1.4
7.5 TO 8.0	1.0	0.6	0.8
8.0 TO 8.5	1.2	1.2	0.6
8.5 TO 9.0	0.7	0.3	0.1
9.0 TO 9.5	0.9	0.3	0.1
9.5 TO 10.0	3.8	1.5	1.6
ENTRIES	4814	4815	4799

Table 57. Frequency distributions of path loss and fading for X-band

DIFFERENCE	% HIGH-LOW	% HIGH-MID	% MID-LOW
-20.0 TO -18.0	7.2	0.5	0.7
-18.0 TO -16.0	2.1	0.5	0.9
-16.0 TO -14.0	2.8	0.7	1.6
-14.0 TO -12.0	3.6	1.5	2.9
-12.0 TO -10.0	4.1	2.4	4.2
-10.0 TO -8.0	4.2	3.1	4.9
-8.0 TO -6.0	4.0	4.8	5.5
-6.0 TO -4.0	5.7	5.2	6.1
-4.0 TO -2.0	6.9	9.5	11.3
-2.0 TO 0.0	6.5	11.4	19.7
0.0 TO 2.0	7.4	14.0	13.0
2.0 TO 4.0	9.2	15.0	9.2
4.0 TO 6.0	8.6	13.0	9.0
6.0 TO 8.0	7.1	8.8	6.0
8.0 TO 10.0	6.4	5.6	2.8
10.0 TO 12.0	3.8	1.9	0.7
12.0 TO 14.0	3.7	1.3	0.3
14.0 TO 16.0	3.0	0.5	0.1
16.0 TO 18.0	1.9	0.2	0.1
18.0 TO 20.0	1.6	0.2	0.1
ENTRIES	4787	4803	4794

DET RANGE	% HIGH	% MID	% LOW
0.0 TO 10.0	0.0	0.0	0.0
10.0 TO 20.0	4.6	10.9	15.0
20.0 TO 30.0	34.0	26.2	21.7
30.0 TO 40.0	19.9	17.4	11.3
40.0 TO 50.0	6.9	7.5	5.7
50.0 TO 60.0	2.9	4.5	2.7
60.0 TO 70.0	2.7	3.2	2.0
70.0 TO 80.0	2.8	2.9	2.1
80.0 TO 90.0	2.6	2.4	2.7
90.0 TO 100.0	3.3	2.6	2.7
100.0 TO 110.0	2.4	3.1	2.4
110.0 TO 120.0	2.7	2.7	2.3
120.0 TO 130.0	1.9	3.4	2.9
130.0 TO 140.0	1.7	2.5	2.3
140.0 TO 150.0	2.5	1.3	3.2
150.0 TO 160.0	1.3	1.9	2.8
160.0 TO 170.0	1.4	1.3	2.2
170.0 TO 180.0	1.6	1.1	2.7
180.0 TO 190.0	1.0	1.1	2.1
190.0 TO 200.0	3.8	3.4	11.3
ENTRIES	4783	4783	4783

Table 38. Frequency distributions of path loss difference and detection range for X-band

DET RANGE	%> HIGH	%> MID	%> LOW
10.0	100.0	100.0	100.0
20.0	95.4	89.1	85.0
30.0	61.4	62.9	63.3
40.0	41.4	45.5	52.1
50.0	34.5	38.0	46.3
60.0	31.7	33.5	43.6
70.0	29.0	30.3	41.6
80.0	26.1	27.4	39.6
90.0	23.5	25.0	35.9
100.0	20.2	22.4	34.1
110.0	17.8	19.3	31.7
120.0	15.1	16.6	29.4
130.0	13.3	13.2	26.5
140.0	11.6	10.6	24.2
150.0	9.2	8.9	21.0
160.0	7.9	6.9	18.2
170.0	6.5	5.7	15.1
180.0	4.9	4.6	13.4
190.0	3.3	3.4	11.3
200.0	-0.0	-0.0	-0.0
ENTRIES	4783	4783	4783

DET RANGE DIFF	% HIGH-LOW	% HIGH-MID	% MID-LOW
-50.0 TO -45.0	27.0	8.9	22.9
-45.0 TO -40.0	1.2	1.3	1.4
-40.0 TO -35.0	1.4	1.5	1.6
-35.0 TO -30.0	0.9	1.7	1.4
-30.0 TO -25.0	1.0	1.7	1.7
-25.0 TO -20.0	1.1	2.4	1.8
-20.0 TO -15.0	1.5	2.9	1.7
-15.0 TO -10.0	2.3	3.6	2.8
-10.0 TO -5.0	4.6	5.2	5.2
-5.0 TO 0.0	6.1	10.5	13.3
0.0 TO 5.0	16.8	26.0	24.2
5.0 TO 10.0	11.5	11.6	7.2
10.0 TO 15.0	5.8	4.4	2.5
15.0 TO 20.0	3.3	4.1	2.2
20.0 TO 25.0	2.2	1.5	1.6
25.0 TO 30.0	1.9	1.9	0.8
30.0 TO 35.0	1.8	2.1	0.8
35.0 TO 40.0	1.2	1.2	0.4
40.0 TO 45.0	1.5	0.9	0.3
45.0 TO 50.0	0.3	6.7	1.2
ENTRIES	4783	4783	4783

Table 59. Cumulative distribution of detection range and frequency distribution of detection range differences for X-band

PATH LOSS	% HIGH	% MID	% LOW
120.0 TO 125.0	0.0	0.0	0.0
125.0 TO 130.0	0.0	0.0	0.0
130.0 TO 135.0	0.2	0.5	0.9
135.0 TO 140.0	0.8	4.9	9.0
140.0 TO 145.0	6.4	15.8	22.8
145.0 TO 150.0	22.0	25.6	15.3
150.0 TO 155.0	25.5	15.2	13.0
155.0 TO 160.0	17.7	13.7	13.6
160.0 TO 165.0	12.3	8.9	11.9
165.0 TO 170.0	7.9	8.5	6.8
170.0 TO 175.0	5.0	4.8	3.3
175.0 TO 180.0	1.3	1.5	1.8
180.0 TO 185.0	0.6	0.3	1.1
185.0 TO 190.0	0.1	0.2	0.6
190.0 TO 195.0	0.1	0.0	0.0
195.0 TO 200.0	0.0	0.0	0.0
200.0 TO 205.0	0.0	0.0	0.0
205.0 TO 210.0	0.0	0.0	0.0
210.0 TO 215.0	0.0	0.0	0.0
215.0 TO 220.0	0.0	0.0	0.0
ENTRIES	1778	1770	1770

FADING	% HIGH	% MID	% LOW
0.0 TO 0.5	1.5	1.3	1.3
0.5 TO 1.0	0.8	0.4	0.2
1.0 TO 1.5	11.2	11.4	8.5
1.5 TO 2.0	2.9	3.0	3.3
2.0 TO 2.5	0.0	1.3	2.3
2.5 TO 3.0	25.3	25.4	27.2
3.0 TO 3.5	1.0	2.3	4.2
3.5 TO 4.0	8.0	7.7	7.9
4.0 TO 4.5	0.7	1.2	2.6
4.5 TO 5.0	0.1	0.3	0.6
5.0 TO 5.5	3.8	3.5	2.7
5.5 TO 6.0	2.0	2.0	1.8
6.0 TO 6.5	6.4	4.5	2.9
6.5 TO 7.0	2.0	1.5	1.5
7.0 TO 7.5	2.5	1.3	1.5
7.5 TO 8.0	1.9	2.5	3.6
8.0 TO 8.5	3.8	2.0	1.2
8.5 TO 9.0	3.9	3.7	2.7
9.0 TO 9.5	1.7	1.5	1.3
9.5 TO 10.0	20.6	22.7	22.8
ENTRIES	1778	1770	1770

Table 50. Frequency distributions of path loss and fading for Ku-band

DIFFERENCE	% HIGH-LOW	% HIGH-MID	% MID-LOW
-20.0 TO -18.0	4.1	0.2	1.4
-18.0 TO -16.0	3.0	0.4	1.3
-16.0 TO -14.0	3.6	1.0	1.8
-14.0 TO -12.0	4.8	1.6	3.2
-12.0 TO -10.0	5.6	3.1	3.6
-10.0 TO -8.0	6.3	5.9	4.9
-8.0 TO -6.0	7.2	10.9	5.6
-6.0 TO -4.0	9.8	14.0	8.8
-4.0 TO -2.0	8.3	14.0	8.4
-2.0 TO 0.0	10.1	12.9	12.6
0.0 TO 2.0	8.5	13.6	11.3
2.0 TO 4.0	9.3	10.6	11.6
4.0 TO 6.0	5.4	6.1	9.5
6.0 TO 8.0	4.1	3.3	6.9
8.0 TO 10.0	3.5	1.6	4.3
10.0 TO 12.0	2.1	0.6	2.1
12.0 TO 14.0	1.1	0.2	1.6
14.0 TO 16.0	1.1	0.1	0.8
16.0 TO 18.0	1.1	0.0	0.3
18.0 TO 20.0	0.8	0.0	0.1
ENTRIES	1768	1769	1765

Table 61. Frequency distributions of path loss differences between antennas for Ku-band

Season	Calculated Reversals in % ($10 < \delta < 30$ m)	Measured Reversals in %
Winter	41	51
Spring	36	28
Summer	33	93
Fall	48	14
Year Average	39	47

Table 62. Calculated and measured antenna reversals

X. APPENDICES

A. Detection Range Calculations

An important consideration in interpreting path loss results is the implied maximum range of detection for some assumed radar and target. A technique has been developed that directly relates the measured path loss at 19 nautical miles for all three antenna heights to predicted detection range. The radar that is assumed is one which can just detect the target at 200 nautical miles in free space. All detection range results presented here are for this same radar and target combination. Figure A 1 shows the theoretical dependence of path loss on range for all three antenna heights at 9.6 GHz for a variety of duct heights. These calculations are the results of a full wave computer solution using realistic log-linear distributions of refractive index in the boundary layer. The free space path loss at 200 nautical miles at 9.6 GHz is 163.5 dB and is indicated in Figure A 1 as a threshold. Any case for which the path loss is less than this threshold is defined as being detectable and any case for which the path loss is greater than this threshold is defined as being undetectable. Thus the maximum range of detection for any of the sample duct heights shown in Figure A 1 is the range at which the path loss first exceeds the 200 nautical mile free space threshold. From the curves in Figure A 1 it is therefore possible to relate certain discrete path loss values at 19 nautical miles to detection range. Figure A 2 shows a tabulation and a plot of these path loss values versus the corresponding detection range for each duct height and antenna height of Figure A 1. The solid curve in Figure A 2 is an empirical fit given by the relation

$$R = 6 - 338/(136-L) \qquad L \geq 142 \qquad (1)$$

$$R = 1397 - 9.4L \qquad L < 142 \qquad (2)$$

where R is detection range in nautical miles and L is path loss in dB. This fit is considered to be conservative since it will normally underestimate the detection range for low path loss values as shown in the table. It will also normally underestimate the detection range for higher path loss values which are due to higher order modal interference as exemplified by the one point for the high antenna which does not fit the curve. It is interesting to note that equations (1) and (2) are independent of antenna height thus making the computation of detection range quite simple. The frequency distributions of detection range shown in this report were prepared by simply calculating the detection range using the above equations on a measurement by measurement basis for all three antenna heights and then distributing them for each measurement period. This procedure has only been carried out for the X-band measurements because of the higher sensitivity of X-band to the evaporation duct but could easily be extended to the other frequencies as well.

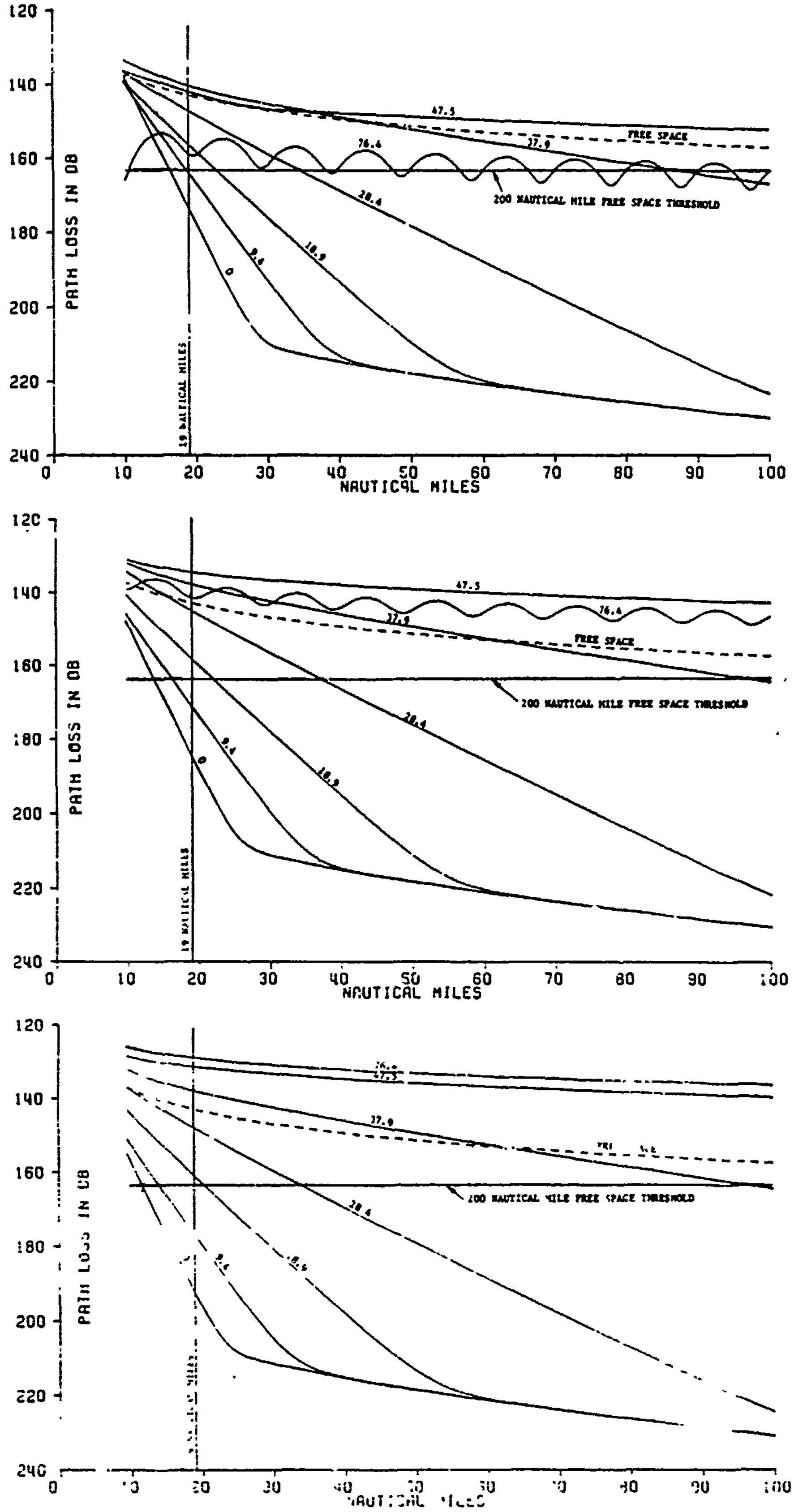

(a) High antenna
Frequency: 9.6 GHz
Transmitter antenna:

Receiver antenna: 64
Duct heights in feet a
indicated

(b) Mid antenna
Receiver antenna: 32
Frequency: 9.6 GHz
Transmitter antenna:

(c) Low antenna
Receiver antenna: 16
Frequency: 9.6 GHz
Transmitter antenna:

Figure A 1. Calculated path loss versus range for the three antenna heights

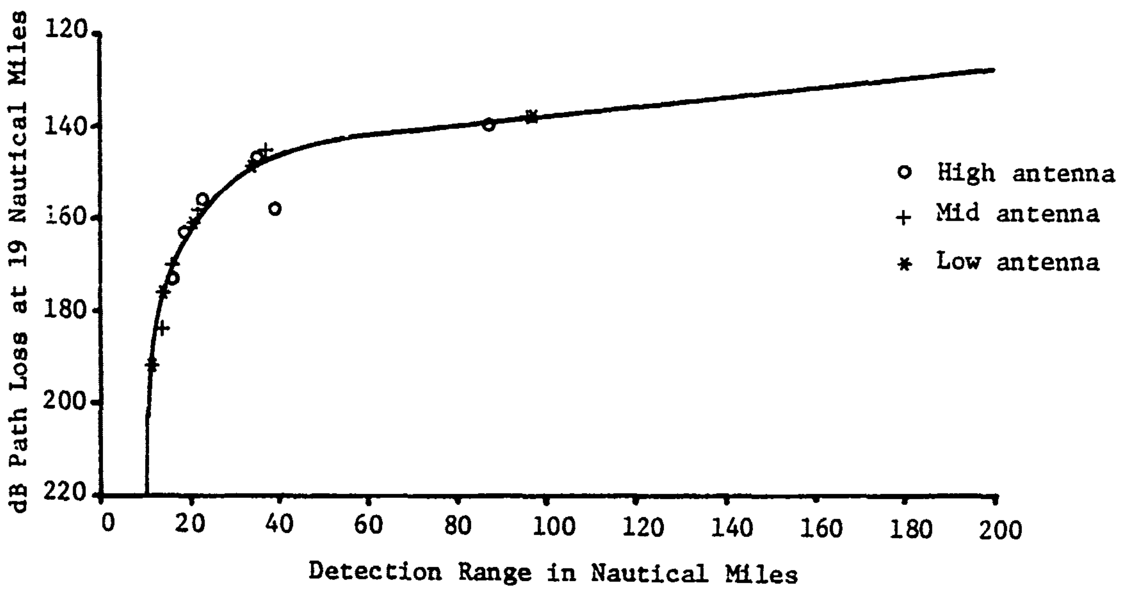

Duct Height (Feet)	High Antenna Path Loss (dB)	High Antenna Det. Range (Nau. mi.)	Mid Antenna Path Loss	Mid Antenna Det. Range	Low Antenna Path Loss	Low Antenna Det. Range
0	173	16	184	14	192	12
9.4	163	19	170	16	176	14
18.9	156	23	158	22	161	21
28.4	147	35	145	37	149	34
37.9	140	87	138	97	138	97
47.3	142	200+	134	200+	132	200+
76.4	158	39	141	200+	129	200+

Figure A 2. Path loss at 19 nautical miles versus detection range

B. Radiosonde Profiles

Radiosonde profiles were obtained using 403 MHz transmitters and Beukers receivers. They were optically tracked for wind information. The individual profiles with the launch time in GMT are listed in the following presentation which is self explanatory. Some of the profiles for the 7 November 1972, 0751 Z launch are shown twice. In the second presentation the original chart recorder trace was read in very small increments and with maximum resolution. This was done in order to show that small fluctuations ignored in the first presentation did not represent significant refractive changes.

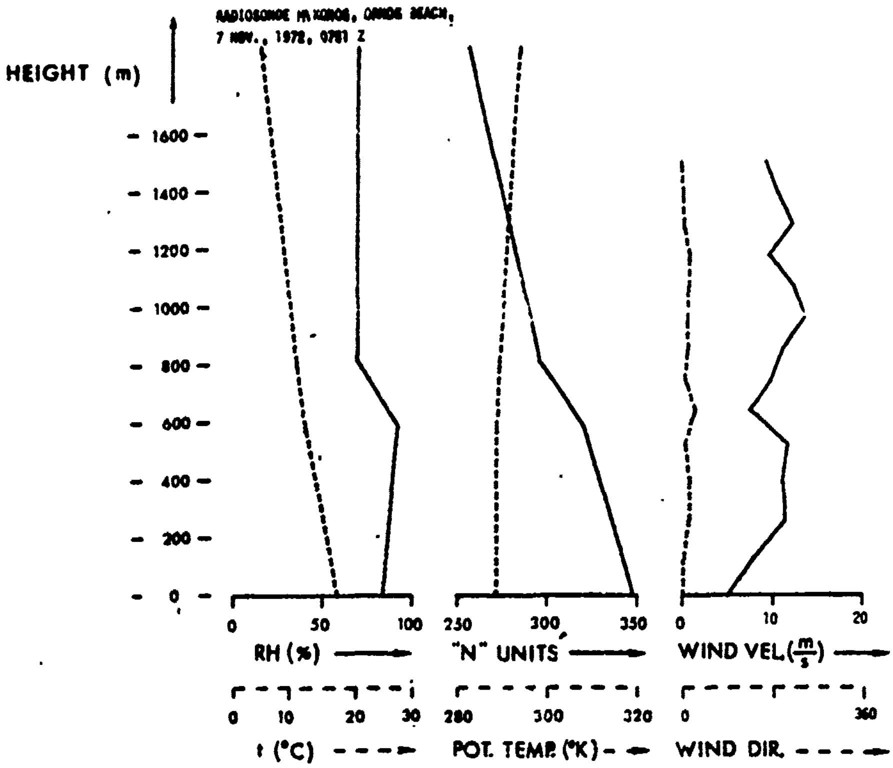
HEIGHT (m)
1600
1400
1200
1000
800
600
400
200
0
0 50 100
RH (%)
250 300 350
"N" UNITS
0 10 20
WIND VEL.(m/s)
0 10 20 30
t (°C)
280 300 320
POT. TEMP. (°K)
0 360
WIND DIR.

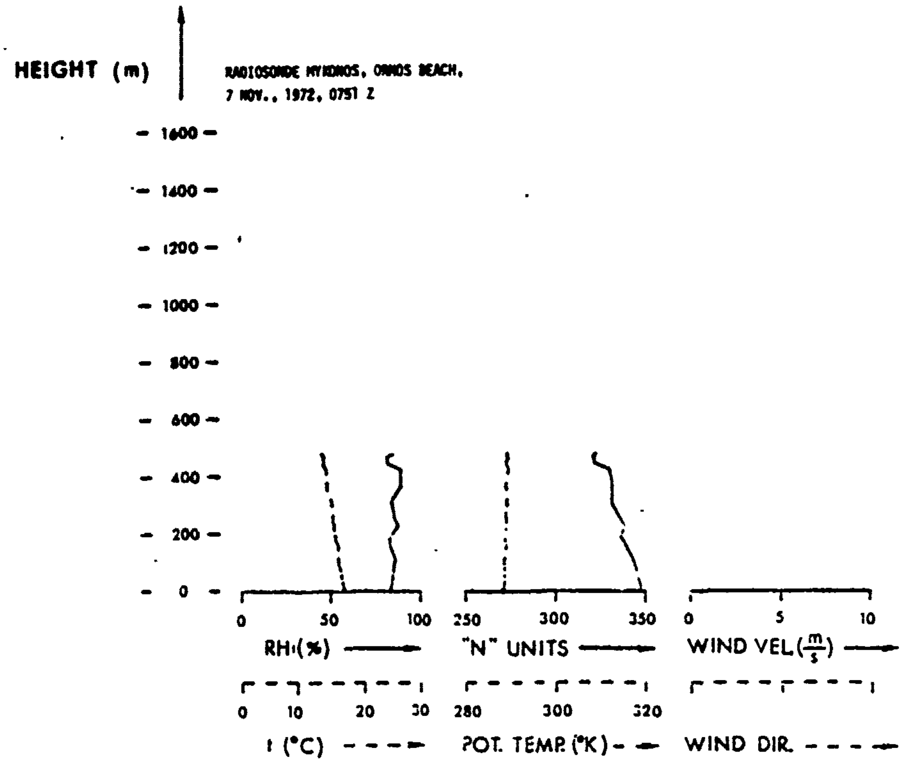
HEIGHT (m)
RADIOSONDE MYKONOS, ORMOS BEACH,
7 NOV., 1972, 0751 Z
1600
1400
1200
1000
800
600
400
200
0
0 50 100
RH (%)
250 300 350
"N" UNITS
0 5 10
WIND VEL.(m/s)
0 10 20 30
t (°C)
280 300 320
POT. TEMP. (°K)
WIND DIR.

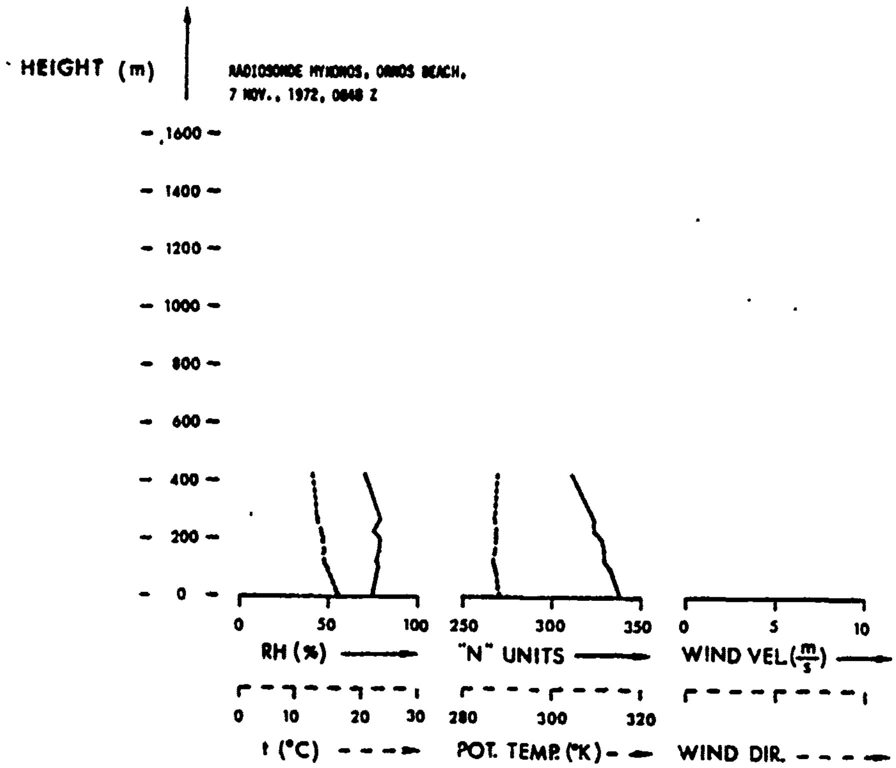
HEIGHT (m)
RADIOSONDE MYKONOS, ORMOS BEACH,
7 NOV., 1972, 0848 Z
1600
1400
1200
1000
800
600
400
200
0
0
50
100
RH (%)
250
300
350
"N" UNITS
0
5
10
WIND VEL.(m/s)
0
10
20
30
t (°C)
280
300
320
POT. TEMP. (°K)
WIND DIR.

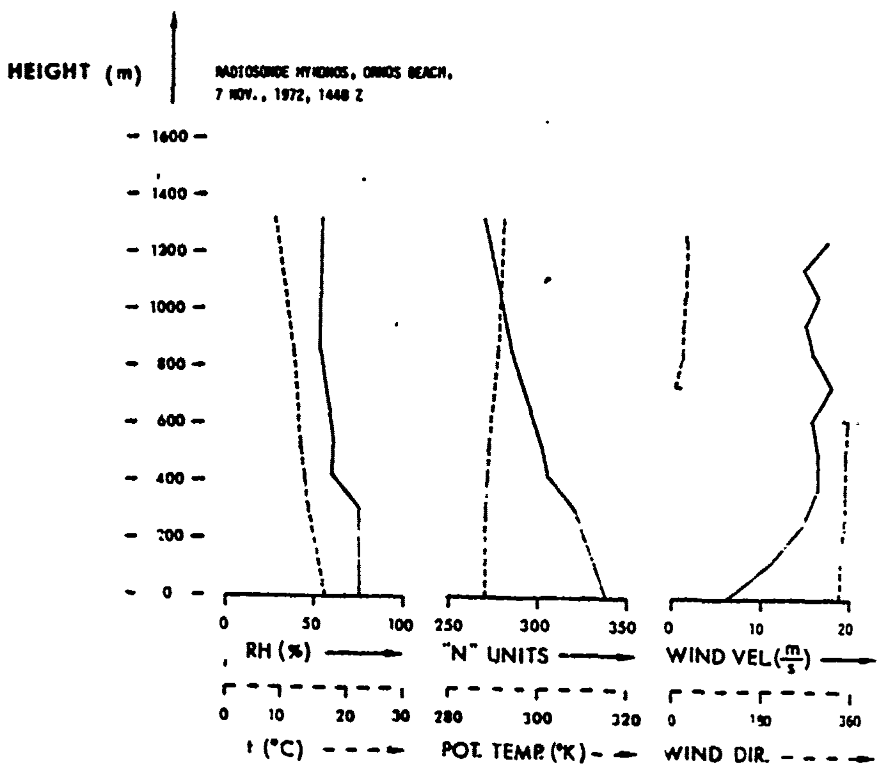
HEIGHT (m)
RADIOSONDE MYKONOS, ORMOS BEACH,
7 NOV., 1972, 1448 Z
1600
1400
1200
1000
800
600
400
200
0
0
50
100
RH (%)
250
300
350
"N" UNITS
0
10
20
WIND VEL.(m/s)
0
10
20
30
t (°C)
280
300
320
POT. TEMP. (°K)
0
180
360
WIND DIR.

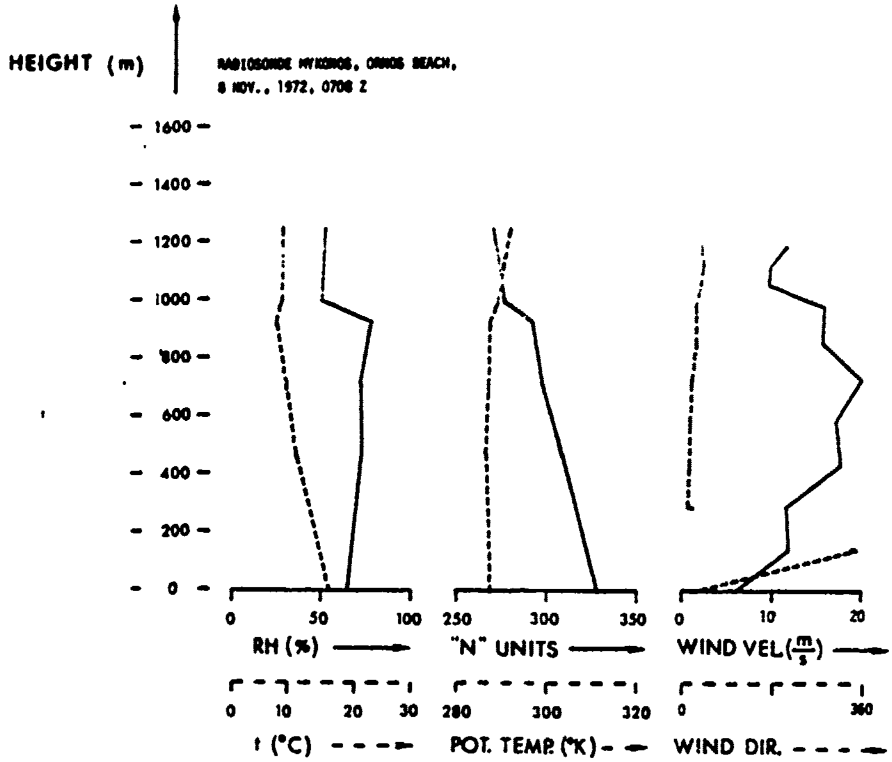
HEIGHT (m)
RADIOSONDE MYKONOS, ORNOS BEACH,
8 NOV., 1972, 0708 Z
1600
1400
1200
1000
800
600
400
200
0
0 50 100
RH (%)
250 300 350
"N" UNITS
0 10 20
WIND VEL.($\frac{m}{s}$)
0 10 20 30
t (°C)
280 300 320
POT. TEMP. (°K)
0 360
WIND DIR.

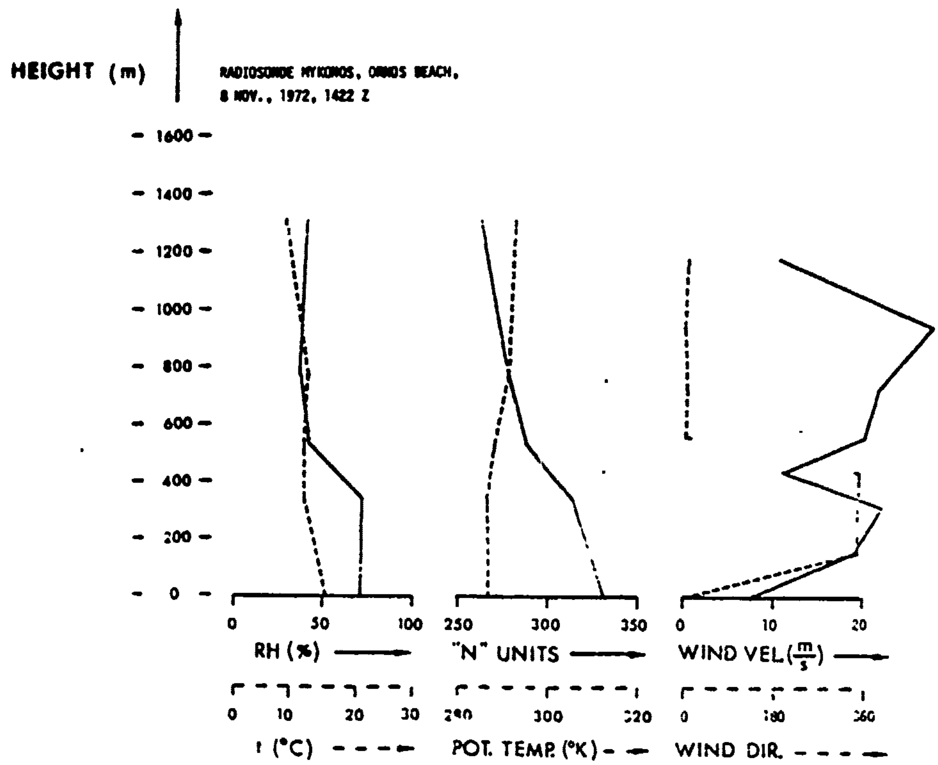
HEIGHT (m)
RADIOSONDE MYKONOS, ORNOS BEACH,
8 NOV., 1972, 1422 Z
1600
1400
1200
1000
800
600
400
200
0
0 50 100
RH (%)
250 300 350
"N" UNITS
0 10 20
WIND VEL.($\frac{m}{s}$)
0 10 20 30
t (°C)
300
POT. TEMP. (°K)
0 180
WIND DIR.

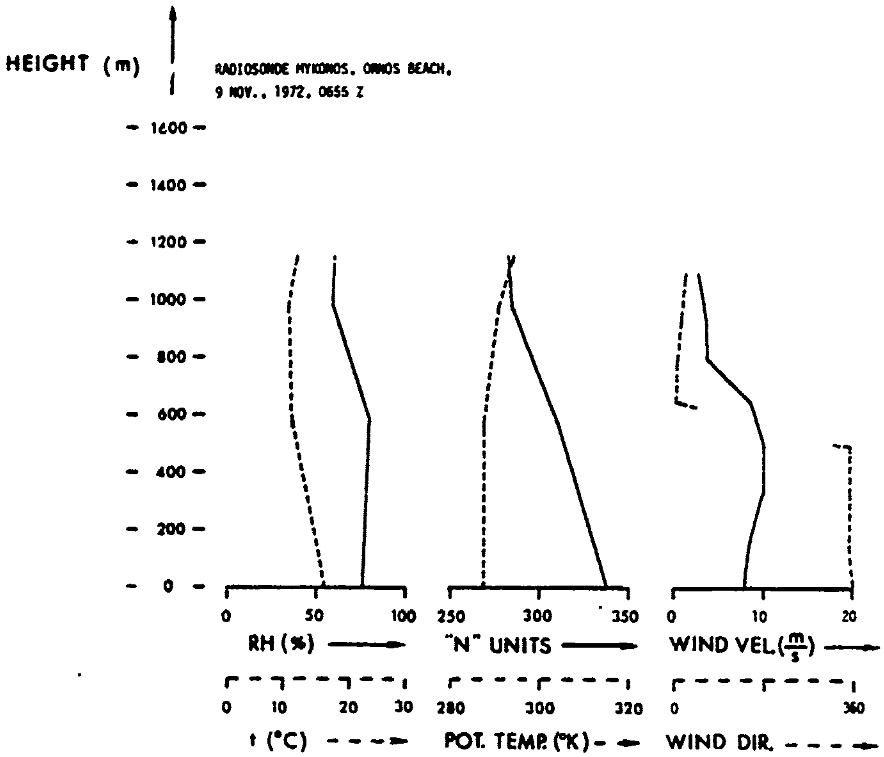
HEIGHT (m)
RADIOSONDE MYKONOS, ORNOS BEACH,
9 NOV., 1972, 0655 Z
1600
1400
1200
1000
800
600
400
200
0
0 50 100
RH (%)
250 300 350
"N" UNITS
0 10 20
WIND VEL.(m/s)
0 10 20 30
t (°C)
280 300 320
POT. TEMP. (°K)
0 360
WIND DIR.

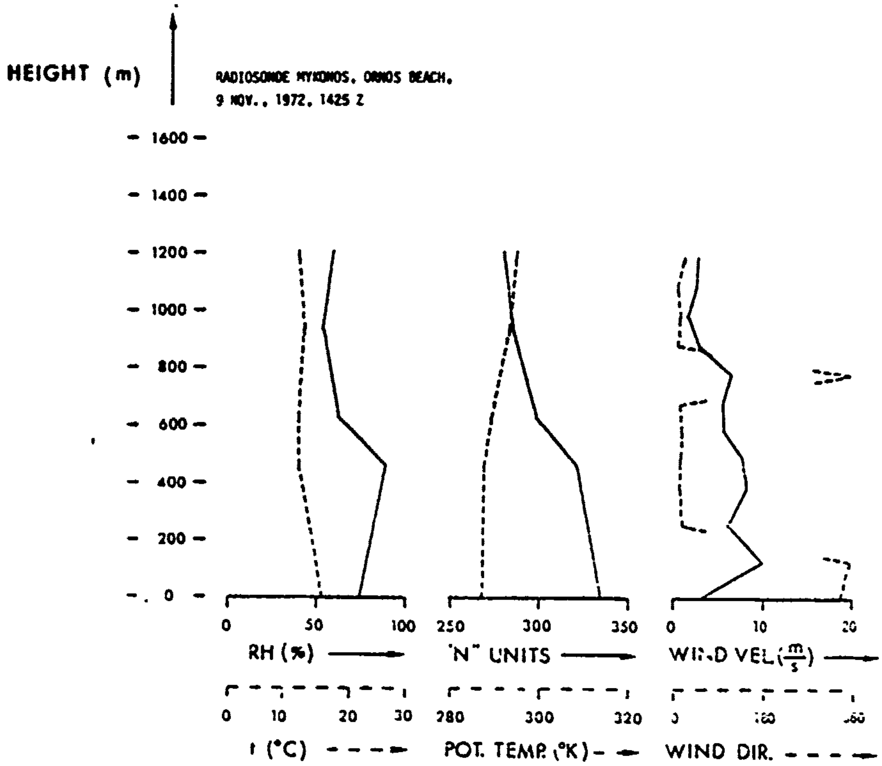
HEIGHT (m)
RADIOSONDE MYKONOS, ORNOS BEACH,
9 NOV., 1972, 1425 Z
1600
1400
1200
1000
800
600
400
200
0
0 50 100
RH (%)
250 300 350
"N" UNITS
0 10 20
WIND VEL.(m/s)
0 10 20 30
t (°C)
280 300 320
POT. TEMP. (°K)
WIND DIR.

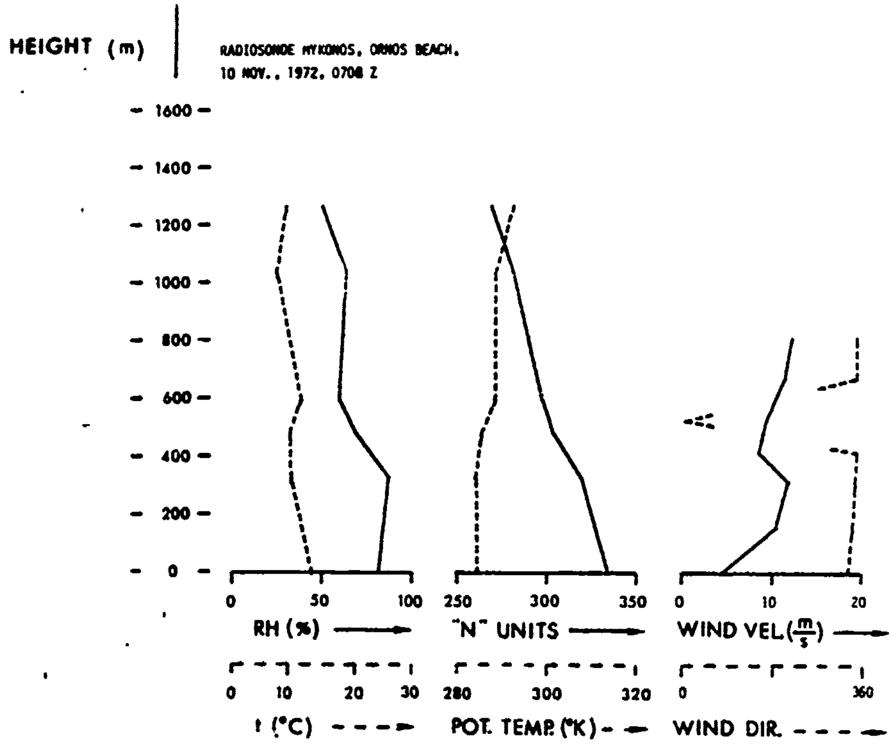

HEIGHT (m)
RADIOSONDE MYKONOS, ORNOS BEACH,
10 NOV., 1972, 0708 Z
RH (%)
"N" UNITS
WIND VEL.(m/s)
t (°C)
POT. TEMP. (°K)
WIND DIR.

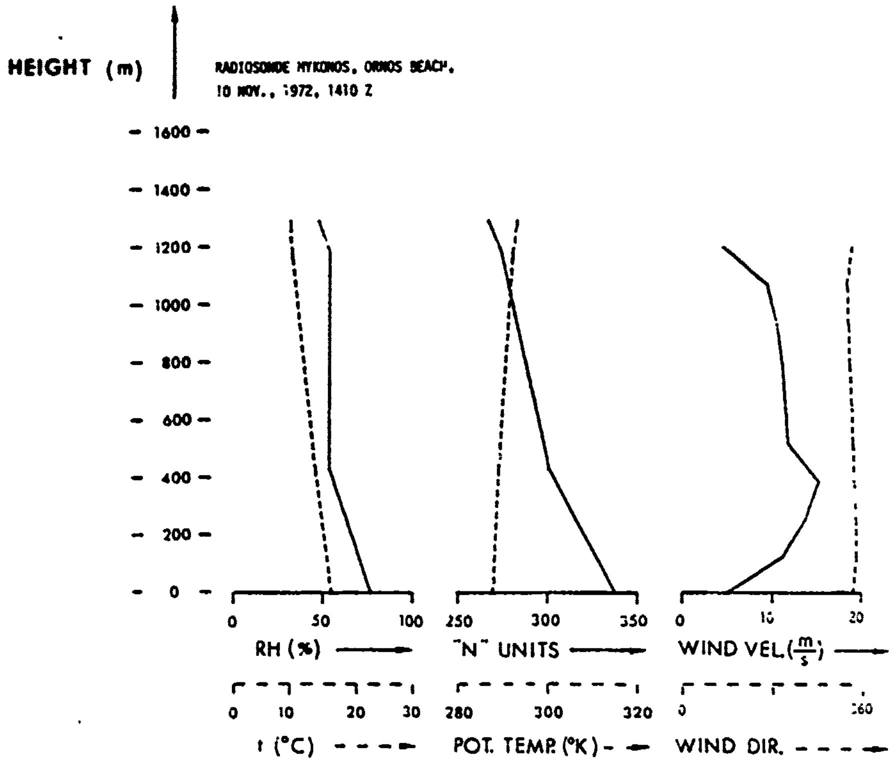

HEIGHT (m)
RADIOSONDE MYKONOS, ORNOS BEACH,
10 NOV., 1972, 1410 Z
RH (%)
"N" UNITS
WIND VEL.(m/s)
t (°C)
POT. TEMP. (°K)
WIND DIR.

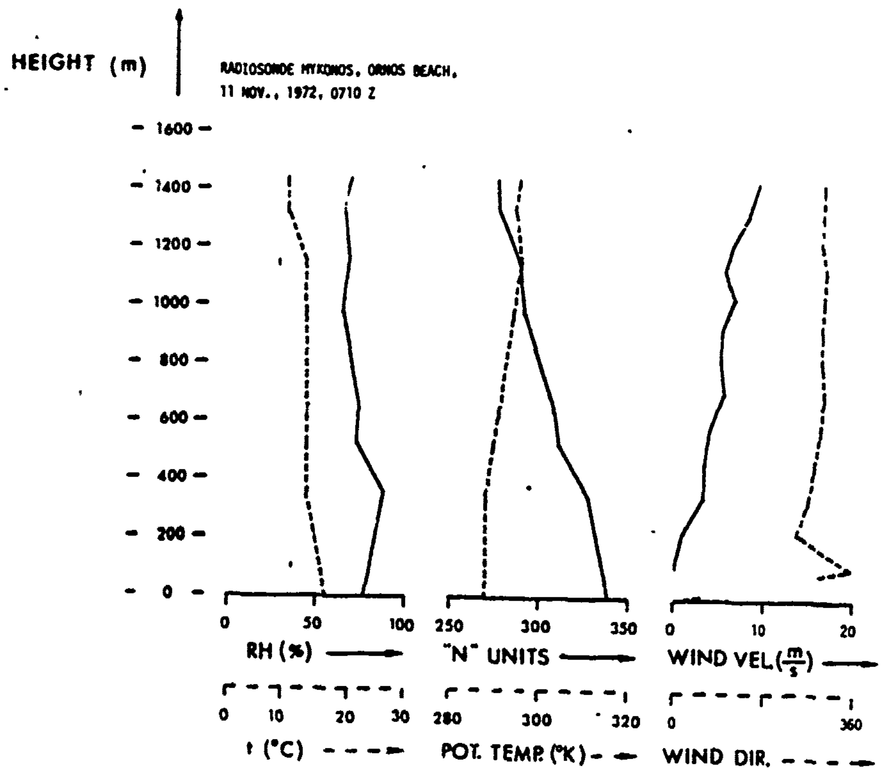
HEIGHT (m)
RADIOSONDE MYKONOS, ORNOS BEACH,
11 NOV., 1972, 0710 Z
1600
1400
1200
1000
800
600
400
200
0
0 50 100
RH (%)
0 10 20 30
t (°C)
250 300 350
"N" UNITS
280 300 320
POT. TEMP. (°K)
0 10 20
WIND VEL.(m/s)
0 360
WIND DIR.

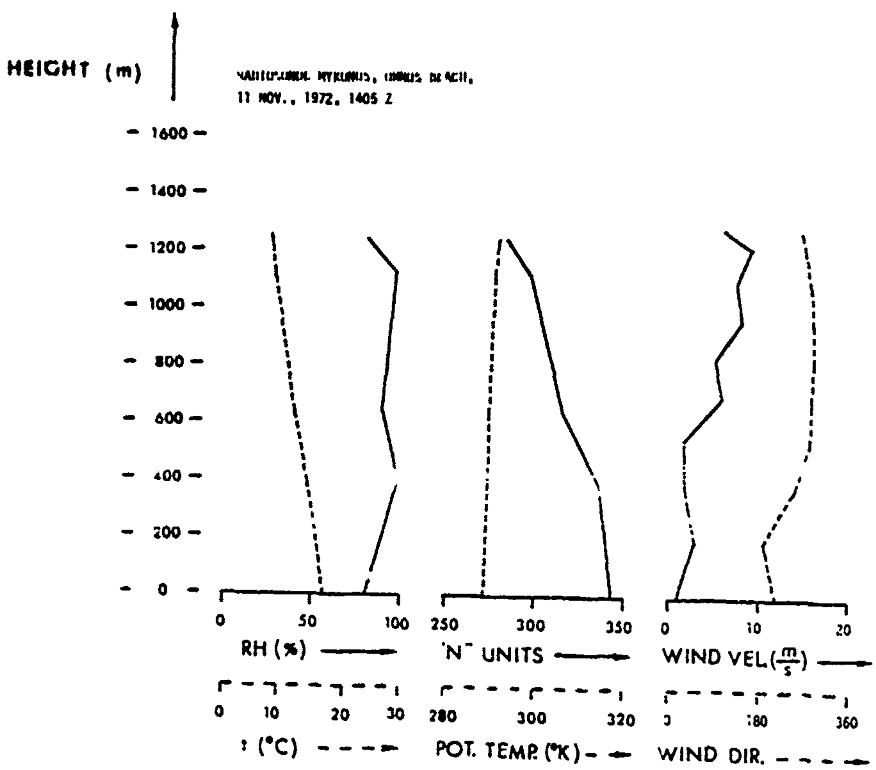
HEIGHT (m)
11 NOV., 1972, 1405 Z
1600
1400
1200
1000
800
600
400
200
0
0 50 100
RH (%)
0 10 20 30
t (°C)
250 300 350
"N" UNITS
280 300 320
POT. TEMP. (°K)
0 10 20
WIND VEL.(m/s)
0 180 360
WIND DIR.

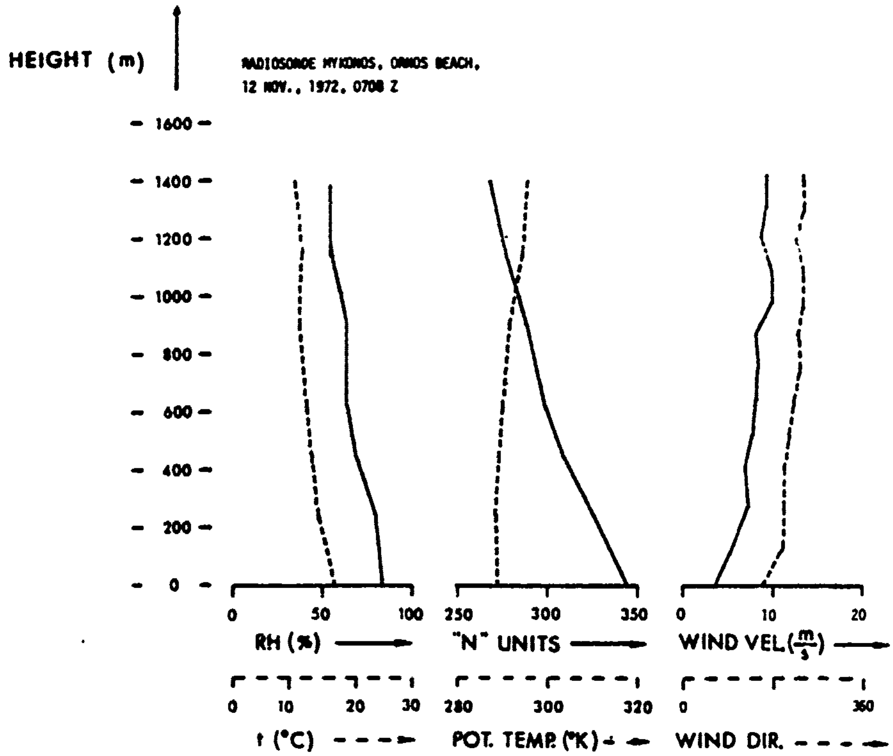
HEIGHT (m)
RADIOSONDE MYKONOS, ORNOS BEACH,
12 NOV., 1972, 0708 Z
1600
1400
1200
1000
800
600
400
200
0
0 50 100
RH (%)
250 300 350
"N" UNITS
0 10 20
WIND VEL.(m/s)
0 10 20 30
t (°C)
280 300 320
POT. TEMP. (°K)
0 360
WIND DIR.

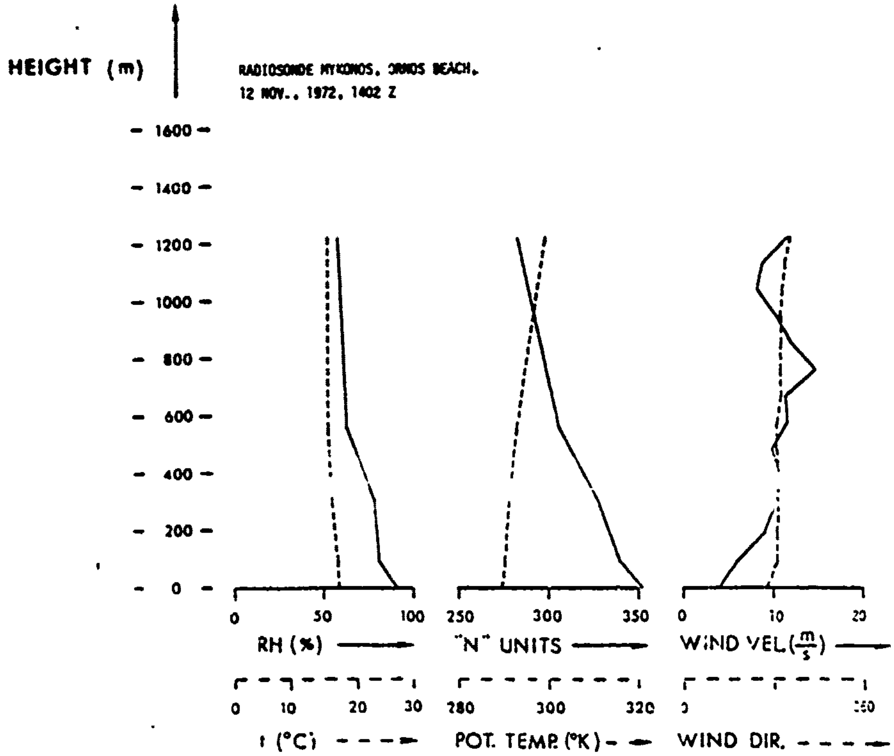
HEIGHT (m)
RADIOSONDE MYKONOS, ORNOS BEACH,
12 NOV., 1972, 1402 Z
1600
1400
1200
1000
800
600
400
200
0
0 50 100
RH (%)
250 300 350
"N" UNITS
0 10 20
WIND VEL.(m/s)
0 10 20 30
t (°C)
280 300 320
POT. TEMP. (°K)
WIND DIR.

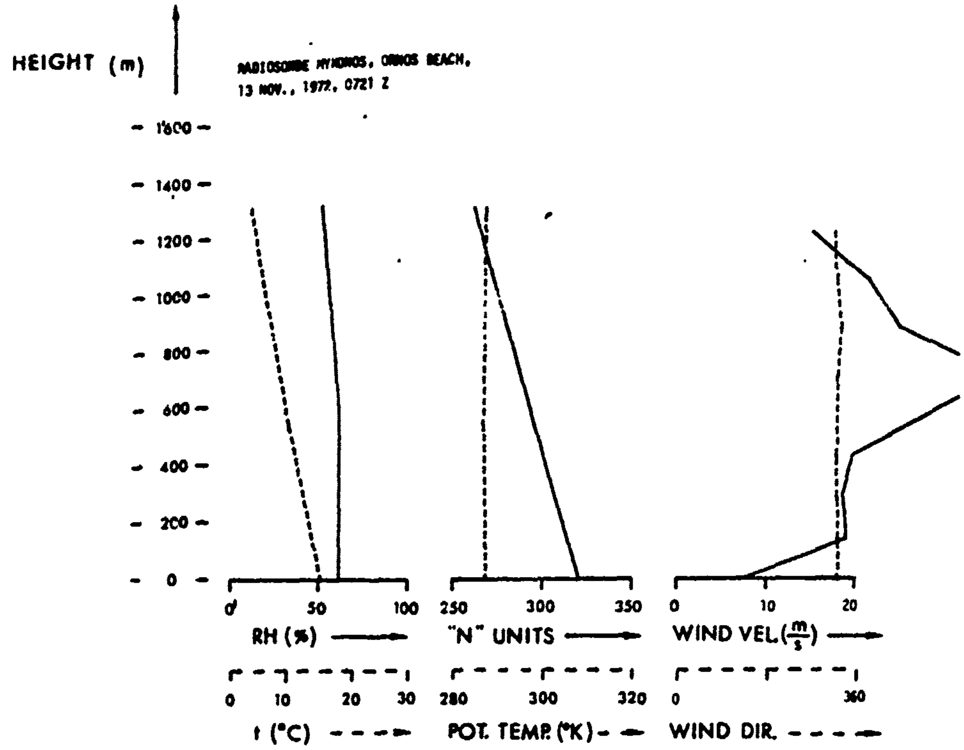
HEIGHT (m)
RADIOSONDE MYKONOS, ORNOS BEACH,
13 NOV., 1972, 0721 Z
1600
1400
1200
1000
800
600
400
200
0
0
50
100
RH (%)
250
300
350
"N" UNITS
0
10
20
WIND VEL.(m/s)
0
10
20
30
t (°C)
280
300
320
POT. TEMP. (°K)
0
360
WIND DIR.

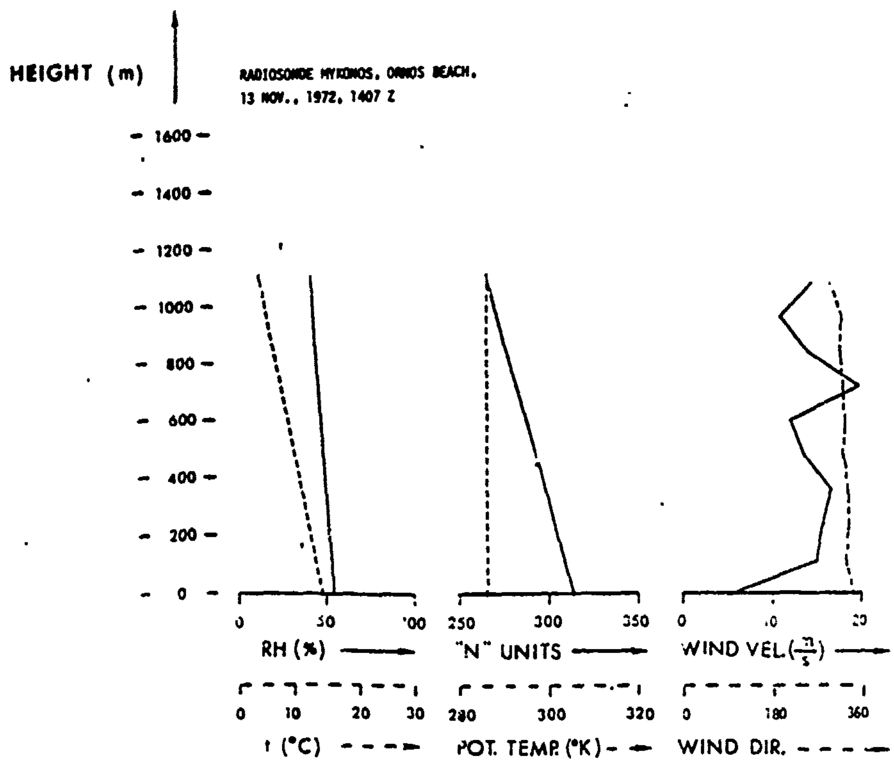
HEIGHT (m)
RADIOSONDE MYKONOS, ORNOS BEACH,
13 NOV., 1972, 1407 Z
1600
1400
1200
1000
800
600
400
200
0
0
50
100
RH (%)
250
300
350
"N" UNITS
0
20
WIND VEL.(m/s)
0
10
20
30
t (°C)
280
300
320
POT. TEMP. (°K)
0
180
360
WIND DIR.

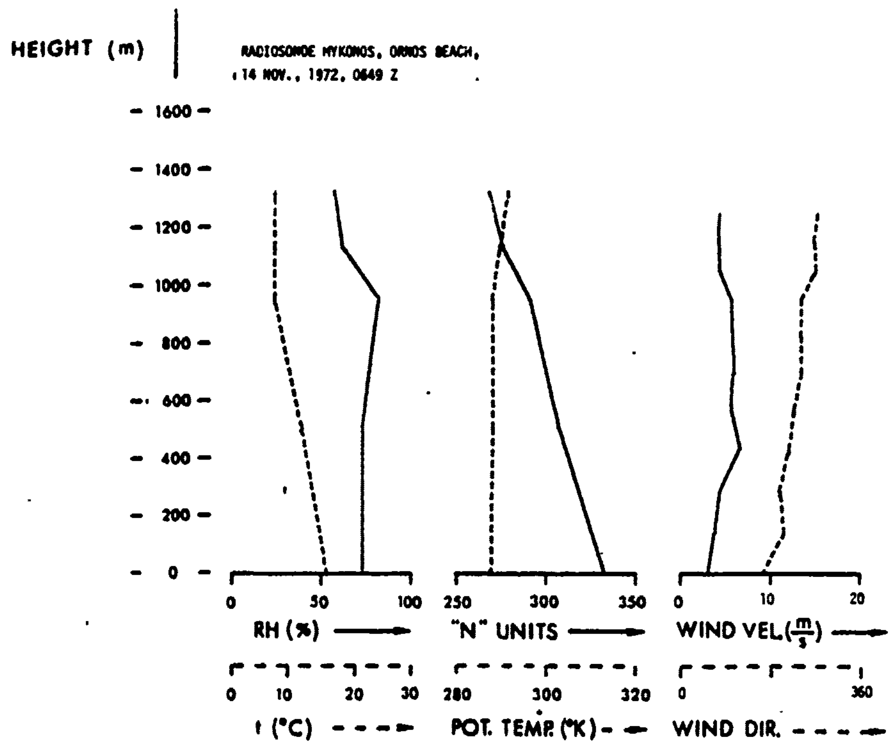
HEIGHT (m)
RADIOSONDE MYKONOS, ORNOS BEACH,
14 NOV., 1972, 0649 Z
1600
1400
1200
1000
800
600
400
200
0
0 50 100
RH (%)
250 300 350
"N" UNITS
0 10 20
WIND VEL.(m/s)
0 10 20 30
t (°C)
280 300 320
POT. TEMP. (°K)
0 360
WIND DIR.

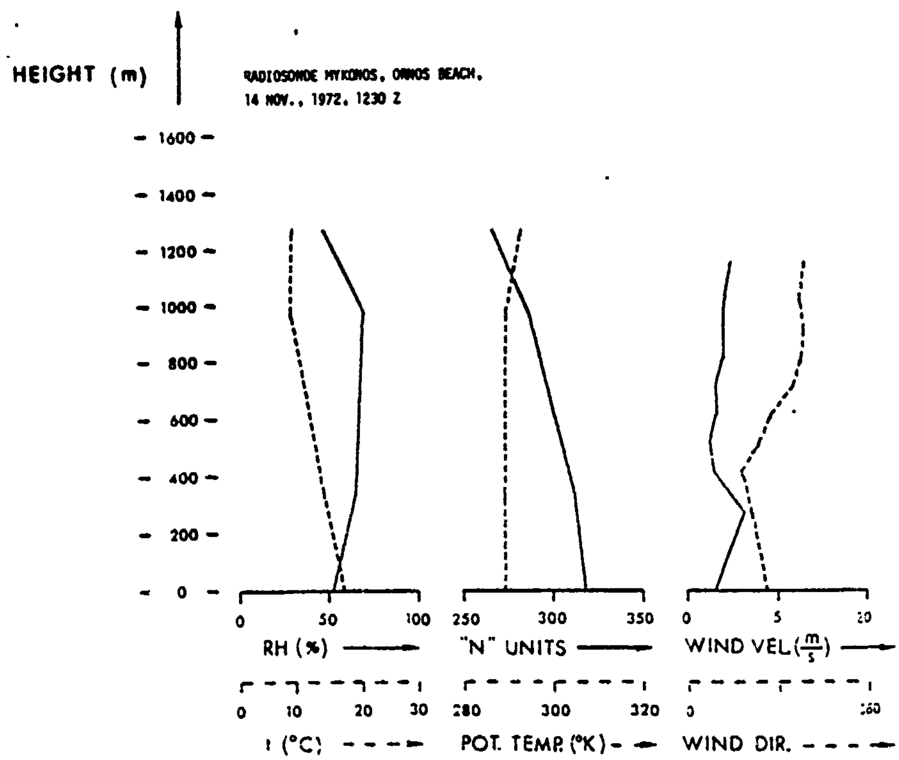
HEIGHT (m)
RADIOSONDE MYKONOS, ORNOS BEACH,
14 NOV., 1972, 1230 Z
1600
1400
1200
1000
800
600
400
200
0
0 50 100
RH (%)
250 300 350
"N" UNITS
0 5 10
WIND VEL.(m/s)
0 10 20 30
t (°C)
280 300 320
POT. TEMP. (°K)
0 360
WIND DIR.

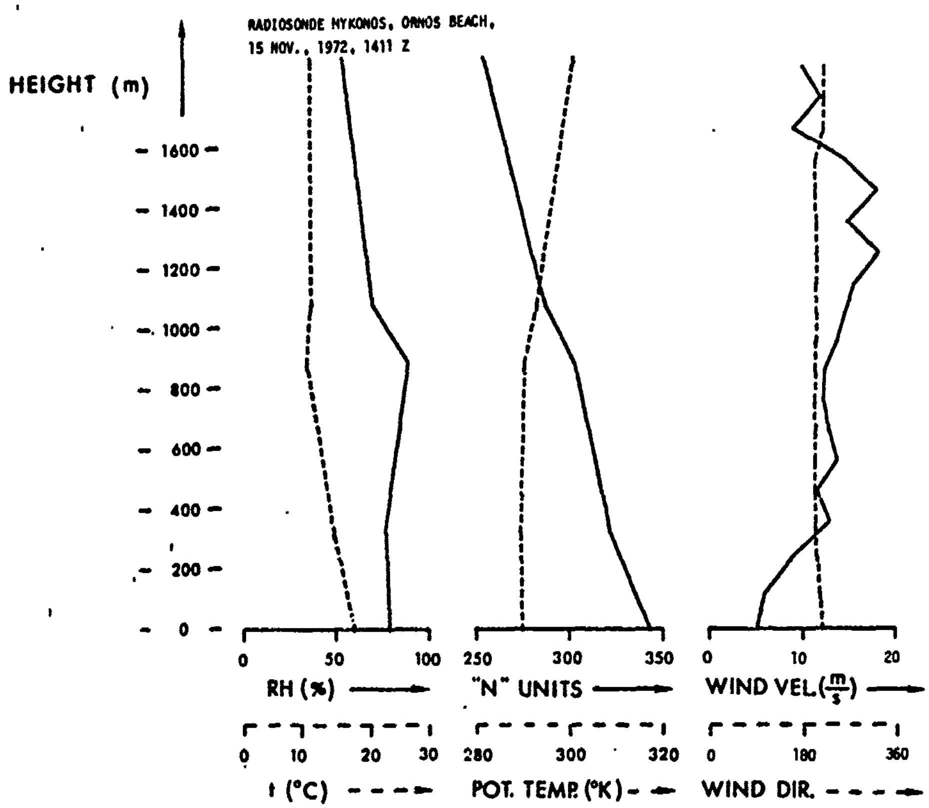
RADIOSONDE MYKONOS, ORNOS BEACH,
15 NOV., 1972, 1411 Z
HEIGHT (m)
1600
1400
1200
1000
800
600
400
200
0
0 50 100
RH (%)
0 10 20 30
t (°C)
250 300 350
"N" UNITS
280 300 320
POT. TEMP. (°K)
0 10 20
WIND VEL.(m/s)
0 180 360
WIND DIR.

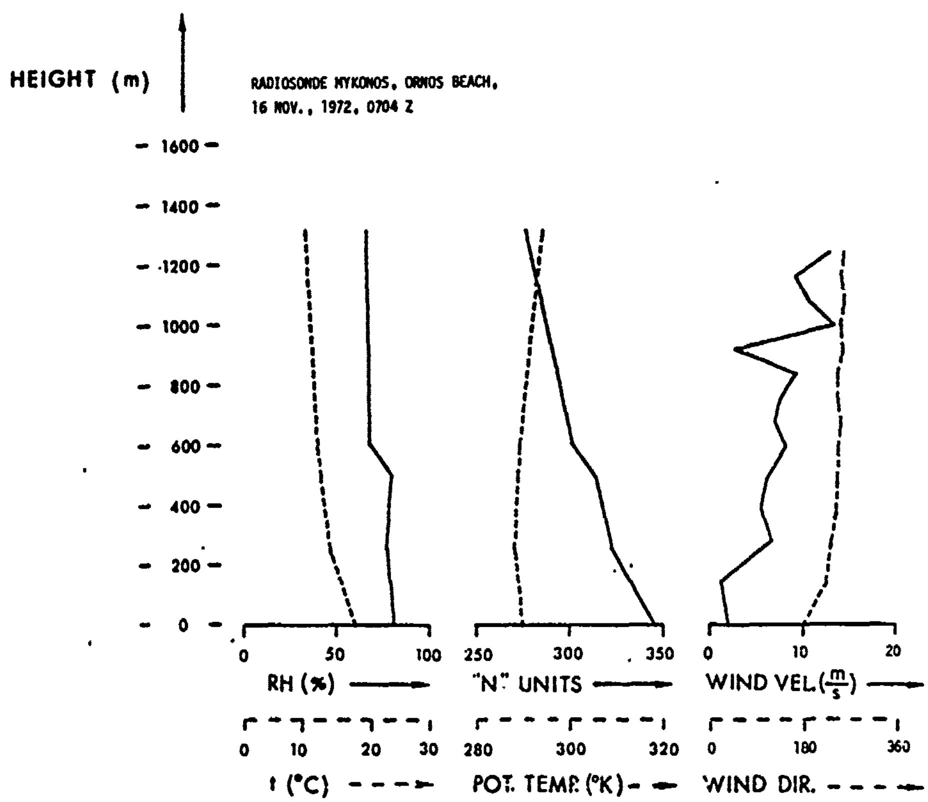
RADIOSONDE MYKONOS, ORNOS BEACH,
16 NOV., 1972, 0704 Z
HEIGHT (m)
1600
1400
1200
1000
800
600
400
200
0
0 50 100
RH (%)
0 10 20 30
t (°C)
250 300 350
"N" UNITS
280 300 320
POT. TEMP. (°K)
0 10 20
WIND VEL.(m/s)
0 180 360
WIND DIR.

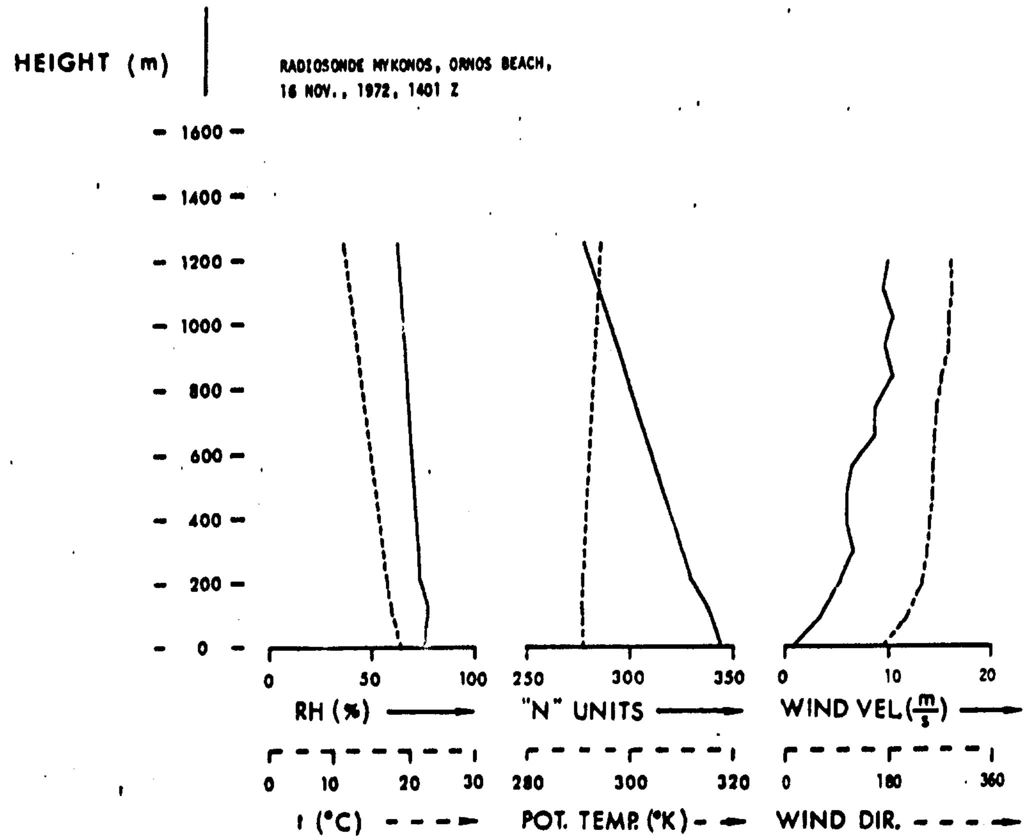
HEIGHT (m)
RADIOSONDE MYKONOS, ORNOS BEACH,
16 NOV., 1972, 1401 Z
1600
1400
1200
1000
800
600
400
200
0
0 50 100
RH (%)
250 300 350
"N" UNITS
0 10 20
WIND VEL.(m/s)
0 10 20 30
t (°C)
280 300 320
POT. TEMP. (°K)
0 180 360
WIND DIR.

XI. ACKNOWLEDGEMENT

The measurement program and the data analysis in this report involved many people. The conscientious effort and enthusiasm of the following people were essential for the successful outcome of the project: K. D. Anderson, L. J. Goodson, W. K. Horner, Dr. D. R. Jensen, M. L. Phares, and J. F. Theisen.

The measurements were conducted with the assistance of University of Athens personnel. We thank Professor Anastassiadis for his support and C. Dragatsis, D. Mavrakis, and S. Prionas for their help during the program.

Also gratefully acknowledged is the assistance and support of the Naval Communication Station in Greece. Captain Brabant took a personal interest in our program and gave us assistance through the entire measurement period. Final thanks go to the 7206th Support Group USAFE in Athens who provided disbursing support and use of their facilities.